MODELING AND SIMULATION OF INFECTIOUS DISEASE USING FRACTIONAL CALCULUS

A Thesis Submitted
in Partial Fulfilment of the Requirements for the
Degree of

DOCTOR OF PHILOSOPHY

in

Mathematics

by

Abhay Srivastava
(Roll No. 2K21/PHDAM/05)

Under the Supervision of

Dr. Nilam

DELHI TECHNOLOGICAL UNIVERSITY
(Formerly Delhi College of Engineering)
Shahbad Daulatpur, Main Bawana Road, Delhi-110042, India

October 2025

Dedicated to my beloved parents

And to my siblings,

For always standing by me with strength and kindness.

ACKNOWLEDGMENTS

First and foremost, I bow with deep gratitude to the Almighty, whose blessings, guidance and grace have given me the strength, clarity and perseverance to complete this thesis. Without His divine will, none of this would have been possible. I am especially thankful to Chitragupta Ji for his blessings and to Surya Dev, Divine Shiva-Parvati and Divine Radhe-Krishna for being my guiding light and for giving me the courage and faith to face life's struggles.

The success of this thesis is not mine alone; it is the result of the encouragement, guidance and support of many individuals. I wish to take this opportunity to express my heartfelt gratitude to all who have played a role in this journey.

This work would not have been possible without the invaluable guidance of my supervisor, Dr. Nilam, to whom I owe my deepest gratitude. Her profound knowledge, patient mentorship and constructive feedback have been instrumental in shaping the direction of this thesis. At every stage, her clarity of thought, meticulous approach and insightful suggestions enhanced the quality of this work. It has been a privilege to learn under her supervision and the scholarly values she has instilled in me will continue to guide my academic endeavors.

My heartfelt gratitude goes to my parents in heaven, who have been the Northern Star to my sailing ship, guiding me always from afar. I remain forever indebted to their unconditional love and sacrifices, which form the foundation of all that I have achieved. Thank you, Mummy and Papa, for being with me in every step of my life and for instilling in me the values that guide me still. To my brother, sister and brother-in-law – Mr. Arpit Srivastava, Mrs. Shweta Srivastava and Mr. Pramod Srivastava – I am grateful for your constant motivation and faith in me, which gave me the strength to keep moving forward. I also extend my heartfelt thanks to my Amma in heaven for her blessings. A special token of appreciation goes to the children, Shreya and Vansh,

whose joy and innocence reminded me to find happiness in the little moments, even during challenging times. Truly, I am blessed to have such a loving family.

I extend my sincere appreciation to the Head of Department, Prof. Ramesh Srivastava; the DRC Chairperson, Prof. Sangita Kansal; Ph.D. Coordinator, Dr. Satyabrata Adhikari; my SRC members, Dr. Vivek Kumar Aggarwal and Dr. M. S. Mehata; along with all other faculty members and office staff of the Department of Applied Mathematics, for their encouragement, guidance and support in facilitating the resources and administrative processes necessary for my research.

I am also grateful to Prof. Rinku Sharma (Dean PG) and the Hon'ble Vice-Chancellor of DTU, Delhi, for providing the facilities that enabled the completion of my research work.

I would like to thank my school principal, Mr. Shiva Ji Rai, for his blessings. My special thanks go to Dr. Mahesh Kumar Yadav, my greatest support and pillar of strength. Your patience, care and unwavering belief in me gave me the confidence to overcome challenges and continue striving forward. I also extend my heartfelt gratitude to Mrs. Nibha Gupta, whose encouragement and inspiration motivated me to embark on this Ph.D. journey, and to Ms. Praggya Chaubey, for her kind support and encouragement during this time. I am equally thankful to Mrs. Tajalli Zehra, my school principal during my teaching years, for her guidance and encouragement, which added greatly to my growth. I am especially grateful to my project supervisor, Dr. K. S. Mathur, whose teaching and insights in epidemiology laid the academic foundation that greatly supported the direction of my doctoral research.

I am deeply thankful to my friends – Mr. Ayush Ojha, Dr. Muneshwar Hembram, Dr. Neelesh Gupta, Dr. Prakash Narayan, Dr. Shivani Khare, Dr. Bhagwan Kumar, Mr. Aditya Khanna, Mr. Kishan Gupta, Mr. Vivek Gupta, Mr. Prashant Chaubey, Mr. Ajay Kumar, Mr. Devraj Maurya, Mr. Uday Chauhan, Mr. Harsh Saxena, Mr. Vikram Singh, Ms. Komal Tanwar, Ms. Richa Rajawat and Dr. Bipin Kumar – for standing by me through thick and thin and for motivating me to persevere and strive for excellence.

My sincere thanks also go to Dr. Kanita, whose unwavering support, motivation and unfailing strength were instrumental in helping me stay focused and complete this Ph.D. journey. I am also thankful to Ms. Suruchi Jain, whose encouragement and kind words provided me with much-needed positivity along the way. Together, their presence made the difficult phases of this Ph.D. more manageable and meaningful. I

also gratefully acknowledge the support of Dr. Vineet Srivastava, Dr. Puneet Pal, Dr. Monu Yadav, Dr. Kartikay Bharadwaj, Dr. Surya Giri, Dr. Ram Pratap, Mr. Krishna Dutta, Ms. Kirti Beniwal, Ms. Vinita Khatri, Mr. Yogesh Bharadwaj, Ms. Anshu Choudhary, Ms. Rachna Sharma and Mrs. Bramhvidya, whose encouragement and cooperation enriched my academic journey.

A special thanks is also due to Dr. Abhishek Kumar, for his support in every way throughout my Ph.D. journey. His readiness to help, thoughtful advice and constant encouragement provided me with both confidence and clarity during challenging phases of my research. I am equally grateful to my seniors – Dr. Kanica Goel, Dr. Ankit Sharma, Dr. Vijay Kumar Yadav, Mr. Anil Kumar Rajak and Dr. Swati – whose guidance, cooperation and companionship made this journey smoother and more enriching. My gratitude further extends to Mr. Sunil Kumar Meena, Ms. Priya Yadav and Mrs. Nishu Mittal, whose timely assistance, collaboration and valuable inputs significantly facilitated my research work.

Finally, I extend my thanks to everyone who may not be mentioned by name here, but who supported, encouraged and inspired me throughout this Ph.D. journey.

Abhay Srivastava
DTU, Delhi

DELHI TECHNOLOGICAL UNIVERSITY
(Formerly Delhi College of Engineering)
Shahbad Daulatpur, Bawana Road, Delhi-110042, India

DECLARATION

I, Abhay Srivastava, hereby declare that the work which is being presented in the thesis entitled "**Modeling and Simulation of Infectious Disease Using Fractional Calculus**" in partial fulfilment of the requirements for the award of the Degree of Doctor of Philosophy, submitted in the Department of Applied Mathematics, Delhi Technological University is an authentic record of my own work carried out during the period from August 2021 to October 2025 under the supervision of ***Dr. Nilam***, Department of Applied Mathematics, Delhi Technological University, Delhi, India.

The matter presented in the thesis has not been submitted by me for the award of any other degree of this or any other Institute.

Abhay Srivastava
(2K21/PHDAM/05)

Date:

DELHI TECHNOLOGICAL UNIVERSITY

(Formerly Delhi College of Engineering)

Shahbad Daulatpur, Bawana Road, Delhi-110042, India

CERTIFICATE

This is to certify that the research work embodied in the thesis entitled **"Modeling and Simulation of Infectious Disease Using Fractional Calculus"** submitted by **Mr. Abhay Srivastava** with enrollment number **2K21/PHDAM/05** is the result of his original research carried out in the Department of Applied Mathematics, Delhi Technological University, Delhi, for the award of **Doctor of Philosophy** under the supervision of **Dr. Nilam**, Department of Applied Mathematics, Delhi Technological University, Delhi, India.

It is further certified that this work is original and has not been submitted in part or fully to any other University or Institute for the award of any degree or diploma.

This is to certify that the above statement made by the candidate is correct to the best of our knowledge.

Date: October 2025
Place: Delhi, India

Dr. Nilam
(Supervisor)

Prof. R Srivastava
(Head of Department)

MODELING AND SIMULATION OF INFECTIOUS DISEASE USING FRACTIONAL CALCULUS

Abhay Srivastava

ABSTRACT

In recent years, the world has faced a sharp rise in infectious diseases, which continue to be a serious threat to public health. Despite progress in medical science, surveillance systems, and control measures, outbreaks such as influenza, SARS, and most recently COVID-19 have shown that our societies remain highly vulnerable. These events have also revealed some of the limitations of the classical models used to study and predict the spread of infections. In particular, standard models often ignore memory effects, individual behaviour, and environmental influences. To overcome these gaps, this thesis applies fractional calculus in the modeling and simulation of infectious diseases. Fractional-order models have the advantage of incorporating memory and history, which makes them more realistic for studying epidemics where past exposure, immunity, and behavioural changes play an important role.

The work begins with a study of vaccination strategies followed in five countries that were badly affected during the first half of 2022: the USA, India, Brazil, France, and the UK. A detailed comparison shows that most countries gave priority first to frontline workers and health professionals, and then to elderly or immunocompromised people. The main difference was how countries divided the age groups for priority. By comparing these strategies with confirmed cases and deaths per population, as well as with population density and median age, the study highlights how vaccine distribution policies must be designed carefully to suit the demographics of each country.

Motivated by these findings, different fractional-order models are developed in this thesis. The first is an *SIS* model with Beddington-De Angelis incidence, used to capture the effect of fear-driven behaviour. When people become afraid of infection, they may self-isolate or reduce contact with others. Such actions can strongly influence disease spread, and fractional calculus is especially suitable to model this because fear and behaviour are shaped by past experiences.

A second contribution is an *SVIR* model that divide vaccinated people into two groups: partially vaccinated (those who did not complete the prescribed course of the doses) and fully vaccinated (those who completed the vaccination schedule and followed health guidelines). This distinction is important, as many people worldwide

showed hesitancy in taking vaccines, often due to doubts about safety or mistrust of governments. The model allows us to study how partial vaccination affects recovery compared with full vaccination, giving a clearer picture of real vaccination outcomes.

The thesis also extends the *SEIQR* model by including two realistic features: psychological effects during transmission (using Monod-Haldane incidence) and a limited quarantine capacity (Holling type-III function). These changes reflect how quarantine in practice cannot be increased indefinitely and is often constrained by resources. An associated fractional optimal control problem is studied using Pontryagin's principle, showing how time-dependent controls can be used to reduce infections at minimum cost.

Beyond vaccination and quarantine, the thesis considers environmental effects. A Susceptible-Pollution affected-Infected-Recovered (*SPIR*) model is proposed to study how exposure to pollutants weakens immunity and increases vulnerability to infections. This model even accounts for prenatal exposure in newborns, reflecting the long-term consequences of pollution. A fractional optimal control problem with two controls is solved to examine how information campaigns and other interventions can help reduce infections in polluted environments.

Another area studied is the role of bacteria. Due to rising household waste and urbanization, bacterial populations in the environment are growing, leading to more bacterial and vector-borne diseases. To address this, a fractional *SIR* model with bacteria in the environment and in organisms is developed. An optimal control problem with three controls is analyzed to show how disease transmission can be reduced efficiently.

Across all these models, the unifying theme is the use of fractional-order systems. By including memory, they allow us to model more realistic epidemic behaviours, whether due to human psychology, environmental stress, or bacterial growth. Numerical simulations are carried out using the Adams-Bashforth-Moulton predictor-corrector method, which validates the theoretical results and demonstrates how the models behave under different conditions.

In summary, this thesis presents a set of new fractional-order models that bring together vaccination strategies, fear and behaviour, quarantine measures, environmental pollution, and bacterial effects in infectious disease dynamics. The results show that fractional models are not only mathematically richer but also practically more meaningful, as they reflect the role of memory and history in epidemic processes. By combining theory, simulations, and control strategies, the thesis provides insights that

can support better decision-making in managing infectious diseases and preparing for future outbreaks.

Table of Contents

List of Figures

List of Tables

Chapter 1

Introduction

"The important thing is not to stop questioning. Curiosity has its own reason for existing."

-Albert Einstein.

1.1 Fractional Calculus

Fractional Calculus, a branch of Calculus dealing with integrals and derivatives of arbitrary orders (including complex orders), has been in the priority of the mathematicians in last few decades [132; 148]. Its applications can be seen in all the classical fields of Mathematics and Physics like Epidemiology, Mathematical Biology, Fluid dynamics etc. Actually, this subject translates the reality of nature in a more better and precise way. In other words, fractional calculus is what nature understands and talking with nature in this language is therefore efficient [104]. The conventional integer order calculus being a part of it, where differintegration is an operator doing differentiation and integration in general sense [42]. In this introductory chapter, the development of fractional calculus is discussed, with several definitions of fractional-order operators presented.

The idea of Fractional Calculus originates from a conversation between L'Hospital and Leibniz in 1695 where L-Hospital asked Leibniz about the n^{th} derivative of a smooth function if $n = \frac{1}{2}$ i.e. differentiation for a non-integer order, a far aspect from classical calculus. In reply from Leibniz to L'Hospital, dated on September 30, 1695, Leibniz wrote: 'This is an apparent paradox from which, one day, useful

consequences will be drawn ...' [94] and here from, the origin of fractional calculus is accepted. Throughout the 18th and 19th centuries, several prominent scientists, including Euler, Abel, Laplace, Grunwald-Letnikov, Riemann-Liouville, Weierstrass, Reisz-Feller Mittag-Leffler, Caputo, Fabrizio, Atangana, Baleanu, and others made substantial contribution to the advancement of fractional calculus. The very first conference with proceedings on 'Fractional calculus and its applications' (Ed. Ross, Lect. Notes Math. 1975, vol. 38) was held in 1974 at the University of New Haven, USA [1]. The second conference with proceedings on 'Fractional Calculus' (Eds A. C. Mcbride and G. F. Roach, Res. Notes Math, 1985 vol. 138). The guesswork of Leibniz (1695-1697) and Euler (1730) start the journey of this field of mathematical analysis. The first book devoted to fractional calculus was a joint contribution of two specialists Oldham (in chemistry) and Spanier (in mathematics) [144] in 1974. The main focus of this monograph is on the evaluation of the fractional integrals and derivatives of the concrete functions and to the applications of the diffusion problems. A book by Podlubny [148] with main focus on fractional differential equations published in 1999 is among most recent work in fractional calculus. Other numerous works include the work done by Hilfer [78] in 2000 on fractional models of anomalous kinetics of complex processes, monograph by Samko [165] which is popular as 'Encyclopedia of Fractional Calculus'. This monograph first published in 1987 in Russian and later was translated in English in 1993 which substantially deals with fractional differential equations.

In modeling physical and engineering processes fractional differential equations are very useful. It is worth noting that in many cases the standard mathematical models incorporating integer order derivatives are not adequate. The beauty of this topic is in its fractional derivatives and integrals, which are not just a local property but also take into account history and locally dispersed effects. That is why this subject better translates nature's reality! Non-integer order fractional derivatives and integrals can be utilized to explain processes with memory. If at each time t, the output of a system depends only upon the input at time t, such system are called memory-less systems while to find the current value of the output of the system need to remember previous values of the input, non memory-less or memory systems. Fractional calculus has expanded its wings even more in the modern age to embrace the complexities of the real world. The first stage of the Memory Revolution in economics is associated with the accomplishments of Granger [70], who received the 'Nobel Memorial Prize in Economic Sciences'; in 2003. He presented the importance of long range time depen-

dence. Because an integer order dynamic system's future states are dependent on the current one (memory-less), but a fractional order system's current state is dependent on the whole history (long memory). This large memory is often used as a nameplate for many fractional order systems

Besides FC, while looking another useful aspect to be analyzed in medical sciences, we see various mathematical models have been modeled to investigate the dynamics of infectious diseases. In recent years, there is a great increase in trend of application of mathematics in infectious diseases which resulted in the emergence of mathematical epidemiology [19; 84; 180; 196]. It is obvious that fractional calculus presents the nature of resultant finer than integral order. It is important to mention that fractional-order system possess the infinite memory which makes the discussion interesting rather than to talk about integer order in new generation researches. Considering these facts, inclusion of memory is important in epidemiology for infectious diseases to improvise the proposed model. Therefore, fractional differential equations (FDEs) in mathematical epidemiology has become a trend of research field in theoretical and as well as in practical sense.

From the discussion mentioned above, it can be concluded that researchers now prefer fractional-order system over the traditional differential equations models mainly because of the following reasons:

- Fractional-order system allow greater degrees of freedom over its integer-order counterpart due to the additional parameter that represents its order [156; 177], and are more suitable for those systems having higher-order dynamics and complex nonlinear phenomena.

- Secondly and more importantly, fractional-order derivatives not only depend on the local conditions but also on the previous history of the function and, therefore, the fractional derivative has become an efficient tool for those systems, where consideration of memory or hereditary properties of the function is essential to represent the system [5].

Before moving further, it is important to recall some basic mathematical tools from fractional calculus that will be used throughout this work. These preliminaries form the foundation for defining fractional derivatives and integrals.

Definition 1.1.1 *[148]* ***Euler's gamma function***

The Euler's gamma function $\Gamma(x)$ *is defined by*

$$\Gamma(x) = \int_0^\infty t^{x-1}e^{-t}dt, \ \text{for } x \in \mathbb{C}, \ Re(x) > 0.$$

Definition 1.1.2 *[148]* ***Mittag-Leffler function***

(i) The one parameter Mittag-Leffler function $E_\alpha(z)$ *is defined by*

$$E_\alpha(z) = \sum_{i=0}^{\infty} \frac{z^i}{\Gamma(\alpha i+1)}; \ z, \ \alpha \in \mathbb{C}, \ Re(\alpha) > 0.$$

(ii) The two parameter Mittag-Leffler function $E_{\alpha,\beta}(z)$ *is defined by*

$$E_{\alpha,\beta}(z) = \sum_{i=0}^{\infty} \frac{z^i}{\Gamma(\alpha i+\beta)}; \ z, \ \alpha, \ \beta \in \mathbb{C}, \ Re(\alpha) > 0.$$

Definition 1.1.3 *[33]* ***Riemann-Liouville fractional integral and derivative***

The Riemann-Liouville fractional integral is given by

$${}_a^{RL}I_x^q f(x) = \frac{1}{\Gamma(q)} \int_a^x (x-u)^{q-1} f(u)du,$$

and the Riemann-Liouville fractional derivative is defined as

$${}_a^{RL}D_x^q f(x) = \frac{d^n}{dx^n} \frac{1}{\Gamma(n-q)} \int_a^x (x-u)^{n-q-1} f(u)du, \quad (n-1) < q < n,$$

where q *is fractional order and* f *is a continuous function.*

Definition 1.1.4 *[33]* ***Caputo fractional derivative***

Caputo fractional derivative was introduced by Michele Caputo in 1967. This derivative proved its identity due to two facts. One is the Caputo fractional derivative of a constant function is equal to zero. Second, the initial conditions depend on integer-order derivative. The Caputo factional derivative is given by:

$${}_a^{c}D_x^q f(x) = \frac{1}{\Gamma(n-q)} \int_a^x (x-u)^{n-q-1} f^n(u)du, \ q > 0, \quad (n-1) < q < n.$$

For $n = 1$ *we have*

$${}_a^{c}D_x^q f(x) = \frac{1}{\Gamma(1-q)} \int_a^x (x-u)^{-q} f'(u)du, \quad q > 0, \ 0 < q < 1.$$

where, $(x-u)^{-q}$ *is called the singular kernel of the integral.*

Definition 1.1.5 *[15]* ***Laplace transform of Caputo fractional derivative***
Let a piece-wise continuous function $D_t^q f(t)$ in Caputo sense, then

$$\mathscr{L}\{{}_0^c D_t^q f(t)\} = s^q \mathscr{L}(f(t)) - \sum_{k=0}^{n-1} s^{q-k-1} g^{(k)}(0), \;\; 0 < q \leq 1$$

where, $\mathscr{L}(D_t^q f(t))$ stands for the Laplace transform of $f(t)$.

Definition 1.1.6 *[142]* ***Generalized mean value theorem***
Suppose that $f(t) \in C[a,b]$ and $D_t^q f(t) \in C(a,b]$ with $0 < q \leq 1$. Then we have $\forall t \in [a,b]$, there exists $\xi(t) \in [a,t]$, such that

$$f(t) = f(a) + \frac{1}{\Gamma(q)} (D_t^q f(\xi))(t-a)^{\alpha}.$$

After recalling these definitions, some important results from fractional calculus, which will be instrumental in the present study, are subsequently presented.

Lemma 1.1.7 *[148] Let $\alpha_1 > 0,\ \alpha_2 > 0$, and $w \in C$. Define*

$$y(t) = t^{\alpha_2 - 1} E_{\alpha_1, \alpha_2}(\pm w t^{\alpha_1}),$$

where $E_{\alpha_1,\alpha_2}(z)$ denotes the two-parameter Mittag-Leffler function with parameters α_1 and α_2. Then the Laplace transformation of y is given by

$$\mathscr{L}[y(t)] = \frac{s^{\alpha_1 - \alpha_2}}{s_1^{\alpha} \mp w}.$$

Lemma 1.1.8 *[148] Let α_2 is and arbitrary real number. If $\alpha_1 < 2$, then there is a constant C_E such that, for all w in the complex plane,*

$$|E_{\alpha_1,\alpha_2}(w)| \leq \frac{C_E}{1+|w|}.$$

Lemma 1.1.9 *[147] Let $h(t) \in \mathbb{R}^+$ be a differentiable function, then*

$${}^c D_t^q \left[h(t) - h^* - h^* \ln \frac{h(t)}{h^*} \right] \leq \left(1 - \frac{h^*}{h(t)} \right) {}^c D_t^q (h(t)),\ h^* \in \mathbb{R}^+, \forall\ q \in (0,1).$$

Lemma 1.1.10 *[109] Given a continuous function $u(t)$ on the interval $[t_0, \infty)$ that satisfies*

$$\begin{cases} {}_{t_0} D_t^q u(t) \leq -\lambda u(t) + \mu, \\ u(t_0) = u_{t_0} \end{cases}, \tag{1.1}$$

where $0 < q < 1,\ \ (\lambda, \mu) \in \mathbb{R}^2$ and $\lambda \neq 0$, and $t_0 \geq 0$ is the initial time. Then

$$u(t) \leq \left(u_{t_0} - \frac{\mu}{\lambda} \right) E_q[-\lambda (t-t_0)^q] + \frac{\mu}{\lambda}.$$

Lemma 1.1.11 *[114] For the Caputo fractional order system,*

$$ {}_{t_0}D_t^q y(t) = f(t,y) \;\; with \;\; y(t_0) = y_0 \;\; and \;\; t_0 > 0, $$

where $q \in (0,1]$ *and* $f : [t_0,\infty] \times \Omega \to \mathbb{R}^n$ *is piecewise continuous on* $[t_0,\infty] \times \Omega$ *and* $\Omega \in \mathbb{R}^n$. *If* $f(t,y)$ *satisfies the Lipschitz condition in y then there exist a unique solution on* $[t_0,\infty] \times \Omega$.

Theorem 1.1.12 *[148] Consider a fractional order non-autonomous system*

$$ {}_{t_0}^{c}D_t^q x(t) = f(t,x), \qquad t > t_0 \tag{1.2} $$

with initial condition x_{t_0}, *where* $0 < q \leq 1$, $f : [t_0,\infty) \times \Omega \to \mathbb{R}^n$, $\Omega \in \mathbb{R}^n$. *If* $f(t,x)$ *is a real-valued continuous function defined in the domain* $[t_0,\infty) \times \Omega$, *satisfying the locally Lipschitz condition with respect to x, i.e.,*

$$ |f(t,x_1) - f(t,x_2)| \leq K\,|x_1 - x_2|, $$

where K is a positive constant, and

$$ |f(t,x)| \leq M < \infty, \qquad \forall (t,x) \in [t_0,\infty) \times \Omega, $$

then the above system has a unique solution in $[t_0,\infty) \times \Omega$.

Lemma 1.1.13 *[49] Assume that* $q \in (0,1]$ *and that both the function* $f(t)$ *and its fractional derivative* ${}_{t_0}D_t^q f(t)$ *belong to the metric space* $C[a,b]$. *If* ${}_{t_0}D_t^q f(t) \geq 0$ *for all* $t \in [a,b]$, *then* $f(t)$ *is monotonically increasing. Conversely, if* ${}_{t_0}D_t^q f(t) \leq 0$ *for all* $t \in [a,b]$, *then* $f(t)$ *is monotonically decreasing.*

The mathematical tools introduced above are useful in modeling real-world problems using fractional calculus. One of the most important areas where these tools have found growing applications is epidemiology, which deals with the study of diseases in populations. To illustrate how fractional models can be employed in this domain, a brief overview of epidemiology is first presented.

1.2 Epidemiology: A brief overview

Epidemiology is the study of the distribution and patterns of disease in a defined population and finding the causes of disease occurrence. The word epidemiology is derived

from Greek word *pi* means 'upon or among', *demos* means 'people' and *logos* means 'study'. Thus, epidemiology literally means "the study of what is upon the people". It is a foundation of public health, based on which public decision makers can identify risk factors for various diseases and employ preventive measures.

The major areas of epidemiology include finding the causes of diseases, how diseases spread, investigating outbreaks, controlling diseases, forensic studies, environmental factors, workplace - related health issues, tracking exposure to harmful substances, and studying the effects of treatments. To better understand how diseases work, epidemiologists use knowledge from different fields - like biology to study life processes, statistics to analyze data and draw conclusions, social sciences to understand both direct and indirect causes, and engineering to measure exposure to risks. Epidemiology is a term that is now commonly used to describe and explain the causes of infectious diseases, epidemics, and diseases in general. Thus, the basis of this epidemiology is the way in which pattern of disease changes human functions.

1.2.1 Mathematical modeling of infectious diseases

Infectious diseases have always been a major threat to human health. It is well known that several factors such as, the type of infectious agent, how it spreads, how vulnerable people are, and what treatments are available - play a role in how these diseases spread. An abstract representation of real-world problems in the framework of mathematics is called a mathematical model and the process is called mathematical modeling. In epidemiology, mathematical modeling is used to investigate the detail mechanisms of disease transmission, to predict disease outbreaks in future, and to analyse effective control measures. Mathematical modeling has been widely utilised in past decades to study various diseases, including dengue, HIV/AIDS, malaria, HBV, SARS, Influenza, COVID-19 etc. Since the beginning of the twentieth century, researchers have developed numerous mathematical models to explain the dynamics of infectious diseases. Depending on the objective and perspective, the mathematical models are formulated in different forms including differential equation models, differintegral equation models, statistical models, models of difference equation etc., and various techniques are employed for theoretical as well as numerical analyses. The parameter values used basically for simulation purposes could be theoretical, or taken from scientific researches, or extracted from statistical modeling.

Epidemic models are broadly classified into two main types: stochastic models and deterministic (or compartmental) models. Stochastic models account for randomness in one or more parameters over time, making them particularly useful for estimating the probability distribution of potential outcomes, especially in small populations or early outbreak stages. In contrast, deterministic models, which are more commonly used in this study, assume a fixed relationship between variables and are typically applied to large populations where random effects are negligible.

Mathematical models of diseases start from the population that can be divided into a set of distinct compartments dependent upon experience with respect to the relevant disease, which provide a significant contributions to Mathematics and public health . The process of mathematical modeling is shown in the Figure 1.1, as below:

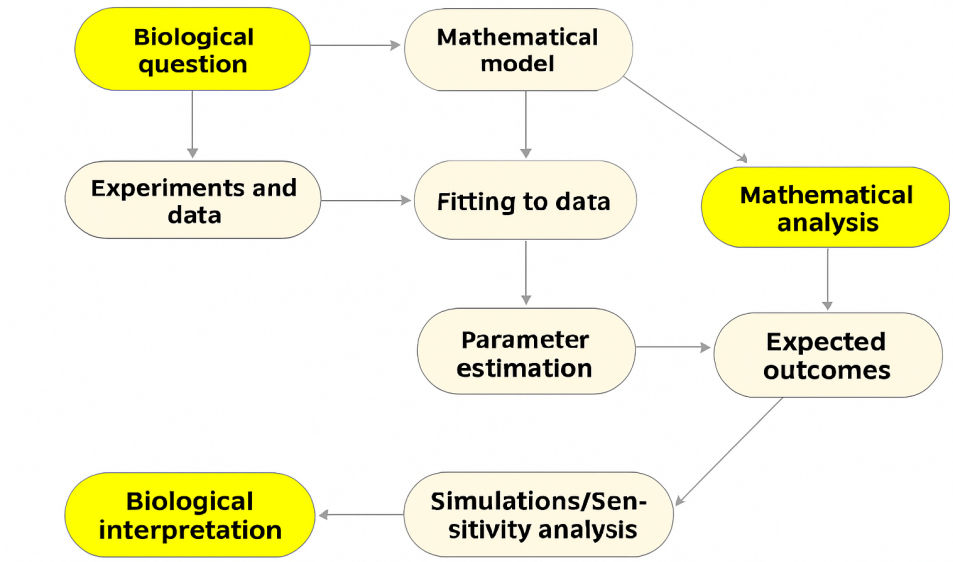

Figure 1.1: Mathematical modeling.

The journey of mathematical modeling of infectious diseases started long back ago. Daniel Bernoulli was the first person who introduced mathematical modeling to study the smallpox outbreak in 1760 [20]. Then the first contributions to the modern Mathematical Epidemiology were set up by P.D. En'ko from 1873 to 1894 [54]. Another revolutionary work is due to Sir Ronald Ross on malaria [154]. He studied malaria transmission dynamics between mosquitoes and humans and was awarded the second Nobel Prize in Medicine. The most well-known and commonly used compart-

mental model in mathematical epidemiology was introduced and studied by Kermack and McKendrick [92]. They proposed a model by categorizing the population into the S-I-R classes and assuming that the total population remains constant at all times in which the infections occur by way of contact between susceptible and infected. Based on these assumptions, they derived the following first-order coupled nonlinear differential equation describing the movement of the population in the three compartments as follows:

$$\begin{aligned}\frac{dS}{dt} &= -\beta SI \\ \frac{dI}{dt} &= \beta SI - \gamma I \\ \frac{dR}{dt} &= \gamma I\end{aligned}$$

where, β denotes the transmission rate and γ is defined as the removal or recovery rate.

Further, in 1990, Anderson [11] and May proposed a model for infectious diseases by introducing and incorporating the natural mortality rate for a fixed population into the above defined Kermack and Mckendrick's model by the following equations:

$$\begin{aligned}\frac{dS}{dt} &= \mu N - \mu S - \beta SI \\ \frac{dI}{dt} &= \beta SI - (\mu + \delta)I \\ \frac{dR}{dt} &= \delta I - \mu R\end{aligned}$$

with the initial conditions $S(0) = S_0$, $I(0) = I_0$ and $R(0) = R_0$, where $t \geq 0$. Through the analysis of this model, they showed that the disease will be eliminated from the society if $\mathscr{R}_0 > 1$.

After that, as time progress, this subject has also been enriched gradually. Due to the advancement of scientific computing, mathematical epidemiology has taken a new shape with more popularity and acceptability (Hethcote [76], Murray [138], Keeling and Rohani [91]). It has been possible for the researchers of interdisciplinary fields to formulate a specific model to analyze the dynamical behaviors of various emerging and re-emerging infectious diseases like malaria, dengue, cholera, HIV-AIDS, zika, influenza, COVID-19, etc. [7; 64; 135; 167; 176].

Since infectious disease models aim to predict whether an outbreak will persist or die out, the study of equilibrium states and stability conditions becomes essential. Accordingly, some fundamental notions from dynamical systems, to be employed throughout the subsequent analysis, are first reviewed.

Definition 1.2.1 ***Fractional-order Autonomus System***
Consider the following fractional-order system

$$ {}_0^cD_t^q x(t) = f(x), \qquad x(0) = x_0 \tag{1.3}$$

with $0 < q \leq 1$, $x \in \mathbb{R}^n$ *and* $f : E(\subset \mathbb{R}^n) \to \mathbb{R}^n$, *it is said to be autonomus if* f *does not depend on* t *explicitly. Here* ${}_0^cD_t^q$ *is the Caputo fractional derivative of order* q.

Definition 1.2.2 ***Equilibrium Solution***
An equilibrium solution (steady state solution or fixed point or critical point) of the system (1.3) *is a solution* $\bar{x} \in E(\subset \mathbb{R}^n)$ *satisfying*

$$f(\bar{x}) = 0.$$

Definition 1.2.3 ***Local Stability***
An equilibrium solution $\bar{x} \in E(\subset \mathbb{R}^n)$ *of* (1.3) *is said to be locally stable if for each* $\varepsilon > 0$ *there exists a* $\delta > 0$ *such that every solution* $x(t)$ *of* (1.3) *with initial condition* $x(0) = x_0$ *and* $\|x_0 - \bar{x}\| < \delta \implies \|x(t) - \bar{x}\| < \varepsilon$ *for all* $t > 0$, *where* $\|.\|$ *is the Euclidean norm. If the equilibrium solution is not locally stable, it is said to be unstable.*

Definition 1.2.4 ***Local Asymptotic Stability***
An equilibrium solution $\bar{x} \in E(\subset \mathbb{R}^n)$ *of* (1.3) *is said to be locally asymptotically stable if it is locally stable and if there exists a* $\sigma > 0$ *such that*

$$\|x_0 - \bar{x}\| < \sigma \implies \lim_{t \to +\infty} \|x(t) - \bar{x}\| = 0.$$

Theorem 1.2.5 *[131]* ***(Local Asymptotic Stability Theorem)*** *The system* (1.3) *is said to be locally asymptotically stable around the equilibrium point* $\bar{x} \in E(\subset \mathbb{R}^n)$ *if all eigenvalues* λ_i *of the jacobian matrix* $J = \dfrac{\partial f}{\partial x}$, $x \in \mathbb{R}^n$ *evaluated at the equilibrium point* $\bar{x}$ *satisfy*

$$|arg(\lambda_i)| > \frac{q\pi}{2}, \quad i = 1, 2, \cdots, n, \tag{1.4}$$

i.e.

$$arg(\lambda_i) > \frac{q\pi}{2} \quad or \quad arg(\lambda_i) < -\frac{q\pi}{2}, \quad i = 1, 2, \cdots, n,$$

where $arg(\lambda_i)$ *is the principal value of argument of the eigenvalue* λ_i *of the Jacobian matrix* J. *If* $arg(\lambda_i)$ *does not satisfy* (1.4), *then the system is unstable around that equilibrium point.*

The graphical representation of the above Theorem (1.2.5) has been shown in Figure 1.2. It clearly shows that the stability region of fractional order system (Figure 1.2 (a)) is greater than the stability region of the integer order system (Figure 1.2 (b))

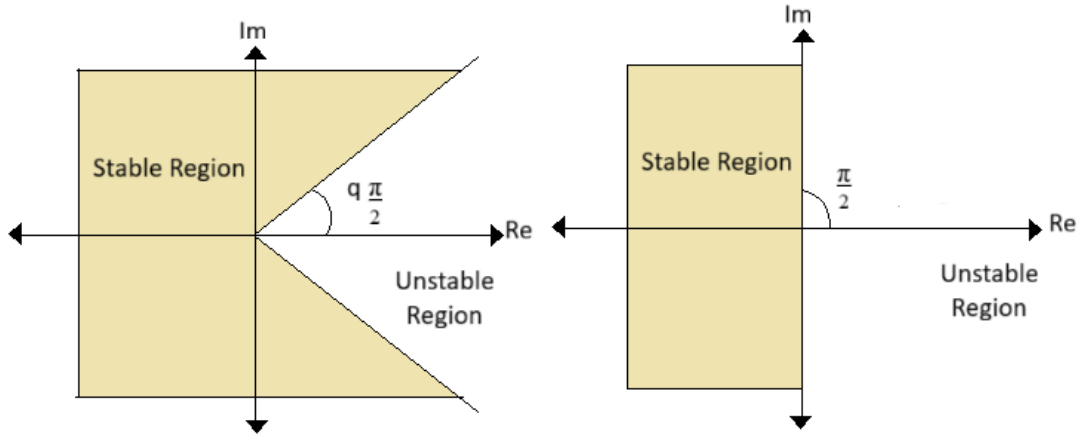

(a) $0 < q < 1$. (b) $q = 1$.

Figure 1.2: Stability regions (shaded area) for (a) fractional order system and (b) integer order systems.

1.2.2 Modes of Transmission

There are several ways to transmit infection from natural reservoir to host. The modes of transmission can be classified as: Direct transmission and Indirect transmission [130]. In direct transmission, an infectious disease is transferred by direct contact of infected person through skin-to-skin contact, sexually transmitted disease (STD), micro organisms in soil etc.. On other hand, droplet spreads the infection which is produced by sneezing, coughing and talking. Transmission can also be made by carriers indirectly by airborne transmission and vector transmission. The infectious agent spreads from one place to another or on person to person by dust or micro organisms presented in air. Mosquitoes, ticks and flea act as a vectors for carrying infected agent to uninfected population. Dengue, Zika, malaria are some examples of vector transmitted diseases.

Even though, the integer model could be suitable for modeling numerous disease processes, but it may not be enough to explain the pandemic dynamics. In recent times, epidemiological research has been diverted to fractional differential research due to its ability to offer a convincing analysis of certain nonlinear dynamics. The study of

fractional order differential equations in the past decades has received a significant attention of researchers [69; 96; 149; 150; 151; 164; 171; 198].

1.3 Incidence and Treatment rates

In the infectious disease model, the incidence rate function has a significant impact on the behaviour of the disease. The incidence function captures the interactions between the healthy and infective ones. It gives the number of new cases per unit time coming from the susceptible population as a result of this interaction. There are many forms of incidence rate functions that are used in the epidemiological literature. The dynamical behaviour of the system is significantly impacted by the choice of incidence rate function. A brief review of the literature on incidence rate functions is presented here.

In the classical Kermack - McKendrick model [92], the monotonic and unsaturated incidence rate function $\beta SI,\ \beta > 0$ is proposed. It represents the bilinear (or mass action) incidence rate. In the bilinear incidence rate, the number of infectives increases linearly, which might be real for a small population of infected individuals, but impractical for a large number of infectives. Therefore, several studies are devoted to considering nonlinear incidence rate for disease transmission dynamics [77; 117; 118].

The incidence rate function in saturated form was first introduced by Capasso and Serio [32] in 1978. They observed population's inhibitory behavior in interaction in presence of disease during the Cholera epidemic in 1973. This bounded interaction pattern inspired them to propose bounded incidence rate function $g(I)S$ provided $0 \leq g(I) \leq c \neq 0, g(0) = 0, g'(0) > 0, g(I) \leq g'(0)I$, while accounting for the psychological effect on people's behavioral responses [155]. Further, they studied an *SIR* model for particular choice of incidence function $Sg(I) = \frac{kSI}{1+\alpha I}, \quad$ where $k, \alpha > 0$.

In 1986, Liu et al.[118] proposed a generalized form of incidence rate function $\frac{\beta SI^p}{1+mI^q}, \quad p,q,\beta,m > 0$. This function can be either monotonic or non-monotonic and saturated or unsaturated for different values of p,q. Here βI^p indicates the force of infection of the disease and $\frac{1}{1+mI^q}$ expresses the inhibitory effect of susceptible due to a large number of infective cases. Ruan and Wang [155] studied the existence and non-existence of limit cycle in a system choosing $p = q = 2$ and found Bogdanov-Takens bifurcation. Gomes et al. [67] observed backward bifurcation in model system when $p = q = 1$. In 2005, Xiao and Ruan [194] focused on the importance of inhibitory effect in disease spread control and proposed the non-monotonic incidence rate taking

$p = 1, q = 2$ i.e., $\frac{\beta SI}{1+mI^2}$, also known as Monod-Haldane type incidence rate where m measures the effect of behavioral change of population.

In addition, some other types of nonlinear incidence rate functions are also established in modeling. Further, Yuan and Li [199] proposed the density-dependent incidence function as $\frac{\beta S(I/S)^p}{1+m(I/S)^q}, \quad \beta, m, p, q > 0$. The works of researchers [30; 97; 100] for specific values of p, q, explore the significance of density-dependent incidence functions. When the number of infective case is very high in population, the population takes protection measures and avoid interactions as much as possible. Therefore the incidence function would become $\frac{\beta SI}{1+a_1S+a_2I}, \quad \beta, a_1, a_2 > 0$, also known as Beddington-DeAngelis function as Beddington [24] and DeAngelis [43] independently established it in 1975 which is also studied later in epidemiology [171; 187].

Before 2004, it was common to consider linear treatment rates in the models. In 2004, Wang and Ruan [186] proposed that disease can be eradicated by using the maximum treatment facility (constant). In 2006, Wang [185] modified the constant treatment to account for increasing costs and medical resources. For this purpose a linear function of infective is used when the number of infective cases is less than the maximum treatment capacity; whereas, a constant treatment rate is used otherwise. Analyzing this non-smooth treatment rate it is found that when the threshold quantity (R_0) is less than unity, the disease would persist at the low level of treatment capacity due to the occurrence of backward bifurcation and bi-stable endemic equilibria [80; 113].

Zhang and Liu [200] underlined that attending to a patient is delayed when the number of infective cases exceeds the available treatment capacity. They proposed a treatment function of the form $\frac{\alpha I}{1+\mu I}$ where α represents the rate of treatment and μ represents the saturation parameter which may be related to the delay in providing treatment. This function grows as the number of infectives grows and saturates to the maximum treatment facility when the number of infectives becomes large. Other forms of saturated functions with the same property can also be found in the literature [97; 143; 201], where treatment functions are dependent on the number of available medical resources. Studying these saturated treatment functions it is observed that if the value of treatment saturation constant parameter exceeds a certain level, then backward bifurcation occurs and the disease persists when the basic reproduction number is less than unity. The saturation parameter also affects the local stability of endemic equilibrium. Upadhyay et al. [183] studied the effect of saturated treatment functions

such as Holling type II and III. They discovered that employing Holling type II treatment is the most effective way to prevent disease spread. Dubey et. al. [58] investigated the impact of saturated treatment function in Holling types III and IV. This thesis investigates the effects of different incidence and treatment rates within the framework of disease transmission dynamics.

1.4 Disease prevention and control

To control the spread of disease, there are several pharmaceutical and non-pharmaceutical control measures such as testing, media awareness, vaccination, social distancing, quarantine, hygiene maintenance or cleanliness, fear effect etc. Effective vaccination and antiviral drugs are the two widely used pharmaceutical interventions that mitigate the disease outbreak. But sometimes the virus mutates, then vaccines become less effective, and most vaccinated people may not acquire protection against new strain of the virus. In that case, antiviral drugs are important in controlling the disease's spread until an effective vaccine is available. The large-scale use of antiviral drugs increases the economic and medical burden. In such situations, non-pharmaceutical interventions can effectively control the disease spread. There are several non-pharmaceutical interventions, such as social distancing, washing hands, wearing face masks, etc. Without an effective vaccine or antiviral drugs, non-pharmaceutical control are only alternative for controlling disease outbreak.

1.4.1 Awareness

Awareness plays a crucial role in educating people about the prevention of infectious diseases and the necessary steps that can be taken to mitigate and control outbreaks. In the case of newly emerging infectious diseases, authorities cannot rely solely on existing vaccines and antiviral drugs, as their efficacy is often uncertain [60]. Therefore, awareness campaigns serve as an essential component of disease control strategies. Such awareness can be disseminated through newspapers, television, and social media platforms, which act as important channels for communicating information about outbreaks [115].

When an infectious disease emerges within a population, the timely dissemination of accurate information is vital to inform people about preventive measures. Media alerts and public health messages guide individuals in reducing their risk of infection. By raising awareness, individuals are encouraged to adopt protective behaviours that

minimize the rate of disease transmission. Awareness programs are particularly valuable for vulnerable populations, as they provide guidance on preventive practices such as regular hand sanitization, the use of face masks and gloves, vaccination, and quarantine measures. The adoption of such practices significantly reduces the impact of illness and helps to control the spread of infection.

Moreover, awareness levels are strongly influenced by educational attainment. Higher education not only enhances the understanding of health-related information but also promotes the adoption of preventive practices. Thus, education plays a critical role in strengthening awareness and enabling individuals to take proactive measures against infectious diseases.

1.4.2 Fear effect

People generally get scared and try to make a significant distance from an infected individual to prevent disease. When the infection increases, it increases the fear level induced by the information about the disease's fatality, which spreads through media. Susceptible individuals try to remain isolated due to fear of contracting the virus, leading to decrease in infection and birth rate. For example, in Hong Knong, during the SARS outbreak, which started in November 2002, peaked on March 2003, and was eliminated on June 2003, the birth rate had fallen from 8742 (in 2002) to 8436 (in 2003) and again increased to 8558 in 2004 [27; 63].

1.4.3 Testing and treatment

Testing is a critical public health strategy that enables authorities to detect and isolate infected individuals from the population, thereby reducing contact with susceptible individuals and minimizing disease transmission. Several infectious diseases, including tuberculosis and HIV/AIDS, underscore the importance of early testing as a life-saving intervention. Although no definitive cure exists for HIV/AIDS, early detection can prolong life expectancy and reduce the overall infection rate within the population. In the case of tuberculosis, timely diagnosis and treatment allow infected individuals to recover fully and lead normal lives. Furthermore, highly transmissible diseases such as influenza and COVID-19 demonstrate the necessity of early testing in combination with appropriate treatment. Such measures not only mitigate the severity of illness but also play a vital role in limiting the spread of infection at the community level.

1.4.4 Vaccination

It is well known that vaccination is an indispensable tool for the control and eradication of infectious diseases. Vaccines strengthen the immune system and protect individuals from life-threatening infections. They lower the risk of contracting diseases, reduce severity, and support the health system in managing outbreaks. Vaccination programs are typically administered to susceptible populations to mitigate disease transmission. Historical evidence demonstrates the success of vaccination in preventing diseases such as smallpox, hepatitis B, diphtheria, measles, polio, cholera, and, more recently, COVID-19. In many cases, a single vaccine dose is insufficient to provide long-term protection, or vaccine-induced immunity diminishes over time; in such instances, booster doses are required to sustain immunity.

During the COVID-19 pandemic, vaccination became the most effective and widely adopted strategy for reducing infection rates, hospitalizations, and deaths worldwide. To further understand the role and effectiveness of vaccination, a comprehensive study has been performed in the review article entitled **"Study on Vaccination strategy employed by the five countries most affected by Covid-19"**. This review highlights how large-scale immunization programs, booster campaigns, and policy decisions shaped the trajectory of the pandemic in the USA, India, Brazil, France, and the UK - the five most affected countries during the first half of 2022.

- **USA:** The United States launched Operation Warp Speed to accelerate vaccine development and delivery. Pfizer, Moderna, and Johnson & Johnson vaccines were domestically produced. Vaccination was carried out in phases: Phase 1a prioritized health care workers and long-term care residents; Phase 1b included frontline essential workers and people aged 75+; Phase 1c covered adults aged 65 - 74 and people with high-risk conditions; and Phase 2 opened vaccination to all adults aged 16+.

- **India:** India relied on indigenous production (Covishield and Covaxin) to vaccinate its large population. The first phase (January 2021) prioritized health care workers (HCWs) and frontline workers (FLWs). Phase II (March 2021) extended to people aged 45+ and those with comorbidities. Phase III (May 2021) expanded coverage to all adults above 18. The Government of India established public vaccination centers (free) and permitted private centers at regulated costs to accelerate nationwide coverage.

- **Brazil:** Brazil adopted a four-phase strategy defined by its Health Ministry. Phase 1 prioritized indigenous groups, health professionals, and people aged 75+. Phase 2 included people aged 60 - 74. Phase 3 focused on individuals with severe health conditions. Phase 4 covered teachers, security forces, and prison staff before opening to the wider population. Vaccine supply constraints, however, slowed progress, as Brazil depended on imports (AstraZeneca, Covax Facility, and J&J).

- **France:** France planned vaccination in five phases. Phase 1 (December 2020-January 2021) targeted nursing home residents and staff over 50. Phase 2 extended to all individuals over 75 and then those aged 65 - 74. Phase 3 (Spring 2021) prioritized adults aged 50 - 64, people with comorbidities, and health professionals in high-risk settings. Phase 4 opened vaccination to adults in essential services and high-exposure occupations. Phase 5 extended to the entire adult population. France's dependence on imported vaccines caused delays in reaching later phases.

- **UK:** The UK followed recommendations from the Joint Committee on Vaccination and Immunisation (JCVI). The first phase prioritized elderly individuals, care home residents, health care staff, and people with high clinical risk. Age-based prioritisation was the main criterion, with vaccination rolled out in descending order of age. Phase 2 (from February 2021) continued with age-based groups until all adults were covered. Occupation-based prioritisation was not formally adopted, which led to criticism, although JCVI defended age as the most effective risk-based criterion. Pfizer-BioNTech and AstraZeneca were the primary vaccines used.

The comparative review makes it clear that while vaccination was universally acknowledged as the most effective preventive tool against COVID-19, the prioritisation strategies varied significantly across countries depending on population structure, vaccine availability, and health infrastructure. A common pattern was the prioritisation of frontline workers and elderly populations, yet differences in the categorization of age groups and occupational risks directly shaped outcomes in terms of transmission control and mortality reduction.

From a broader perspective, this study also highlights the importance of country-specific vaccination policies. Nations with younger populations, like India and Brazil,

faced challenges of vaccinating large cohorts rapidly, while countries with older populations, like France and the UK, emphasized early protection of the elderly to minimize fatalities. Moreover, domestic vaccine production capacity played a decisive role: the USA and India benefited from self-sufficiency, whereas Brazil and France were heavily dependent on external suppliers, slowing their rollouts.

In the context of this thesis, the findings from the review article highlight that vaccination not only reduces disease transmission and mortality but also interacts with demographic and infrastructural factors, thereby serving as a central pillar of disease prevention and control strategies. Building on these insights, the challenges and problem areas identified in the review will be further examined through the development and analysis of mathematical models presented in the subsequent chapters of this thesis.

1.5 Mathematical Preliminaries and Methodology

In this section, some basic definitions and theorems on fractional-order systems are presented, along with mathematical tools from recent literature, that will be of interest to the whole thesis.

Definition 1.5.1 ***Linearization***
For the system (1.3)*, we assume* $f \in C^1(E)$ *and* $\bar{x}$ *is an equilibrium point. Then the linarization of* ${}_0^cD_t^q = f(x), \quad x \in \mathbb{R}^n$ *at the equilibrium* $\bar{x} \in E$ *can be expressed as*

$$ {}_0^cD_t^q X(t) = JX(t), $$

where the Jacobian matrix or variational matrix

$$ J = \begin{pmatrix} \frac{\partial f_1}{\partial x_1} & \frac{\partial f_1}{\partial x_2} & \cdots & \frac{\partial f_1}{\partial x_n} \\ \frac{\partial f_2}{\partial x_1} & \frac{\partial f_2}{\partial x_2} & \cdots & \frac{\partial f_2}{\partial x_n} \\ \vdots & \vdots & \vdots & \vdots \\ \frac{\partial f_n}{\partial x_1} & \frac{\partial f_n}{\partial x_2} & \cdots & \frac{\partial f_n}{\partial x_n} \end{pmatrix}_{x=\bar{x}} $$

is evaluated at $\bar{x} \in E(\subset \mathbb{R}^n)$ *and*

$$X = \begin{pmatrix} x_1 \\ x_2 \\ \vdots \\ x_n \end{pmatrix}.$$

Theorem 1.5.2 *[4]* ***Routh-Hurwitz criteria for fractional order system***
Let $P(\lambda) = 0$ *be a characteristic equation of the jacobian matrix* $J = \frac{\partial f}{\partial x}$, $x \in \mathbb{R}^n$ *of the fractional order system* (1.3)*, where*

$$P(\lambda) = \lambda^n + a_1\lambda^{n-1} + \cdots + a_{n-1}\lambda + a_n \tag{1.5}$$

with real coefficients a_i, $i = 1, 2, \ldots, n$. *The conditions in which all the roots of* (1.5) *will satisfy*

$$|\arg(\lambda_i)| > \frac{q\pi}{2}, \quad i = 1, 2, \ldots, n, \quad 0 < q < 1, \tag{1.6}$$

are generally known as fractional order Routh-Hurwitz conditions. Following are the fractional order Routh-Hurwitz criteria for different $n \in \mathbb{N}$ *for which* (1.6) *is satisfied:*

- $n = 1$*:* $a_1 > 0$.
- $n = 2$*:*
  - *(i)* $D(P) \geq 0$, $a_1 > 0$, $a_2 > 0$.
  - *(ii)* $D(P) < 0$, $a_1 < 0$, *and* $\left|\tan^{-1}\left(\frac{\sqrt{4a_2 - a_1{}^2}}{a_1}\right)\right| > \frac{q\pi}{2}$, *where* $0 < q < 1$.
- $n = 3$*:*
  - *(i)* $D(P) > 0$, $a_1 > 0$, $a_3 > 0$, *and* $a_1a_2 - a_3 > 0$.
  - *(ii)* $D(P) < 0$, $a_1 \geq 0$, $a_2 \geq 0$, $a_3 > 0$, *and* $0 < q < \frac{2}{3}$.
  - *(iii)* $D(P) < 0$, $a_1 > 0$, $a_2 > 0$, $a_1a_2 = a_3$, *and* $0 < q < 1$.

  Where $D(P)$ *is the discriminant for the polynomial* $P(\lambda)$.

Lemma 1.5.3 *[139] Let* $P \neq \phi$ *be a subset of Banach space which is closed, convex and bounded. Let the two functions* T_1, T_2 *be such that*

(i) $T_1w_1 + T_2w_2 \in P$ *whenever* $w_1, w_2 \in P$,

(ii) T_2 *is compact and continuous, and*

(iii) T_1 *is contraction.*

Then operator equations $T_1w + T_2w = w$*, for* $w \in P$*, has at least one solution.*

Lemma 1.5.4 *[82]* ***Generalized LaSalle's Invariance Principle***
Suppose $A \subset \mathbb{R}^n$ *is a bounded closed set. Every solution of* (1.3) *starts from A and remains in A for all time if there exists a Lyapunov function* $V(x) : A \to \mathbb{R}^n$ *with continuous first order partial derivatives satisfying the following condition:*

$$ {}_0^cD_t^qV \leq 0, \qquad \forall q \in (0,1]. \tag{1.7}$$

Let $Z = \{x \in A \mid {}_0^cD_t^qV = 0\}$ *be the set and L is the largest invariant subset of Z. Then every solution* $x(t) \in \mathbb{R}^n$ *originating in A tends to L as* $t \to \infty$ *and eventually becomes globally stable in A. Particularly, when* $L = \{0\}$*, then* $x \to 0$ *as* $t \to \infty$*.*

Definition 1.5.5 *[168]* ***Bifurcation***
The qualitative behavior of a dynamical system changes suddenly when parameter values change. This phenomenon is known as bifurcation. Bifurcation may alter equilibrium points, stability, or periodic orbits. The parameter values at which bifurcations occur are called bifurcation points. Here, different types of bifurcations are discussed.

Saddle-node bifurcation
This basic mechanism is responsible for the creation or destruction of equilibrium points for any dynamical system. In this bifurcation, two equilibrium points, out of which one is a saddle point, and another is a stable node, collide at the bifurcating point and annihilate each other.

Transcritical bifurcation
In this bifurcation, two equilibria of the system collide and interchange their stability. In this scenario, one equilibrium point becomes stable from unstable, and another one becomes unstable from stable, as the parameter passes through its critical value. However, in this case, no equilibrium point is created or vanished.

Hopf bifurcation
In this bifurcation, an equilibrium point losses its stability, and a limit cycle is created at the critical value of the bifurcation parameter. In this case, a pair of purely

imaginary eigenvalues crosses the imaginary axis from left to right half-plane. As a result, a limit cycle exists in the system. There are mainly two types of Hopf bifurcation depending on the nature of the limit cycle. When the limit cycle is orbitally stable, it is called Supercritical Hopf bifurcation, and if the limit cycle is orbitally unstable, then it is called Subcritical Hopf bifurcation.

Definition 1.5.6 *[130]* ***Basic reproduction number***

A major concern regarding any infectious disease is its potential to spread within a population. The basic reproduction number, often denoted as $\mathscr{R}_0$ is a key concept in epidemiology which is used to describe this potential of a certain disease would spread in a population or not. In the context of compartmental models of disease transmission, it represents the expected number of secondary infections produced by a typical infected individual in a completely susceptible population. The next generation matrix, introduced by Diekmann and Heesterbeek in 1990 [48], technique is commonly used to calculate the basic reproduction number. It is defined as the largest absolute value of eigenvalue in the spectrum of next generation matrix.

There are several techniques in the literature to derive the next-generation matrix from compartmental models. The working rule of the most popular approach [56] is given below.

Let $X \in \mathbb{R}^n$ and $Y \in \mathbb{R}^m$ be the n and m dimensional infected and non-infected population compartments respectively. Consider the following fractional order system

$$D^q(X_j) = \mathscr{F}_j(X,Y) - \mathscr{V}_j(X,Y), \quad j = 1,\ldots,n,$$

and

$$D^q(Y_k) = \mathscr{H}_k(X,Y), \quad k = 1,\ldots,m,$$

where $\mathscr{F}_j$ represents the rate of appearance of new infections in compartment j and $\mathscr{V}_j$ denotes the transmission rate of individuals from compartment j because of death or immunization. This method is based on linearization of the system at disease free equilibrium $(0,Y_0)$ and the functions satisfy the following assumptions:

(A1) If $X_j \geq 0$, then $\mathscr{F}_j \geq 0$ and $\mathscr{V}_j \geq 0$, for all $j = 1,\ldots,n$, suggesting all transmission rates are non-negative.

(A2) If $X_j = 0$, then $\mathscr{V}_j(X,Y) = 0$. It means that no transfer of individuals from an empty compartment.

(A3) *For $X_j = 0$, $\mathscr{F}_j(X,Y) = 0$. Suggests that new infections are not possible for uninfected compartment.*

(A4) *If $X \in Y$, then $\mathscr{F}_j(X,Y) = \mathscr{V}_j(X,Y) = 0$, for all $j = 1,\ldots,n$. Indicates a population is infection free invariant. That means, there is no entry of infected people.*

(A5) *The infection free system*

$$D^q(Y) = \mathscr{H}(0,Y),$$

has unique fixed point or equilibrium point which is asymptotically stable.

If the above assumptions $(A1-A5)$ are satisfied by $\mathscr{F}_j(X,Y)$ and $\mathscr{V}_j(X,Y)$, then it is possible to construct the $n \times n$ matrices $F = [\mathscr{F}_{jk}]$ and $V = [\mathscr{V}_{jk}]$ at disease free equilibrium as follows:

$$F = \left[\frac{\partial \mathscr{F}_j}{\partial X_k}(0,Y_0)\right] \quad \text{and} \quad V = \left[\frac{\partial \mathscr{V}_j}{\partial X_k}(0,Y_0)\right].$$

In addition, F is non-negative and V is invertible. Thus, the basic reproduction number is given by spectral radius of matrix FV^{-1}.

Definition 1.5.7 *[158]* ***Sensitivity analysis***

Sensitivity analysis is a useful tool for assessing the influence of model parameters on disease transmission and prevalence. It quantifies the variation of state variables in response to changes in biological parameters. Since disease spread is closely linked to the basic reproduction number, $\mathscr{R}_0$, it is crucial to identify the parameters that most strongly affect it. By evaluating the variation of $\mathscr{R}_0$ with respect to different model parameters, the normalized forward sensitivity index can be computed, thereby identifying the parameters that play the most significant role in controlling disease transmission.

The normalized forward sensitivity index of a variable z, which depends on a parameter x, is defined as

$$W_x^z = \frac{\partial z}{\partial x} \times \frac{x}{z}.$$

So, for $\mathscr{R}_0$, the sensitivity index is $W_x^{\mathscr{R}_0} = \dfrac{\partial \mathscr{R}_0}{\partial x} \times \dfrac{x}{\mathscr{R}_0}$, which shows how sensitive $\mathscr{R}_0$ to the parameter x.

Definition 1.5.8 *[25]* ***Ulam-Hyers stability***

The global stability of the fractional-order model is analyzed within the framework of

the Ulam-Hyers stability criteria, following the approach in [83; 179]. To this end, the following inequality is introduced:

$$\left|D_t^q M(t) - f(t, M(t))\right| \leq \varepsilon, \quad t \in [0, t_0]. \tag{1.8}$$

A function M^o satisfies (1.8)*, if there exists $\chi \in \Omega$ such that:*

- $|\chi(t)| \leq \varepsilon$
- $D_t^q M^o(t) = f(t, M^o(t)) + \chi(t); \;\; t \in [0, t_0]$.

A fractional order system is Ulam-Hyers stable if $\exists$ a real number $\phi > 0$ such that for given $\varepsilon > 0$ and for any solution $M^o(t)$ of equation (1.8)*, there exists a unique solution $M(t)$ of corresponding model with*

$$\|M(t) - M^o(t)\| \leq \varepsilon\phi; \;\; t \in [0, t_0].$$

Consider the inequality,

$$\left|D_t^q M(t) - f(t, M(t))\right| \leq \varepsilon\theta(t), \;\; \text{for some} \;\; \theta(t) \in C([0, t_0]; \mathbb{R}^+). \tag{1.9}$$

A function M^o satisfies equation (1.9) iff there exists a function $\nu(t) \in \Omega$ such that

- $|\nu(t)| \leq \varepsilon\theta(t)$
- $D_t^q M^o(t) = f(t, M^o(t)) + \nu(t); \;\; t \in [0, t_0]$.

Definition 1.5.9 *[25] The fractional order model is generalized Ulam-Hyers stable with respect to function $\theta(t)$ if there exists real number $\phi > 0$ such that for given $\varepsilon > 0$ and for any solution $M^o(t)$ of equation* (1.9)*, there exists a unique solution $M(t)$ of model equation with*

$$\|M(t) - M^o(t)\| \leq \varepsilon\phi\theta(t); \;\; t \in [0, t_0].$$

1.6 Fractional order optimal control

The applications of Fractional ordered optimal control problem (FOCP) have grown in recent decades. Agrawal [2] explored fractional-order variational problems of the Riemann-Liouville type in 2002 and developed a framework for studying fractional optimal control problems (FOCP) and suggests a numerical method to solve FOCP using Lagrange multiplier technique. Building on this framework, Ding studied the

FOCP of the Caputo HIV model in 2012 and presented related numerical techniques [55]. Pontryagin's principle is one of the most useful approaches to solve optimal control problem. There are several works where these methods are employed in Fractional ordered optimal control problems [62; 169].

Here a brief review of the mathematical formulation of Caputo fractional optimal control model.

Let $u = [u_1(t), u_2(t), \ldots, u_m(t)] \in \mathscr{U} \subset \mathbb{R}^m$ be the time-dependent control variables and U be the set of admissible controls of the dynamical system

$$ {}^cD_t^q x(t) = f(x(t), u(t)), \quad x(0) = x_0, $$

where ${}^cD_t^q$ denotes the Caputo fractional derivative of order $0 < q < 1$.

The control $u \in \mathscr{U}$ must be chosen for all $t \in [0, T_f]$ to minimize the objective functional $\mathscr{J}$, where T_f is the final time, which is defined by

$$ \mathscr{J}[u] = \Theta(x(T_f)) + \int_0^{T_f} \mathscr{F}(x(t), u(t))\, dt, $$

where $\Theta(x(T))$ is the terminal cost and $\mathscr{F}(x(t), u(t))$ is the running cost.

Step 1. Hamiltonian construction.

Introduce the adjoint (co-state) vector $\lambda(t)$ and define the Hamiltonian as

$$ \mathscr{H}(x(t), u(t), \lambda(t)) = \lambda^T(t) f(x(t), u(t)) + \mathscr{F}(x(t), u(t)), $$

where λ^T stands for transpose of λ.

Step 2. Necessary conditions (Fractional Pontryagin's Principle).

The following conditions must be satisfied for the optimal state trajectory $x^*(t)$, optimal control $u^*(t)$, and adjoint λ^*:

1. $\mathscr{H}(x^*(t), u(t), \lambda(t)) \leq \mathscr{H}(x^*(t), u^*(t), \lambda(t))$
2. $\left.\frac{\partial \Theta(x)}{\partial T_f}\right|_{x=x(T_f)} + \mathscr{H}(T_f) = 0$
3. ${}^cD_t^q \lambda^T(t) = \left.\frac{\partial \mathscr{H}}{\partial x}\right|_{x=x^*}$ with transversality conditions $\lambda(T_f) = 0$.
4. $\left.\frac{\partial \mathscr{H}}{\partial u}\right|_{u=u^*} = 0 \quad \text{and} \quad \left.\frac{\partial^2 \mathscr{H}}{\partial u^2}\right|_{u=u^*} \leq 0$

These four conditions are the necessary conditions for optimal control.

1.7 Chapter-wise Overview of the Thesis

The thesis consists of seven chapters, including a concluding chapter on future scope, followed by a bibliography. The organization of the thesis is as follows:

Chapter 1 presents an introduction and background literature relevant to the title of the thesis. It provides a comprehensive overview of a fractional-order mathematical model for analyzing the dynamics of infectious diseases, along with the fundamental terminologies and key concepts associated with the study. The preliminary section of this chapter includes essential definitions, theorems, and lemmas that form the foundation for the subsequent work. In addition, the chapter offers a concise outline of the overall structure of the thesis, summarizing the content of the following chapters. Disease prevention and control measures, with particular emphasis on vaccination, are also discussed.

The work reported in this chapter has been communicated in a research paper entitled **"Study on Vaccination Strategy Employed by the Five Countries Most Affected by Covid-19"**, which has been submitted for publication.

Chapter 2 focuses on the formulation and analysis of a fractional-order SIS compartmental model that incorporates the influence of fear on disease dynamics. The presence of fear induces behavioural changes such as reduced social interactions and adoption of preventive measures, which significantly affect the transmission process. To capture these effects, the model employs a Beddington-De Angelis type incidence rate, which provides a realistic representation of interactions between susceptible and infected individuals, as it accounts for inhibition measures adopted by both groups. The chapter establishes fundamental mathematical properties of the system, derives the basic reproduction number $\mathscr{R}_0$, and examines the existence and stability of both disease-free and endemic equilibria. Furthermore, numerical simulations are presented to validate and illustrate the analytical results.

The work reported in this chapter has been communicated in the paper entitled **"A Study of Fractional Order SIS Model with Fear Effect and Beddington-De**

Angelis Incidence Rate" for publication.

Chapter 3 deals with the formulation and analysis of a fractional-order *SVIR* model that incorporates different vaccination strategies. The model distinguishes between partially and fully vaccinated individuals, thereby providing a more realistic framework for studying the role of vaccination in disease dynamics. To reflect constraints such as limited medical resources and the possibility of disease reemergence, a Holling type-III saturated treatment function is included. The chapter establishes well-posedness of the system and examines the stability of both the disease-free and endemic equilibria. Local stability is analyzed using the linearization method and the Routh-Hurwitz criterion, while global stability is investigated through suitable Lyapunov functions. In addition, numerical simulations are performed to validate the analytical results. The quantification of vaccination effects demonstrates that full vaccination leads to a higher proportion of recovered individuals compared to partial vaccination, underscoring the importance of effective full vaccination strategies in public health planning.

The work reported in this chapter has been published as **"Stability Analysis and Quantification of Effects of Partial and Full Vaccination Using Fractional Order** *SVIR* **Model"**, in *Mathematical Medicine and Biology: A Journal of the IMA*, (SCIE Indexed), Impact Factor: 1.5, Oxford University Press (2025).

Chapter 4 presents a fractional-order *SEIQR* model that incorporates quarantine measures and behavioural responses during an epidemic outbreak. To capture psychological effects in disease transmission, the Monod-Haldane incidence rate is adopted, while a Holling type-III saturated quarantine function is employed to reflect the limitations of quarantine facilities arising from the unavailability of a sufficient number of quarantine places. The system is formulated using Caputo fractional derivatives, allowing the inclusion of memory effects in epidemic dynamics. The chapter establishes the well-posedness of the model, ensuring nonnegativity and boundedness of solutions, and identifies two possible equilibria: the disease-free and endemic states. Stability analysis is carried out for both equilibria, where local stability is studied using the linearization method and the Routh-Hurwitz criterion, while global stability is investigated with the help of Lyapunov functions

for fractional-order systems. The thresholds governing these stability behaviours, including the basic reproduction number $\mathscr{R}_0$ and its alternative $\mathscr{T}_0$, are derived using the Next-Generation Matrix method. In addition, a fractional optimal control problem is formulated using Pontryagin's maximum principle to minimize disease spread while balancing control costs, introducing a time-dependent control function representing behavioural interventions. Numerical simulations using the Adams-Bashforth-Moulton scheme are provided to illustrate and validate the analytical results.

The work reported in this chapter has been published as **"Optimal Control of a Fractional Order *SEIQR* Epidemic Model with Non-monotonic Incidence and Quarantine Class"**, in *Computers in Biology and Medicine* (SCIE Indexed, Impact Factor: 6.3), Elsevier (2024).

Chapter 5 introduces a fractional-order *SPIR* model to study the impact of environmental pollution on disease dynamics. The model developed in this chapter accounts for the role of long-term exposure to polluted environments, which increases susceptibility to infection, and incorporates prenatal exposure effects through a Monod-Haldane incidence rate to capture psychological influences during transmission. The system is formulated using Caputo fractional derivatives, and its well-posedness is established by proving existence, uniqueness, positivity, and boundedness of solutions. The chapter investigates the disease-free and endemic equilibria, with stability analyzed using the basic reproduction number $\mathscr{R}_0$, derived via the Next-Generation Matrix method. Local stability is examined using the linearization method and the Routh-Hurwitz criterion, while global stability is studied with Lyapunov functions. The model also reveals the occurrence of a forward transcritical bifurcation at $\mathscr{R}_0 = 1$. Furthermore, a fractional optimal control problem is developed using Pontryagin's maximum principle, introducing two non-pharmaceutical, time-dependent control measures. Numerical simulations, carried out using the Adams-Bashforth-Moulton scheme, support the theoretical findings and show that the simultaneous implementation of both controls is most effective in flattening the epidemic curve within a short time frame.

The work reported in this chapter has been communicated in the paper entitled **"Mathematical Modeling and Qualitative Analysis of a Fractional-Order *SPIR***

Epidemic Model with Non-monotonic Incidences and Optimal Control" for publication.

Chapter 6 develops a fractional-order *SIR* model to investigate the impact of household waste on the spread of infectious diseases. The model incorporates two bacterial populations, namely bacteria present in the environment (B_e) and bacteria within organisms (B_o), to capture the dual role of pathogens in transmission. The system is formulated using Caputo fractional derivatives, and its well-posedness is established by proving existence and uniqueness through the Banach contraction principle and Schaefer's fixed point theorem. The basic reproduction number $\mathscr{R}_0$ is derived, and a sensitivity analysis is carried out to identify the most influential parameters affecting disease dynamics. Stability is further studied in the sense of Ulam-Hyers criteria. In addition, an optimal control problem is formulated to minimize the disease burden and associated costs, introducing three time-dependent controls that target transmission reduction. The existence and characterization of these controls are derived using Pontryagin's maximum principle. Numerical simulations, performed with the Adams-Bashforth-Moulton method, illustrate the effectiveness of the proposed strategies and highlight cost-effective approaches to mitigating health risks associated with household waste.

The work reported in this chapter has been communicated in the paper entitled **"Analysis of a Fractional Order *SIR* Model for Infectious Diseases Spread by Household Waste with Optimal Control Strategies"** for publication.

Chapter 7 presents a comprehensive summary of the work along with an outline of the future scope and social impact of the research. The thesis concludes with a bibliography and a list of the author's publications.

Chapter 2

A study of Fractional order SIS model with fear effect and Beddington-De Angelis incidence rate

---

Many studies have demonstrated that, during epidemics, fear can significantly influence human behavior, often leading to a decline in birth rates. This chapter presents a fractional-order SIS compartmental model that incorporates the effects of fear and employs a Beddington-De Angelis type incidence rate. This incidence function captures the impact of preventive measures taken by both susceptible and infected individuals, thereby providing a more realistic representation of disease transmission dynamics. Following the model formulation, fundamental properties such as positivity and boundedness of solutions are established. The basic reproduction number, $\mathscr{R}_0$, is then computed, and the existence of an endemic equilibrium for $\mathscr{R}_0 > 1$ is demonstrated. Furthermore, the local stability of both the disease-free and endemic equilibria is analyzed using the linearized system. Numerical simulations, conducted via the Adams-Bashforth-Moulton Predictor-Corrector method, are provided to support the analytical results.

2.1 Introduction

Infectious diseases continue to pose a significant threat to public health and human lifestyles. Illnesses such as chickenpox, measles, cholera, tuberculosis, and influenza

have far-reaching societal impacts due to their ability to spread rapidly through direct contact or intermediary carriers. Because of this high transmissibility, outbreaks can escalate into regional or even global epidemics in a short period. Consequently, researchers from diverse disciplines are increasingly involved in understanding the transmission dynamics of infectious diseases and developing strategies for their control.

Public awareness and behavioural responses to infectious disease outbreaks have also intensified in recent times. The fear of infection often drives individuals to limit social interactions, thereby influencing the spread of the disease. Such fear-induced behaviour can result in self-isolation, reduced fertility rates, and changes in survival outcomes. Furthermore, studies in pathology suggest that psychological stress, including fear, can impair immune function, particularly the body's capacity to produce antibodies. Media coverage plays a pivotal role in amplifying this fear, as evidenced during the SARS outbreak (November 2002 to June 2003), which coincided with a noticeable drop in Hong Kong's birth rate- from 8,742 births in 2002 to 8,436 in 2003 [22; 27; 63].

Based on these observations, a fractional-order *SIS* (Susceptible-Infected-Susceptible) epidemic model is proposed, in which individuals who recover from the infection can become susceptible again. The model incorporates fear-driven behavioral changes that affect both susceptible and infected individuals. To more accurately represent contact dynamics under such behavioral responses, a Beddington-De Angelis type incidence function is employed, accounting for mutual interference and saturation effects during disease transmission.

The chapter is organized as follows: Section 2.2 presents the assumptions and mathematical formulation of the model. Sections 2.3 and 2.4 analyze the non-negativity and boundedness of solutions, derive the basic reproduction number, and examine the existence of equilibria. Section 2.5 investigates the local stability of the equilibrium points using linearization. Numerical simulations validating the theoretical results are provided in Section 2.6. Finally, Section 2.7 concludes the chapter with a summary and potential directions for future research.

2.2 Formulation of fractional order epidemic model

This section develops a fractional-order *SIS* (Susceptible-Infected-Susceptible) epidemic model based on the Caputo derivative framework, incorporating both treatment interventions and fear-driven behavioral changes. The total population is divided into

two distinct and time-dependent compartments: the susceptible class, $S(t)$, consisting of individuals vulnerable to infection, and the infected class, $I(t)$, which includes individuals currently carrying and capable of transmitting the disease. The dynamics of the epidemic are described using the following system of nonlinear fractional differential equations:

$$\begin{aligned} {}_0D_t^{\alpha} S(t) &= \frac{\Lambda}{1+\delta I} - \frac{\beta SI}{1+\rho S+\gamma I} + (\psi+u)I - \mu S, \\ {}_0D_t^{\alpha} I(t) &= \frac{\beta SI}{1+\rho S+\gamma I} - (\psi+u)I - (\mu+d)I, \end{aligned} \tag{2.1}$$

subject to the conditions

$$S(0) = S_0 \geq 0, I(0) = I_0 \geq 0, \tag{2.2}$$

and the different model parameters are defined in Table 2.1.

Table 2.1: Parameters of the model *SIS*.

Parameter	**Description**
Λ	Birth rate of susceptible population
β	Disease transmission rate
δ	Level of fear
ρ	Preventive measures taken by susceptibles
γ	Preventive measures taken by infectives
μ	Natural death rate
ψ	Natural recovery rate
u	Recovery rate due to treatment
d	Disease induced death rate

2.3 Non-negativity and Boundedness

To ensure biological relevance, the solutions of system (2.1) must remain non-negative and bounded over time. In this context, the feasible region is defined as $\Omega^+ = (S,I) \in \Omega : S,I \in \mathbb{R}^+$, where $\mathbb{R}^+$ denotes the set of non-negative real numbers. This ensures that population variables retain meaningful interpretations within a biological framework.

Theorem 2.3.1 *Every solution of the system* (2.1) *remain non-negative and uniformly bounded starting in* Ω^+.

Proof 2.3.2 *Let the initial solution of the system be* $\Gamma_{t_0} = (S_{t_0}, I_{t_0}) \in \Omega^+$. *It then follows from system* (2.1) *that,*

$$D^\alpha S|_{S_{t_0}=0} = \frac{\Lambda}{1+\delta I} + (\psi + u)I > 0,$$
$$D^\alpha I|_{I_{t_0}=0} = 0.$$

Using Lemma 1.1.13, we have $S(t), I(t) \geq 0$ *for any* $t \geq t_0$. *Therefore, the solution of the system* (2.1) *will remain in* Ω^+.

Again, consider the function $N(t) = S(t) + I(t)$, *then*

$$D^\alpha N = D^\alpha S + D^\alpha I$$
$$\leq \Lambda - \mu N - dI$$
$$i.e.\ D^\alpha N + \mu N \leq \Lambda \quad as\ I > 0.$$

So, $N(t) \leq \left(N(t_0) - \frac{\Lambda}{\mu}\right) E_\alpha[-\mu(t-t_0)] + \frac{\Lambda}{\mu} \to \frac{\Lambda}{\mu}$ *as* $t \to \infty$.

Therefore, solutions of the system (2.1) *starting in the region* Ω^+ *are always lying in the region* $\left\{(S,I) \in \Omega : 0 \leq S + I \leq \frac{\Lambda}{\mu}\right\}$.

2.4 Basic Reproduction Number and Equilibria

It is straightforward to observe that the system (2.1) admits a disease-free equilibrium (DFE) given by $E_0 = E_0\left(\frac{\Lambda}{\mu}, 0\right)$, where the entire population is susceptible and no infection is present. Our next objective is to determine the basic reproduction number, denoted by $\mathscr{R}_0$, which quantifies the expected number of secondary infections generated by a single infectious individual introduced into a fully susceptible population. The value of $\mathscr{R}_0$ is a crucial threshold parameter for assessing the potential for disease spread or elimination. We compute $\mathscr{R}_0$ using the next-generation matrix approach as outlined in [47]. To proceed, it is assumed that

$$D_t^\rho X = \mathscr{F}(X) - \mathscr{V}(X),$$

where $X = (I)^T$ and $\mathscr{F}(X)$ be the matrix of new infection term, $\mathscr{V}(X)$ be the matrix of outgoing terms. The Jacobian matrices F and V of $\mathscr{F}(X)$ and $\mathscr{V}(X)$, respectively, are given as:

$$F = \left[\frac{\beta S(1+\rho S)}{(1+\rho S+\gamma I)^2}\right],$$

$$V = [\psi + u + \mu + d].$$

The next generation matrix, at infection-free equilibrium E_0 is,

$$FV^{-1} = \left[\frac{\beta\Lambda}{(\mu+\rho\Lambda)(\psi+u+\mu+d)}\right].$$

Thus,

$$\mathscr{R}_0 = \frac{\beta\Lambda}{(\mu+\rho\Lambda)(\psi+u+\mu+d)}.$$

In addition, it will be shown that the model (2.1) admits an endemic equilibrium when $\mathscr{R}_0 > 1$. Let $E_1 = E_1(S_*, I_*)$ denote an endemic equilibrium such that $S_* > 0$, $I_* > 0$ and

$$\begin{cases} \frac{\Lambda}{1+\delta I_*} - \frac{\beta S_* I_*}{1+\rho S_*+\gamma I_*} + (\psi+u) I_* - \mu S_* = 0, \\ \frac{\beta S_* I_*}{1+\rho S_*+\gamma I_*} - (\psi+u) I_* - (\mu+d) I_* = 0, \end{cases} \tag{2.3}$$

It follows that,

$$S_* = \frac{(\psi+u+\mu+d)(1+\gamma I_*)}{\beta - (\psi+u+\mu+d)\rho}$$

and I_* can be obtained by solving the following equation:

$$A_2 {I_*}^2 + A_1 I_* + A_0 = 0, \tag{2.4}$$

where,

$$\begin{aligned} A_2 &= \delta\left(d^2\rho + d(-\beta-\gamma\mu+\rho(2\mu+u+\psi)) - \mu(\beta+(\gamma-\rho)(\mu+u+\psi))\right), \\ A_1 &= d^2\rho - d(\beta+\gamma\mu+\delta\mu-2\mu\rho-\rho\psi-\rho u) - \mu(\beta+(\gamma+\delta-\rho)(\mu+u+\psi)), \\ A_0 &= (\mathscr{R}_0 - 1)(\Lambda\rho+\mu)(d+\mu+u+\psi). \end{aligned} \tag{2.5}$$

Thus, it can be observed that, A_2 and A_1 can be positive or negative but $A_0 > 0$ for $\mathscr{R}_0 > 1$. So, according to Descarte's rule of sign, the polynomial (2.4) will have at least one positive root I_* for $\mathscr{R}_0 > 1$. The present study focuses on the existence of a unique positive equilibrium point. Consider $\mathscr{R}_0 > 1$, then the combinations of signs of coefficients A_1 and A_2 that allow the existence of a unique positive root for the polynomial (2.4) are as follows:

(i) $A_2 < 0$ and $A_1 < 0$,

(ii) $A_2 < 0$ and $A_1 > 0$.

Once the value of I_* is determined, the unique positive endemic equilibrium point can be obtained as $E_1 = E_1(S_*, I_*)$.

2.5 Stability Analysis

This section presents the stability analysis of the equilibrium points of the system. Local stability determines whether small perturbations around an equilibrium point will return to the equilibrium (stable) or move away from it (unstable). Let us assume the subsequent coordinate transform $S(t) = S_*(t) + s(t); I(t) = I_*(t) + i(t)$, where $(S_*(t), I_*(t))$ denotes the equilibrium point of the model. The linearised system at any steady state is given by

$$\begin{cases} {}_0D_t^{\alpha} S(t) = -\left(\frac{\beta I_*(1+\gamma I_*)}{(1+\rho S_* + \gamma I_*)^2} + \mu\right) S - \left(\frac{\delta\Lambda}{(1+\delta I_*)^2} + \frac{\beta S_*(1+\rho S_*)}{(1+\rho S_* + \gamma I_*)^2} - (\psi + u)\right) I, \\ {}_0D_t^{\alpha} I(t) = \left(\frac{\beta I_*(1+\gamma I_*)}{(1+\rho S_* + \gamma I_*)^2}\right) S + \left(\frac{\beta S_*(1+\rho S_*)}{(1+\rho S_* + \gamma I_*)^2} - (\psi + u + \mu + d)\right) I. \end{cases} \tag{2.6}$$

Applying the Laplace transform on both side of equation (2.6), the reduced system can be written in the following matrix form:

$$\bigtriangledown(s) \begin{pmatrix} \mathscr{L}\{S(t)\} \\ \mathscr{L}\{I(t)\} \end{pmatrix} = \begin{pmatrix} \nu_1(s) \\ \nu_2(s) \end{pmatrix},$$

where,

$$\nu_1(s) = s^{\alpha-1} S(0),\ \nu_2(s) = s^{\alpha-1} I(0),$$

and

$$\bigtriangledown(s) = \begin{pmatrix} s^{\alpha} + \frac{\beta I_*(1+\gamma I_*)}{(1+\rho S_* + \gamma I_*)^2} + \mu & \frac{\delta\Lambda}{(1+\delta I_*)^2} + \frac{\beta S_*(1+\rho S_*)}{(1+\rho S_* + \gamma I_*)^2} - (\psi + u) \\ -\frac{\beta I_*(1+\gamma I_*)}{(1+\rho S_* + \gamma I_*)^2} & s^{\alpha} - \left(\frac{\beta S_*(1+\rho S_*)}{(1+\rho S_* + \gamma I_*)^2} - (\psi + u + \mu + d)\right) \end{pmatrix}. \tag{2.7}$$

In this case, the characteristic polynomial of system (2.1) is $\det(\bigtriangledown(s))$, and the characteristic matrix is $\bigtriangledown(s)$. The distribution of eigenvalues of the characteristic polynomial $\det(\bigtriangledown(s))$ provides a means to analyze the local stability of the system (2.1).

2.5.1 Local stability of disease-free equilibrium

This subsection establishes the local stability of the disease-free equilibrium (DFE) point, $E_0 = E_0\left(\frac{\Lambda}{\mu}, 0\right)$, for which the characteristic matrix at the DFE is given by:

$$\bigtriangledown(s) = \begin{pmatrix} s^{\alpha} + \mu & \delta\Lambda + \frac{\beta\Lambda}{\mu + \rho\Lambda} - (\psi + u) \\ 0 & s^{\alpha} - \left(\frac{\beta\Lambda}{\mu + \rho\Lambda} - (\psi + u + \mu + d)\right) \end{pmatrix}, \tag{2.8}$$

or

$$\bigtriangledown(s) = \begin{pmatrix} s^{\alpha}+\mu & \delta\Lambda + \dfrac{\beta\Lambda}{\mu+\rho\Lambda} - (\psi+u) \\ 0 & s^{\alpha} - (\psi+u+\mu+d)\big(\mathscr{R}_0 - 1\big) \end{pmatrix}. \tag{2.9}$$

Since stability is determined by the eigenvalues of the characteristic matrix (2.9), we obtain two eigenvalues: $\omega_1 = -\mu$ and $\omega_2 = (\psi+u+\mu+d)\big(\mathscr{R}_0 - 1\big)$. The disease-free equilibrium is locally asymptotically stable if all eigenvalues are negative. In particular, the second eigenvalue ω_2 is negative when $\mathscr{R}_0 < 1$, indicating local stability, and becomes positive when $\mathscr{R}_0 > 1$, leading to instability. Thus, the following theorem holds.

Theorem 2.5.1 *The disease-free equilibrium E_0 is locally asymptotically stable if and only if the threshold value $\mathscr{R}_0$ is less than one, otherwise unstable.*

2.5.1.a Local stability of endemic equilibrium

This subsection examines the local stability of the endemic equilibrium, $E_1 = E_1(S_*, I_*)$. The characteristic matrix $\bigtriangledown(s)$ corresponding to equation (2.7) at E_1 is given by:

$$\bigtriangledown(s) = \begin{pmatrix} s^{\alpha} + \dfrac{\beta I_*(1+\gamma I_*)}{(1+\rho S_* + \gamma I_*)^2} + \mu & \dfrac{\delta\Lambda}{(1+\delta I_*)^2} + \dfrac{\beta S_*(1+\rho S_*)}{(1+\rho S_* + \gamma I_*)^2} - (\psi+u) \\ -\dfrac{\beta I_*(1+\gamma I_*)}{(1+\rho S_* + \gamma I_*)^2} & s^{\alpha} - \left(\dfrac{\beta S_*(1+\rho S_*)}{(1+\rho S_* + \gamma I_*)^2} - (\psi+u+\mu+d)\right) \end{pmatrix}. \tag{2.10}$$

Let $s^{\alpha} = \lambda$, then the characteristic equation corresponding to characteristic matrix (2.10) is:

$$\begin{aligned} &\frac{I_*^2\beta\gamma\delta\Lambda}{(I_*\delta+1)^2(I_*\gamma+\rho S_*+1)^2} + \frac{I_*^2\beta\gamma\lambda}{(I_*\gamma+\rho S_*+1)^2} + d\left(\frac{I_*\beta(I_*\gamma+1)}{(I_*\gamma+\rho S_*+1)^2} + \lambda + \mu\right) - \\ &\frac{\beta\lambda\rho S_*^2}{(I_*\gamma+\rho S_*+1)^2} - \frac{\beta\mu\rho S_*^2}{(I_*\gamma+\rho S_*+1)^2} + \frac{I_*\beta\delta\Lambda}{(I_*\delta+1)^2(I_*\gamma+\rho S_*+1)^2} + \frac{I_*\beta\lambda}{(I_*\gamma+\rho S_*+1)^2} \\ &- \frac{\beta\lambda S_*}{(I_*\gamma+\rho S_*+1)^2} - \frac{\beta\mu S_*}{(I_*\gamma+\rho S_*+1)^2} + u\left(\frac{I_*\beta(I_*\gamma+1)}{(I_*\gamma+\rho S_*+1)^2} + \lambda + \mu\right) \\ &+ \lambda^2 + \psi(\lambda+\mu) + 2\lambda\mu + \mu^2 = 0 \end{aligned}$$

which can be simplified into the following polynomial form:

$$\lambda^2 - 2A_1\lambda + A_0 = 0, \tag{2.11}$$

where

$$A_1 = \frac{\beta(S_*(\rho S_*+1)-I_*(I_*\gamma+1))}{2(I_*\gamma+\rho S_*+1)^2} - \frac{(d+2\mu+u+\psi)}{2},$$
$$A_0 = \frac{\beta\left(I_*^2\gamma(d+u)+I_*(d+u)-\mu S_*(\rho S_*+1)\right)}{(I_*\gamma+\rho S_*+1)^2} + \frac{I_*\beta\delta\Lambda(I_*\gamma+1)}{(I_*\delta+1)^2(I_*\gamma+\rho S_*+1)^2} + \mu(d+\mu+u+\psi).$$

The eigenvalues are

$$\lambda_{1,2} = A_1 \pm \sqrt{{A_1}^2 - A_0}.$$

The different values of λ_1 and λ_2 are depending on the coefficients A_1 and A_0. Thus, the possibilities arises for which the eigenvalues will be negative and endemic equilibrium will be locally stable, according to Lemma 1.2.5, are given in the following theorem:

Theorem 2.5.2 *Consider the endemic equilibrium point $E_1 = (S_*, I_*)$ of the system. The local asymptotic stability of E_1 depends on the characteristic equation coefficients A_0 and A_1, and it is determined by the following conditions:*

(i) If $A_1 < 0$ and $A_1^2 \geq A_0$, then the equilibrium E_1 is locally asymptotically stable.

(ii) If $A_1 \geq 0$ and $A_1^2 \geq A_0$, then the equilibrium E_1 is unstable.

(iii) If $A_1 > 0$ and $A_1^2 < A_0$, then the equilibrium E_1 is locally asymptotically stable.

(iv) If $A_1 < 0$ and $A_1^2 < A_0$, then the equilibrium E_1 is locally asymptotically stable.

(v) If $A_1 = 0$ and $A_1^2 < A_0$, then the equilibrium E_1 is locally asymptotically stable.

2.6 Numerical Simulation and Discussion

In this section, numerical simulations are carried out using MATLAB 2012b to validate the theoretical results, employing the set of parameter values listed in Table 2.2. The simulations utilize the fractional Adams-Bashforth-Moulton method, as described in [52], to solve the system of equations. For the initial conditions, the susceptible and infected populations are taken as $S(0) = 73$ and $I(0) = 1$, respectively. Based on the parameter values provided in Table 2.2, the coefficients of the polynomial equation (2.4) are computed as follows:

$$A_2 = -2.0172 \times 10^{-6}, \quad A_1 = -0.000377, \quad A_0 = 0.00418.$$

Table 2.2: Parameter values for simulation.

Parameter	Values
Λ	3
β	0.004
δ	0.006
ρ	0.002
γ	0.001
μ	0.04
ψ	0.05
u	0.03
d	0.05

These values satisfy the necessary conditions for the existence of a unique, biologically feasible endemic equilibrium. Consequently, the system admits a single endemic equilibrium point given by $E^* = (S^*, I^*) = (46.9357, 10.4979)$, for which the basic reproduction number is calculated as $\mathscr{R}_0 = 1.5345$.

Figures 2.1 and 2.2, plotted using the initial population values, illustrate the effect of fractional-order parameter α on the susceptible and infected sub-populations.

Figure 2.1 highlights how variations in α influence the convergence behavior of system (2.1). An increase in α leads to faster stabilization of the susceptible population toward its steady state. In contrast, decreasing α strengthens the memory effect inherent in the fractional-order system, thereby slowing down the rate of convergence. In practical terms, a lower value of α results in a prolonged presence of the disease in the population.

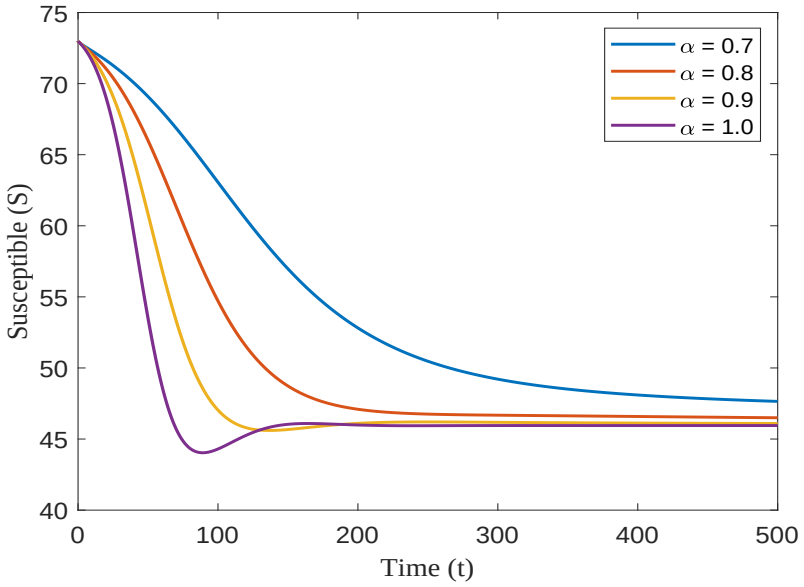

Figure 2.1: Time series plot of susceptible population for different values of fractional order α.

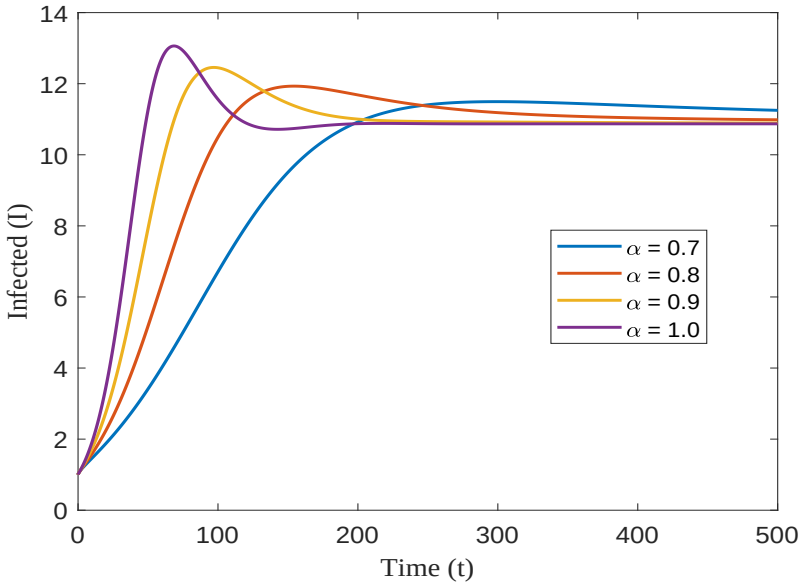

Figure 2.2: Time series plot of infected population for different values of fractional order α.

Figure 2.2 shows that when $\alpha = 1$ the infected population quickly reach a steady state. However, as the value of α decreases, the time it takes for these populations to reach the steady state increases. This shows how the epidemic evolves over time.

Furthermore, Figures 2.1 and 2.2 indicate that, as the disease progresses, the number of susceptible individuals decreases while the number of infected individuals increases, eventually stabilizing at their respective steady states.

Figure 2.3 provides valuable insights into the long-term behaviour of disease transmission within a population by depicting a phase portrait of susceptible versus infected individuals. This graphical representation allows us to visualize how the populations of susceptible and infected individuals evolve over time and interact with one another. From the phase portrait, it can be observe that as time progresses, the number of susceptible individuals increases while the number of infected individuals decreases. This inverse relationship suggests that the disease is gradually being brought under control. The increase in the susceptible population may initially seem strange, however this reflects the effect of reduced transmission of infection, that is, fewer individuals are becoming infected, allowing more individuals to remain in the susceptible class.

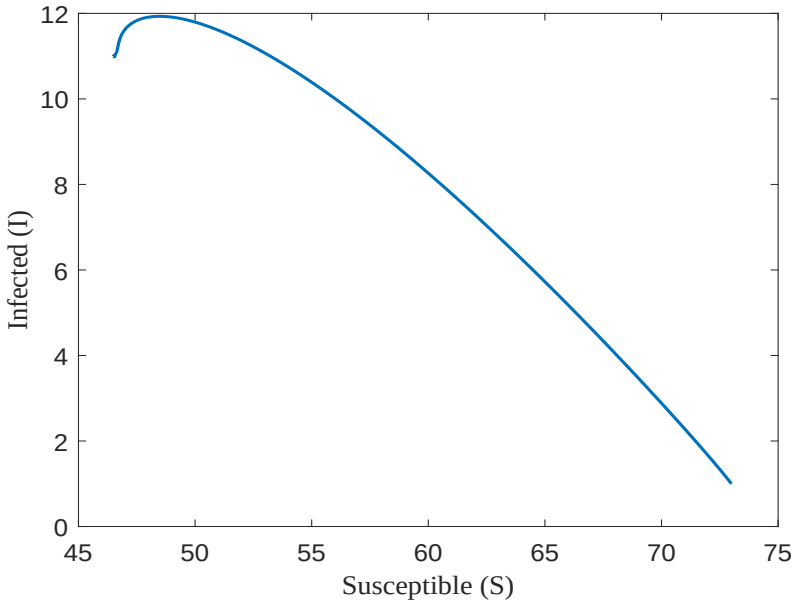

Figure 2.3: Phase diagram for susceptible and infected population for fractional order $\alpha = 0.8$.

The work done in this chapter focuses on the role of fear and the Beddington-De Anglis incidence rate in shaping the dynamics of infectious disease transmission. Specifically, it explores how behavioural responses driven by fear and preventive actions influence the susceptible and infected populations. Figures 2.4, 2.5 and 2.6 illus-

trate the impact of these key parameters, namely the level of fear δ and the rates of preventive measures (ρ and γ), on the disease dynamics.

From Figure 2.4, it is observed that as the fear level within the population increases, there is a decline in the number of infected individuals. This outcome can be attributed to fear-induced behavioural changes such as social distancing, improved hygiene, and reduced contact rates, all of which contribute to lowering disease transmission.

Figures 2.5 and 2.6 further demonstrates that higher values of ρ and γ, which represent the rates at which susceptible individuals adopt preventive measures, lead to an increase in the susceptible population. This is because effective preventive behaviours reduce the likelihood of infection, thereby increasing the susceptible population over time.

Altogether, these findings highlight the critical role of psychological and behavioural factors, particularly fear and preventive actions, in modulating epidemic outcomes. Incorporating these elements into epidemiological models helps capture more realistic disease dynamics and can inform more effective public health interventions.

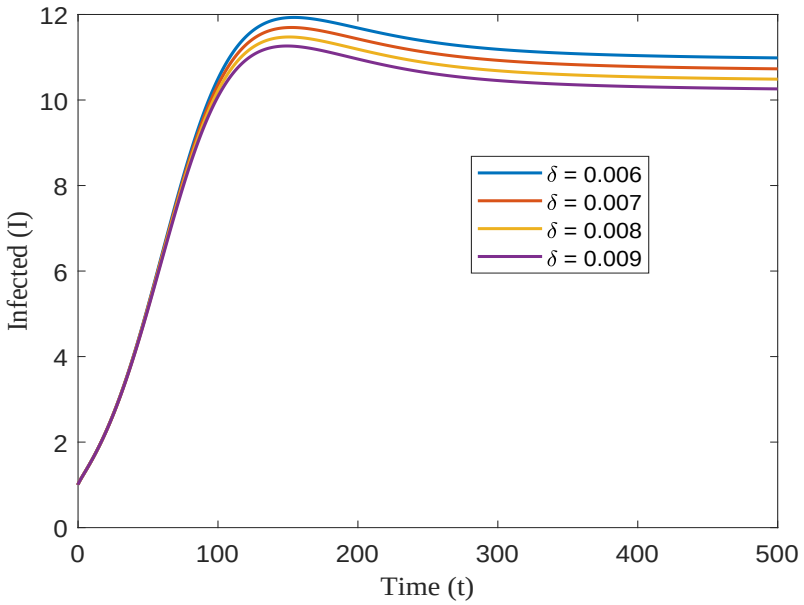

Figure 2.4: Effect of fear level δ on I for fractional order $\alpha = 0.8$.

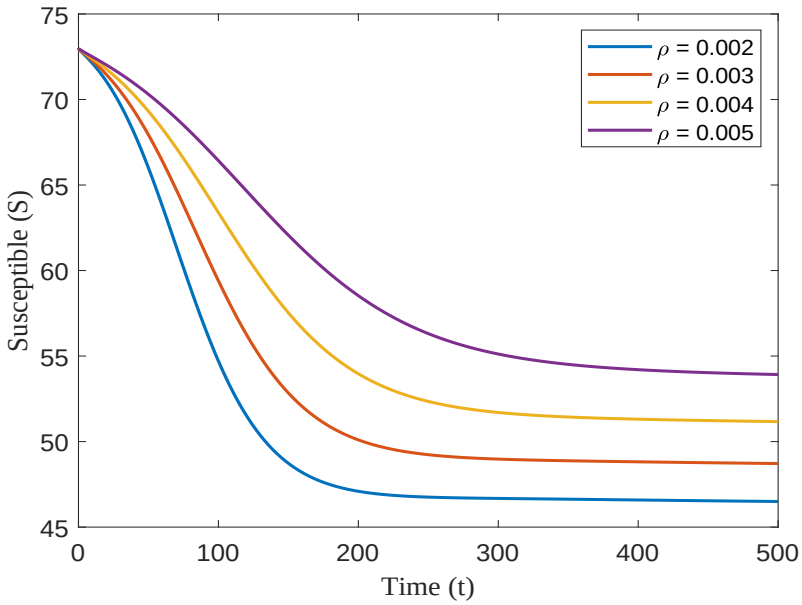

Figure 2.5: Effect of preventive measures ρ on S for fractional order $\alpha = 0.8$.

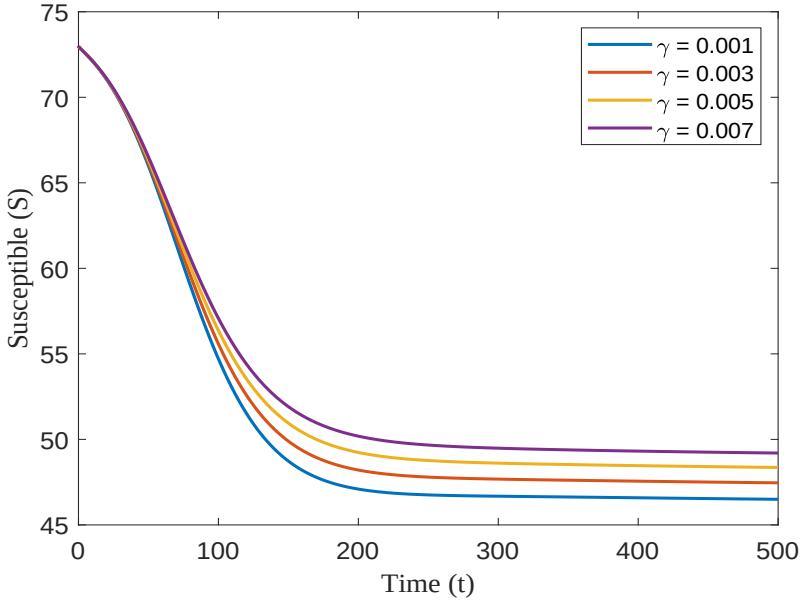

Figure 2.6: Effect of preventive measures γ on S for fractional order $\alpha = 0.8$.

2.7 Conclusion

Mathematical modeling is a valuable tool for understanding the dynamics of epidemics and for planning and evaluating intervention strategies. This chapter presented and

analyzed a Caputo-type fractional-order Susceptible-Infected-Susceptible (SIS) model that incorporates the fear effect and preventive measures adopted by both susceptible and infected individuals. These behavioural effects are modeled through a Beddington-De Angelis type incidence rate. The well-posedness of the model was first established by proving the positivity and boundedness of the solutions, ensuring that they remain positive and uniformly bounded within a biologically relevant region. The analysis showed that the model admits two equilibria: a disease-free equilibrium point E_0, and an endemic equilibrium point E_1, which exists when the basic reproduction number $\mathscr{R}_0 > 1$. The basic reproduction number $\mathscr{R}_0$ was derived using the next-generation matrix approach, and the stability of the disease-free equilibrium was characterized in terms of $\mathscr{R}_0$. Specifically, the disease dies out when $\mathscr{R}_0 < 1$ and persists when $\mathscr{R}_0 > 1$. The local stability behaviour of the endemic equilibrium point was also discussed. Furthermore, numerical simulations were conducted to validate theoretical results and to study the effects of memory (fractional-order dynamics) using the Adams-Bashforth-Moulton Predictor-Corrector method in MATLAB. The simulations further illustrated the influence of fear on the infected population, as well as the impact of preventive measures ρ and γ on the susceptible population. The results indicate that these preventive measures are highly effective in controlling the spread of the disease, and the fear effect significantly reduces the disease burden in the population. Overall, the proposed model, incorporating both the fear effect and the Beddington-De Angelis incidence rate within a fractional-order framework, offers valuable insights for epidemiologists, policymakers, and public health officials.

Chapter 3

Stability Analysis and Quantification of Effects of Partial and Full Vaccination Using Fractional Order *SVIR* model

---

An infectious disease such as COVID-19 poses a global threat to public health due to its high infection rate and continued mutation into novel variants. Vaccination serves as a vital tool to interrupt its transmission cycle and mitigate its far-reaching effects. However, the effectiveness of vaccination depends on a well-planned strategy. This chapter compares full and partial vaccination strategies using a novel fractional SVIR mathematical model with a Caputo fractional derivative. The model categorizes vaccinated individuals into two groups: partially vaccinated and fully vaccinated. To account for limited medical resources and the possibility of virus reemergence, the Holling type III saturated treatment function is adopted for the treatment rate. The analysis begins by establishing the well-posedness of the model solutions. Subsequently, the stability of the two equilibria exhibited by the system-the disease-free equilibrium (DFE) and the endemic equilibrium (EE)-is examined. It is shown that the DFE is locally asymptotically stable when $\mathscr{R}_0 < 1$, and that the EE is locally asymptotically stable according to the Routh-Hurwitz criterion. Moreover, both equilibrium points are proved to be globally stable under certain conditions, using appropriate Lyapunov functions. Additionally, sensitivity analysis for $\mathscr{R}_0$ is performed. Numerical

simulations, conducted in MATLAB, validate the analytical findings. The quantification of the effects of partial and full vaccination reveals that full vaccination results in a higher percentage of recovered individuals. This demonstrates that policymakers and public health professionals should emphasize the importance of effective full vaccination among susceptible populations.

3.1 Introduction

In late December 2019, a novel respiratory illness emerged in Wuhan, located in China's Hubei Province. This infectious disease, later termed coronavirus disease 2019 (COVID-19), is caused by the newly identified severe acute respiratory syndrome coronavirus 2 (SARS-CoV-2) [9; 178]. Initially, the World Health Organization (WHO) designated the outbreak as a Public Health Emergency of International Concern. However, as infections rapidly increased both between and within countries, the WHO subsequently characterized COVID-19 as a global pandemic on 11 March 2020 [191]. The pandemic posed new problems to the worldwide community, particularly in the context of attempts to ensure equitable vaccine distribution, lessen the load on healthcare systems and mitigate the virus's economic impact. In response, most countries adopted rigorous containment strategies to promote physical distancing, which included closing schools and workplaces and limiting travel and public gatherings to different extents [107].

The spread of COVID-19 and the resurgence of the pandemic in 2022 have significantly affected people's mental health, despite the government's implementation of various effective measures to control its spread. It is important to note that public opinion regarding vaccines has undergone a significant shift in light of the pandemic's impact. Vaccination is widely regarded as one of the most effective public health measures and a key strategy for controlling the spread of infectious diseases [12]. However, sustained progress depends on widespread public acceptance to preserve herd immunity, curb outbreaks of vaccine-preventable infections, and facilitate the uptake of newly developed vaccines [31]. The recent resurgence of vaccine-preventable diseases has even prompted the World Health Organization (WHO) to list vaccine hesitancy as one of the top ten global health threats in 2019 [190]. There is a considerable number of individuals worldwide who are hesitant to receive vaccinations [174]. This hesitancy may be attributed to doubts concerning the credibility of vaccine development and

the government's approval process. Existing research articles, however, have mostly examined vaccine hesitancy for vaccines with long-term safety records. Such data are not yet available for novel COVID-19 vaccines, which likely exaggerates existing fears about vaccine safety resulting in partial vaccination in the population [121].

Several mathematical models have been proposed to evaluate the role of vaccination, its effectiveness, and the influence of vaccination campaigns on the progression of COVID-19 [10; 45; 197]. In addition, many studies have employed compartmental models to examine the impact and significance of vaccination strategies against various infectious diseases [29; 112]. More recently, mathematical modeling approaches have been utilized to explore the long-term effects of vaccination on COVID-19 incidence and control, as can be found in the literature and references therein [106; 172]. To the best of our knowledge, very few studies have been performed to consider the classes of vaccinated people bases on their vaccine doses [136; 145] but not much attention has been paid to investigate the impact of vaccination in a way such that the vaccinated population is categorised into two parts by considering the fact that some people take all the doses of vaccine allowed by the health agencies of respective country and some population could not take all the doses. This chapter incorporates this scenario by defining two cohorts: the partially vaccinated population and the fully vaccinated population. Here, the population that cannot follow the SOPs of the government for vaccination due to vaccine hesitancy, careless human behaviour, lack of awareness or any other reason will be kept in the Partially Vaccinated class and the others who follow SOPs and get all the vaccine doses will be kept in the Fully Vaccinated class.

As noted by several researchers, saturation effects in medical treatment can produce complex and often nonlinear disease dynamics [39; 81; 129]. Wang and Ruan [186] investigated an *SIR* model where the treatment rate $T(I)$ is zero at $I = 0$ and becomes a constant r once $I > 0$. In a related study, Dubey et al. [59] considered a Holling type III treatment rate, which increases rapidly with the number of infectives in the beginning and then gradually approaches a saturation level as the infectious population grows. In the context of several infectious diseases, where limited medical resources can affect the treatment rate and where treatment effectiveness may vary with disease prevalence, Holling Type III treatment offers a more realistic representation. It captures the idea that medical facilities may be overwhelmed during outbreaks, leading to a slower response initially and then a more rapid one as resources become available.

Keeping the above considerations in mind, the Holling type-III treatment rate is incorporated into the proposed $SVIR$ fractional compartmental model. This approach, which extends the $SVIR$ model by classifying the vaccinated population into partially and fully vaccinated groups, is expected to be highly valuable for health agencies in decision-making. The structure of this chapter is organized as follows. Section 3.2 presents the formulation of the fractional-order mathematical model. In Section 3.3, the positivity and boundedness of the solutions are established. Section 3.4 investigates the existence of equilibrium points and derives the basic reproduction number using the next-generation approach. The local and global stability of the equilibria are analyzed in Section 3.5. Sensitivity nalysis of $\mathscr{R}_0$ is performed in Section 3.6. Numerical simulations, provided in Section 3.7, are used to compare the partially and fully vaccinated populations with recovered individuals and to validate the analytical results. Finally, Section 3.8 summarizes the main findings of the study and provides concluding remarks.

3.2 Formulation of fractional order epidemic model

This section develops a fractional-order compartmental model in the Caputo sense, incorporating a Holling type III treatment rate. The total population at time t, denoted by $N(t)$, is subdivided into five compartments: susceptible individuals denoted as $S(t)$, partially vaccinated individuals as $V_p(t)$, fully vaccinated individuals as $V_f(t)$, infected individuals as $I(t)$, and recovered individuals as $R(t)$.

The basic assumptions of our model are as follows:

(A1) The growth rate of susceptibles is taken as constant which is K and contact rate of susceptible with infected population has taken as β.

(A2) It is assumed that there are some population that cannot follow the SOPs of government and not been vaccinated properly, those people will be kept in partially vaccinated class and rest of the vaccinated people will be in the fully vaccinated class.

(A3) It is possible that some partially vaccinated individuals may become fully vaccinated over time but at the same time, there are also some populations that could not be administered all the doses of allocated vaccines for their respective countries due to allergic reactions, pregnancy, logistic issues, personal choices,

vaccine hesitancy and many more. That is why the model is developed under the assumption that there is no transfer between partially and fully vaccinated individuals to study the effects of partial vaccination more closely.

(A4) The vaccinated population will also become infected due to close contact with infected individual. So the rate of infection of partially and fully vaccinated populations have been considered different and taken as f_1 and f_2 respectively.

(A5) The natural and disease induced mortality have been considered. The treatment of infected populations is taken as the function $h(I) = \frac{aI^2}{1+bI^2}$ which is Holling type-III treatment rate, where a is the treatment rate of the disease and b is the limitation of medical and pharmaceutical facilities.

(A6) Infected population will also be recovered by the natural recovery rate θ.

(A7) Death rate for each category population is μ.

Considering the aforementioned information, the propagation dynamics of the system can be represented by the flow chart given in Figure 3.1 and described by the following set of fractional differential equations:

$$
\begin{aligned}
{}_0D_t^{\alpha} S(t) &= K - \beta S(t)I(t) - \alpha_p S(t) - \alpha_f S(t) - \mu S(t),\\
{}_0D_t^{\alpha} V_p(t) &= \alpha_p S(t) - f_1 V_p(t)I(t) - \mu V_p(t),\\
{}_0D_t^{\alpha} V_f(t) &= \alpha_f S(t) - f_2 V_f(t)I(t) - \mu V_f(t),\\
{}_0D_t^{\alpha} I(t) &= \beta S(t)I(t) + f_1 V_p(t)I(t) + f_2 V_f(t)I(t) - (\mu + d + \theta) I(t) - h(I(t)),\\
{}_0D_t^{\alpha} R(t) &= h(I(t)) + \theta I(t) - \mu R(t),
\end{aligned}
\tag{3.1}
$$

where, $h(I) = \frac{aI^2}{1+bI^2}$, is the Holling type III treatment rate with treatment capacity $\frac{a}{b}$. So our model becomes

$$
\begin{aligned}
{}_0D_t^{\alpha} S(t) &= K - \beta S(t) I(t) - (\alpha_p + \alpha_f + \mu) S(t), \\
{}_0D_t^{\alpha} V_p(t) &= \alpha_p S(t) - f_1 V_p(t) I(t) - \mu V_p(t), \\
{}_0D_t^{\alpha} V_f(t) &= \alpha_f S(t) - f_2 V_f(t) I(t) - \mu V_f(t), \\
{}_0D_t^{\alpha} I(t) &= \beta S(t) I(t) + f_1 V_p(t) I(t) + f_2 V_f(t) I(t) - (\mu + d + \theta) I(t) - \frac{aI^2}{1+bI^2}, \\
{}_0D_t^{\alpha} R(t) &= \frac{aI^2}{1+bI^2} + \theta I(t) - \mu R(t)
\end{aligned}
\tag{3.2}
$$

subject to the conditions

$$
S(0) = S_0 \geq 0, V_p(0) = V_{p0} \geq 0, V_f(0) = V_{f0} \geq 0, I(0) = I_0 \geq 0, R(0) = R_0 \geq 0, \tag{3.3}
$$

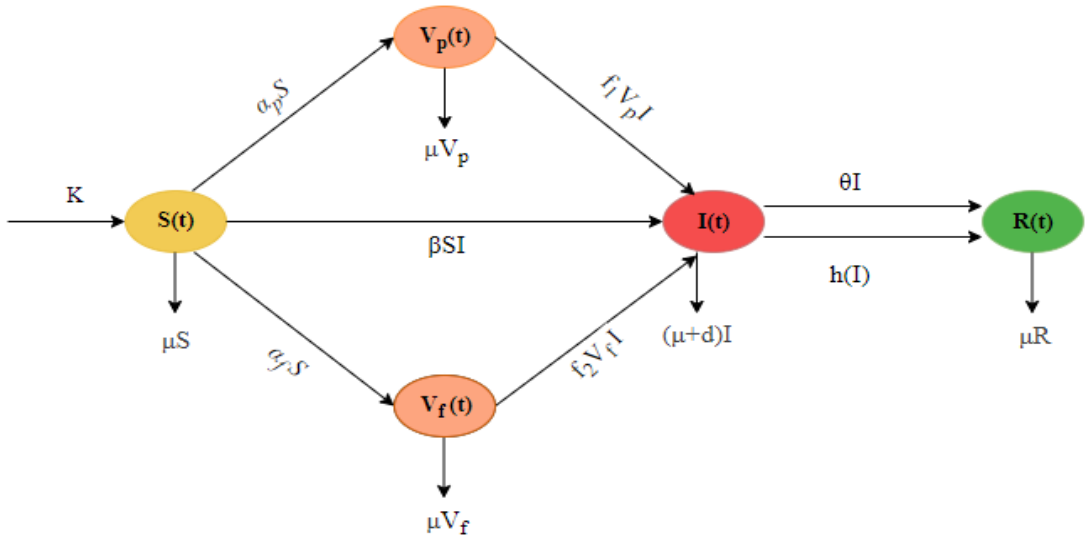

Figure 3.1: Propagation diagram of disease.

The fractional order derivative ${}_0D_t^{\alpha}$, where $\alpha \in (0,1]$, is employed in the Caputo sense. All the parameters relevant to the model can be found in Table 3.1.

Table 3.1: Parameter descriptions of the model $SVIR$ and the their units.

Parameters	**Description**	**Unit**
K	Recruitment rate	ind. time^{-1}
β	The transmission rate of infection in	
μ	Natural death rate	time^{-1}
	susceptibles	ind^{-1}. time^{-1}
α_p	Partial vaccination rate	time^{-1}
α_f	Full vaccination rate	time^{-1}
f_1	Contact rate of partially vaccinated population	ind. time^{-1}
f_2	Contact rate of fully vaccinated population	ind.time^{-1}
d	Death rate induced by disease	time^{-1}
θ	Recovery rate of infected population	time^{-1}
a	Treatment rate	ind^{-1}.time^{-1}
b	Treatment limitation	ind^{-1}.time^{-1}

3.3 Positivity and boundedness

For epidemiological reasons, all the state variables describe the evolution of population and hence they should be non-negative because it would not make sense if the solution of system (3.2) is negative.

Theorem 3.3.1 *All solutions of the system described by* (3.2) *and subject to the initial condition* (3.3) *are non-negative and uniformly bounded for all* $t \geq 0$.

Proof 3.3.2 ***(Positivity)*** *Let us consider the scenario where* $S(0) > 0$. *To begin with, we aim to establish the claim that* $S(t)$ *remains non-negative for all* $t \geq 0$ *through contradiction.*

Let us assume that $S(t) < 0$. *Consequently, there exists a specific value* $\tau_1 > 0$ *such that* $S(t) > 0$ *holds true for* $0 \leq t < \tau_1$, $S(t) = 0$ *precisely at* $t = \tau_1$, *and* $S(t) < 0$ *for* $\tau_1 < t < \tau_1 + \varepsilon_1$, *where* ε_1 *is chosen to be sufficiently small.*

From the first equation of the model (3.2), *we get* $D_t^{\alpha} S(t)|_{t=\tau_1} = K > 0$. *According to generalized mean value theorem [142], for any* $0 < \varepsilon_1 \ll 1$, *we get*

$$S(\tau_1 + \varepsilon_1) = S(\tau_1) + \frac{1}{\Gamma(\alpha)} {}_{\tau_1}D_t^{\alpha} S(\xi)(\varepsilon_1)^{\alpha}, \ \ with \ \ \tau_1 < \xi \leq \tau_1 + \varepsilon_1.$$

Consequently, we can conclude that $S(\tau_1+\varepsilon_1) \geq 0$, *which contradicts the established fact that* $S(t) < 0$ *for* $\tau_1 \leq t \leq \tau_1+\varepsilon_1$. *Hence, we can affirm that* $S(t) \geq 0$ *for all* $t \geq 0$.

In a similar manner, we can demonstrate that $V_p(t) \geq 0,\ V_f(t) \geq 0,\ I(t) \geq 0$ *and* $R(t) \geq 0$ *holds for* $t \geq 0$. *Consequently, it can be concluded that all solutions* $(S(t), V_p(t), V_f(t), I(t), R(t))$ *of the model described by* (3.2) *and subject to the conditions outlined in* (3.3) *are non-negative.*

*Now, (**Boundedness**) using the identity* $S+V_p+V_f+I+R=N$ *i.e. adding all the equations of the model* (3.2), *we obtain,*

$$\begin{aligned} D_t^{\alpha} N &= K-\mu N-dI, \\ D_t^{\alpha} N &\leq K-\mu N \end{aligned} \tag{3.4}$$

Now consider the initial value problem

$$D_t^{\alpha}\bar{N} = K-\mu\bar{N},\ \ \bar{N}(0)=\bar{N}_0.$$

Using comparison principle [120], we obtain the following inequality:

$$N(t) \leq \bar{N}(t),\ \forall t \geq 0.$$

Applying the Laplace transform to the above initial value problem, we have

$$S^{\alpha}\mathscr{L}[\bar{N}(t)] - s^{\alpha-1}\bar{N}_0 = \frac{K}{s} - \mu\mathscr{L}[\bar{N}(t)]$$

$$\implies \mathscr{L}[\bar{N}(t)] = \frac{s^{\alpha-1}\bar{N}_0}{s^{\alpha}+\mu} + \frac{Ks^{-1}}{s^{\alpha}+\mu}.$$

Now, according to Lemma 3 of [171], we obtain

$$\mathscr{L}[E_{\alpha,1}(-\mu t^{\alpha})] = \frac{s^{\alpha-1}}{s^{\alpha}+\mu},\quad \mathscr{L}[t^{\alpha}E_{\alpha,\alpha+1}(-\mu t^{\alpha})] = \frac{s^{-1}}{s^{\alpha}+\mu}.$$

Applying the inverse Laplace transform in above equation, we obtain

$$\bar{N}(t) = \bar{N}_0 E_{\alpha,1}(-\mu t^{\alpha}) + Kt^{\alpha}E_{\alpha,\alpha+1}(-\mu t^{\alpha}).$$

Combining this with (3.4) *gives*

$$N(t) \leq [N_0 E_{\alpha,1}(-\mu t^{\alpha}) + Kt^{\alpha}E_{\alpha,\alpha+1}(-\mu t^{\alpha})].$$

Moreover, by Lemma 3 of [96], we obtain

$$|N(t)| \leq \frac{N_0 C_E}{1+\mu t^{\alpha}} + \frac{Kt^{\alpha}C_E}{1+\mu t^{\alpha}},$$

where C_E is the constant defined in Lemma 4 of [171]. Therefore, as $t \to \infty$, we have $N(t) \leq \bar{M}$ with $\bar{M} \geq C_E \frac{K}{\mu}$. Hence, all the solutions are bounded and will remain in attracting biological feasible domain Ω of system (3.2)*, which is given below:*

$$\Omega = \left\{ (S, V_p, V_f, I, R) \in \mathbb{R}^5_+ : 0 < S + V_p + V_f + I + R \leq \bar{M}, \bar{M} \geq C_E \frac{K}{\mu} \right\}.$$

The proof is completed.

It is worth noting that in the model system (3.2), the variable $R(t)$ does not directly appear in the first four equations. Instead, the first four equations can be seen as providing input to the equation concerning R. As a result, we can consider the following subsystem:

$$\begin{aligned}
{}_0D_t^{\alpha} S(t) &= K - \beta S(t) I(t) - \eta S(t), \\
{}_0D_t^{\alpha} V_p(t) &= \alpha_p S(t) - f_1 V_p(t) I(t) - \mu V_p(t), \\
{}_0D_t^{\alpha} V_f(t) &= \alpha_f S(t) - f_2 V_f(t) I(t) - \mu V_f(t), \\
{}_0D_t^{\alpha} I(t) &= \beta S(t) I(t) + f_1 V_p(t) I(t) + f_2 V_f(t) I(t) - \rho I(t) - \frac{a I^2}{1 + b I^2},
\end{aligned} \tag{3.5}$$

where $\rho = (\mu + d + \theta)$ and $\eta = (\alpha_p + \alpha_f + \mu)$.

3.4 Possible Equilibria and Basic Reproduction Number

Within this section, our objective is to determine all biologically and feasibly relevant equilibria that are supported by the system. To obtain these equilibria, we set the right-hand side of system (3.5) to zero. Thus, we found the model system (3.5) has a disease free equilibrium (DFE) point also, given by $\bar{E} = (\bar{S}, \bar{V_p}, \bar{V_f}, 0)$, at which the whole population is free from the disease, where

$$\bar{S} = \frac{K}{\eta}, \ \bar{V_p} = \frac{K \alpha_p}{\mu \eta}, \ \bar{V_f} = \frac{K \alpha_f}{\mu \eta}.$$

Now, the basic reproduction number $\mathscr{R}_0$ can be find by using the recipes of next generation approach given in [47]. Let

$$D_t^{\alpha}(x) = \mathscr{F}(x) - \mathscr{V}(x),$$

where, $x = (I, V_f, V_p)$. The non-negative matrix $\mathscr{F}$, which represents the new infection terms, and the matrix $\mathscr{V}$, comprising the remaining terms, are provided as follows:

$$\mathscr{F} = \begin{pmatrix} \beta SI + f_1 V_w I + f_2 V_s I \\ 0 \\ 0 \end{pmatrix} \quad \text{and} \quad \mathscr{V} = \begin{pmatrix} \rho I + \frac{aI^2}{1+bI^2} \\ f_2 V_s I + \mu V_s - \alpha_s S \\ f_1 V_w I + \mu V_w - \alpha_w S \end{pmatrix}$$

The corresponding linearized matrices evaluated at DFE $\bar{E}$ are respectively,

$$F = \begin{pmatrix} \frac{\beta K}{\eta} + \frac{f_1 K \alpha_w}{\mu \eta} + \frac{f_2 K \alpha_s}{\mu \eta} & 0 & 0 \\ 0 & 0 & 0 \\ 0 & 0 & 0 \end{pmatrix} \quad \text{and} \quad V = \begin{pmatrix} \rho & 0 & 0 \\ \frac{f_2 K \alpha_s}{\mu \eta} & \mu & 0 \\ \frac{f_1 K \alpha_w}{\mu \eta} & 0 & \mu \end{pmatrix}.$$

It follows that,

$$FV^{-1} = \begin{pmatrix} \frac{K(\mu\beta + f_1\alpha_p + f_2\alpha_f)}{\rho\mu\eta} & 0 & 0 \\ 0 & 0 & 0 \\ 0 & 0 & 0 \end{pmatrix}.$$

The basic reproduction number $\mathscr{R}_0$ is the spectral radius i.e. the largest eigen value of above matrix FV^{-1}, i.e.

$$\mathscr{R}_0 = \frac{K(\mu\beta + f_1\alpha_p + f_2\alpha_f)}{\rho\mu\eta},$$

which shows the average number of secondary cases generated by a typical infective individual in an otherwise susceptible population. Further, for the endemic equilibrium point $E^* = (S^*, {V_p}^*, {V_f}^*, I^*)$ of the system (3.5), we get the following set of algebraic equations:

$$\begin{aligned} &K - \beta S^* I^* - (\alpha_p + \alpha_f + \mu) S^* = 0, \\ &\alpha_p S^* - f_1 V_p^* I^* - \mu V_p^* = 0, \\ &\alpha_f S^* - f_2 V_f^* I^* - \mu V_f^* = 0, \\ &\beta S^* I^* + f_1 V_p^* I^* + f_2 V_f^* I^* - \rho I^* - \tfrac{aI^{*2}}{1+bI^{*2}} = 0. \end{aligned} \tag{3.6}$$

All the components of E^* can be obtained by solving equation (3.6) for $I^* \neq 0$, as follows:

$${S^*} = \frac{K}{\beta I^* + \eta}, \quad {V_p}^* = \frac{K\alpha_p}{(f_1 I^* + \mu)(\beta I^* + \eta)}, \quad \text{and} \quad {V_f}^* = \frac{K\alpha_f}{(f_2 I^* + \mu)(\beta I^* + \eta)},$$

with I^* satisfying the equation

$$A_5 I^{*5} + A_4 I^{*4} + A_3 I^{*3} + A_2 I^{*2} + A_1 I^* + A_0 = 0, \tag{3.7}$$

with

$$\begin{aligned}
A_5 &= f_1 f_2 \beta \rho b, \\
A_4 &= f_1 f_2 (\eta \rho b + a\beta - \beta K b) + \beta \rho b \mu (f_1 + f_2), \\
A_3 &= \beta \rho b \mu^2 + (\eta \rho b + a\beta - \beta K b)(\mu (f_1 + f_2)) + f_1 f_2 (\rho \beta + a\eta) - bK f_1 f_2 (\alpha_w + \alpha_s), \\
A_2 &= (\rho \eta - K\beta) f_1 f_2 + \mu (f_1 + f_2)(\rho \beta + a\eta) + \mu^2 a\beta + b\mu^2 \rho \eta (1 - \mathscr{R}_0), \\
A_1 &= \mu^2 (\rho \beta + a\eta) + \mu (f_1 + f_2)(\rho \eta - K\beta) - K f_1 f_2 (\alpha_w + \alpha_s), \\
A_0 &= \mu^2 \rho \eta (1 - \mathscr{R}_0).
\end{aligned} \tag{3.8}$$

Theorem 3.4.1 *For $\mathscr{R}_0 > 1$, the system* (3.5) *exhibits either a unique positive endemic equilibrium or three or five positive endemic equilibria, assuming that all equilibria are simple roots.*

Proof 3.4.2 *Let $\mathscr{R}_0 > 1$. From equation* (3.7) *we have fifth degree polynomial I^* :*

$$A_5 I^{*5} + A_4 I^{*4} + A_3 I^{*3} + A_2 I^{*2} + A_1 I^* + A_0.$$

Applying the fundamental theorem of algebra, we can deduce that this polynomial can have at most five real roots.

Here, we examine only the case of unique endemic equilibrium. Since, $A_5 > 0$ and $A_0 < 0$ for $\mathscr{R}_0 > 1$ then with the help of Descartes' rule of signs [188], equation (3.7) has a unique positive real root I^* if any one of the following holds:

$$\begin{aligned}
&(i) \quad A_4 < 0,\ A_3 < 0,\ A_2 < 0 \text{ and } A_1 < 0, \\
&(ii) \quad A_4 > 0,\ A_3 < 0,\ A_2 < 0 \text{ and } A_1 < 0, \\
&(iii) \quad A_4 > 0,\ A_3 > 0,\ A_2 < 0 \text{ and } A_1 < 0, \\
&(iv) \quad A_4 > 0,\ A_3 > 0,\ A_2 > 0 \text{ and } A_1 < 0, \\
&(v) \quad A_4 > 0,\ A_3 > 0,\ A_2 > 0 \text{ and } A_1 > 0.
\end{aligned} \tag{3.9}$$

Upon establishing the value of I^*, we can subsequently determine the values of S^*, ${V_p}^*$, and ${V_f}^*$. This implies that there exists a single positive endemic equilibrium if any of the conditions specified in (3.9) are met.

3.5 Stability Analysis

In this particular section, our focus shifts towards investigating the stability of the equilibria in the system (3.5) by computing the corresponding variational matrix, denoted as J. The Jacobian matrix associated with the system (3.5) is presented below:

$$J=\begin{pmatrix} -\eta-\beta I & 0 & 0 & -\beta S \\ \alpha_p & -\mu-f_1 I & 0 & -f_1 V_p \\ \alpha_f & 0 & -\mu-f_2 I & -f_2 V_f \\ \beta I & f_1 I & f_2 I & -\rho+\beta S+f_1 V_p+f_2 V_f-\dfrac{2aI}{(1+bI^2)^2} \end{pmatrix}.$$

3.5.1 Local stability of DFE and endemic equilibrium

The Jacobian matrix at the DFE point $\bar{E}$ is given by

$$J_{\bar{E}}=\begin{pmatrix} -(\alpha_p+\alpha_f+\mu) & 0 & 0 & \dfrac{-\beta K}{(\alpha_p+\alpha_f+\mu)} \\ \alpha_p & -\mu & 0 & \dfrac{-f_1 K\alpha_p}{\mu(\alpha_p+\alpha_f+\mu)} \\ \alpha_f & 0 & -\mu & \dfrac{-f_2 K\alpha_f}{\mu(\alpha_p+\alpha_f+\mu)} \\ 0 & 0 & 0 & -\rho(1-\mathscr{R}_0) \end{pmatrix}.$$

The characteristic equation corresponding to the DFE $\bar{E}=(\bar{S},\bar{V}_p,\bar{V}_f,0)$ takes the form:

$$(-\lambda-\rho(1-\mathscr{R}_0))\left(\lambda+\left(\alpha_p+\alpha_f+\mu\right)\right)(\lambda+\mu)^2=0.$$

Hence, the eigenvalues of system (3.5) at DFE $\bar{E}$ are

$$\lambda_1=-\eta,\ \ \lambda_2=-\mu,\ \ \lambda_3=-\mu,\ \ \lambda_4=-\rho(1-\mathscr{R}_0).$$

Here, see that λ_i for $i=1,2,3$ are all with negative sign, and therefore

$$|\arg(\lambda_i)|=\pi>\alpha\frac{\pi}{2}\quad \text{for}\quad i=1,2,3$$

and $|\arg(\lambda_4)|=\pi>\alpha\frac{\pi}{2}$ if $-\rho(1-\mathscr{R}_0)<0$, i.e. $\mathscr{R}_0<1$, where $\alpha\in(0,1]$. In an opposite manner, when $\mathscr{R}_0>1$, then $\lambda_4>0$ and so $|\arg(\lambda_4)|=0<\alpha\frac{\pi}{2}$. Thus, the DFE $\bar{E}$ will be unstable. Hence, by Lemma 3.4 of [128], we can say that DFE is locally asymptotically stable when $\mathscr{R}_0$ is less that unity and unstable otherwise. Then we have the following theorem:

Theorem 3.5.1 *The disease free equilibrium of the model* (3.5) *is locally asymptotically stable if* $\mathscr{R}_0<1$, *otherwise unstable.*

3.5.1.a Local stability analysis at $\mathscr{R}_0 = 1$ around $\bar{E}$

This subsection analyzes the behavior of system (3.5) at $\mathscr{R}_0 = 1$, for which the linearized matrix at $\bar{E}$ has at least one eigenvalue with real part equal to zero. By performing this analysis, we determine the direction of bifurcation and describe the local behaviour of $\bar{E}$ around $\mathscr{R}_0 = 1$. To do so, we apply center manifold theory as described in [35]. Although this theory was originally developed for integer-order systems, its extension to Caputo-type fractional-order systems has been established by Ma and Li [123], which justifies its use in our fractional-order model. This methodology has been adopted in several recent studies on bifurcation analysis of fractional-order epidemic models [16; 126].

Let us redefine $(S, V_p, V_f, I) = (x_1, x_2, x_3, x_4)$, then the system (3.5) can be rewritten as:

$$\begin{aligned}
D_t^\alpha x_1 &= K - \beta x_1 x_4 - (\alpha_p + \alpha_f + \mu) x_1 \equiv z_1, \\
D_t^\alpha x_2 &= \alpha_p x_1 - f_1 x_2 x_4 - \mu x_2 \equiv z_2, \\
D_t^\alpha x_3 &= \alpha_f x_1 - f_2 x_3 x_4 - \mu x_3 \equiv z_3, \\
D_t^\alpha x_4 &= \beta x_1 x_4 + f_1 x_2 x_4 + f_2 x_3 x_4 - (\mu + d + \theta) x_4 - \frac{a {x_4}^2}{1 + b {x_4}^2} \equiv z_4,
\end{aligned} \tag{3.10}$$

Recall that, $\mathscr{R}_0 = \dfrac{K(\mu\beta + f_1\alpha_p + f_2\alpha_f)}{\mu(\mu + d + \theta)(\alpha_p + \alpha_f + \mu)}$. Select β as a bifurcation parameter for $\mathscr{R}_0 = 1$ which takes the following form:

$$\beta = \beta^* = \frac{\mu(\mu + d + \theta)(\alpha_p + \alpha_f + \mu) - K(f_1\alpha_p + f_2\alpha_f)}{K\mu}.$$

Further, the Jacobian matrix of the system (3.5) at $\bar{E}$ and at the chosen bifurcation parameter $\beta = \beta^*$ it is given by $J_{[\bar{E},\beta^*]}$ as:

$$J_{[\bar{E},\beta^*]} = \begin{pmatrix}
-(\alpha_p+\alpha_f+\mu) & 0 & 0 & \dfrac{-\beta^* K}{(\alpha_p+\alpha_f+\mu)} \\
\alpha_p & -\mu & 0 & \dfrac{-f_1 K \alpha_p}{\mu(\alpha_p+\alpha_f+\mu)} \\
\alpha_f & 0 & -\mu & \dfrac{-f_2 K \alpha_f}{\mu(\alpha_p+\alpha_f+\mu)} \\
0 & 0 & 0 & 0
\end{pmatrix}.$$

The matrix $J_{[\bar{E},\beta^*]}$ has a simple zero eigen value and other eigen value with negative real part.

Let $v=(v_1,v_2,v_3,v_4)$ be the left eigenvector and $w=(w_1,w_2,w_3,w_4)^T$ be the right eigen vector corresponding to the zero eigen value. Then, we have

$v_1=0,\ v_2=0,\ v_3=0,\ v_4=1$

and $w_1=-\frac{K\beta}{(\alpha_p+\alpha_f+\mu)^2}$, $w_2=-\frac{K\alpha_p[\beta\mu+f_1(\alpha_p+\alpha_f+\mu)]}{\mu^2(\alpha_p+\alpha_f+\mu)^2}$, $w_3=-\frac{K\alpha_f[\beta\mu+f_2(\alpha_p+\alpha_f+\mu)]}{\mu^2(\alpha_p+\alpha_f+\mu)^2}$, $w_4=1$.

The non-zero partial derivatives of $z_k's$ at $\bar{E}$ and $\beta=\beta^*$ are evaluated as follows:

$$\frac{\partial^2 z_1}{\partial x_1\partial x_4}=-\beta^*=\frac{\partial^2 z_1}{\partial x_4\partial x_1},\ \frac{\partial^2 z_2}{\partial x_2\partial x_4}=-f_1=\frac{\partial^2 z_2}{\partial x_4\partial x_2},\ \frac{\partial^2 z_3}{\partial x_3\partial x_4}=-f_2=\frac{\partial^2 z_3}{\partial x_4\partial x_3},$$
$$\frac{\partial^2 z_4}{\partial {x_4}^2}=-2a,\ \frac{\partial^2 z_4}{\partial x_3\partial x_4}=f_2=\frac{\partial^2 z_4}{\partial x_4\partial x_3},\ \frac{\partial^2 z_4}{\partial x_1\partial x_4}=\beta^*=\frac{\partial^2 z_4}{\partial x_4\partial x_1},\ \frac{\partial^2 z_4}{\partial x_2\partial x_4}=f_1=\frac{\partial^2 z_4}{\partial x_4\partial x_2},$$
$$\frac{\partial^2 z_1}{\partial x_4\partial\beta^*}=-\frac{K}{(\alpha_p+\alpha_f+\mu)},\ \frac{\partial^2 z_4}{\partial x_4\partial\beta^*}=\frac{K}{(\alpha_p+\alpha_f+\mu)}.$$

The bifurcation constants a_1 and b_1 can be computed by using Theorem 4.1 given in [35] as follows:

$$\begin{aligned}
a_1&=\sum_{k,i,j=1}^{4}v_kw_iw_j\left(\frac{\partial^2 z_k}{\partial x_i\partial x_j}\right)_{[\bar{E},\beta^*]}\\
&=v_4{w_4}^2\frac{\partial^2 z_4}{\partial {x_4}^2}+2v_4w_3w_4\frac{\partial^2 z_4}{\partial x_3\partial x_4}+2v_4w_1w_4\frac{\partial^2 z_4}{\partial x_1\partial x_4}+2v_4w_2w_4\frac{\partial^2 z_4}{\partial x_2\partial x_4}\\
&=2\Bigg(\frac{K{\beta^*}^2}{(\alpha_p+\alpha_f+\mu)^2}-\Bigg(a+\frac{f_1K\alpha_p[\beta\mu+f_1(\alpha_p+\alpha_f+\mu)]}{\mu^2(\alpha_p+\alpha_f+\mu)^2}+\\
&\qquad\qquad\frac{f_2K\alpha_f[\beta\mu+f_2(\alpha_p+\alpha_f+\mu)]}{\mu^2(\alpha_p+\alpha_f+\mu)^2}\Bigg)\Bigg)\\
&=2\Big(L_1-L_2\Big),
\end{aligned}$$

where $L_1=\frac{K{\beta^*}^2}{(\alpha_p+\alpha_f+\mu)^2}$, $L_2=\left(a+\frac{f_1K\alpha_p[\beta\mu+f_1(\alpha_p+\alpha_f+\mu)]}{\mu^2(\alpha_p+\alpha_f+\mu)^2}+\frac{f_2K\alpha_f[\beta\mu+f_2(\alpha_p+\alpha_f+\mu)]}{\mu^2(\alpha_p+\alpha_f+\mu)^2}\right)$ and

$$\begin{aligned}
b_1&=\sum_{k,i=1}^{4}v_kw_i\left(\frac{\partial^2 z_k}{\partial x_i\partial\beta^*}\right)_{[\bar{E},\beta^*]}\\
&=v_4w_4\frac{\partial^2 z_4}{\partial x_4\partial\beta^*}=\frac{K}{(\alpha_p+\alpha_f+\mu)}>0.
\end{aligned}$$

Thus, the following theorem may be stated by using Theorem 4.1 of [35].

Theorem 3.5.2 *The following results are obtained for the transcritical bifurcation:*

1. *If $L_1 < L_2$ i.e. $a_1 < 0$, then system* (3.5) *exhibits a transcritical forward bifurcation at $\bar{E}$ and $\mathscr{R}_0 = 1$.*

2. *If $L_1 > L_2$ i.e. $a_1 > 0$, then system* (3.5) *exhibits either a transcritical backward bifurcation or a saddle-node bifurcation at $\bar{E}$ and $\mathscr{R}_0 = 1$.*

The transcritical forward bifurcation is illustrated in Figure 3.2.

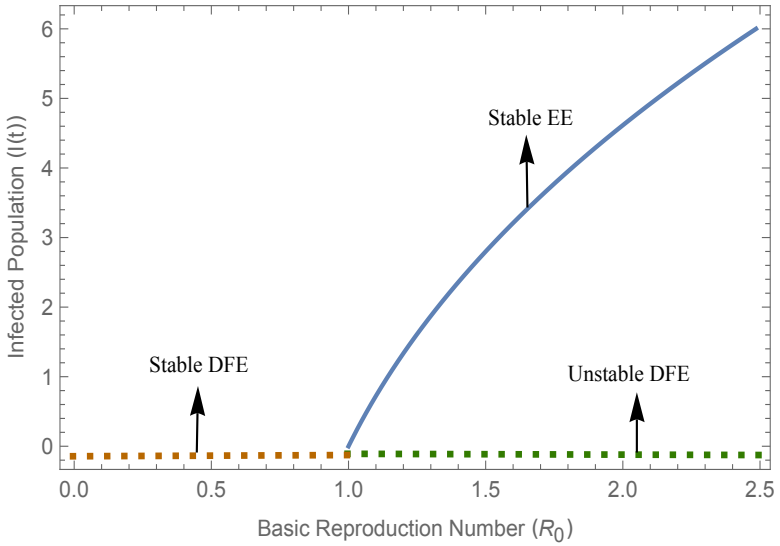

Figure 3.2: Diagram for forward bifurcation in $(\mathscr{R}_0, I)$ plane for the data set given in Table 3.2.

Now for the local stability of endemic equilibrium $E^* = (S^*, V_p{}^*, V_f{}^*, I^*)$, the corresponding Jacobian matrix by using the equation (3.6) is given by

$$J_{E^*} = \begin{pmatrix} -\beta I^* + \eta & 0 & 0 & -\dfrac{\beta K}{\beta I^* + \eta} \\ \alpha_p & -\mu - f_1 I^* & 0 & -\dfrac{K f_1 \alpha_p}{(f_1 I^* + \mu)(\beta I^* + \eta)} \\ \alpha_f & 0 & -\mu - f_2 I^* & -\dfrac{K f_2 \alpha_f}{(f_2 I^* + \mu)(\beta I^* + \eta)} \\ \beta I^* & f_1 I^* & f_2 I^* & \dfrac{a I^* (b I^{*2} - 1)}{(1 + b I^{*2})^2} \end{pmatrix}.$$

The characteristic equation corresponding to the above Jacobian matrix takes the form:

$$(-\eta - \beta I^* - \lambda)(C_3 \lambda^3 + C_2 \lambda^2 + C_1 \lambda + C_0) = 0. \tag{3.11}$$

where,

$$
\begin{aligned}
C_3 &= \left(bI^{*2}+1\right)^2 (f_1 I^* + \mu)\,(f_2 I^* + \mu)\,(\eta + \beta I^*),\\
C_2 &= \mu\big(f_2\big(I^*(\eta+\beta I^*)\big(2aI^* + \big(bI^{*2}+1\big)^2(3\mu+\rho)\big) + f_2\big(bI^{*3}+I^*\big)^2(\eta+\beta I^*)\\
&\quad - K\big(bI^{*2}+1\big)^2\alpha_f + \beta(-K)I^*\big(bI^{*2}+1\big)^2\big) + \mu\big((\eta+\beta I^*)\big(2aI^*\\
&\quad + \big(bI^{*2}+1\big)^2(2\mu+\rho)\big) - \beta K\big(bI^{*2}+1\big)^2\big)\big) + f_1\big(f_2 I^*\big(I^*(\eta+\beta I^*)\big(2aI^*\\
&\quad + \big(bI^{*2}+1\big)^2(4\mu+\rho)\big) - K\big(bI^{*2}+1\big)^2\big(\alpha_f+\alpha_p\big) + \beta(-K)I^*\big(bI^{*2}+1\big)^2\big)\\
&\quad + \mu I^*\big((\eta+\beta I^*)\big(2aI^* + \big(bI^{*2}+1\big)^2(3\mu+\rho)\big) - \beta K\big(bI^{*2}+1\big)^2\big)\\
&\quad + f_2^2 I^{*3}\big(bI^{*2}+1\big)^2(\eta+\beta I^*) - K\mu\big(bI^{*2}+1\big)^2\alpha_p\big)\\
&\quad + f_1^2\big(bI^{*3}+T\big)^2\big(f_2 I^*+\mu\big)(\eta+\beta I^*),
\end{aligned}
$$

$$
\begin{aligned}
C_1 &= f_2\mu\big(f_2 I^{*2}\big((\eta+\beta I^*)\big(2aI^* + \big(bI^{*2}+1\big)^2(\mu+\rho)\big) - \beta K\big(bI^{*2}+1\big)^2\big)\\
&\quad + \mu\big(I^*(\eta+\beta I^*)\big(6aI^* + \big(bI^{*2}+1\big)^2(2\mu+3\rho)\big) - 2K\big(bI^{*2}+1\big)^2\alpha_f\\
&\quad - 3\beta K I^*\big(bI^{*2}+1\big)^2\big)\big) + f_1\big(f_2\mu I^*\big(4I^*(\eta+\beta I^*)\big(2aI^* + \big(bI^{*2}+1\big)^2(\mu+\rho)\big)\big)\\
&\quad - 3K\big(bI^{*2}+1\big)^2\big(\alpha_f+\alpha_p\big) - 4\beta K I^*\big(bI^{*2}+1\big)^2\big) + f_2^2 I^{*2}\big(I^*(\eta+\beta I^*)\big(2aI^*\\
&\quad + \big(bI^{*2}+1\big)^2(2\mu+\rho)\big) + \beta(-K)I^*\big(bI^{*2}+1\big)^2 - K\big(bI^{*2}+1\big)^2\alpha_p\big)\\
&\quad + \mu^2\big(I^*(\eta+\beta I^*)\big(6aI^* + \big(bI^{*2}+1\big)^2(2\mu+3\rho)\big) - 3\beta K I^*\big(bI^{*2}+1\big)^2\\
&\quad - 2K\big(bI^{*2}+1\big)^2\alpha_p\big)\big) + f_1^2 I^{*2}\big(f_2\big(I^*(\eta+\beta I^*)\big(2aI^* + \big(bI^{*2}+1\big)^2(2\mu+\rho)\big)\big)\\
&\quad + f_2\big(bI^{*3}+T\big)^2(\eta+\beta I^*) - K\big(bI^{*2}+1\big)^2\alpha_f + \beta(-K)I^*\big(bI^{*2}+1\big)^2\big)\\
&\quad + \mu\big((\eta+\beta I^*)\big(2aI^* + \big(bI^{*2}+1\big)^2(\mu+\rho)\big) - \beta K\big(bI^{*2}+1\big)^2\big)\big)\\
&\quad + \mu^3\big((\eta+\beta I^*)\big(4aI^* + \big(bI^{*2}+1\big)^2(\mu+2\rho)\big) - 2\beta K\big(bI^{*2}+1\big)^2\big),\\
C_0 &= f_2\mu^2\big(f_2 I^{*2}\big((\eta+\beta I^*)\big(2aI^* + \rho\big(bI^{*2}+1\big)^2\big) - \beta K\big(bI^{*2}+1\big)^2\big)\\
&\quad + 2\mu I^*\big((\eta+\beta I^*)\big(2aI^* + \rho\big(bI^{*2}+1\big)^2\big) - \beta K\big(bI^{*2}+1\big)^2\big) - K\mu\big(bI^{*2}+1\big)^2\alpha_f\big)\\
&\quad + f_1^2 I^{*2}\big(f_2\mu\big(2I^*(\eta+\beta I^*)\big(2aI^* + \rho\big(bI^{*2}+1\big)^2\big) - K\big(bI^{*2}+1\big)^2\alpha_f\\
&\quad - 2\beta K I^*\big(bI^{*2}+1\big)^2\big) + f_2^2 I^{*2}\big((\eta+\beta I^*)\big(2aI^* + \rho\big(bI^{*2}+1\big)^2\big) - \beta K\big(bI^{*2}+1\big)^2\big)\\
&\quad + \mu^2\big((\eta+\beta I^*)\big(2aI^* + \rho\big(bI^{*2}+1\big)^2\big) - \beta K\big(bI^{*2}+1\big)^2\big)\big)\\
&\quad + f_1\mu\big(2f_2\mu I^*\big(2I^*(\eta+\beta I^*)\big(2aI^* + \rho\big(bI^{*2}+1\big)^2\big) - K\big(bI^{*2}+1\big)^2\big(\alpha_f+\alpha_p\big)\\
&\quad - 2\beta K I^*\big(bI^{*2}+1\big)^2\big) + f_2^2 I^{*2}\big(2I^*(\eta+\beta I^*)\big(2aI^* + \rho\big(bI^{*2}+1\big)^2\big)\\
&\quad - 2\beta K I^*\big(bI^{*2}+1\big)^2 - K\big(bI^{*2}+1\big)^2\alpha_p\big) + \mu^2\big(2I^*(\eta+\beta I^*)\big(2aI^* + \rho\big(bI^{*2}+1\big)^2\big)\\
&\quad - 2\beta K I^*\big(bI^{*2}+1\big)^2 - K\big(bI^{*2}+1\big)^2\alpha_p\big)\big) + \mu^4\big((\eta+\beta I^*)\big(2aI^* + \rho\big(bI^{*2}+1\big)^2\big)\\
&\quad - \beta K\big(bI^{*2}+1\big)^2\big).
\end{aligned}
$$

From equation (3.11), the polynomial $C_3\lambda^3 + C_2\lambda^2 + C_1\lambda + C_0$ can be written as, say $P(\lambda) = \lambda^3 + k_2\lambda^2 + k_1\lambda + k_0$, and corresponding to this $P(\lambda)$, the discriminant is

$$D(\lambda) = 18k_2k_1k_0 + {k_2}^2{k_1}^2 - 4k_0{k_2}^3 - 4{k_1}^3 - 27{k_0}^2.$$

If $P(\lambda) = 0$ has three roots with negative real parts, then the endemic equilibrium is stable. Therefore, following Ahmed et al. [4], the following theorem is stated:

Theorem 3.5.3 *The endemic equilibrium $E^*(S^*, {V_p}^*, {V_f}^*, I^*)$ is locally asymptotically stable when any of the following conditions hold:*

- $D(P) > 0,\ k_2 > 0,\ k_0 > 0,\ k_2k_1 > k_0$.
- $D(P) < 0,\ k_2 \geq 0,\ k_1 \geq 0,\ k_0 > 0,\ \alpha < \frac{2}{3}$.
- $D(P) < 0,\ k_2 > 0,\ k_1 > 0,\ k_2k_1 = k_0,\ \alpha \in (0,1]$. *Otherwise, the endemic equilibrium $E^*(S^*, {V_p}^*, {V_f}^*, I^*)$ is unstable when the condition $D(P) < 0, k_2 < 0, k_1 < 0, \alpha > \frac{2}{3}$ holds.*

3.5.2 Global stability of disease-free equilibrium (DFE)

This subsection presents the theorem concerning the global stability behavior of the disease-free equilibrium (DFE) point.

Theorem 3.5.4 *The DFE point of the system* (3.5) *is GAS (Globally asymptotically Stable) if the basic reproduction number $\mathscr{R}_0$ is strictly less than unity i.e. $\mathscr{R}_0 < 1$.*

Proof 3.5.5 *To prove this theorem, consider a positive definite Lyapunov function*

$$\mathscr{L} = I.$$

Then for order α we have,

$$
\begin{aligned}
{}_{t_0}D_t^{\alpha}\mathscr{L} &= {}_{t_0}D_t^{\alpha}I(t)\\
&= \left[\beta SI + f_1V_pI + f_2V_fI - (\mu+d+\theta)I - \frac{aI^2}{1+bI^2}\right]\\
&\leq \left[\beta SI + f_1V_pI + f_2V_fI - (\mu+d+\theta)I\right]\\
&= \left[\beta S + f_1V_p + f_2V_f - (\mu+d+\theta)\right]I(t)\\
&= \left[\frac{\beta K}{(\alpha_p+\alpha_f+\mu)} + \frac{f_1K\alpha_p}{\mu(\alpha_p+\alpha_f+\mu)} + \frac{f_2K\alpha_f}{\mu(\alpha_p+\alpha_f+\mu)} - (\mu+d+\theta)\right]I(t)\\
&= \left[\frac{1}{(\mu+d+\theta)}\left\{\frac{\beta K}{(\alpha_p+\alpha_f+\mu)} + \frac{f_1K\alpha_p}{\mu(\alpha_p+\alpha_f+\mu)} + \frac{f_2K\alpha_f}{\mu(\alpha_p+\alpha_f+\mu)}\right\} - 1\right]I(t)\\
&= (\mathbb{R}_0-1)I(t)\\
&\leq 0 \quad \textit{if } \mathbb{R}_0 \leq 1.
\end{aligned}
$$

So, by Lemma 4.6 of [82], any solution starting in $\mathbb{R}$ converges to the largest invariant set $S = \left\{(S,V_p,V_f,I) \in \mathbb{R} : {}_{t_0}D_t^{\alpha}\mathscr{L} = 0\right\}$. Hence $\lim_{t\to\infty} I(t) = 0$.

3.5.3 Global stability of endemic equilibrium

This subsection examines the global stability behavior of the endemic equilibrium E^* under certain constraints, for which it is assumed that

$$G(I) = \frac{I}{1+bI^2}.$$

Theorem 3.5.6 *The endemic equilibrium $E^*(S^*,{V_p}^*,{V_f}^*,I^*)$ is globally asymptotically stable when $\mathscr{R}_0 > 1$.*

Proof 3.5.7 *From the system* (3.5) *following conditions are derived at $E^*(S^*,{V_p}^*,{V_f}^*,I^*)$,*

$$K = \beta S^*I^* + \eta S^*;\ \ \alpha_p = \frac{f_1{V_p}^*I^*}{S^*} + \frac{\mu{V_p}^*}{S^*};\ \ \alpha_f = \frac{f_2{V_f}^*I^*}{S^*} + \frac{\mu{V_f}^*}{S^*}$$

$$\rho = \beta S^* + f_1{V_p}^* + f_2{V_f}^* - aG(I^*).$$

Now, to prove the global stability behaviour of E^*, we construct the following positive definite Lyapunov function:

$$
\begin{aligned}
\mathscr{L}(t) = &\left(S - S^* - S^*\log\frac{S}{S^*}\right) + \left(V_p - {V_p}^* - {V_p}^*\log\frac{V_p}{{V_p}^*}\right)\\
&+ \left(V_f - {V_f}^* - {V_f}^*\log\frac{V_f}{{V_f}^*}\right) + \left(I - I^* - I^*\log\frac{I}{I^*}\right).
\end{aligned}
$$

The derivative of $\mathscr{L}(t)$ along the solution of system (3.5)*, with the help of Lemma 3 of [140], becomes:*

$$
\begin{aligned}
{}_0D_t^{\alpha}\mathscr{L}(t) \leq{}& \left(1-\frac{S^*}{S}\right){}_0D_t^{\alpha}S(t)+\left(1-\frac{{V_p}^*}{V_p}\right){}_0D_t^{\alpha}V_p(t)+\left(1-\frac{{V_f}^*}{V_f}\right){}_0D_t^{\alpha}V_f(t)\\
&+\left(1-\frac{I^*}{I}\right){}_0D_t^{\alpha}I(t)\\
&=\left(1-\frac{S^*}{S}\right)(K-\beta SI-\eta S)+\left(1-\frac{{V_p}^*}{V_p}\right)(\alpha_p S-f_1V_pI-\mu V_p)\\
&+\left(1-\frac{{V_f}^*}{V_f}\right)\left(\alpha_f S-f_2V_fI-\mu V_f\right)+\left(1-\frac{I^*}{I}\right)\left(\beta S+f_1V_p+f_2V_f-\rho-aG(I)\right)\\
&=\left(1-\frac{S^*}{S}\right)(\beta S^*I^*+\eta S^*-\beta SI-\eta S)\\
&+\left(1-\frac{{V_p}^*}{V_p}\right)\left(\frac{f_1{V_p}^*I^*}{S^*}S+\frac{\mu {V_p}^*}{S^*}S-f_1V_pI-\mu V_p\right)\\
&+\left(1-\frac{{V_f}^*}{V_f}\right)\left(\frac{f_2{V_f}^*I^*}{S^*}S+\frac{\mu {V_f}^*}{S^*}S-f_2V_fI-\mu V_f\right)\\
&+\left(1-\frac{I^*}{I}\right)\left(\beta S^*+f_1{V_p}^*+f_2{V_f}^*-aG(I^*)+\beta S+f_1V_p+f_2V_f-aG(I)\right)\\
&=\eta S^*\left(2-\frac{S^*}{S}-\frac{S}{S^*}\right)+\beta S^*I^*\left(1-\frac{S^*}{S}+\frac{I}{I^*}-\frac{SI}{S^*I^*}\right)\\
&+f_1{V_p}^*I^*\left(\frac{S}{S^*}-\frac{{V_p}^*S}{V_pS^*}+\frac{I}{I^*}-\frac{V_pI}{{V_p}^*I^*}\right)+\mu {V_p}^*\left(\frac{S}{S^*}-\frac{{V_p}^*S}{V_pS^*}+1-\frac{V_p}{{V_p}^*}\right)\\
&+f_2{V_f}^*I^*\left(\frac{S}{S^*}-\frac{{V_f}^*S}{V_fS^*}+\frac{I}{I^*}-\frac{V_fI}{{V_f}^*I^*}\right)+\mu {V_f}^*\left(\frac{S}{S^*}-\frac{{V_f}^*S}{V_fS^*}+1-\frac{V_f}{{V_f}^*}\right)\\
&+\beta S^*\left(1+\frac{S}{S^*}-\frac{I^*}{I}-\frac{SI^*}{S^*I^*}\right)+f_1{V_p}^*\left(1-\frac{I^*}{I}+\frac{V_p}{{V_p}^*}-\frac{V_pI^*}{{V_p}^*I}\right)\\
&+f_2{V_f}^*\left(1-\frac{I^*}{I}+\frac{V_f}{{V_f}^*}-\frac{V_fI^*}{{V_f}^*I}\right)+aG(I^*)\left(\frac{I^*}{I}+\frac{G(I)}{G(I^*)}+\frac{G(I)I^*}{G(I^*)I}-1\right).
\end{aligned}
$$

Now, from the property of the arithmetic mean, we have

$$\left(2-\frac{S^*}{S}-\frac{S}{S^*}\right)\leq 0.$$

and if

$$\left.\begin{array}{ll}
\left(1-\frac{S^*}{S}+\frac{I}{I^*}-\frac{SI}{S^*I^*}\right)\leq 0, & \left(\frac{S}{S^*}-\frac{{V_p}^*S}{V_pS^*}+\frac{I}{I^*}-\frac{V_pI}{{V_p}^*I^*}\right)\leq 0,\\
\left(\frac{S}{S^*}-\frac{{V_p}^*S}{V_pS^*}+1-\frac{V_p}{{V_p}^*}\right)\leq 0, & \left(\frac{S}{S^*}-\frac{{V_f}^*S}{V_fS^*}+\frac{I}{I^*}-\frac{V_fI}{{V_f}^*I^*}\right)\leq 0,\\
\left(\frac{S}{S^*}-\frac{{V_f}^*S}{V_fS^*}+1-\frac{V_f}{{V_f}^*}\right)\leq 0, & \left(1+\frac{S}{S^*}-\frac{I^*}{I}-\frac{SI^*}{S^*I^*}\right)\leq 0,\\
\left(1-\frac{I^*}{I}+\frac{V_p}{{V_p}^*}-\frac{V_pI^*}{{V_p}^*I}\right)\leq 0, & \left(1-\frac{I^*}{I}+\frac{V_f}{{V_f}^*}-\frac{V_fI^*}{{V_f}^*I}\right)\leq 0,\\
\left(\frac{I^*}{I}+\frac{G(I)}{G(I^*)}+\frac{G(I)I^*}{G(I^*)I}-1\right)\leq 0, &
\end{array}\right\} \quad (3.12)$$

then ${}_0D_t^{\alpha}\mathscr{L}(t)\leq 0$. *Hence, when the inequalities in equation*(3.12) *are satisfied simultaneously then* ${}_0D_t^{\alpha}\mathscr{L}(t)\leq 0$. *Besides, the largest invariant set in* $\left\{(S,V_p,V_f,I)|{}_0D_t^{\alpha}\mathscr{L}(t)=0\right\}$ *is the singleton set* $\{E^*\}$. *Consequently, in accordance with Lassalle's invariance principle, it can be concluded that the endemic equilibrium* E^* *of the model* (3.5) *exhibits global stability when* $\mathscr{R}_0>1$.

3.6 Sensitivity analysis of $\mathscr{R}_0$

Here, the results of a sensitivity analysis for the basic reproduction $\mathscr{R}_0$ number are presented. The objective of this analysis is to identify parameters that exert the greatest influence on $\mathscr{R}_0$, allowing us to prioritize them in the implementation of effective intervention strategies. Sensitivity indices quantify the relative variation in a given outcome as a parameter changes. Specifically, we compute the normalized forward sensitivity index of a variable with respect to a parameter as the ratio of the variable's relative change to the corresponding relative change in that parameter.

Definition[164]: The normalized forward sensitivity index of a variable z, which depends on a parameter x, is defined as

$$W_x^z=\frac{\partial z}{\partial x}\times\frac{x}{z}.$$

So, for $\mathscr{R}_0$, the sensitivity index is $W_x^{\mathscr{R}_0}=\dfrac{\partial\mathscr{R}_0}{\partial x}\times\dfrac{x}{\mathscr{R}_0}$. The expressions of sensitivity

index for the parameters of interest are:

$$W_K^{\mathscr{R}_0} = 1,\ W_\beta^{\mathscr{R}_0} = \frac{\beta\mu}{\beta\mu + f_2\alpha_f + f_1\alpha_p},\ W_{f_1}^{\mathscr{R}_0} = \frac{f_1\alpha_p}{\beta\mu + f_2\alpha_f + f_1\alpha_p},$$
$$W_{f_2}^{\mathscr{R}_0} = \frac{f_2\alpha_f}{\beta\mu + f_2\alpha_f + f_1\alpha_p},\ W_{\alpha_p}^{\mathscr{R}_0} = \frac{\alpha_f + \mu}{\alpha_f + \mu + \alpha_p} - \frac{\beta\mu + f_2\alpha_f}{\beta\mu + f_2\alpha_f + f_1\alpha_p},$$
$$W_{\alpha_f}^{\mathscr{R}_0} = \alpha_f\left(\frac{f_2}{\beta\mu + f_2\alpha_f + f_1\alpha_p} - \frac{1}{\alpha_f + \mu + \alpha_p}\right),\ W_d^{\mathscr{R}_0} = -\frac{d}{d + \theta + \mu},$$
$$W_\theta^{\mathscr{R}_0} = -\frac{\theta}{d + \theta + \mu},\ W_\mu^{\mathscr{R}_0} = -2 + \frac{d + \theta}{d + \theta + \mu} + \frac{\beta\mu}{\beta\mu + f_2\alpha_f + f_1\alpha_p} - \frac{\mu}{\alpha_f + \mu + \alpha_p}$$

These sensitivity indices are evaluated with the help of parametric values given in Table 3.2 and depicted by the bar diagram in Figure 3.3.

$$W_K^{\mathscr{R}_0} = 1,\ W_\beta^{\mathscr{R}_0} = 0.162791,\ W_{f_1}^{\mathscr{R}_0} = 0.55814,\ W_{f_2}^{\mathscr{R}_0} = 0.27907,$$
$$W_{\alpha_p}^{\mathscr{R}_0} = 0.038659,\ W_{\alpha_f}^{\mathscr{R}_0} = -0.110541,\ W_d^{\mathscr{R}_0} = -0.277778,$$
$$W_\theta^{\mathscr{R}_0} = -0.33333,\ W_\mu^{\mathscr{R}_0} = -1.31701.$$

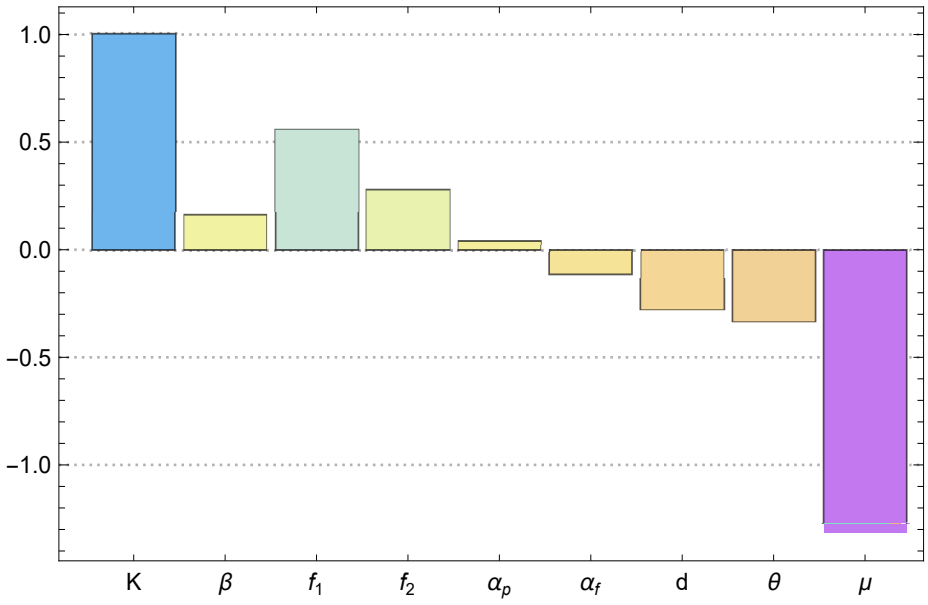

Figure 3.3: Sensitivity indices of $\mathscr{R}_0$.

From the above, it is seen that these sensitivity indices with respect to parameters can either have positive impact or negative impact on $\mathscr{R}_0$. Specifically, the parameters K, f_1 and f_2 have strongest positive impact while β and α_p have less positive impact on $\mathscr{R}_0$. This means that if these parameters increase while keeping the others unchanged, the basic reproduction number $\mathscr{R}_0$ will also increase, leading to a faster spread of the

disease. Similarly, if they decrease, the spread of the disease will be slowed down. For example, $W_{f_1}^{\mathscr{R}_0} = 0.55814$ indicates that if the parameter f_1 increases (or decreases) by 10%, then $\mathscr{R}_0$ will increase (or decrease) by 5.58%. Similarly, $W_{\mu}^{\mathscr{R}_0} = -1.31701$ means that if μ increases (or decreases) by 10%, then $\mathscr{R}_0$ will decrease (or increase) by 13.17%, respectively. This helps us to understand the sensitivity of the parameters and their impact on $\mathscr{R}_0$ in both positive and negative ways.

3.7 Numerical Simulation

This section provides numerical computations, performed in MATLAB 2012b using the Predictor-Corrector method [50], to validate the analysis of the existence and stability conditions of the equilibria of model system (3.5). For the numerical simulation the initial sub-populations are taken as $S(0) = 200, V_p(0) = 45, V_f(0) = 35, I(0) = 3, R(0) = 2$ and the numerical data-set used for simulation, given in Table 3.2, is experimental data satisfying the analysis of the system (3.5).

Table 3.2: Numerical values of parameters of the model.

Parameters	**Description**	**Values**
K	Recruitment rate	2
β	The transmission rate of infection in susceptibles	0.0005
μ	Natural death rate	0.007
α_p	Partial vaccination rate	0.04
α_f	Full vaccination rate	0.03
f_1	Contact rate of partially vaccinated population	0.0003
f_2	Contact rate of fully vaccinated population	0.0002
d	Death rate induced by disease	0.005
θ	Recovery rate of infected population	0.006
a	Treatment rate	0.004
b	Treatment limitation	0.00001

From the parametric values given in 3.2, the value of the coefficients of equation (3.7) is $A_5 = 5.4 \times 10^{-18}$, $A_4 = 1.20547 \times 10^{-13}$, $A_3 = 2.59539 \times 10^{-11}$, $A_2 = 1.22833 \times 10^{-9}$, $A_1 = 8.484 \times 10^{-9}$, $A_0 = -2.33086 \times 10^{-7}$. These coefficient values satisfy Theorem3.4.1 and one of the possibility of the existence of unique positive equilibrium. Thus the endemic equilibrium is $E^*(S^*, V_p{}^*, V_f{}^*, I^*) =$

$(24.3965, 97.7104, 81.3985, 9.95763)$ for which the basic reproduction number $\mathscr{R}_0$ is 4.43208. The values of coefficients of equation (3.11) are calculated as $C_3 = 7.37638 \times 10^{-6}$, $C_2 = 4.32928 \times 10^{-7}$, $C_1 = 7.107 \times 10^{-9}$, $C_0 = 3.4502 \times 10^{-11}$ and the eigen values corresponding the equation (3.11) are $\lambda_1 = -0.0819788$, $\lambda_2 = -0.0349566$, $\lambda_3 = -0.0145179$, $\lambda_4 = -0.00921651$, and the discriminant of polynomial term of the equation (3.11) is calculated as $D(\lambda) = 7.77873 \times 10^{-12} > 0$. The values of k_0, k_1, k_2 and $D(\lambda)$ satisfy the first condition of the Theorem 3.5.3. Using the initial population conditions, Figures 3.4, 3.5, 3.6, and 3.7 are plotted, which shows the effect of fractional derivative order $\alpha(\alpha = 0.7, 0.8, 0.9, 1)$ on the Susceptible, Partially Vaccinated, Fully Vaccinated and Infected population, respectively. In the virtue of Theorem 3.5.3, the endemic equilibrium E^* is stable for each value of fractional order α, which is being depicted from the figures.

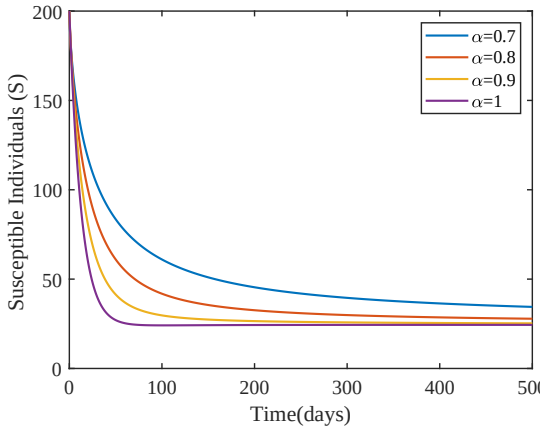

Figure 3.4: Effect of fractional order α on the susceptible population.

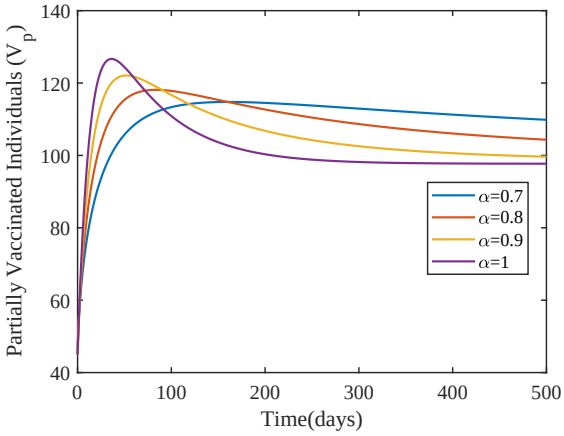

Figure 3.5: Effect of fractional order α on the partially vaccinated population.

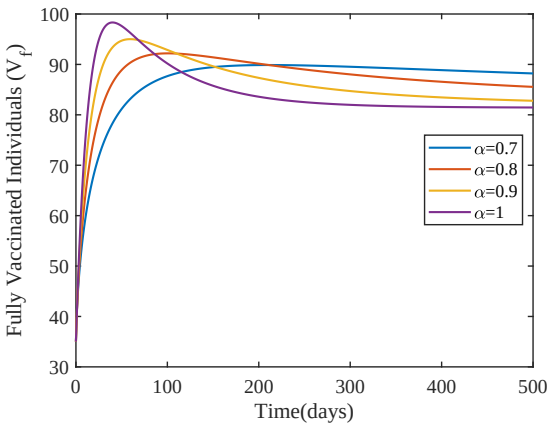

Figure 3.6: Effect of fractional order α on the fully vaccinated population.

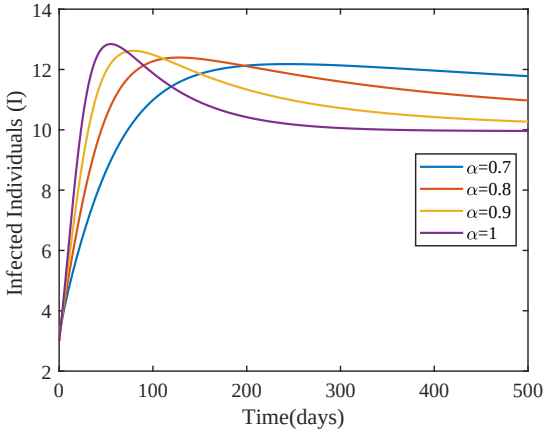

Figure 3.7: Effect of fractional order α on the infected population.

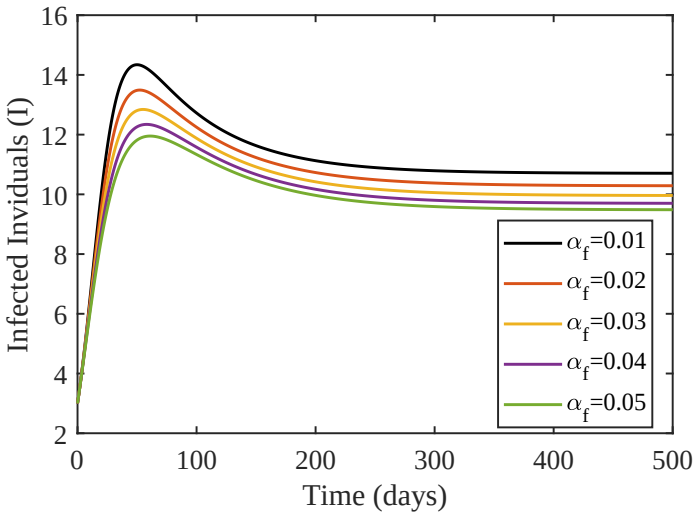

Figure 3.8: Effect of full vaccination rate on the Infected population.

The figures indicate that the disease is endemic, as all solutions of system 3.5 converge towards the endemic equilibrium E^*. Furthermore, an important observation to note is that for $\alpha = 1$, the system reaches a stationary state relatively quickly, whereas as the value of α decreases, the system takes longer to reach a stationary state. This behaviour highlights the time evolution of the epidemic.

Figure 3.4 illustrates the behaviour of the number of susceptible individuals over time for various values of α. As time progresses, the number of susceptible individuals decreases, ultimately leading to the population reaching the endemic equilibrium E^*.

Additionally, it is noteworthy that as the value of α approaches one, the trajectories converge to the steady state in a considerably shorter duration.

Figures 3.5 and 3.6 show the impact of fractional order α on the partially vaccinated and fully vaccinated individuals and it is observed that by increasing the value of α, strength of both partially and fully vaccinated individuals increases initially and gradually decreases after some time and the pattern of trajectories is reversed i.e. by decreasing the value of α, the count of vaccinated individuals increases, which is also a benefit of memory effect.

Figure 3.7 provides insights into the impact of the fractional order derivative α on the population of infected individuals. Notably, it is observed that as the value of α decreases, the time required to reach a steady state increases. Conversely, as α approaches one, the infected population achieves a steady state in a significantly shorter time frame. This indicates that when α decreases, there is a presence of a memory effect, causing the infected population to require more time to diminish or vanish entirely. In Figure 3.8, we have shown by effect of full vaccination rate α_f on the infected individuals. Here it can be seen that by increasing the value of full vaccination rate the number of infected individuals getting decrease. So, vaccination plays an important role in lowering of disease burden.

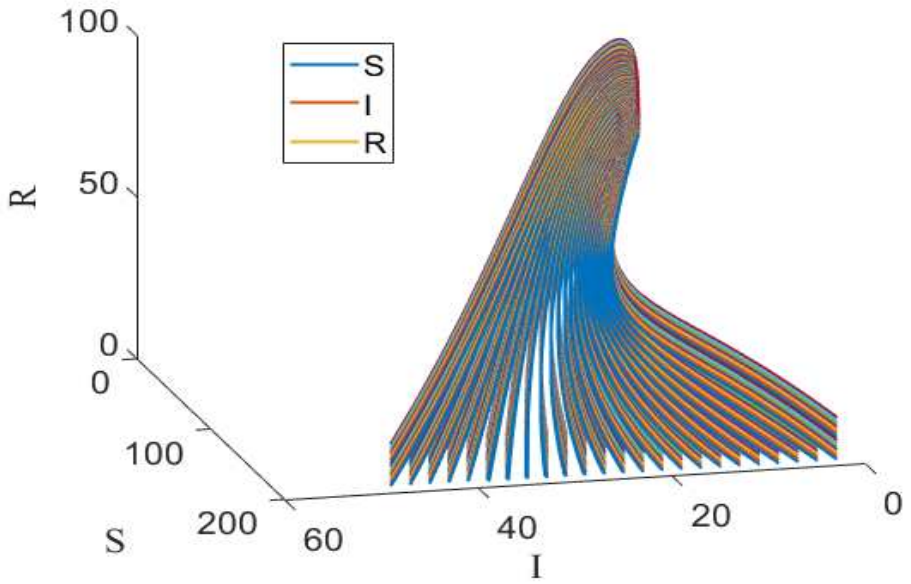

Figure 3.9: Phase plot of susceptible-infected-recovered population.

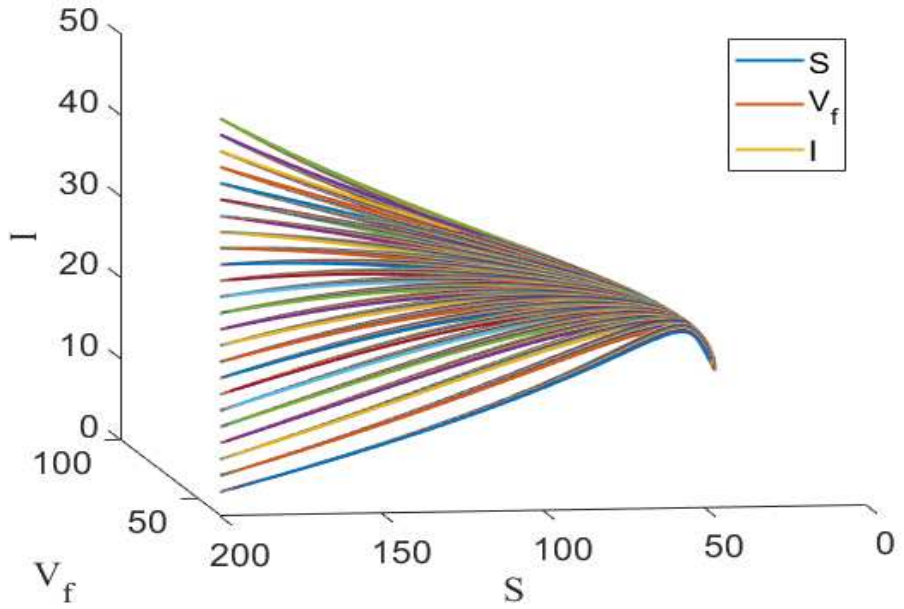

Figure 3.10: Phase plot of susceptible-fully vaccinated-infected population.

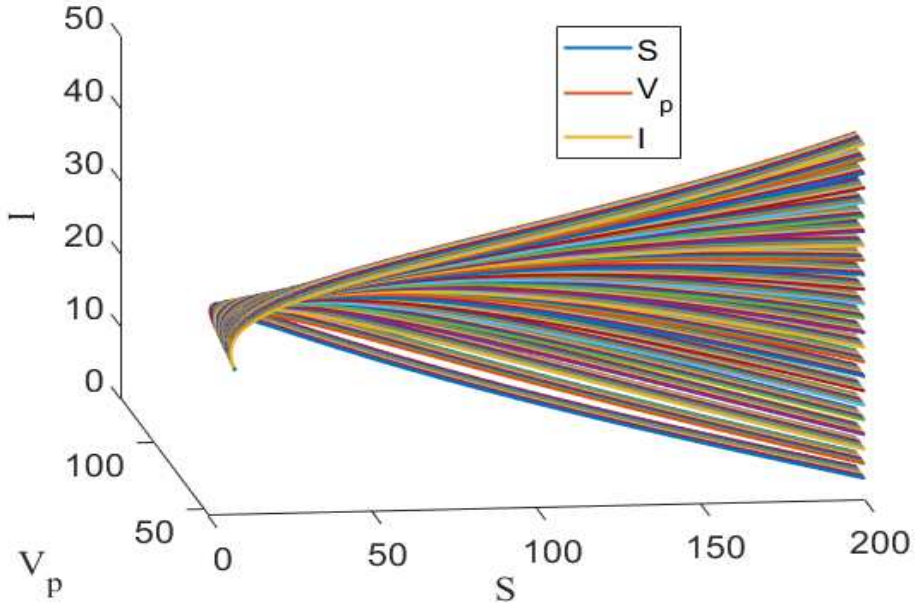

Figure 3.11: Phase plot of susceptible-partially vaccinated-infected population.

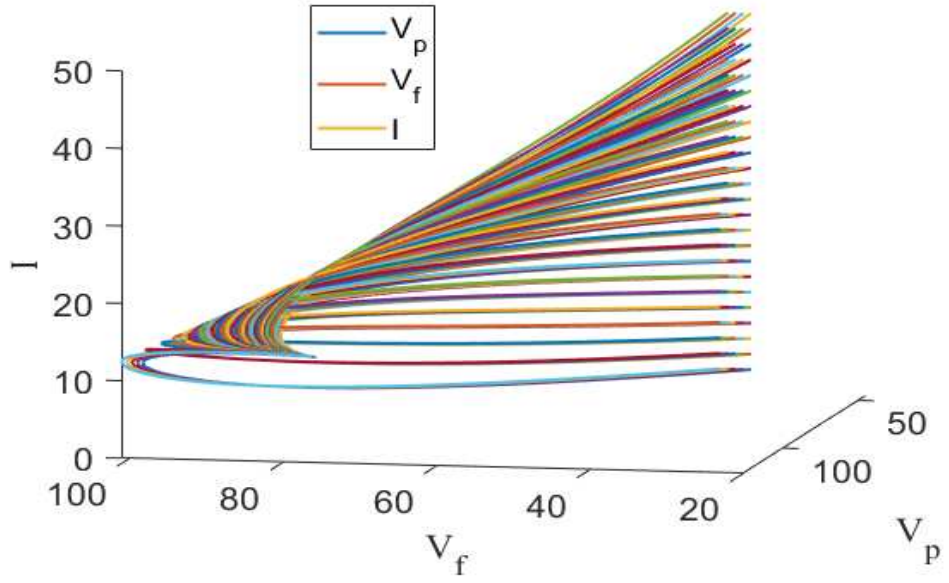

Figure 3.12: Phase plot of partially vaccinated-fully vaccinated-infected population.

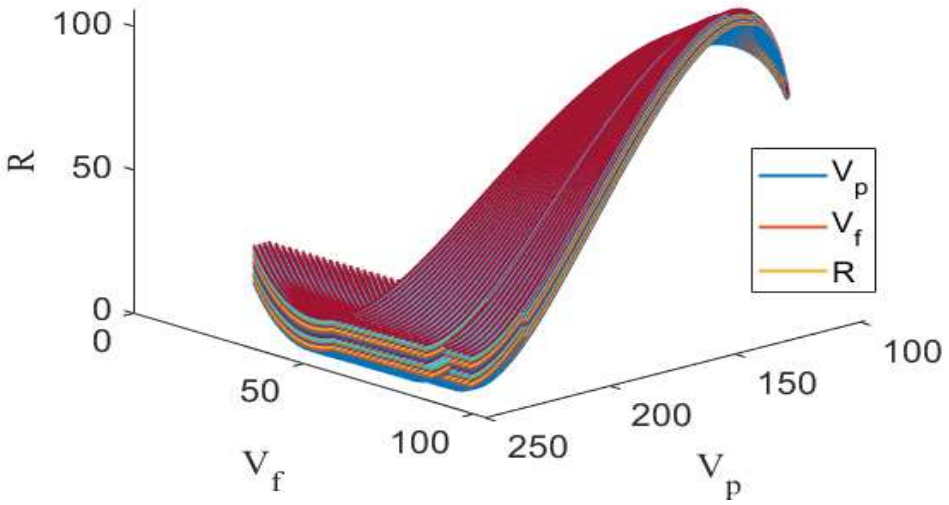

Figure 3.13: Phase plot of partially vaccinated-fully vaccinated-recovered population.

Figure 3.9, shows the phase portrait of the Susceptible, Infected and Recovered population in which it can be seen that the trajectories starting form anywhere i.e. with various initial conditions, within the region of consideration, are converging to a point which is equilibrium point (S^*, I^*, R^*). Similarly, Figure 3.10 shows the phase plot of

Susceptible, Fully Vaccinated and Infected population in which trajectories are converging to the respective equilibrium point $(S^*, {V_f}^*, I^*)$. In Figure 3.11, the converging behaviour of trajectories can be seen towards the equilibrium point $(S^*, {V_p}^*, I^*)$. The same thing can be also observed in Figure 3.12 and 3.13 that the trajectories initiating from different initial conditions are going to converge to the equilibrium point $({V_p}^*, {V_f}^*, I^*)$ and $({V_p}^*, {V_f}^*, R^*)$, respectively.

Collectively the Figures 3.9, 3.10, 3.11, 3.12 and 3.13 show that the solution trajectories are independent of the initial conditions which is nothing but the global stability of the equilibrium point $(S^*, {V_p}^*, {V_f}^*, I^*, R^*)$.

3.7.1 Quantification of effects partial and full vaccination

Assessing partial vaccination in terms of recovered population with respect to time is depicted in Figure 3.14, at different values of α and similarly, Figure 3.15 depicts the quantification of fully vaccinated and recovered individuals with time at different values of α.

It can be seen from these figures that at time 64 days and for $\alpha = 0.7$ the percentage of recovered population in case of partial vaccination is 6.42%, where as for the same time and fractional order the percentage of recovered population in case of full vaccination is 8.46%. In a similar way for fractional order $0.8, 0.9$ and 1.0 at the time $t = 57, 42,$ and 34 the percent count of recovered populations in case of partial vaccination are $8.59\%, 9.132\%$ and 9.57% and in case of full vaccination the percentage of recovered population are $11.33\%, 11.57\%$ and 12.66%. So, from here it can be seen that the percentage of recovered population is larger in case of full vaccination while less in case of partial vaccination. This gap of percentage will make significant impact in case of large population. This indicates that the full vaccination is very beneficial for public health and health agencies should also focus towards this side so that the count of partial vaccination could be as less as possible which will helpful in lowering the disease burden by enlarging the recovered population.

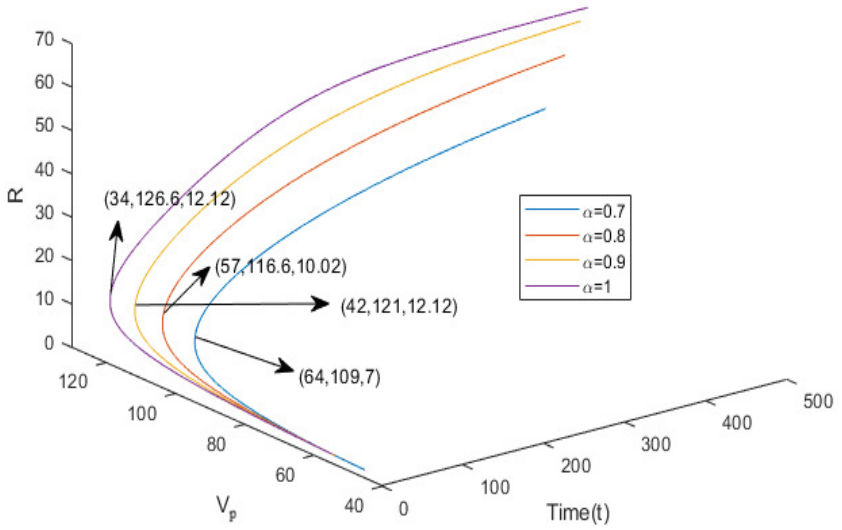

Figure 3.14: Variation in partially vaccinated and recovered individuals with respect to time at different values of α.

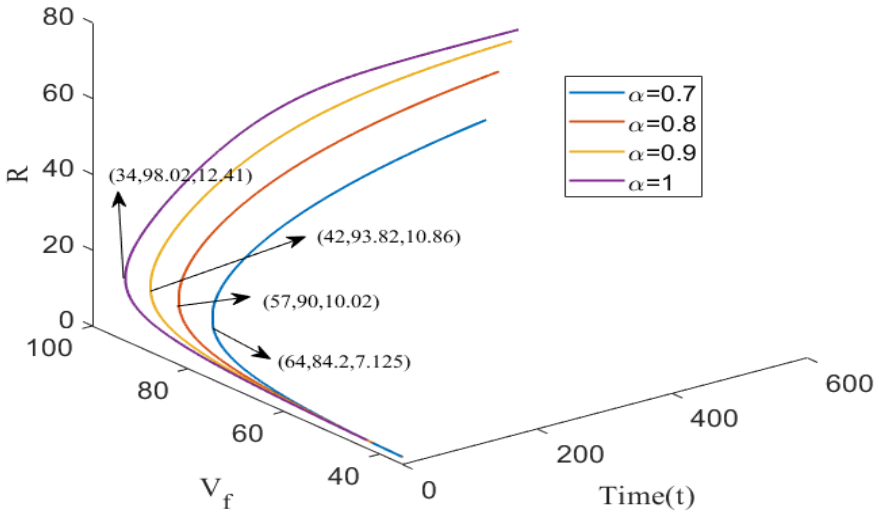

Figure 3.15: Variation in fully vaccinated and recovered individuals with respect to time at different values of α.

3.8 Discussion and Conclusion

In this chapter, a novel Caputo-fractional order *SVIR* model with Holling type-III treatment rate has been proposed by categorising the vaccinated population into two further compartments, namely, Partially vaccinated and Fully vaccinated populations. Firstly, we established the well-posedness of the fractional model with the help of the Generalized mean value theorem and Mittag-Leffler functions. Further the stability behaviour of the equilibrium points are discussed, namely DFE and EE, and also the basic reproduction number has been calculated with the help of next generation approach. It has been investigated that DFE is locally asymptotically stable for $\mathscr{R}_0 \leq 1$. Furthermore, the existence of unique positive equilibrium has shown under some feasible constraints and local stability of EE is analyzed. Through our analysis, it is determined that the endemic equilibrium (EE) is locally asymptotically stable if the condition $\mathscr{R}_0 > 1$ holds, provided that the conditions outlined in Theorem 3.5.3 are met. Additionally, the global stability behaviour of the disease-free equilibrium (DFE) and EE using a Lyapunov function under specific conditions are analyzed. The analysis has led us to conclude that the DFE is globally asymptotically stable when $\mathscr{R}_0 \leq 1$, while the EE is globally asymptotically stable when $\mathscr{R}_0 > 1$ and the conditions specified in equation (3.12) are satisfied. Further, sensitivity analysis shown in Figure 3.3 to observe the highly sensitive parameters in positive and negative manner.

In the section of numerical simulation, with the help of some experimental data given in Table 3.2, we perform some numerical simulations in favor of validation of our analytical findings. It is worth noting that the inclusion of the fractional-order derivative introduces a memory effect that influences the dynamics of the system, as evident from the time-series plot of the model. Interestingly, it was observed that the stability of the equilibria remains unaffected by variations in the fractional order α. However, the time required to reach a steady state is significantly influenced by the choice of α. Increasing the order of the fractional derivative leads to faster convergence, while lower values of α result in slower convergence. This highlights the utility of fractional derivatives over integer-order derivatives, as they offer better control over convergence rate and allow for more flexible modeling of dynamical systems.

It is also observed from the phase plots of the system that the solutions trajectories are independent of the initial population i.e. the initial population does not affect the steady state of the system. Further, as the effect of full vaccination rate over in-

fected population depict that by increasing the rate of vaccination the count of infected population will decrease. Additionally, Figures 3.14 and 3.15 depict the variations in partially and fully vaccinated with recovered individuals over time (with different memory effects). Full vaccination resulted in a higher percentage of recovered population compared to partial vaccination, indicating its greater effectiveness. This quantification highlights the importance and effects of full vaccination for public health and reducing disease burden. Thus, focus should be on full vaccination to lower the disease burden, and it will play a paramount role in controlling the epidemic spread in society.

In conclusion, the findings of this study highlight the significance of including a more realistic modeling method that involves fractional order dynamics and considers separate groups of partially and fully vaccinated populations. Policymakers and professionals can obtain more accurate projections of disease dynamics by focusing on the implications of effective full vaccination among susceptible individuals. Also it is evident that partial vaccination is not capable enough to control the spread of disease as well as it may be an unnecessary economic burden on the society. This strategy has the ability to lessen the effect of epidemics while also shortening the duration of outbreaks. Implementing such a comprehensive strategy can provide significant insights for decision-making as well as aid in the development of effective intervention measures to reduce disease spread.

Chapter 4

Optimal Control of a Fractional Order $SEIQR$ Epidemic Model with Non-monotonic Incidence and Quarantine class

---

During any infectious disease outbreak, effective and timely quarantine of infected individuals, along with preventive measures by the population, is vital for controlling the spread of infection in society. Therefore, this chapter attempts to provide a mathematically validated approach for managing the epidemic spread by incorporating the Monod-Haldane incidence rate, which accounts for psychological effects, and a saturated quarantine rate as Holling functional type III that considers the limitation in quarantining of infected individuals into the standard Susceptible-Exposed-Infected-Quarantine-Recovered $(SEIQR)$ model. The rate of change of each subpopulation is considered as the Caputo form of fractional derivative where the order of derivative represents the memory effects in epidemic transmission dynamics and can enhance the accuracy of disease prediction by considering the experience of individuals with previously encountered. The mathematical study of the model reveals that the solutions are well-posed, ensuring nonnegativity and boundedness within an attractive region. Further, the study identifies two equilibria, namely, disease-free equilibrium (DFE) and endemic equilibrium (EE); and stability analysis of equilibria is performed for local as well as global behaviours for the same. The stability behaviours of equilibria mainly

depend on the basic reproduction number $\mathscr{R}_0$ and its alternative threshold $\mathscr{T}_0$ which is computed using the Next-generation matrix method. It is investigated that DFE is locally and globally asymptotic stable when $\mathscr{R}_0 < 1$. Furthermore, the existence of the endemic equilibrium (EE) is established, and its local and global asymptotic stability is investigated using the Routh-Hurwitz criterion and the Lyapunov stability theorem for fractional order systems with $\mathscr{R}_0 > 1$ under certain conditions. Additionally, sensitivity analysis is also performed corresponding to $\mathscr{R}_0$. This chapter also addresses a fractional optimal control problem (FOCP) using Pontryagin's maximum principle aiming to minimize the spread of infection with minimal expenditure. This approach involves introducing a time-dependent control measure, $u(t)$, representing the behavioural response of susceptible individuals. Finally, numerical simulations are presented to support the analytical findings using the Adams Bashforth Moulton scheme in MATLAB, providing a comprehensive understanding of the proposed SEIQR model.

4.1 Introduction

The dynamics of disease in an epidemic model are shaped by the incidence and treatment rates [146]. The incidence rate, assessing new cases in a population over time, is pivotal. Kermack and McKendrick's bilinear form βSI becomes impractical for large populations due to susceptibles increasing the rate [92]. Researchers proposed alternative nonlinear forms, like Beddington-DeAngelis, Crowley-Martin, Holling types II and III [32; 57; 59; 98; 108; 150; 171]. In 1986, Liu et al. [118], introduced a saturated incidence rate:

$$f(S,I) = \frac{\beta I^l S}{I + \alpha I^h}, \tag{4.1}$$

capturing infectivity and behavioural inhibitions. Nonlinear rates offer realistic disease transmission aspects, displaying broader dynamic behaviours. This study focuses on the non-monotone incidence rate for $l = 1$ and $h = 2$:

$$f(S,I) = \frac{\beta IS}{I + \alpha I^2},$$

where $\frac{1}{1+\alpha I^2}$ describes the psychological effect resulting from behavioural changes in susceptibles when the number of infectives reaches a high level, and βI is a measure of the disease's infection intensity [173]. The parameter α serves as a measure of the

psychological influence of the disease on the population when the count of infectives reaches a substantial level. The functional expression $\frac{\beta IS}{I+\alpha I^2}$ is non-monotonic, also referred as the simplified Monod-Haldane (M-H) incidence rate [99]. If the incidence function is nonmonotone, that is function is increasing when I is small and decreasing when I is large, it can be used to interpret the psychological effect: for a very large number of infective individuals the infection force may decrease as the number of infective individuals increases, because, in the presence of a large number of infectives, the population may tend to reduce the number of contacts per unit time. This is important because the number of effective contacts between infective individuals and susceptible individuals decreases at high infective levels due to the quarantine of infective individuals or due to the protection measures by the susceptible individuals.

Implementing quarantine measures for infected persons is a highly successful method in controlling the spread of an epidemic in the case of an outbreak. Thus, the significance of the role played by quarantined individuals in controlling the transmission of disease cannot be ignored. This study introduces a specific quarantine class into the conventional epidemic model to investigate the impact of quarantine people. The term "quarantine" here refers to the enforced isolation or restrictions placed on the movement of infected individuals to prevent further disease dissemination. By quarantining those who have tested positive, one can significantly reduce new infection cases among susceptibles. For example, in the context of COVID-19, individuals in quarantine are those who have tested positive and are isolating in a dedicated space at home or in designated facilities like hotels, depending on the severity of the infection and associated risk factors [150]. This study also considers individuals hospitalized based on symptom severity during an infectious disease outbreak as part of the quarantined category. An assumption made in our study is that quarantined individuals remain isolated from others, preventing additional infections and contributing to a reduction in the incidence rate for new cases.

We have used nonlinear Holing type III quarantine rate for the infected individuals to transfer them into quarantined class in our model. The Holling Type III quarantine rate is characterized by a saturation effect, signifying that as the number of infected individuals increases, healthcare resources may become overwhelmed, leading to diminishing returns on additional quarantine efforts. A non-linear saturated quarantine rate captures this saturation effect by modeling how the effectiveness of

quarantine measures levels off as the number of quarantined individuals approaches a certain threshold.

For some infectious diseases, there is a proportion of population who have experienced exposure to the infectious agent but are not yet able to transmit the infection. This class is particularly relevant in models that incorporate an "incubation period", which is the time between exposure to the pathogen and the onset of infectiousness. These are referred to as exposed population. For instance, diseases such as chickenpox, measles, tuberculosis, rubella, and more, involve an extended duration wherein individuals who are infected belong to the exposed class before becoming capable of spreading the infection (see [14; 46; 85; 89]).

In this chapter, building upon the insights gained from the existing literature, our objective is to delve into the dynamics of a fractional-order *SEIQR* epidemic model. We deal with non-monotonic Monod-Haldane (M-H) incidence rate which is most suitable for widely spread epidemics and also incorporates the psychological effects of susceptibles. The nonlinear quarantine rate has been considered in the sense of Holling type III which incorporates the effects of limitations in quarantine. The combination of these two makes our model more realistic in case of an outbreak of a deadly epidemic. This study aims to attain a profound understanding that can guide the implementation of effective measures for the prevention and control of infectious diseases within populations.

The works [18; 40; 169; 182; 195] underscore the pressing need for comprehensive and effective strategies to manage the transmission of COVID-19. Current models of virus transmission frequently ignore the vital role that community awareness plays in determining an individual's vulnerability to the infection. For example, it is generally acknowledged that people who are aware of the COVID-19 hazards are more likely to take preventative action and adjust their behaviour accordingly. On the other hand, those who are unaware could act in a less careful manner, increasing their susceptibility to infection and aiding in the virus's spread. These circumstances highlight the requirement for a novel strategy that specifically incorporates community awareness into the modeling framework. The approach seeks to quantify the impact of information or community awareness on disease by examining the "behavioural response of susceptible individuals". As susceptible individuals become informed about the disease, they are likely to adopt protective measures. This emphasis on behavioural response adds a nuanced dimension to the modeling process, capturing the dynamic interplay between

awareness, individual actions, and disease transmission. By incorporating community awareness in this manner, we aim to provide a more comprehensive and realistic representation of the factors influencing the spread of infectious diseases.

This chapter emphasizes the importance of developing an appropriate model to evaluate the effectiveness of control strategies during disease outbreaks. An optimal control analysis is introduced for a transmission model that incorporates the behavioral responses of susceptible individuals, simulating the reduction of effective contacts between susceptible and infected individuals. Agrawal [2] explored fractional-order variational problems of the Riemann-Liouville type in 2002 and developed a framework for studying fractional optimal control problems (FOCP). Afterwards, Agrawal investigated FOCP for fractional-order Riemann-Liouville systems in 2004 [3]. Building on this framework, Ding studied the FOCP of the Caputo HIV model in 2012 and presented related numerical techniques [55]. While there exists substantial research on optimal control of various models, studies specifically focused on fractional-order models are relatively sparse [195]. The Adams-Bashforth-Moulton forward-backward predict-evaluate-correct-evaluate (PECE) technique and Pontryagin's maximum principle (PMP) are employed to solve the optimal control problem (OCP) and determine the most cost-effective combination of control interventions. The validity of the results is further confirmed through numerical simulations.

The remaining portions of this chapter are organized as follows: The basic presumptions of the model are presented together with a mathematical framework based on the Caputo fractional-order derivative in Section 4.2. Basic properties, encompassing aspects like positivity and boundedness, the basic reproduction number, existence of equilibria of the model and absence of backward bifurcation, are addressed in Section 4.3. Section 4.4 explores stability analysis, both locally and globally. Sensitivity analysis of basic reproduction $\mathscr{R}_0$ is given in Section 4.5. The corresponding fractional optimal control problem (FOCP) is introduced and analytically solved in Section 4.6. Section 4.7 gives the numerical scheme of the adopted numerical method and 4.8 validates the relevant theoretical results and provides a numerical solution to the corresponding fractional optimal control problem (FOCP). The chapter concludes in Section 4.9.

4.2 Formulation of fractional order epidemic model

The epidemic processes, evolution and control, in human societies, cannot be considered without any memory effect. When a disease spreads within a human population, the experience or knowledge of individuals about that disease should affect their response. If people know about the history of a certain disease in the area where they live, they use different precautions. Thus, some endogenously controlled suppression of the spreading is expected. Based on the aforementioned studies, this section proposes a new fractional-order nonlinear epidemic model employing the Caputo form of the fractional-order derivative. The model assumes a total population size denoted as $N(t)$ at any time t, divided into five sub-populations or classes: susceptible $S(t)$, exposed $E(t)$, infected $I(t)$, quarantined $Q(t)$, and recovered $R(t)$. The susceptible class $S(t)$ comprises individuals at risk of infection, while the exposed class $E(t)$ includes individuals in close contact with infected people but not yet infectious. The infected class $I(t)$ consists of individuals capable of transmitting the infection, and the quarantine class $Q(t)$ comprises those who have tested positive but are not showing symptoms of the disease yet and are either quarantined, at private suitable places or in quarantine centers, or hospitalized based on the severity of infection with time. The recovered class $R(t)$ includes individuals transitioning from $I(t)$ and $Q(t)$ due to either auto-immune response or medical treatment. For the formulation of the model, we make the following assumptions:

(A1) All the newly recruited population by births or immigration goes to the susceptible class initially, with a constant recruitment rate Λ.

(A2) When susceptible individuals come in close contact with infectious individuals, they will be infected at a rate β and move to the exposed class with a transition rate $\frac{\beta SI}{(1+\alpha I^2)}$. This transition rate function is referred to as the Monod-Haldane type incidence rate, which describes a non-monotonic behaviour of incidence rate due to psychological effects or behavioural changes of susceptible individuals in case of a high density of infectives in the community.

(A3) The progression rate from exposed to the infected class is taken as ν.

(A4) The transition rate function for quarantine to the infected population is taken as Holling type III, i.e.,$\frac{\gamma I^2}{(1+\delta I^2)}$, where γ is the quarantine rate and δ is the limitation in quarantining the people because of the limitation in the quarantine

facilities due to the unavailability of a significant number of quarantine places. The limiting value for the quarantine rate is $\frac{\gamma}{\delta}$ for the transition rate function, i.e., $\lim_{I\to\infty} \frac{\gamma I^2}{(1+\delta I^2)} = \frac{\gamma}{\delta}$.

(A5) The disease-induced death rate is considered as d_1 and d_2 for the infected and quarantined classes, respectively. Whereas, the natural death rate in all the compartments is considered as μ.

(A6) The recovery rate of the infected population due to auto-immune or treatment is taken as σ, and the recovery rate for quarantined infected individuals is taken as ω.

(A7) Recovery is assumed to be permanent here, which means recovered people are no longer susceptible to the disease and will not take part in further spreading of the disease.

(A8) It is also assumed that there is no time delay (latency period) in the model.

(A9) It is assumed that the population is homogeneously mixed.

In the presented study, the fractional-order epidemic model is presented under these assumptions. The model is presented by considering the non-monotone incidences and saturated quarantining rate for infectives along with the Caputo form of derivative for the rate of change of population in compartments into the standard $SEIQR$ model. Therefore, it can be considered a novel fractional-order epidemic model for disease transmission dynamics. The resulting fractional-order epidemic model presented under these assumptions is:

$$\begin{aligned}
{}_0D_t^{\rho} S(t) &= \Lambda - \frac{\beta SI}{1+\alpha I^2} - \mu S,\\
{}_0D_t^{\rho} E(t) &= \frac{\beta SI}{1+\alpha I^2} - \nu E - \mu E,\\
{}_0D_t^{\rho} I(t) &= \nu E - \frac{\gamma I^2}{1+\delta I^2} - \sigma I - (\mu + d_1) I,\\
{}_0D_t^{\rho} Q(t) &= \frac{\gamma I^2}{1+\delta I^2} - \omega Q - (\mu + d_2) Q,\\
{}_0D_t^{\rho} R(t) &= \sigma I + \omega Q - \mu R,
\end{aligned} \tag{4.2}$$

subject to the conditions

$$S(0) = S_0 > 0, E(0) = E_0 \geq 0, I(0) = I_0 \geq 0, Q(0) = Q_0 \geq 0, R(0) = R_0 \geq 0. \tag{4.3}$$

4.3 Basic Properties and Equilibria

4.3.1 Positivity and Boundedness of solutions

Theorem 4.3.1 *For any initial condition satisfying* (4.3)*, the solutions of the system* (4.2) *remains non-negative and uniformly bounded* $\forall\ t \geq 0$ *in the region of attraction given by*

$$\Omega = \left\{ (S,E,I,Q,R) \in \mathbb{R}^5_+ : 0 < N \leq \frac{\Lambda}{\mu} \right\}.$$

Proof 4.3.2 *After adding all the model equations, we have*

$$\begin{aligned} {}_0D^{\rho}_t (S+E+I+Q+R)(t) &= \Lambda - \mu(S+E+I+Q+R)(t) - d_1 I(t) - d_2 Q(t) \\ D^{\rho}_t (N(t)) &\leq \Lambda - \mu N(t) \end{aligned},$$

where, $N = S+E+I+Q+R$.

According to Lemma 1.1.10, it can be illustrated that,

$$N(t) \leq \left(N(0) - \frac{\Lambda}{\mu} \right) E_{\rho}(-\mu t^{\rho}) + \frac{\Lambda}{\mu},$$

where E_{α} *stands for Mittag-Leffler function as defined in Definition 1.1.2.*

Therefore,

$$\limsup_{t \to 0} N(t) \leq \frac{\Lambda}{\mu}.$$

Finally, $S(t), E(t), I(t), Q(t)$ *and* $R(t)$ *are non-negative and uniformly bounded.*

4.3.2 The Basic Reproduction Number and Equilibria

It is worth noting that the variable $R(t)$ is absent from the initial four equations. Consequently, without sacrificing generality, it can be excluded from model (4.2) for the purposes of subsequent mathematical analysis. The resulting reduced system is:

$$\begin{aligned} {}_0D^{\rho}_t S(t) &= \Lambda - \frac{\beta SI}{1+\alpha I^2} - \mu S, \\ {}_0D^{\rho}_t E(t) &= \frac{\beta SI}{1+\alpha I^2} - \nu E - \mu E, \\ {}_0D^{\rho}_t I(t) &= \nu E - \frac{\gamma I^2}{1+\delta I^2} - \sigma I - (\mu + d_1) I, \\ {}_0D^{\rho}_t Q(t) &= \frac{\gamma I^2}{1+\delta I^2} - \omega Q - (\mu + d_2) Q. \end{aligned} \tag{4.4}$$

It is evident that model (4.4) always admits a disease-free equilibrium $E_0 = E_0(\frac{\Lambda}{\mu}, 0, 0, 0)$. Now further, the basic reproduction number $\mathscr{R}_0$ associated with the system 4.4 is determined. $\mathscr{R}_0$ represents the average number of infections produced by a single infected individual in a susceptible population during their entire infectious period. If $\mathscr{R}_0$ is greater than 1, each existing infection is expected to cause more than one new infection, leading to exponential growth of the disease. Conversely, if $\mathscr{R}_0$ is less than 1, the infection is likely to die out eventually as each existing infection leads to fewer than one new infection on average. It is computed using the next-generation matrix method [47]. To this end, the right-hand side of the infected compartments is expressed as the difference $\mathscr{F}(X) - \mathscr{V}(X)$, where $\mathscr{F}(X)$ represents the rate of appearance of new infections in the compartments, and $\mathscr{V}(X)$ incorporates the remaining transitional terms, namely births, deaths, disease progression, and recovery. So, assume that

$$D_t^{\rho} X = \mathscr{F}(X) - \mathscr{V}(X),$$

where $X = (E, I, Q)^T$ and $\mathscr{F}(X)$ be the matrix of new infection term, $\mathscr{V}(X)$ be the matrix of outgoing terms. The Jacobian matrices F and V of $\mathscr{F}(X)$ and $\mathscr{V}(X)$, respectively, at infection-free equilibrium E_0 are given as:

$$F = \begin{pmatrix} 0 & \frac{\beta\Lambda}{\mu} & 0 \\ \nu & 0 & 0 \\ 0 & 0 & 0 \end{pmatrix},$$

$$V = \begin{pmatrix} \nu+\mu & 0 & 0 \\ 0 & \sigma+\mu+d_1 & 0 \\ 0 & 0 & \omega+\mu+d_2 \end{pmatrix}.$$

The next generation matrix is

$$FV^{-1} = \begin{pmatrix} 0 & \frac{\beta\Lambda}{\mu(\mu+\sigma+d_1)} & 0 \\ \frac{\nu}{\mu+\nu} & 0 & 0 \\ 0 & 0 & 0 \end{pmatrix}.$$

Now, the spectral radius, i.e., the largest eigen value of the matrix FV^{-1} represent the basic reproduction number and is given by,

$$\mathscr{R}_0 = \sqrt{\frac{\beta\Lambda\nu}{\mu(\mu+\nu)(\sigma+\mu+d_1)}}.$$

In addition, it can be shown that the model 4.4 admits an endemic steady state when $\mathscr{R}_0 > 1$. Let $E_1 = E_1(S^*, E^*, I^*, Q^*)$ be an endemic equilibrium such that $S^* > 0$, $E^* > 0$, $I^* > 0$, $Q^* > 0$ and

$$\begin{cases} \Lambda - \frac{\beta S^* I^*}{1+\alpha I^{*2}} - \mu S^* = 0, \\ \frac{\beta S^* I^*}{1+\alpha I^{*2}} - \nu E^* - \mu E^* = 0, \\ \nu E^* - \frac{\gamma I^{*2}}{1+\delta I^{*2}} - \sigma I^* - (\mu + d_1) I^* = 0, \\ \frac{\gamma I^{*2}}{1+\delta I^{*2}} - \omega Q^* - (\mu + d_2) Q^* = 0. \end{cases} \tag{4.5}$$

It follows that,

$$S^* = \frac{\Lambda(1+\alpha I^{*2})}{\beta I^* + \mu(1+\alpha I^{*2})}, \quad E^* = \frac{1}{\nu}\left[\frac{\gamma I^{*2}}{1+\delta I^{*2}} + (\sigma + \mu + d_1) I^*\right],$$

$$Q^* = \frac{\gamma I^{*2}}{(1+\delta I^{*2})(\omega + \mu + d_2)}$$

and I^* can be obtained by solving the following equation:

$$A_4 I^{*4} + A_3 I^{*3} + A_2 I^{*2} + A_1 I^* + A_0 = 0, \tag{4.6}$$

where,

$$\begin{aligned} A_4 &= \alpha\delta\mu(\mu+\nu)(\sigma+\mu+d_1), \\ A_3 &= (\mu+\nu)(\alpha\gamma\mu + \beta\delta(\sigma+\mu+d_1)), \\ A_2 &= \mu(\alpha+\delta)(\mu+\nu)(\sigma+\mu+d_1) + \beta(\nu(\gamma-\delta\Lambda) + \gamma\mu), \\ A_1 &= (\mu+\nu)(\gamma\mu + \beta(\sigma+\mu+d_1)), \\ A_0 &= \mu(\mu+\nu)(\sigma+\mu+d_1)(1-\mathscr{T}_0), \end{aligned} \tag{4.7}$$

where,

$$\mathscr{T}_0 = \frac{\beta\Lambda\nu}{\mu(\mu+\nu)(\sigma+\mu+d_1)}.$$

The coefficients A_4, A_3, A_1 are always positive. Now, there are two cases for $\mathscr{T}_0$ which are $\mathscr{T}_0 < 1$ and $\mathscr{T}_0 > 1$.

Case I: When $\mathscr{T}_0 < 1$

For $\mathscr{T}_0 < 1$, the coefficient $A_0 > 0$. So, we only need to check the sign of the coefficient A_2. Backward bifurcation may arises here depending on the sign of A_2. Backward bifurcation shows the presence of multiple positive equilibrium points, that is, even

when the alternative threshold $\mathscr{T}_0$ (or the basic reproduction number $\mathscr{R}_0$, according to proposition (4.3.5)) is below unity, disease can still persist in the society, which makes the control of the disease more challenging. Since its presence or absence can be justified by the sign of A_2 for $\mathscr{T}_0 < 1$, so incorporating $\mathscr{T}_0$ into A_2 gives us,

$$\begin{aligned}
A_2 &= \mu(\alpha+\delta)(\mu+\nu)(\sigma+\mu+d_1)+\beta(\nu(\gamma-\delta\Lambda)+\gamma\mu),\\
&= \mu(\mu+\nu)(\sigma+\mu+d_1)\left[(\alpha+\delta)+\frac{\beta\gamma(\gamma+\mu)-\beta\nu\delta\Lambda}{\mu(\mu+\nu)(\sigma+\mu+d_1)}\right],\\
&= \mu(\mu+\nu)(\sigma+\mu+d_1)\left[(\alpha+\delta)+\frac{\beta\gamma}{\mu(\sigma+\mu+d_1)}-\frac{\beta\Lambda\nu\delta}{\mu(\mu+\nu)(\sigma+\mu+d_1)}\right],\\
&= \mu(\mu+\nu)(\sigma+\mu+d_1)\left[(\alpha+\delta)+\frac{\beta\gamma}{\mu(\sigma+\mu+d_1)}-\delta\mathscr{T}_0\right]
\end{aligned} \tag{4.8}$$

As $\mathscr{T}_0 < 1$,

$$\left[(\alpha+\delta)+\frac{\beta\gamma}{\mu(\sigma+\mu+d_1)}-\delta\mathscr{T}_0\right] > \alpha+\frac{\beta\gamma}{\mu(\sigma+\mu+d_1)} \text{ (A positive quantity),}$$

i.e.

$$\left[(\alpha+\delta)+\frac{\beta\gamma}{\mu(\sigma+\mu+d_1)}-\delta\mathscr{T}_0\right] > 0,$$

This implies that sign of A_2 is positive for $\mathscr{T}_0 < 1$. Since, all the coefficients of equation (4.6) are positive i.e. there is no variation of sign therefore, the Descartes's rule of sign [188] confirms that there is no positive real root (positive equilibrium point) for $\mathscr{T}_0 < 1$. Thus, there is absence of backward bifurcation.

Theorem 4.3.3 *When* $\mathscr{T}_0 < 1$, *the equation* (4.6) *along with* (4.7) *indicates the absence of backward bifurcation in system 4.4.*

Case II: When $\mathscr{T}_0 > 1$

For $\mathscr{T}_0 > 1$, the coefficient A_0 will be of negative sign. The following will be the possibilities on the variation of signs of the coefficients of equation (4.6).

$$\begin{aligned}
&(i) \quad A_4 > 0,\ A_3 > 0,\ A_2 > 0,\ A_1 > 0 \text{ and } A_0 < 0,\\
&(ii) \quad A_4 > 0,\ A_3 > 0,\ A_2 < 0,\ A_1 > 0 \text{ and } A_0 < 0.
\end{aligned} \tag{4.9}$$

Here, we examine the case of unique endemic equilibrium only. For $\mathscr{T}_0 > 1$ and with the help of Descartes' rule of signs [188], equation (4.6) has a unique positive real root I^* possible in the case of (i). Once I^* is determined, values for S^*, E^*, and Q^* can be derived, leading to a unique positive endemic equilibrium $E_1(S^*, E^*, Q^*, I^*)$. Consequently, the following theorem establishes the existence of this equilibrium.

Theorem 4.3.4 *If $\mathscr{T}_0 > 1$, then the system 4.4 has a unique endemic equilibrium $E_1(S^*, E^*, I^*, Q^*)$.*

The numerical illustration of Theorems 4.3.3 and 4.3.4 is given in Figure 4.1 below by taking the parameter values given in Table 4.1.

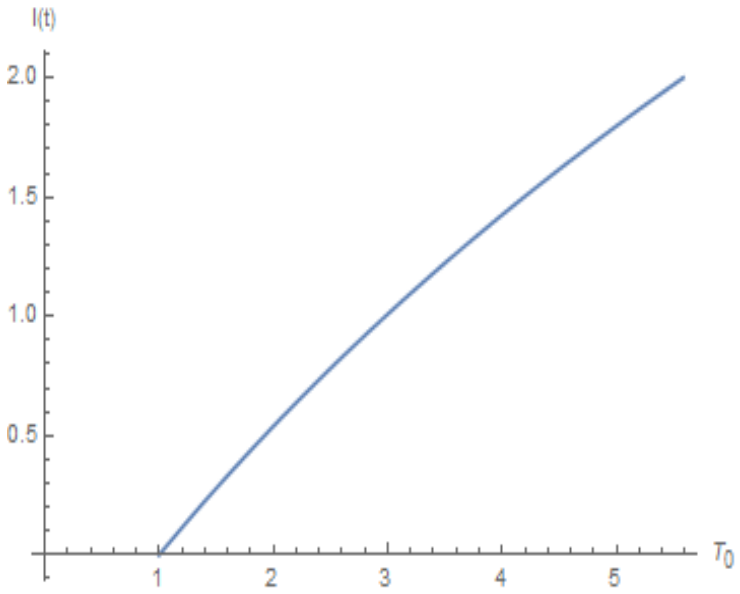

Figure 4.1: Plot of $\mathscr{T}_0$ versus $I(t)$.

Proposition 4.3.5 *(Alternative Threshold). Set*

$$\mathscr{T}_0 = \frac{\beta\Lambda\nu}{\mu(\mu+\nu)(\sigma+\mu+d_1)}.$$

Then $\mathscr{R}_0$ is smaller than (respectively, equal to or greater than) 1 if and only if the same relation holds for $\mathscr{T}_0$.

Proof 4.3.6 *By a straightforward computation we see that*

$$\begin{aligned}
\mathscr{R}_0 \leq 1 &\iff \sqrt{\frac{\beta\Lambda\nu}{\mu(\mu+\nu)(\sigma+\mu+d_1)}} \leq 1 \\
&\iff 0 < \sqrt{\frac{\beta\Lambda\nu}{\mu(\mu+\nu)(\sigma+\mu+d_1)}} \leq 1 \\
&\iff \frac{\beta\Lambda\nu}{\mu(\mu+\nu)(\sigma+\mu+d_1)} \leq 1 \\
&\iff \mathscr{T}_0 \leq 1
\end{aligned} \tag{4.10}$$

and also $\mathscr{R}_0 > 1$ is equivalent to $\mathscr{T}_0 > 1$.

This section outlined the basic properties, encompassing aspects like positivity and boundedness, the basic reproduction number $\mathscr{R}_0$ and equilibria of the model. The theorems given here determine the conditions under which an epidemic can persist or die out depending on $\mathscr{R}_0$ as well as on defined alternative threshold $\mathscr{T}_0$. Understanding these thresholds helps in devising effective control measures. Moreover, the absence of backward bifurcation is shown, which makes the control of the disease less challenging.

4.4 Stability Analysis

This section addresses the local and global staility analysis of both the equilibria. The local stability analysis involves examining the behaviour of a system in the neighborhood of an equilibrium point. It determines whether small perturbations in the equilibrium point leads the system back towards that point (stable) or diverge away from it (unstable). Whereas, the global stability analysis examines the behaviour of a system over its entire state space, not just in the neighborhood of equilibrium points.

4.4.1 Local Stability

At any equilibrium point (S_*, E_*, I_*, Q_*), the linearized system of (4.4) is derived as follows to establish local asymptotic stability:

$$\begin{cases} {}_0D_t^\rho S(t) = -\left(\dfrac{\beta I_*}{1+\alpha {I_*}^2} + \mu\right) S - \dfrac{\beta S_*(1-\alpha {I_*}^2)}{(1+\alpha {I_*}^2)^2} I, \\ {}_0D_t^\rho E(t) = \left(\dfrac{\beta I_*}{1+\alpha {I_*}^2}\right) S - (\nu+\mu)E + \dfrac{\beta S_*(1-\alpha {I_*}^2)}{(1+\alpha {I_*}^2)^2} I, \\ {}_0D_t^\rho I(t) = \nu E - \left(\dfrac{2\gamma I_*}{(1+\delta {I_*}^2)^2} + (\sigma+\mu+d_1)\right) I, \\ {}_0D_t^\rho Q(t) = \dfrac{2\gamma I_*}{(1+\delta {I_*}^2)^2} I - (\omega+\mu+d_2)Q. \end{cases} \tag{4.11}$$

Taking the Laplace transform on both sides of the system (4.11), we have

$$\begin{aligned}
s^{\rho}\mathscr{L}\{S(t)\} - s^{\rho-1}S(0) &= -\left(\frac{\beta I_*}{1+\alpha {I_*}^2} + \mu\right)\mathscr{L}\{S(t)\} - \frac{\beta S_*(1-\alpha {I_*}^2)}{(1+\alpha {I_*}^2)^2}\mathscr{L}\{I(t)\},\\
s^{\rho}\mathscr{L}\{E(t)\} - s^{\rho-1}E(0) &= \left(\frac{\beta I_*}{1+\alpha {I_*}^2}\right)\mathscr{L}\{S(t)\} - (\nu+\mu)\mathscr{L}\{E(t)\} + \frac{\beta S_*(1-\alpha {I_*}^2)}{(1+\alpha {I_*}^2)^2}\mathscr{L}\{I(t)\},\\
s^{\rho}\mathscr{L}\{I(t)\} - s^{\rho-1}I(0) &= \nu\mathscr{L}\{E(t)\} - \left(\frac{2\gamma I_*}{(1+\delta {I_*}^2)^2} + (\sigma+\mu+d_1)\right)\mathscr{L}\{I(t)\},\\
s^{\rho}\mathscr{L}\{Q(t)\} - s^{\rho-1}Q(0) &= \frac{2\gamma I_*}{(1+\delta {I_*}^2)^2}\mathscr{L}\{I(t)\} - (\omega+\mu+d_2)\mathscr{L}\{Q(t)\}.
\end{aligned} \tag{4.12}$$

The system (4.12) can be written in the following matrix form:

$$\bigtriangledown(s)\begin{pmatrix} \mathscr{L}\{S(t)\} \\ \mathscr{L}\{E(t)\} \\ \mathscr{L}\{I(t)\} \\ \mathscr{L}\{Q(t)\} \end{pmatrix} = \begin{pmatrix} a_1(s) \\ a_2(s) \\ a_3(s) \\ a_4(s) \end{pmatrix},$$

where

$$a_1(s) = s^{\rho-1}S(0),\ a_2(s) = s^{\rho-1}E(0),\ a_3(s) = s^{\rho-1}I(0),\ a_4(s) = s^{\rho-1}Q(0),$$

and

$$\bigtriangledown(s) = \begin{pmatrix} s^{\rho} + \frac{\beta I_*}{1+\alpha {I_*}^2} + \mu & 0 & \frac{\beta S_*(1-\alpha {I_*}^2)}{(1+\alpha {I_*}^2)^2} & 0 \\ -\frac{\beta I_*}{1+\alpha {I_*}^2} & s^{\rho}+\nu+\mu & -\frac{\beta S_*(1-\alpha {I_*}^2)}{(1+\alpha {I_*}^2)^2} & 0 \\ 0 & -\nu & s^{\rho} + \frac{2\gamma I_*}{(1+\delta {I_*}^2)^2} + \sigma + \mu + d_1 & 0 \\ 0 & 0 & -\frac{2\gamma I_*}{(1+\delta {I_*}^2)^2} & s^{\rho}+\omega+\mu+d_2 \end{pmatrix}. \tag{4.13}$$

In this case, the characteristic polynomial of the system 4.4 is $det(\bigtriangledown(s))$, and the characteristic matrix is $\bigtriangledown(s)$. The distribution of eigenvalues of the characteristic polynomial $det(\bigtriangledown(s))$ may be utilized to examine the local stability of system (4.4).

Now, to analyze the local stability of disease-free equilibrium $E_0\left(\frac{\Lambda}{\mu},0,0,0\right)$, the characteristic matrix of system 4.4 at E_0 is determined as follows:

$$\bigtriangledown(s)=\begin{pmatrix} s^{\rho}+\mu & 0 & \frac{\beta\Lambda}{\mu} & 0 \\ 0 & s^{\rho}+\nu+\mu & -\frac{\beta\Lambda}{\mu} & 0 \\ 0 & -\nu & s^{\rho}+\sigma+\mu+d_1 & 0 \\ 0 & 0 & 0 & s^{\rho}+\omega+\mu+d_2 \end{pmatrix}. \tag{4.14}$$

So, the characteristic equation is:

$$det(\bigtriangledown(s))=\frac{(s^{\rho}+\mu)\,(s^{\rho}+d_2+\mu+\omega)\,[\beta\Lambda\nu+\mu\,(\mu+\nu+s^{\rho})\,(d_1+\mu+s^{\rho}+\sigma)]}{\mu}=0$$

Let $\lambda=s^{\rho}$, then the characteristic equation can be written as:

$$(\lambda+\mu)\,(\lambda+d_2+\mu+\omega)\,[-\beta\Lambda\nu+\mu\,(\mu+\nu+\lambda)\,(d_1+\mu+\lambda+\sigma)]=0 \tag{4.15}$$

Since the stability can be justified by the negative eigen value of characteristic equation, from equation (4.15) we have two negative eigenvalues $\lambda_1=-\mu$ and $\lambda_2=-(\omega+\mu+d_2)$ and the rest of the eigen values can be analyzed by the following factor of equation (4.15):

$$[-\beta\Lambda\nu+\mu\,(\mu+\nu+\lambda)\,(d_1+\mu+\lambda+\sigma)]=0,$$

which can be re-written as the following quadratic equation:

$$\left[\mu\lambda^2+\mu\lambda\,(\mu(\mu+\nu)+(\sigma+\mu+d_1))+\mu(\mu+\nu)(\sigma+\mu+d_1)(1-\mathscr{T}_0)\right]=0,$$

$$\lambda^2+\lambda\,(\mu(\mu+\nu)+(\sigma+\mu+d_1))+(\mu+\nu)(\sigma+\mu+d_1)(1-\mathscr{T}_0)=0.$$

Now, it can be seen that all the coefficients of the above quadratic equations are positive. So, Routh-Hurwitz criterion [4] assures that the equation has two roots with negative real parts. So, finally all the eigen values of characteristic equation (4.15) are with negative real part and therefore the disease-free equilibrium E_0 is locally asymptotically stable. Thus, we have the following theorem.

Theorem 4.4.1 *The disease-free equilibrium E_0 is locally asymptotically stable when the threshold value $\mathscr{T}_0$ (or $\mathscr{R}_0$ by Proposition 4.3.5) is less than unity.*

To analyze the local stability of the endemic equilibrium E_1, the characteristic matrix $\bigtriangledown(s)$ corresponding to equation (4.13) at E_1 is obtained as follows:

$$\bigtriangledown(s)=\begin{pmatrix} s^\rho+\frac{\beta I^*}{1+\alpha I^{*2}}+\mu & 0 & \frac{\beta S^*(1-\alpha I^{*2})}{(1+\alpha I^{*2})^2} & 0 \\ -\frac{\beta I^*}{1+\alpha I^{*2}} & s^\rho+\nu+\mu & -\frac{\beta S^*(1-\alpha I^{*2})}{(1+\alpha I^{*2})^2} & 0 \\ 0 & -\nu & s^\rho+\frac{2\gamma I^*}{(1+\delta I^{*2})^2}+\sigma+\mu+d_1 & 0 \\ 0 & 0 & -\frac{2\gamma I^*}{(1+\delta I^{*2})^2} & s^\rho+\omega+\mu+d_2 \end{pmatrix} \tag{4.16}$$

Let $\Omega=s^\rho$, then the characteristic equation of the characteristic matrix (4.16) is

$$\begin{aligned} det(\bigtriangledown(s))=\frac{\begin{aligned}&(d_2+\mu+\omega+\Omega)\big[(\alpha I^{*2}+1)^3(\alpha I^{*2}\mu+\alpha I^{*2}\Omega+I^*\beta+\mu+\Omega)\\ &(\mu+\nu+\Omega)(I^{*4}\delta^2\mu+I^{*4}\delta^2\sigma+I^{*4}\delta^2\Omega+I^{*4}\delta^2 d_1+2I^{*2}\delta d_1\\ &+2I^{*2}\delta\mu+2I^{*2}\delta\sigma+2I^{*2}\delta\Omega+2I^*\gamma+d_1+\mu+\sigma+\Omega)\\ &+\nu(I^{*2}\delta+1)^2(\alpha^3I^{*6}\beta\mu S+\alpha^3I^{*6}\beta S\Omega+\alpha^2I^{*4}\beta\mu S+\alpha^2I^{*4}\beta S\Omega\\ &-\alpha I^{*2}\beta\mu S-\alpha I^{*2}\beta S\Omega-\beta\mu S-\beta S\Omega)\big]\end{aligned}}{(\alpha I^{*2}+1)^4(I^{*2}\delta+1)^2}=0. \end{aligned} \tag{4.17}$$

This can be re-written as,

$$\begin{aligned} det(\bigtriangledown(s))=&(d_2+\mu+\omega+\Omega)\big[(\alpha I^{*2}+1)^3(\alpha I^{*2}\mu+\alpha I^{*2}\Omega+I^*\beta+\mu+\Omega)\\ &(\mu+\nu+\Omega)(I^{*4}\delta^2\mu+I^{*4}\delta^2\sigma+I^{*4}\delta^2\Omega+I^{*4}\delta^2 d_1+2I^{*2}\delta d_1\\ &+2I^{*2}\delta\mu+2I^{*2}\delta\sigma+2I^{*2}\delta\Omega+2I^*\gamma+d_1+\mu+\sigma+\Omega)\\ &+\nu(I^{*2}\delta+1)^2(\alpha^3I^{*6}\beta\mu S+\alpha^3I^{*6}\beta S\Omega+\alpha^2I^{*4}\beta\mu S\\ &+\alpha^2I^{*4}\beta S\Omega-\alpha I^{*2}\beta\mu S-\alpha I^{*2}\beta S\Omega-\beta\mu S-\beta S\Omega)\big]=0. \end{aligned} \tag{4.18}$$

From here, one of the eigen values is $\Omega_1=-(\omega+\mu+d_2)$ and rest of the eigen values are analyzed by the equation,

$$\begin{aligned} &(\alpha I^{*2}+1)^3(\alpha I^{*2}\mu+\alpha I^{*2}\Omega+I^*\beta+\mu+\Omega)(\mu+\nu+\Omega)\\ &(I^{*4}\delta^2\mu+I^{*4}\delta^2\sigma+I^{*4}\delta^2\Omega+I^{*4}\delta^2 d_1+2I^{*2}\delta d_1+2I^{*2}\delta\mu+2I^{*2}\delta\sigma+2I^{*2}\delta\Omega\\ &+2I^*\gamma+d_1+\mu+\sigma+\Omega)+\nu(I^{*2}\delta+1)^2(\alpha^3I^{*6}\beta\mu S+\alpha^3I^{*6}\beta S\Omega\\ &+\alpha^2I^{*4}\beta\mu S+\alpha^2I^{*4}\beta S\Omega-\alpha I^{*2}\beta\mu S-\alpha I^{*2}\beta S\Omega-\beta\mu S-\beta S\Omega)=0, \end{aligned} \tag{4.19}$$

which reduces into the following polynomial:

$$A_3\Omega^3+A_2\Omega^2+A_1\Omega+A_0=0, \tag{4.20}$$

where,

$$A_3 = \left(\alpha I^{*2}+1\right)^4\left(I^{*2}\delta+1\right)^2,$$
$$A_2 = \left(\alpha I^{*2}+1\right)^3\left(I^*\left(2\left(\alpha I^{*2}\gamma+\gamma\right)+I^*\left(\alpha\left(I^{*2}\delta+1\right)^2+\delta\left(I^{*2}\delta+2\right)\right)(3\mu+\nu+\sigma)\right.\right.$$
$$\left.\left.+\beta\left(I^{*2}\delta+1\right)^2\right)+d_1\left(\alpha I^{*2}+1\right)\left(I^{*2}\delta+1\right)^2+3\mu+\nu+\sigma\right),$$

$$A_1 = \left(\alpha I^{*2}+1\right)^2\left(\alpha^2 I^{*8}\delta^2\left(3\mu^2+2\mu(\nu+\sigma)+\nu\sigma\right)+\alpha I^{*7}\beta\delta^2(2\mu+\nu+\sigma)\right.$$
$$+\alpha I^{*6}\delta\left(2\sigma(\alpha+\delta)(2\mu+\nu)+6\alpha\mu^2+4\alpha\mu\nu+6\delta\mu^2+4\delta\mu\nu+\beta\delta\nu S^*\right)$$
$$+I^{*5}\left((2\mu+\nu)\left(2\alpha^2\gamma+2\alpha\beta\delta+\beta\delta^2\right)+\beta\delta\sigma(2\alpha+\delta)\right)$$
$$+I^{*4}\left(\alpha^2\left(3\mu^2+2\mu(\nu+\sigma)+\nu\sigma\right)+2\alpha\left(2\delta\left(3\mu^2+2\mu(\nu+\sigma)+\nu\sigma\right)\right.\right.$$
$$\left.\left.+\beta(\gamma+\delta\nu S^*)\right)+\delta^2\left(3\mu^2+2\mu(\nu+\sigma)+\nu(\sigma-\beta S^*)\right)\right)+I^{*3}(\alpha(\beta+4\gamma)(2\mu+\nu)$$
$$+\alpha\beta\sigma+2\beta\delta(2\mu+\nu+\sigma))+d_1\left(\alpha I^{*2}+1\right)\left(I^{*2}\delta+1\right)^2(I^*(\alpha I^*(2\mu+\nu)+\beta)$$
$$+2\mu+\nu)+I^{*2}\left(2(\alpha+\delta)\left(3\mu^2+2\mu(\nu+\sigma)+\nu\sigma\right)+2\beta\gamma+\beta\nu S^*(\alpha-2\delta)\right)$$
$$\left.+I^*(\beta+2\gamma)(2\mu+\nu)+I^*\beta\sigma+3\mu^2+2\mu(\nu+\sigma)+\nu(\sigma-\beta S^*)\right),$$
$$A_0 = \left(\alpha I^{*2}+1\right)^2\left(\alpha^2 I^{*8}\delta^2\mu(\mu+\nu)(\mu+\sigma)+\alpha I^{*7}\beta\delta^2(\mu+\nu)(\mu+\sigma)\right.$$
$$+\alpha I^{*6}\delta\mu(2\alpha(\mu+\nu)(\mu+\sigma)+\delta(2(\mu+\nu)(\mu+\sigma)+\beta\nu S^*))$$
$$+I^{*5}(\mu+\nu)\left(2\alpha^2\gamma\mu+2\alpha\beta\delta(\mu+\sigma)+\beta\delta^2(\mu+\sigma)\right)+I^{*4}\left(\alpha^2\mu(\mu+\nu)(\mu+\sigma)\right.$$
$$+2\alpha(2\delta\mu(\mu+\nu)(\mu+\sigma)+\beta(\gamma(\mu+\nu)+\delta\mu\nu S^*))+\delta^2\mu((\mu+\nu)(\mu+\sigma)$$
$$\left.-\beta\nu S^*)\right)+I^{*3}(\mu+\nu)(\alpha(\beta(\mu+\sigma)+4\gamma\mu)+2\beta\delta(\mu+\sigma))$$
$$+d_1\left(\alpha I^{*2}+1\right)\left(I^{*2}\delta+1\right)^2(\mu+\nu)(I^*(\alpha I^*\mu+\beta)+\mu)+I^{*2}(2\mu(\alpha+\delta)$$
$$(\mu+\nu)(\mu+\sigma)+\beta(2\gamma(\mu+\nu)+\mu\nu S^*(\alpha-2\delta)))+I^*(\mu+\nu)(\beta(\mu+\sigma)$$
$$\left.+2\gamma\mu)+\mu((\mu+\nu)(\mu+\sigma)-\beta\nu S^*)\right).$$

Considering $K_0 = \dfrac{A_0}{A_3}$, $K_1 = \dfrac{A_1}{A_3}$, and $K_2 = \frac{A_2}{A_3}$, equation (4.20) becomes,

$$P(\Omega) = \Omega^3 + K_2\Omega^2 + K_1\Omega + K_0. \tag{4.21}$$

The Routh-Hurwitz criteria for fractional order systems [4] demonstrates that the roots of the aforementioned polynomial, which meet $|arg\Omega_i| > \frac{\rho\pi}{2}$, $i = 1,2,3$, indicates local

stability. So, corresponding to the above polynomial $P(\Omega)$, the discriminant $D(\Omega)$ is,

$$D(\Omega) = \begin{vmatrix} 1 & K_2 & K_1 & K_0 & 0 \\ 0 & 1 & K_2 & K_1 & K_0 \\ 3 & 2K_2 & K_1 & 0 & 0 \\ 0 & 3 & K_2 & K_1 & 0 \\ 0 & 0 & 3 & 2K_2 & K_1 \end{vmatrix}$$
$$= 18K_2K_1K_0 + (K_2K_1)^2 - 4K_0{K_2}^3 - 4{K_1}^3 - 27{K_0}^2.$$

For $P(\Omega) = 0$ having three roots with negative real parts, we have the following theorem which ensures the local stability of $E_1(S^*, E^*, I^*, Q^*)$ using [4]:

Theorem 4.4.2 *The endemic equilibrium $E_1(S^*, E^*, I^*, Q^*)$ is locally asymptotically stable when any of the following conditions hold:*

(i) $K_2 > 0,\ K_0 > 0,\ K_2K_1 > K_0$ *if* $D(\Omega) > 0$,

(ii) *If* $D(\Omega) < 0,\ K_2 \geq 0,\ K_1 \geq 0,\ K_0 > 0,\ \rho < \frac{2}{3}$,

(iii) *If* $D(\Omega) < 0,\ K_2 > 0,\ K_1 > 0,\ K_2K_1 = K_0,\ \rho \in (0, 1]$.
Otherwise, the endemic equilibrium $E_1(S^*, E^*, I^*, Q^*)$ is unstable when the condition $D(\Omega) < 0,\ K_2 < 0,\ K_1 < 0,\ \rho > \frac{2}{3}$ holds because in this case all the roots satisfy the condition $|arg(\Omega_i)| < \frac{\rho\pi}{2}$.

4.4.2 Global Stability

This subsection analyzes the global stability of disease-free equilibrium E_0 and endemic equilibrium E_1 with the help of Lyapunov stability method for fractional order system. The global stability of the disease-free equilibrium E_0 is first discussed. To this end, the following positive definite Lyapunov function is constructed:

$$\mathbb{L}(t) = \frac{\nu}{(\mu + \nu)} E(t) + I(t).$$

Differentiating both sides with respect to t along with E_0 for order ρ, we get,

$$
\begin{aligned}
{}_0D_t^{\rho}\mathbb{L}(t) &= \frac{\nu}{(\mu+\nu)}\,{}_0D_t^{\rho}E(t) + {}_0D_t^{\rho}I(t) \\
&= \frac{\nu}{(\mu+\nu)}\left[\frac{\beta SI}{1+\alpha I^2} - (\nu+\mu)E\right] + \left[\nu E - \frac{\gamma I^2}{1+\delta I^2} - (\sigma+\mu+d_1)I\right] \\
&= \frac{\nu}{(\mu+\nu)}\frac{\beta SI}{1+\alpha I^2} - \frac{\gamma I^2}{1+\delta I^2} - (\sigma+\mu+d_1)I \\
&\leq \frac{\nu}{(\mu+\nu)}\beta SI - (\sigma+\mu+d_1)I - \frac{\gamma I^2}{1+\delta I^2} \\
&\leq \left[\frac{\nu}{(\mu+\nu)}\beta S - (\sigma+\mu+d_1)\right]I - \frac{\gamma I^2}{1+\delta I^2} \\
&\leq (\sigma+\mu+d_1)\left[\frac{\beta\Lambda\nu}{\mu(\mu+\nu)(\sigma+\mu+d_1)} - 1\right]I - \frac{\gamma I^2}{1+\delta I^2} \\
&\leq (\sigma+\mu+d_1)\,(\mathscr{T}_0 - 1)\,I - \frac{\gamma I^2}{1+\delta I^2} \\
&\leq 0 \quad \text{if} \quad \mathscr{T}_0 \leq 1.
\end{aligned}
$$

It is clear that ${}_0D_t^{\rho}\mathbb{L}(t)$ is negative when $\mathscr{T}_0 < 1$ (or $\mathscr{R}_0 < 1$, by proposition (4.3.5)) and equal to 0 at E_0. Hence, by the Lyapunov stability theorem [116; 44], E_0 is globally asymptotically stable when $\mathscr{T}_0 < 1$ (or $\mathscr{R}_0 < 1$) and thus we have the following theorem:

Theorem 4.4.3 *The disease free equilibrium E_0 is globally asymptotically stable when the threshold vale $\mathscr{T}_0$ (or $\mathscr{R}_0$ by Proposition* (4.3.5)*) is less than unity.*

Now, moving towards the global stability of endemic equilibrium. To prove this, we constructed the following positive definite Lyapunov function,

$$
\begin{aligned}
\mathbb{L}(t) = &\left(S - S^* - S^*\log\frac{S}{S^*}\right) + \left(E - E^* - E^*\log\frac{E}{E^*}\right) \\
&+ \left(I - I^* - I^*\log\frac{I}{I^*}\right) + \left(Q - Q^* - Q^*\log\frac{Q}{Q^*}\right).
\end{aligned}
$$

The differentiation of both sides with respect to t along with the endemic equilibrium E_1 for order ρ with the help of Lemma 1.1.9 is:

$$\begin{aligned}
{}_0D_t^{\rho}\mathbb{L}(t) &\leq \left(1-\frac{S^*}{S}\right){}_0D_t^{\rho}S(t)+\left(1-\frac{E^*}{E}\right){}_0D_t^{\rho}E(t)+\left(1-\frac{I^*}{I}\right){}_0D_t^{\rho}I(t)\\
&+\left(1-\frac{Q^*}{Q}\right){}_0D_t^{\rho}Q(t)\\
&\leq \left(1-\frac{S^*}{S}\right)\left(\Lambda-\frac{\beta SI}{1+\alpha I^2}-\mu S\right)+\left(1-\frac{E^*}{E}\right)\left(\frac{\beta SI}{1+\alpha I^2}-(\nu+\mu)E\right)\\
&+\left(1-\frac{I^*}{I}\right)\left(\nu E-\frac{\gamma I^2}{1+\delta I^2}-(\sigma+\mu+d_1)I\right)\\
&+\left(1-\frac{Q^*}{Q}\right)\left(\frac{\gamma I^2}{1+\delta I^2}-(\omega+\mu+d_2)Q\right).
\end{aligned}$$

Let $G(I)=\frac{I}{1+\alpha I^2}$, $F(I)=\frac{I^2}{1+\delta I^2}$, then from the steady state equation (4.5), we also have:

$$\Lambda=\beta S^*G(I^*)+\mu S^*,\quad (\nu+\mu)=\frac{\beta S^*G(I^*)}{E^*},$$
$$\nu=\frac{\gamma F(I^*)}{E^*}+(\sigma+\mu+d_1)\frac{I^*}{E^*},\quad (\omega+\mu+d_2)=\frac{\gamma F(I^*)}{Q^*}.$$

Thus,

$$\begin{aligned}
{}_0D_t^{\rho}\mathbb{L}(t) &\leq \left(1-\frac{S^*}{S}\right)(\beta S^*G(I^*)+\mu S^*-\beta SG(I)-\mu S)\\
&+\left(1-\frac{E^*}{E}\right)\left(\beta SG(I)-\beta S^*G(I^*)\frac{E}{E^*}\right)\\
&+\left(1-\frac{I^*}{I}\right)\left(\gamma F(I^*)\frac{E}{E^*}+(\sigma+\mu+d_1)I^*\frac{E}{E^*}-\gamma F(I)-(\sigma+\mu+d_1)I\right)\\
&+\left(1-\frac{Q^*}{Q}\right)\left(\gamma F(I)-\gamma F(I^*)\frac{Q}{Q^*}\right)
\end{aligned}$$

$$
\begin{aligned}
&= \mu S^* \left(2 - \frac{S^*}{S} - \frac{S}{S^*}\right) + \beta S^* G(I^*) \left(1 - \frac{S^*}{S} + \frac{G(I)}{G(I^*)} - \frac{S}{S^*}\frac{G(I)}{G(I^*)}\right) \\
&\quad + \beta S^* G(I^*) \left(1 - \frac{E}{E^*} - \frac{E^*}{E}\frac{S}{S^*}\frac{G(I)}{G(I^*)} + \frac{S}{S^*}\frac{G(I)}{G(I^*)}\right) \\
&\quad + \gamma F(I^*)\frac{E}{E^*}\left(1 - \frac{I^*}{I} - \frac{E^*}{E}\frac{F(I)}{F(I^*)} + \frac{I^*}{I}\frac{E^*}{E}\frac{F(I)}{F(I^*)}\right) \\
&\quad + (\sigma + \mu + d_1) I^* \left(1 + \frac{E}{E^*} - \frac{E}{E^*}\frac{I^*}{I} - \frac{I}{I^*}\right) \\
&\quad + \gamma F(I^*)\left(1 + \frac{F(I)}{F(I^*)} - \frac{Q^*}{Q}\frac{F(I)}{F(I^*)} - \frac{Q}{Q^*}\right) \\
&\leq \mu S^* \left(2 - \frac{S^*}{S} - \frac{S}{S^*}\right) \\
&\quad + \beta S^* G(I^*) \left(2 - \frac{S^*}{S} - \frac{E}{E^*} + \frac{G(I)}{G(I^*)}\left(1 - \frac{E^*}{E}\frac{S}{S^*}\right)\right) \\
&\quad + \gamma F(I^*)\frac{E}{E^*}\left(1 - \frac{I^*}{I} - \frac{E^*}{E}\frac{F(I)}{F(I^*)} + \frac{I^*}{I}\frac{E^*}{E}\frac{F(I)}{F(I^*)}\right) \\
&\quad + (\sigma + \mu + d_1) I^* \left(1 + \frac{E}{E^*} - \frac{E}{E^*}\frac{I^*}{I} - \frac{I}{I^*}\right) \\
&\quad + \gamma F(I^*)\left(1 + \frac{F(I)}{F(I^*)} - \frac{Q^*}{Q}\frac{F(I)}{F(I^*)} - \frac{Q}{Q^*}\right).
\end{aligned}
$$

Clearly, by the property of arithmetic mean, we have

$$
\left(2 - \frac{S^*}{S} - \frac{S}{S^*}\right) \leq 0,
$$

and if

$$
\left.
\begin{aligned}
&\left(2 - \frac{S^*}{S} - \frac{E}{E^*} + \frac{G(I)}{G(I^*)}\left(1 - \frac{E^*}{E}\frac{S}{S^*}\right)\right) \leq 0, \\
&\left(1 - \frac{I^*}{I} - \frac{E^*}{E}\frac{F(I)}{F(I^*)} + \frac{I^*}{I}\frac{E^*}{E}\frac{F(I)}{F(I^*)}\right) \leq 0, \\
&\left(1 + \frac{E}{E^*} - \frac{E}{E^*}\frac{I^*}{I} - \frac{I}{I^*}\right) \leq 0, \\
&\left(1 + \frac{F(I)}{F(I^*)} - \frac{Q^*}{Q}\frac{F(I)}{F(I^*)} - \frac{Q}{Q^*}\right) \leq 0,
\end{aligned}
\right\} \tag{4.22}
$$

then, ${}_0D_t^{\rho}\mathbb{L}(t) \leq 0$. Hence, the Lyapunov stability theorem [116; 44], ensures that the endemic equilibrium $E_1(S^*, E^*, I^*, Q^*)$ is globally asymptotically stable when $\mathscr{T}_0 > 1$ (*or* $\mathscr{R}_0 > 1$ by Proposition (4.3.5)). Thus, we have the following theorem:

Theorem 4.4.4 *The endemic equilibrium $E_1(S^*, E^*, I^*, Q^*)$ is globally asymptotically stable when $\mathscr{T}_0 > 1$ (or $\mathscr{R}_0 > 1$ by Proposition (4.3.5)) for all $\alpha \in [0, 1)$.*

In summary, this section explored the stability analysis which helps in understanding the long-term behaviour of the epidemic. By studying the stability of different equilibria (e.g., disease-free equilibrium or endemic equilibrium), one can assess whether the disease will persist at a certain level in the population or eventually die out. As stated in the theorems, the threshold value $\mathscr{T}_0$ indicates that $\mathscr{T}_0 < 1$ signifies the asymptotic stability of the disease-free equilibrium (Theorems 4.4.1 and 4.4.3). On the other hand, for the disease to persist in the society, the threshold value $\mathscr{T}_0$ must be greater than 1. In other words, we can say that the endemic equilibrium will be asymptotically stable when $\mathscr{T}_0 > 1$ (theorems 4.4.2 and 4.4.4). This information is crucial for public health planning and resource allocation.

4.5 Sensitivity Analysis

Sensitivity analysis is used to determine the model factors that affect the fundamental rate of reproduction of various infectious diseases financially. Using this method, epidemiologists may predict crucial elements required for the dynamics of disease transmission. We must ascertain the values of the sensitivity indices in order to comprehend the model parameters that must be maintained or watched over in order to prevent or control the impacts of illness. To stop the spread of infection, we need to determine the model parameters that are sensitive to comprehend the dynamics of disease transmission. We need to estimate the change in the basic reproduction number with respect to various model parameters to get the normalized forward sensitivity index of the basic reproduction number.

Definition 4.5.1 *[158] The normalized forward sensitivity index of a variable z, which depends on a parameter x, is defined as*

$$W_x^z = \frac{\partial z}{\partial x} \times \frac{x}{z}.$$

So, for $\mathscr{R}_0$, the sensitivity index is $W_x^{\mathscr{R}_0} = \dfrac{\partial \mathscr{R}_0}{\partial x} \times \dfrac{x}{\mathscr{R}_0}$, which shows how sensitive $\mathscr{R}_0$ to the parameter x. The sensitivity index for the parameters of interest are:

$$W_\beta^{\mathscr{R}_0} = \frac{1}{2},\ W_\mu^{\mathscr{R}_0} = -\frac{d_1(2\mu+\nu)+3\mu^2+2\mu(\nu+\sigma)+\nu\sigma}{2(\mu+\nu)(d_1+\mu+\sigma)},\ W_\Lambda^{\mathscr{R}_0} = \frac{1}{2},$$
$$W_\sigma^{\mathscr{R}_0} = -\frac{\sigma}{2(d_1+\mu+\sigma)},\ W_\nu^{\mathscr{R}_0} = \frac{\mu}{2(\mu+\nu)},\ W_{d_1}^{\mathscr{R}_0} = -\frac{d_1}{2(d_1+\mu+\sigma)}.$$

These sensitivity indices are evaluated with the help of parametric values given in Table 4.1, as follows and also given by the bar diagram in Figure 4.2.

$$W_{\beta}^{\mathscr{R}_0} = 0.5,\ W_{\mu}^{\mathscr{R}_0} = -0.7727,\ W_{\Lambda}^{\mathscr{R}_0} = 0.5,\ W_{\sigma}^{\mathscr{R}_0} = -0.0455,$$
$$W_{\nu}^{\mathscr{R}_0} = 0.0909,\ W_{d_1}^{\mathscr{R}_0} = -0.2727.$$

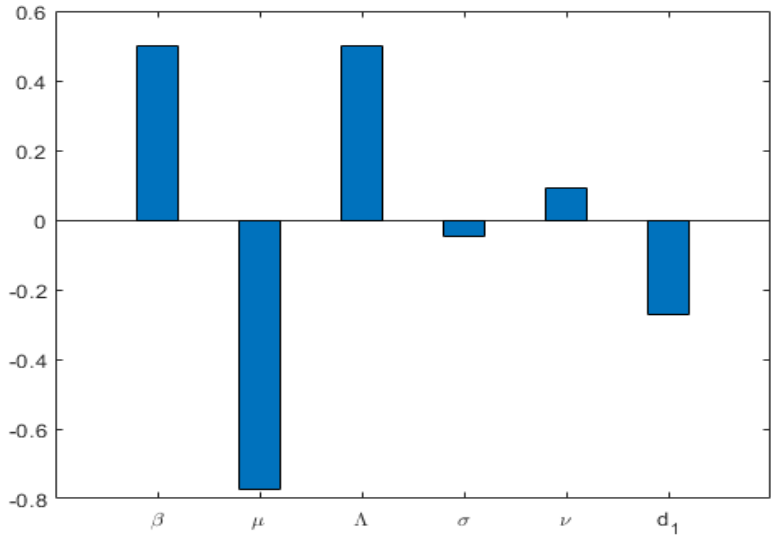

Figure 4.2: Sensitivity indices of $\mathscr{R}_0$.

Figure 4.2 indicates that the most sensitive parameters for $\mathscr{R}_0$ are β, μ and Λ. Parameters ν and d_1 also have some sensitivity to $\mathscr{R}_0$ while the parameter σ is least sensitive. Thus, for example, if the transmission rate β varies i.e. increased or (decreased) by 10%, then the value of $\mathscr{R}_0$ will increase or (decrease) by 5%. Likewise, a 10% increase or (decrease) in value of μ would correspond to a 7.72% decrease or (increase) in the value of $\mathscr{R}_0$. By doing so, the sensitivity of parameters is observed in both positive and negative aspects.

4.6 Optimal Control Problem

In this section, we establish an optimal control problem aligned with the model system (4.2), incorporating the influence of information (non-pharmaceutical intervention) as a control policy. The optimal control problem, formulated using fractional differential equations, can provide a more accurate representation of the system dynamics compared to integer order models [93]. Our objective is to explore the effects of these

control interventions on disease progression and to optimize the associated implementation costs. Initially, we outline the control policy and subsequently assess the corresponding cost implications.

Enhancing the response of susceptible population via information: During the spread of an epidemic, the rate at which the susceptible people become infected can be reduced by changing their behaviours by getting aware of the risk of disease transmission within their community, informed by public health campaigns, media coverage, and personal experiences. It is assumed that susceptible individuals, after awareness, adopt the preventive measures; such as wearing masks, social-distancing, regular sanitation, etc.; but disparities in resources and attitudes can impact implementation. This behavioural response is represented by the control variable $u(t)$. In our model system (4.2), u represents the response intensity via information, where $0 \leq u \leq 1$. Here, 0 means no response, and 1 means a full response from informed individuals. So, this response intensity is directly related with an individual's behavioural response. Now, we treat this response intensity $u(t)$ as a control variable. There will be a cost involved, which is a nonlinear function of $u(t)$, to boost individuals' response to information, prompting them to change their behaviour.

Our primary goal is to determine the optimal response intensity using available data while executing them at the lowest possible cost through the spread of information. The admissible set, as discussed above, for the control variable $u(t)$ is given by,

$$U = \{u(t) |\ u \text{ is Lebesgue measurable, } 0 \leq u(t) \leq 1,\ t \in [0,T]\}.$$

Here, T is the final time of implemented control policy and $u(t)$ is measurable and bounded function.

The motivation for implementing control variable $u(t)$ is to minimize the proportion of infected and quarantined populations, and the cost of its implementation, given by,

$$\mathscr{J}[u] = \int_0^T \left(w_1 E + w_2 I + w_3 Q + \frac{1}{2} z_1 u^2 \right) dt, \tag{4.23}$$

subject to model system

$$\begin{aligned}
D^{\rho}S(t) &= \Lambda - (1-u(t))\frac{\beta SI}{1+\alpha I^2} - \mu S,\\
D^{\rho}E(t) &= (1-u(t))\frac{\beta SI}{1+\alpha I^2} - \nu E - \mu E,\\
D^{\rho}I(t) &= \nu E - \frac{\gamma I^2}{1+\delta I^2} - \sigma I - (\mu + d_1)I,\\
D^{\rho}Q(t) &= \frac{\gamma I^2}{1+\delta I^2} - \omega Q - (\mu + d_2)Q,\\
D^{\rho}R(t) &= \sigma I + \omega Q - \mu R,
\end{aligned} \tag{4.24}$$

with $S(0) \geq 0,\ E(0) \geq 0,\ I(0) \geq 0,\ Q(0) \geq 0$ and $R(0) \geq 0$.

Here, the function $\mathscr{J}$ represents the overall cost, and the expression $L(E,I,Q,u(t)) = w_1E + w_2I + w_3Q + \frac{1}{2}z_1u^2$ shows the current cost at any given time t. The parameters w_1, w_2, w_3 are positive constants that balance the units of the different parts of the expression [62; 90]. The control effort is represented by the quadratic term u^2. For convenience, we use $u(t) = u$.

In the following, the Pontryagin's maximum principle [105] is used to solve optimal control problems. According to the literature [124; 66], an optimal solution for (4.24) exists if the following conditions are met:

(i) The state variables and control set are not empty.

(ii) The set U is both convex and closed.

(iii) The system's right side in equation (4.24) is constrained by a linear function involving both the control and state variables.

(iv) The integrand of the objective function

$$L(E,I,Q,u) = w_1E + w_2I + w_3Q + \frac{1}{2}z_1u^2$$

is convex on the set U.

(v) There exist constants $k_1,\ k_2 > 0$ and $\varepsilon > 1$ such that the integrand $L(E,I,Q,u)$ satisfies

$$L(E,I,Q,u) = k_1\left(|u|^2\right)^{\frac{\varepsilon}{2}} - k_2.$$

Similar to Theorem (4.3.1), we have

$$D^{\rho}N = \Lambda - \mu N - d_1 I - d_2 Q$$
$$D^{\rho}N \leq \Lambda - \mu N$$

Now from the prior bounds of the populations as $N \leq \frac{\Lambda}{\mu}$, for bounded control in U, it can be concluded that the solutions of the system (4.24) are also bounded. It is evident that the functions on the right-hand side of the system (4.24) meet the Lipschitz condition concerning the state variables.

Thus, we can satisfy condition (i) by applying the Picard-Lindelof Theorem [38]. Since the solution to the system (4.24) is bounded, and the control set is convex, conditions (ii) are also met. According to the literature [122], it is straightforward to confirm that conditions (iii) and (iv) are equally valid. Moreover,

$$L(E,I,Q,u) \geq k_1 \left(|u|^2\right)^{\frac{\varepsilon}{2}} - k_2,$$

where $k_1 = \frac{1}{2}\min\{k_1,k_2\},\ k_2 = 1,\ \varepsilon = 2$. Thus, condition (v) is verified. Considering the above discussion, we reach the following conclusion.

Theorem 4.6.1 *There exists an optimal control solution $\bar{u}$ such that*

$$\mathscr{J}(\bar{u}) = \min[\mathscr{J}(u)]$$

subject to the fractional system (4.24).

To obtain the optimal control solution, the Lagrangian function is defined as:

$$L = w_1 E + w_2 I + w_3 Q + \frac{1}{2} z_1 u^2,$$

and Hamiltonian function

$$\begin{aligned}
H(S,E,I,Q,R,u,\lambda_i) &= L + \lambda_1 D^{\rho}S + \lambda_2 D^{\rho}E + \lambda_3 D^{\rho}I + \lambda_4 D^{\rho}Q + \lambda_5 D^{\rho}R \\
&= w_1 E + w_2 I + w_3 Q + \frac{1}{2} z_1 u^2 \\
&\quad + \lambda_1 \left(\Lambda - (1-u)\frac{\beta SI}{1+\alpha I^2} - \mu S\right) \\
&\quad + \lambda_2 \left((1-u)\frac{\beta SI}{1+\alpha I^2} - (\nu+\mu)E\right) \\
&\quad + \lambda_3 \left(\nu E - \frac{\gamma I^2}{1+\delta I^2} - (\sigma+\mu+d_1)I\right) \\
&\quad + \lambda_4 \left(\frac{\gamma I^2}{1+\delta I^2} - (\omega+\mu+d_2)Q\right) \\
&\quad + \lambda_5 (\sigma I + \omega Q - \mu R).
\end{aligned}$$

Here, $\lambda_i = (\lambda_1, \lambda_2, \lambda_3, \lambda_4, \lambda_5)$ is referred to as the adjoint variable. Using Pontryagin's Maximum Principle, the minimized Hamiltonian that reduces the cost is obtained. Pontryagin's Maximum Principle contributes significantly in connecting the cost with the state equations by introducing adjoint variables.

Theorem 4.6.2 *In the control system* (4.23)-(4.24)*, let* $\bar{u}$ *be the optimal control variable and* $\bar{S}$, $\bar{E}$, $\bar{I}$, $\bar{Q}$, *and* $\bar{R}$ *the corresponding optimal state variables. Then, there exists* $\lambda_i = (\lambda_1, \lambda_2, \lambda_3, \lambda_4, \lambda_5) \in \mathbb{R}^5$ *as an adjoint variable that satisfies the following canonical equations:*

$$D^{\rho}\lambda_1(t) = \left((1-\bar{u})\frac{\beta\bar{I}}{1+\alpha\bar{I}^2} + \mu\right)\lambda_1 - \left((1-\bar{u})\frac{\beta\bar{I}}{1+\alpha\bar{I}^2}\right)\lambda_2,$$

$$D^{\rho}\lambda_2(t) = -w_1 + (\nu+\mu)\lambda_2 - (\nu\bar{E})\lambda_3,$$

$$D^{\rho}\lambda_3(t) = -w_2 + \left((1-\bar{u})\frac{\beta\bar{S}(1-\alpha\bar{I}^2)}{(1+\alpha\bar{I}^2)^2}\right)\lambda_1 - \left((1-\bar{u})\frac{\beta\bar{S}(1-\alpha\bar{I}^2)}{(1+\alpha\bar{I}^2)^2}\right)\lambda_2$$
$$+ \left(\frac{2\gamma\bar{I}}{(1+\delta\bar{I}^2)^2} + (\sigma+\mu+d_1)\right)\lambda_3 - \left(\frac{2\gamma\bar{I}}{(1+\delta\bar{I}^2)^2}\right)\lambda_4 - (\sigma)\lambda_5, \quad (4.25)$$

$$D^{\rho}\lambda_4(t) = -w_3 + (\omega+\mu+d_2)\lambda_4 - (\omega)\lambda_5,$$

$$D_t^{\rho}\lambda_5(t) = (\mu)\lambda_5,$$

with transversality conditions

$$\lambda_i(T) = 0. \quad (4.26)$$

Further, the optimal control $\bar{u}$ *is given by*

$$\bar{u} = \min\left\{max\left\{0, \frac{1}{z_1}\frac{\beta\bar{S}\bar{I}}{1+\alpha\bar{I}^2}(\lambda_2-\lambda_1)\right\}, 1\right\}. \quad (4.27)$$

Proof 4.6.3 *The adjoint variable equations and the transversality condition may be derived as follows by applying Pontryagin's maximal principle:*

$$D^{\rho}\lambda_1(t) = -\frac{\partial H}{\partial S} = \left((1-\bar{u})\frac{\beta\bar{I}}{1+\alpha\bar{I}^2}+\mu\right)\lambda_1 - \left((1-\bar{u})\frac{\beta\bar{I}}{1+\alpha\bar{I}^2}\right)\lambda_2,$$

$$D^{\rho}\lambda_2(t) = -\frac{\partial H}{\partial E} = -w_1 + (\nu+\mu)\lambda_2 - (\nu\bar{E})\lambda_3,$$

$$\begin{aligned} D^{\rho}\lambda_3(t) = -\frac{\partial H}{\partial I} = &-w_2 + \left((1-\bar{u})\frac{\beta\bar{S}(1-\alpha\bar{I}^2)}{(1+\alpha\bar{I}^2)^2}\right)\lambda_1 \\ &- \left((1-\bar{u})\frac{\beta\bar{S}(1-\alpha\bar{I}^2)}{(1+\alpha\bar{I}^2)^2}\right)\lambda_2 + \left(\frac{2\gamma\bar{I}}{(1+\delta\bar{I}^2)^2}+(\sigma+\mu+d_1)\right)\lambda_3 \\ &- \left(\frac{2\gamma\bar{I}}{(1+\delta\bar{I}^2)^2}\right)\lambda_4 - (\sigma)\lambda_5, \end{aligned}$$

$$D^{\rho}\lambda_4(t) = -\frac{\partial H}{\partial Q} = -w_3 + (\omega+\mu+d_2)\lambda_4 - (\omega)\lambda_5,$$

$$D_t^{\rho}\lambda_5(t) = -\frac{\partial H}{\partial R} = (\mu)\lambda_5,$$

with $\lambda_i(T) = 0$, *for any* $i = 1,2,\ldots,5$. *The characteristic equation of optimal control* $\bar{u}$, *can be obtain by solving the equation:*

$$\frac{\partial H}{\partial u} = 0, \;\; at \;\; u = \bar{u}.$$

Thus we get,

$$\bar{u} = \frac{1}{z_1}\frac{\beta\bar{S}\bar{I}}{1+\alpha\bar{I}^2}(\lambda_2-\lambda_1).$$

Thus, we have the control set U as:

$$\bar{u} = \begin{cases} 0 & if \;\; \frac{1}{z_1}\frac{\beta\bar{S}\bar{I}}{1+\alpha\bar{I}^2}(\lambda_2-\lambda_1) < 0 \\ \frac{1}{z_1}\frac{\beta\bar{S}\bar{I}}{1+\alpha\bar{I}^2}(\lambda_2-\lambda_1) & if \;\; 0 \le \frac{1}{z_1}\frac{\beta\bar{S}\bar{I}}{1+\alpha\bar{I}^2}(\lambda_2-\lambda_1) \le 1 \\ 1 & if \;\; \frac{1}{z_1}\frac{\beta\bar{S}\bar{I}}{1+\alpha\bar{I}^2}(\lambda_2-\lambda_1) > 1, \end{cases}$$

which can be equivalently written as:

$$\bar{u} = \min\left\{max\left\{0, \frac{1}{z_1}\frac{\beta\bar{S}\bar{I}}{1+\alpha\bar{I}^2}(\lambda_1-\lambda_2)\right\}, 1\right\}. \tag{4.28}$$

Hence, the theorem proved.

This section focused on the optimal control problem to reduce the spread of disease in an optimal manner. Theorem 4.6.1 established the existence of an optimal intervention strategy, minimizing disease spread or maximizing public health outcomes. Pontryagin's Maximum Principle characterized this strategy, defining when and how interventions should occur. Theorem 4.6.2 confirmed the existence of adjoint variables meeting canonical equations and a transversality condition, ensuring the strategy's long-term sustainability. This condition prevents short-term disease control gains from causing long-term harm, aiding in effective decision-making for disease management.

4.7 Numerical Scheme

The Adams-Bashforth-Moulton predictor corrector method is the most employed numerical method for the fractional order system of differential equations with initial values [50]. The implementation of this method is given below. Consider the following non-autonomous *SEIQR* system for the same.

$$\begin{aligned} D^{\rho}S(t) &= f_1\big(t,S,E,I,Q,R\big),\\ D^{\rho}E(t) &= f_2\big(t,S,E,I,Q,R\big),\\ D^{\rho}I(t) &= f_3\big(t,S,E,I,Q,R\big),\\ D^{\rho}Q(t) &= f_4\big(t,S,E,I,Q,R\big),\\ D^{\rho}R(t) &= f_5\big(t,S,E,I,Q,R\big), \end{aligned} \tag{4.29}$$

with $S(0)=S_0,\ E(0)=E_0,\ I(0)=I_0,\ Q(0)=Q_0$ and $R(0)=R_0$, where $0<\rho\leq 1$. Let $t_j=jh,\ j=0,1,2,\ldots,N$ with some integer N and $h=T/N$, in the interval $[0,T]$. By utilizing the method given in [50], system (4.29) can be written as follows.

Predictor values for (4.29) are

$$S^P_{n+1} = S_0 + \frac{1}{\Gamma(\rho)} \sum_{j=0}^{n} b_{j,n+1} f_1\big(t_j, S_j, E_j, I_j, Q_j, R_j\big),$$

$$E^P_{n+1} = E_0 + \frac{1}{\Gamma(\rho)} \sum_{j=0}^{n} b_{j,n+1} f_2\big(t_j, S_j, E_j, I_j, Q_j, R_j\big),$$

$$I^P_{n+1} = I_0 + \frac{1}{\Gamma(\rho)} \sum_{j=0}^{n} b_{j,n+1} f_3\big(t_j, S_j, E_j, I_j, Q_j, R_j\big),$$

$$Q^P_{n+1} = Q_0 + \frac{1}{\Gamma(\rho)} \sum_{j=0}^{n} b_{j,n+1} f_4\big(t_j, S_j, E_j, I_j, Q_j, R_j\big),$$

$$R^P_{n+1} = R_0 + \frac{1}{\Gamma(\rho)} \sum_{j=0}^{n} b_{j,n+1} f_5\big(t_j, S_j, E_j, I_j, Q_j, R_j\big),$$

where, $b_{j,n+1} = \frac{h^\rho}{\rho}\big((n-j+1)^\rho - (n-j)^\rho\big)$.

Corrector values are obtained by using predictor values as follows:

$$S_{n+1} = S_0 + \frac{h^\rho}{\Gamma(\rho+2)} f_1\big(t_{n+1}, S^P_{n+1}, E^P_{n+1}, I^P_{n+1}, Q^P_{n+1}, R^P_{n+1}\big) + \frac{h^\rho}{\Gamma(\rho+2)} \sum_{j=0}^{n} a_{j,n+1} f_1\big(t_j, S_j, E_j, I_j, Q_j, R_j\big),$$

$$E_{n+1} = E_0 + \frac{h^\rho}{\Gamma(\rho+2)} f_2\big(t_{n+1}, S^P_{n+1}, E^P_{n+1}, I^P_{n+1}, Q^P_{n+1}, R^P_{n+1}\big) + \frac{h^\rho}{\Gamma(\rho+2)} \sum_{j=0}^{n} a_{j,n+1} f_2\big(t_j, S_j, E_j, I_j, Q_j, R_j\big),$$

$$I_{n+1} = I_0 + \frac{h^\rho}{\Gamma(\rho+2)} f_3\big(t_{n+1}, S^P_{n+1}, E^P_{n+1}, I^P_{n+1}, Q^P_{n+1}, R^P_{n+1}\big) + \frac{h^\rho}{\Gamma(\rho+2)} \sum_{j=0}^{n} a_{j,n+1} f_3\big(t_j, S_j, E_j, I_j, Q_j, R_j\big),$$

$$Q_{n+1} = Q_0 + \frac{h^\rho}{\Gamma(\rho+2)} f_4\big(t_{n+1}, S^P_{n+1}, E^P_{n+1}, I^P_{n+1}, Q^P_{n+1}, R^P_{n+1}\big) + \frac{h^\rho}{\Gamma(\rho+2)} \sum_{j=0}^{n} a_{j,n+1} f_4\big(t_j, S_j, E_j, I_j, Q_j, R_j\big),$$

$$R_{n+1} = R_0 + \frac{h^\rho}{\Gamma(\rho+2)} f_5\big(t_{n+1}, S^P_{n+1}, E^P_{n+1}, I^P_{n+1}, Q^P_{n+1}, R^P_{n+1}\big) + \frac{h^\rho}{\Gamma(\rho+2)} \sum_{j=0}^{n} a_{j,n+1} f_5\big(t_j, S_j, E_j, I_j, Q_j, R_j\big),$$

where,

$$a_{j,n+1} = \begin{cases} n^{\rho+1} - (n-\rho)(n+1)^{\rho}, & j = 0 \\ (n-j+2)^{\rho+1} + (n-j)^{\rho+1} - 2(n-j+1)^{\rho+1}, & 1 \leq j \leq n. \end{cases}$$

According to the mathematical analysis of this method in [51], the order of accuracy is $\psi = min(2, 1+\rho)$. This is because it can be demonstrated that ψ must be the minimum among the order of the corrector (which is 2 in our scenario) and the sum of the order of the predictor method (which is 1 in this case) and the order of the differential operator (denoted as ρ). It is noteworthy that the Adams-Bashforth-Moulton scheme's convergence order ψ increases with an increase in ρ, which denotes the order of differential equation, as described the algorithm behaviour in [53]. Regarding the algorithm's stability properties, it is observed that it follows that the fractional Adams-Bashforth-Moulton scheme's stability properties are at least as good as those of its counterpart for first-order equations, i.e., the traditional second-order Adams-Bashforth-Moulton method [53].

4.8 Numerical Simulations and Discussion

In this section, MATLAB 2012b is used to execute numerical simulation with the set of numerical experimental data as given in Table 4.1, to verify the accuracy of the theoretical derivation using the fractional Adams-Bashforth-Moulton technique by using scheme given in Section 4.7. When numerical analysis is performed with the help of real data, it might lead to fluctuations in pricing, expenditures, and technology, making it challenging to identify causes and effects. On the other hand, numerical analysis with a set of numerical experimental data makes it easier to distinguish the effects of interactions between different classes, which is crucial for the observation of long term behaviour of the system [125]. Therefore, a qualitative analysis is presented, which provides a conceptual understanding, as researchers examine the underlying mechanisms and assumptions of the model to develop a deeper understanding of the complex dynamics of disease transmission and control, identifying areas where further empirical validation or adjustment is possible. For the numerical computations, the initial sub-populations are taken as $S(0) = 310, E(0) = 25, I(0) = 5, Q(0) = 5$, and $R(0) = 5$ and set of numerically experimental data has been given in Table 4.1.

4.8.1 Numerical Analysis without Control Strategy

In this subsection, to confirm the feasibility of our analysis regarding the existence and stability conditions of equilibria corresponding to model system (4.2), some numerical computations are performed.

Table 4.1: Parameters of the model *SEIQR*.

Parameters	**Description**	**Values**
Λ	Recruitment rate	7
β	Transmission rate	0.009
α	Psychological saturation constant	0.02
μ	Natural mortality rate	0.02
ν	Rate of progression from exposed to the infected group	0.09
γ	Quarantine rate	0.07
δ	Quarantine saturation constant	0.008
σ	Auto recovery rate	0.005
ω	Recovery rate due to treatment	0.007
d_1	Death rate due to disease in I class	0.03
d_2	Death rate due to disease in Q class	0.03

For the data given in Table 4.1, the value of the coefficients of equation (4.6) is $A_4 = 1.936 \times 10^{-8}, A_3 = 3.5156 \times 10^{-6}, A_2 = 2.7328 \times 10^{-5}, A_1 = 2.0845 \times 10^{-4}, A_0 = -5.549 \times 10^{-3}$. These coefficient values satisfy Theorem 4.3.4 and the possibility of the existence of unique positive equilibrium provided the condition $\gamma > \delta\Lambda$ which is $(0.07 > 0.056)$. Thus the endemic equilibrium is $E^*(S^*, E^*, I^*, Q^*) = (135.966, 34.5256, 8.18312, 53.5491)$ for which the basic reproduction number $\mathscr{R}_0$ is 6.8454 and simultaneously the alternative threshold $\mathscr{T}_0$ is 46.85954.

The values of coefficients of equation (4.20) are calculated as $A_3 = 70.6216, A_2 = 49.5942, A_1 = 7.0492, A_0 = 0.225921$. One of the eigen values corresponding the equation (4.18) are $\Omega_1 = -0.057$, and the rest of the eigen values are the root of the equation (4.21) i.e. of the equation $\Omega^3 + 0.702252\Omega^2 + 0.0998165\Omega + 0.00319903$ which are $\Omega_2 = -0.523139,\ \Omega_3 = -0.133208,\ \Omega_4 = -0.0459063$. The discriminant of polynomial term of the equation (4.21) is calculated as $D(\lambda) = 0.000263922$. The values of the coefficients of equation (4.21) are $K_0 = 0.00319903, K_1 = 0.0998165, K_2 =$

0.702252 and these also satisfy the condition $K_2K_1 > K_0$, so together with the discriminant $D(\lambda)$, these are satisfying the first condition of the Theorem 4.4.2. Using the initial population conditions, Figures 4.3a, 4.3b, 4.4a, 4.4b, are plotted, depicting the impact of the fractional order ρ on the sub-populations.

As depicted in Figure 4.3a, the variation in the fractional order value ρ influences the convergence rate of the system (4.4). Specifically, when the value of ρ increases, the susceptible population reaches its steady state more rapidly. On the other hand, if the value of ρ decreases, the memory of the system (4.4) is strengthened, leading to a slower convergence speed. In simpler terms, reducing ρ makes it take longer to eliminate the disease.

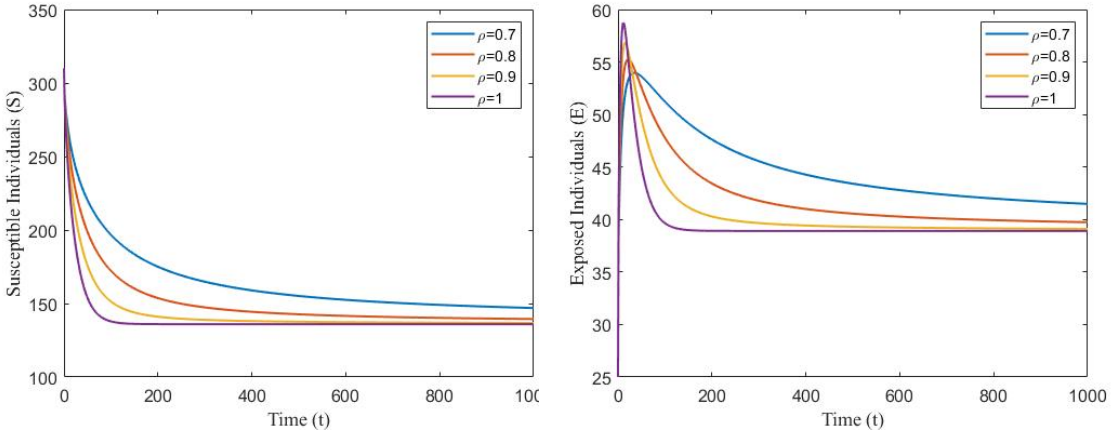

(a) Profiles of susceptible population with different fractional order.

(b) Profiles of exposed population with different fractional order.

Figure 4.3: Effect of fractional order ρ on susceptible and exposed populations.

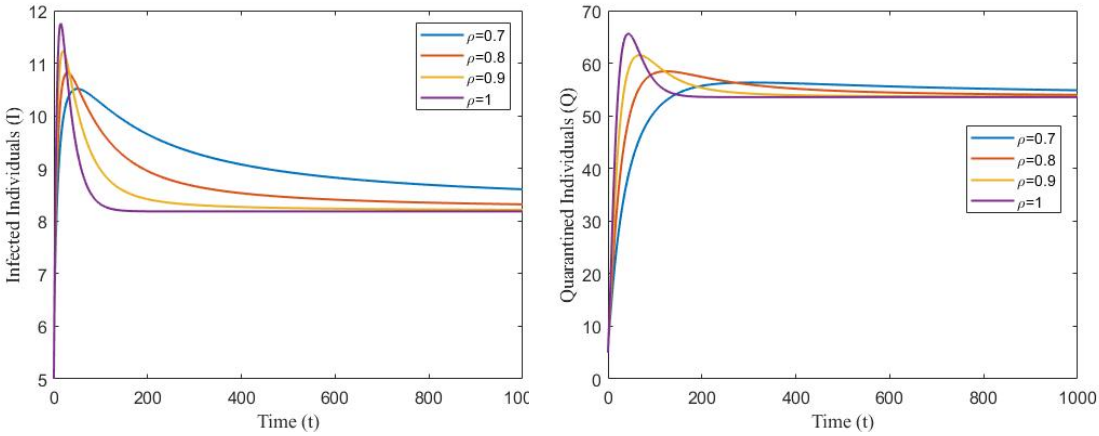

(a) Profiles of infected population with different fractional order.

(b) Profiles of quarantined population with different fractional order.

Figure 4.4: Effect of fractional order ρ on infected and quarantined populations.

In Figures 4.3b, 4.4a, 4.4b, it can be seen that when $\rho = 1$, the populations E, I, and Q quickly reach a steady state. However, as the value of ρ decreases, the time it takes for these populations to reach the steady state increases. This shows how the epidemic evolves over time. According to Theorem 4.4.4, the endemic equilibrium $(135.966, 34.5256, 8.18312, 53.5491)$ is stable for all fractional order values $(\rho = 0.7, 0.8, 0.9, 1)$, as demonstrated in Figures 4.3a, 4.3b, 4.4a, 4.4b.

Biologically, it can be said that a higher value of ρ implies that individuals are less influenced by past experiences, leading to a quicker convergence to the steady state. On the other hand, when the value of ρ is relatively low, the memory effect is stronger, and the susceptible population takes more time to reach a steady state. A lower value of ρ implies that society retains more memory of past experiences during the emergence of an infectious disease. Moreover, with a weaker memory effect, individuals might take longer to recognize and respond to the disease's presence that is the peak of infected individuals is high in case of higher values of ρ.

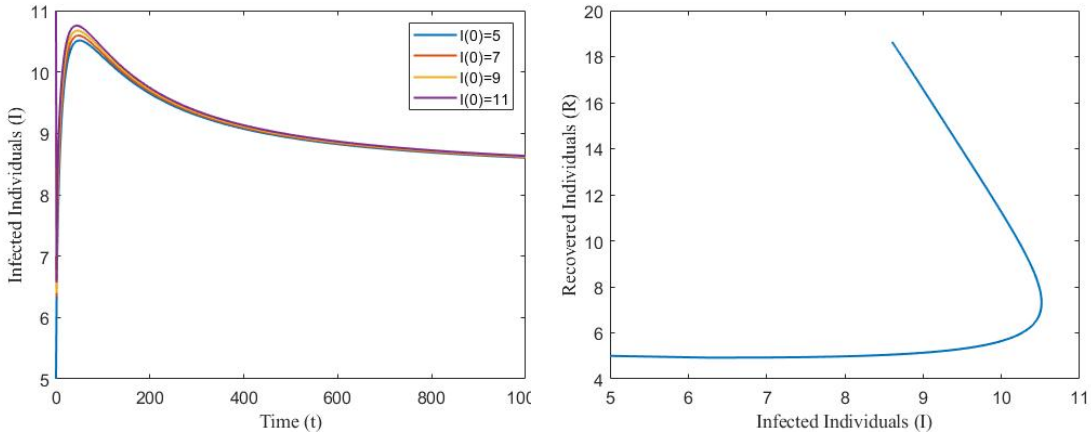

(a) Profiles of infected population with different initial conditions $I(0)$ for $\rho = 0.7$.

(b) Phase portrait of infected and recovered population at $\rho = 0.7$.

Figure 4.5: Effect of different initial conditions $I(0)$ on infected population and the phase diagram of infected vs recovered population at fixed $\rho = 0.7$.

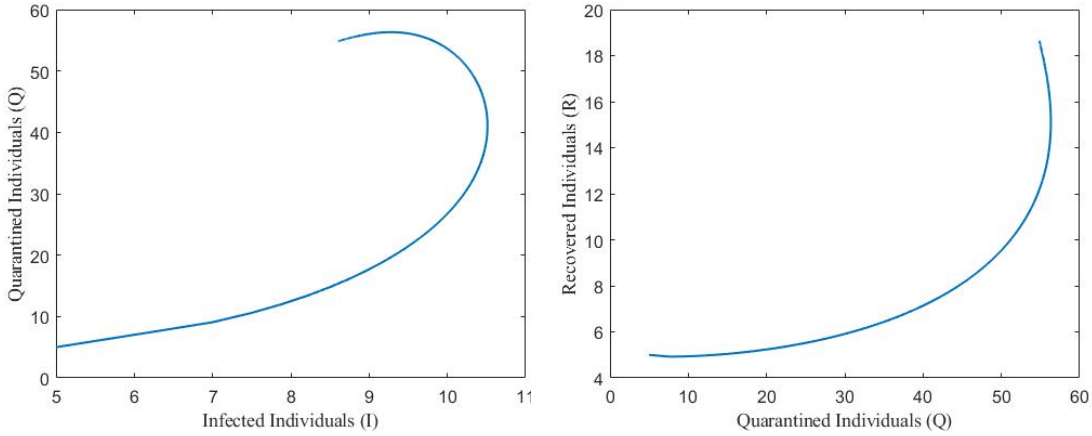

(a) Phase portrait of infected and quarantined population at $\rho = 0.7$.

(b) Phase portrait of quarantined and recovered population at $\rho = 0.7$.

Figure 4.6: Phase diagram at fixed $\rho = 0.7$.

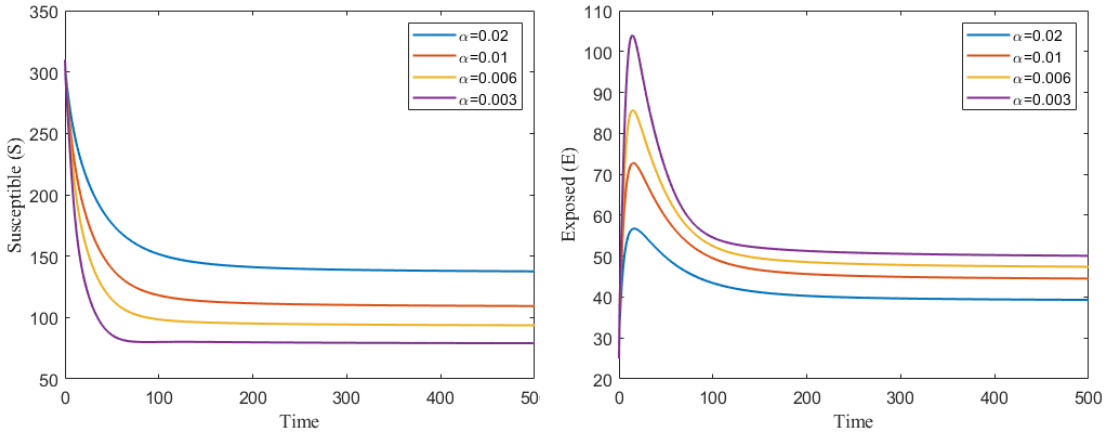

(a) Impact of psychological effects (α) on susceptible individuals at $\rho = 0.9$.

(b) Impact of psychological effects (α) on exposed individuals at $\rho = 0.9$.

Figure 4.7: Phase diagram at fixed $\rho = 0.7$.

Important insights into the dynamics of disease transmission within a population may be gained from Figures 4.5a, 4.5b, 4.6a, and 4.6b. Figure 4.5a illustrates the stability of the model under different initial conditions. The stability of the model is confirmed when the infected population reaches a steady-state, regardless of the starting number of infected people. For instance, steady-state behaviour is consistent in simulations with varied beginning infected people $(I(0) = 5, 7, 9, 11)$. The recovered population is initially at a low level as the number of infected persons grows, as seen in Figure 4.5b. However, with time, recovery increases along with the number of infected individuals and reaches to its steady state. Figure 4.6a shows how timely quarantine affects the number of infected individuals. The graph indicates that when quarantine measures are initiated, the number of infected individuals initially increases. However, because of the timely quarantine, the infection reaches its highest point and then goes down significantly. This emphasizes the importance of timely quarantine in controlling the peak of infection during an epidemic. In Figure 4.6b, we can see how putting people in quarantine on time affects the number of individuals who have recovered. Clearly, when quarantine happens on time, the number of people recovering increases and eventually levels off at a steady state.

Figures 4.7a and 4.7b are presented to study how psychological factors affect both susceptible and exposed populations. When the rate of psychological effects α increases, the number of susceptible individuals increases, and the peak of exposed individuals starts to decrease, as illustrated in Figures 4.7a and 4.7b. Therefore, using

psychological effects can be an effective way to lower the peak of infection in society during an outbreak.

4.8.2 Numerical Analysis with Control Strategy

This subsection explains the outcomes of the Fractional Optimal Control Problem (FOCP) and discusses the implications of the study. To analyze the results, Pontryagin's maximum principle along with its optimality conditions is applied, using the forward-backward predict-evaluate-correct-evaluate (PECE) method. The simulations and discussion of results are conducted through this approach, which involves the Adams Bashforth Moulton FBSM method [153].

The values of the state variables S, E, I, Q, and R are obtained by first solving system (4.24) using the PECE process with initial conditions for the state variables, in the forward direction (time), and an estimate for the control across the time interval $[0, T]$. Using the PECE approach, the resulting state solution is then applied to solve the adjoint system (4.25) in the backward direction (time) with transversality conditions. Next, the control set U is updated by a convex combination of the previous and present values of the control characterizations, after the control variables are calculated using the characterizations provided in (4.28). Until the control values, adjoint variables, and state variables converge, this procedure is repeated. The same set of parameters and initial values is used as previously established in order to numerically simulate our FOCP.

The proper weights for the goal cost functional (4.23) were established to ensure effective optimization. In particular, $z_1 = 240$ and $w_1 = w_2 = w_3 = 1$ is considered. These weights were chosen to account for the varying degrees of significance and work associated with each control. To get the required results for our optimization problem, the controls were applied for $T = 200$ (in days). Through the proper selection of parameters and initialization of the system with suitable conditions, we get trustworthy and accurate findings.

For a more insightful examination and interpretation of optimal control analysis, an implementation of control policy $u(t)$, i.e., response via information is considered. The corresponding population profiles are plotted in Figures 4.8a, 4.8b,4.9a, 4.9b and the path of the applied control response via information $u(t)$ for $\rho = 0.9$ is depicted in Figure 4.10.

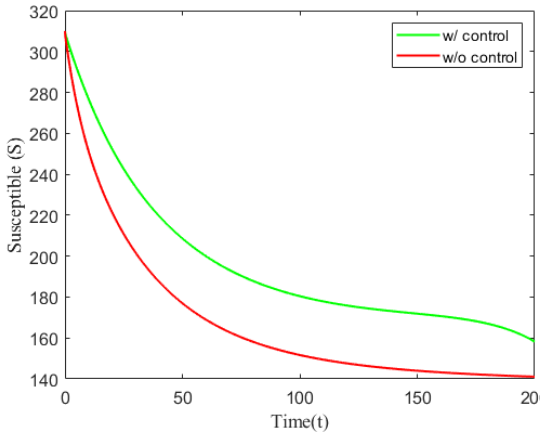

(a) Impact of applying u on susceptible population S.

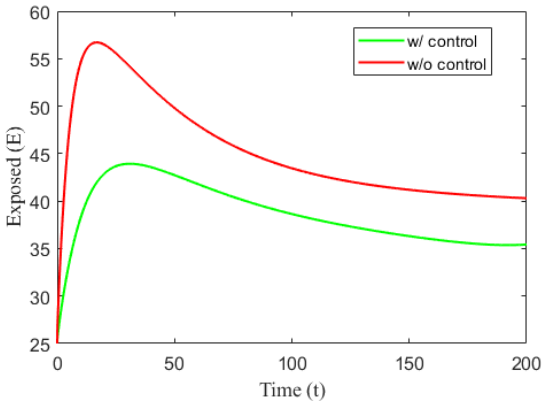

(b) Impact of applying u on exposed population E.

Figure 4.8: Profiles of susceptible and exposed population with applied optimal control of response via information u for $\rho = 0.9$.

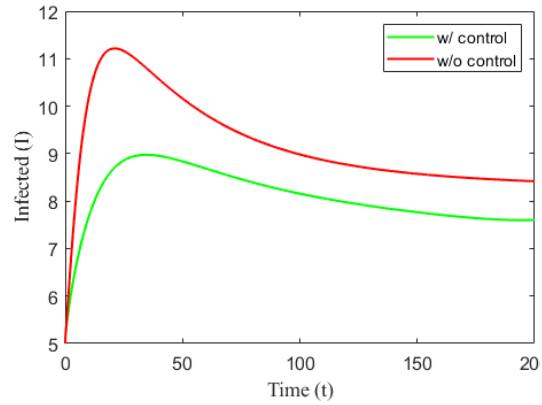

(a) Impact of applying u on infected population I.

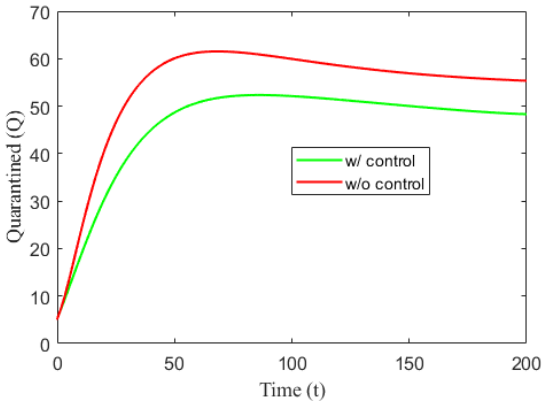

(b) Impact of applying u on quarantined population Q.

Figure 4.9: Profiles of infected and quarantined population with applied optimal control of response via information u for $\rho = 0.9$.

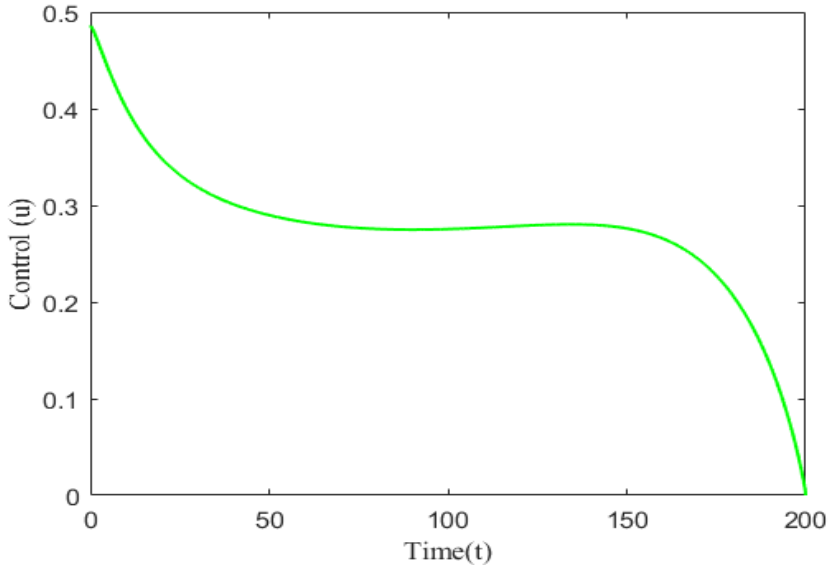

Figure 4.10: Optimal control path of response via information u for $\rho = 0.9$.

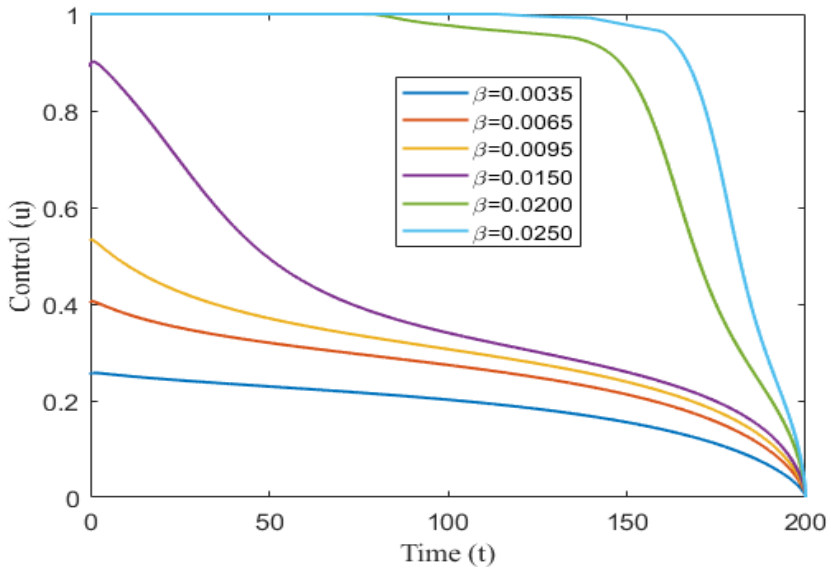

Figure 4.11: Optimal control path of response via information u with different values of contact rate β for $\rho = 0.9$.

The profile of optimal control u, as shown in Figure 4.10, indicates that if it is implemented as a control intervention strategy, it would require high implementation efforts initially, then constant efforts for a longer period of time. Gradually, lower implementations can be applied and finally, it can be removed from employment at the end. Furthermore, Figures 4.8a, 4.8b, 4.9a, 4.9b demonstrates the impact of im-

plementing u on the S, E, I and Q population. It is noteworthy that if individuals in susceptible will go through the implemented control u, the count of susceptibles increase and infected decrease in comparison of without any control. So, conclusively, information-based behavioural response effectively lowers the number of infected people, and in this instance, the epidemic peaks considerably lower than it would have if no controls were in place. Furthermore, the profile of control $u(t)$ for various values of contact rate of susceptible population β is shown in Figure 4.11 to further explore how optimal control relies upon various factors in the model. It shows that for a higher value of contact rate of susceptible population β, to achieve the optimal scenario, information spreading process must be implemented with the maximum rate of 140 days (approx). On the other hand, the best result may be achieved with a smaller value of β by using a shorter information-spreading method in terms of days.

4.9 Conclusion

This chapter endeavors to propose and conduct a mathematical analysis of a fractional-order *SEIQR* epidemic model. The primary goal is to gain insights into the dynamics of disease transmission during an outbreak by incorporating the impact of quarantined individuals and delving into the psychological effects on susceptible individuals. The model extends the conventional susceptible-exposed-infected-recovered (*SEIR*) compartmental epidemic model by introducing a distinct class of quarantined individuals. The incidence rate of infection is modeled using the Monod-Haldane type, which captures the nonmonotonic effects associated with the psychological state of susceptibles during an epidemic.

Moreover, the quarantine rate is characterized by the Holling type-III, providing a nuanced understanding of the dynamics of isolating individuals. The choice of the Caputo derivative for the population rate of each subpopulation is crucial, as it accounts for fractional-order dynamics and incorporates memory effects. This is particularly relevant in the context of emerging diseases, where initial responses draw upon knowledge accumulated from past outbreaks. The Caputo derivative, being fractional-order, acknowledges the inherent memory effects associated with the societal response to novel diseases. Essentially, it recognizes that the control measures implemented at the onset of an outbreak are influenced by the collective memory and experiences gained from previous instances, a dimension not adequately captured by traditional integer-order derivative-based epidemic models.

The analysis of the proposed model demonstrates its well-posed nature, ensuring that the solutions are non-negative and confined within a compact region. The model reveals two equilibria: a disease-free state and an endemic state. Employing the next-generation matrix method, the basic reproduction number $\mathscr{R}_0$ was computed, and an alternative threshold, denoted as $\mathscr{T}_0$, was also determined. The outcomes, detailed in Theorems 4.4.4 and 4.4.3, assert that EE achieves global asymptotic stability when $\mathscr{R}_0 > 1$, while DFE attains global asymptotic stability when $\mathscr{R}_0 < 1$. Furthermore, sensitivity analysis of $\mathscr{R}_0$ shows that parameters β, μ and Λ are highly sensitive parameters.

The numerical results presented in this study complement the analytical findings, with Figures 4.3a, 4.3b, 4.4a, and 4.4b providing visual insights into the influence of the fractional order ρ on the susceptible, exposed, infected, and quarantine sub-populations, respectively. These graphical representations highlight a notable trend: as the fractional order ρ approaches one, each sub-population exhibits a quicker convergence to its steady state. The observation emerges that varying values of ρ do not impact the stability nature of the equilibrium points but solely influence the time required for each sub-population to reach its equilibrium state. These graphical depictions align with the findings of Theorem 4.4.2, affirming the local asymptotic stability of the endemic equilibrium (EE) when $\mathscr{R}_0$ exceeds one. Additionally, the simulations reveal an intriguing aspect: the initial population of infectives does not exert any influence on the steady-state of the infected population, as illustrated in Figure 4.5a. Furthermore, the numerical simulations underscore the effectiveness of timely quarantining of infected individuals. This proactive measure not only significantly reduces new infection cases but also contributes to an increase in the recovered population. The simulations thus underscore the importance of strategic interventions, particularly in the form of timely quarantine, in shaping the dynamics of disease spread and recovery. Analyzing the graphs highlights that diligently monitoring psychological effects and implementing timely measures to boost the rate of psychological effects can significantly decrease new infections within society.

Furthermore, the model was modified into a corresponding optimal control problem through the implementation of an optimal control policy, where the response of the susceptible population via information emerges as a powerful strategy in epidemic modeling. Existence of such optimal control functions is also established. Analytical characterization of optimal control paths has been performed with the help of Pontrya-

gin's Maximum Principle. Examining the population profiles in Figures 4.8a, 4.8b, 4.9a, 4.9b provides a comprehensive understanding of the impact of the implemented control response on susceptible (S), exposed (E), infected (I), and quarantined (Q) individuals. Notably, the implementation of the control strategy demonstrates a significant reduction in the count of infected individuals, accompanied by an increase in susceptibles, highlighting the effectiveness of the control policy in curbing the spread of the epidemic. The count of infective individuals and the duration of the disease prevalence is minimized by the optimal response via information. The control measures are found economical for an early phase of the epidemic. It was found that the effect of information on behavioral change plays an important role in reducing both the disease burden and the economic load. Thus, the comprehensive use of control interventions is found more effective and highly economical during epidemic outbreaks. Furthermore, this chapter incorporates a saturation effect in the quarantine process, meaning that the quarantine rate saturates as the number of infected individuals increases, with the help of the non-monotonic simplified Monod-Haldane incidence rate. This mirrors the real-world scenario where the transmission of infectious diseases tends to slow down as a larger proportion of the population becomes infected. This is essential for modeling scenarios where resources for transmission are limited.

In conclusion, this study introduces a fractional-order *SEIQR* epidemic model, aiming to analyze disease transmission dynamics incorporating quarantined individuals and the psychological effects on susceptibles. It extends the conventional *SIR* model, introducing an exposed and quarantined class and utilizing a non-monotonic Monod-Haldane incidence rate to capture psychological effects and nonlinear Holling type III quarantine rate. The well-posed nature of our model is demonstrated, revealing equilibria and thresholds in the stability analysis. Numerical simulations show the impact of fractional order on population dynamics and highlight the effectiveness of timely quarantining and psychological interventions. An optimal control framework is proposed, emphasizing the role of information in shaping susceptible population responses. The unique contributions of our study lie in memory effects, timely quarantines, and psychological interventions for accurate disease prediction and epidemic management.

The proposed *SEIQR* model is flexible and can be adapted to include other compartments or factors as needed. For example, it can be extended to include compartments for vaccination, different stages of disease severity, or demographic characteris-

tics of the population. If one can deal with the complexities then time delay can also be incorporated to take the model one more step closer towards realism.

Chapter 5

Mathematical Modeling and Qualitative Analysis of a Fractional-Order *SPIR* Epidemic Model with Non-monotonic Incidences and Optimal Control

---

Environmental pollution is a major global health concern and is linked to increased mortality. Long-term exposure to polluted environments weakens the immune system, making individuals more susceptible to infections. Therefore, this chapter proposes a novel fractional SPIR (Susceptible, Pollution-affected or Stressed, Infected, Recovered) compartmental model based on the Caputo fractional derivative. The model incorporates the effects of prenatal exposure on newborns with Monod-Haldane incidence rate to capture psychological impacts during disease transmission. It also considers how environmental stress increases the likelihood of infection (transition from P to I). The existence, uniqueness, positivity, and boundedness of the system's solutions are established to ensure its well-posedness. Qualitative analysis reveals two equilibria: disease-free and endemic, whose stability is assessed using the basic reproduction number $\mathscr{R}_0$, derived via the next-generation matrix method. The disease-free equilibrium is locally and globally asymptotically stable when $\mathscr{R}_0 < 1$, while the endemic equilibrium becomes locally and globally asymptotically stable for $\mathscr{R}_0 > 1$, under cer-

tain conditions, as confirmed by the Routh-Hurwitz criterion and Lyapunov functions. A forward transcritical bifurcation at $\mathscr{R}_0 = 1$ is also observed. Moreover, a fractional optimal control problem is formulated using Pontryagin's maximum principle, involving two time-dependent non-pharmaceutical controls, $v_1(t)$ and $v_2(t)$. Finally, numerical simulations are performed using the Adams-Bashforth-Moulton Predictor-Corrector method in MATLAB to validate the analytical results. Findings indicate that simultaneous implementation of both controls is more effective in flattening epidemic curves in short time, offering valuable insights.

5.1 Introduction

The world has seen a noticeable increase in infectious diseases which continues to pose a serious threat to public health, in past years, despite various advancements in technology, medical science, surveillance, and control strategies [86; 137; 192]. The burden of infectious diseases remains one of the major challenges in today's time. Recent decades have witnessed recurrent outbreaks and pandemics, including those caused by respiratory pathogens such as influenza viruses, SARS, and more recently, COVID-19 [134; 175].

The occurrence of infectious diseases often leads to substantial losses, both in human lives and economic resources. For instance, the 2002-03 SARS outbreak infected over 8,000 individuals across 30 countries, resulting in 774 deaths and economically, regions like Hong Kong and Singapore experienced GDP contractions of 4.75% and 1%, respectively [37]. The COVID-19 pandemic, which began in late 2019, had resulted in over 20 million deaths worldwide. The global economy contracted by 3.2% in 2020, with an estimated 8.5 trillion dollars output loss over two years [23; 181]. Researchers have made several attempts to develop mathematical models to deal with such alarming situations.

Numerous mathematical models have been developed and studied to analyze the effects of infectious disease so as to control and curb them. Controlling the outbreak of infectious diseases has long relied on measures such as vaccination, awareness programs, medical treatments etc. [87; 88; 95; 162]. Despite ongoing efforts, infectious diseases remain a serious burden on modern society [163]. Numerous studies have been conducted to extensively examine how infectious diseases transmit within populations, by dividing the total considered population into different compartments, in

order to devise effective strategies to contain and mitigate them (see [28; 71; 105; 119] and references within).

As a result, compartmental modeling frameworks have become fundamental tools in epidemiological research, enabling researchers to capture the dynamics of disease spread and evaluate the effectiveness of various control strategies. These models often categorize a population into compartments such as Susceptible (S), Infected (I), and Recovered (R) (SIR model), or with the addition of other compartments, such as Exposed (E) compartment ($SEIR$ model), Vaccinated (V) compartment ($SVIR$ model), Quarantined (Q) compartment ($SQIR$ model) or a combination of these, to capture the flow of individuals through different disease states [8; 72; 92; 110; 111; 141; 184].

However, these conventional models often overlook the critical role of environmental factors in shaping disease susceptibility and transmission. Notably, the escalating levels of environmental pollution worldwide have emerged as a significant concern for human health. Exposure to various pollutants can compromise the respiratory system, weaken the immune response, and induce physiological stress in individuals [65; 68]. This environmentally induced stress can render a larger proportion of the population more vulnerable to infectious agents, potentially altering the course and severity of epidemics. In 2003, Lafferty and Holt [102] modeled how environmental stress affects the population dynamics of infectious diseases by influencing host susceptibility, parasite mortality, and host population parameters, thus proposing that stress can both increase and decrease disease impact depending on specific interactions between infected and uninfected hosts. Kumari and Sharma [101], in 2018, analyzed how pollution increases susceptibility to infectious diseases, particularly among newborns, by compromising immunity. Very recently, Anthony and Bhatia [13] introduced a novel fuzzy epidemic model that incorporated the effects of environmental pollution and viral-load uncertainty using fuzzy parameters showing that both these factors significantly increased the basic reproduction number, thereby highlighting the importance of integrating pollution control with public health measures.

Our model introduces the compartment of pollution-affected or stressed population, to explicitly represent the population segment that is physically stressed and rendered more susceptible to infection due to environmental pollution. This compartment also considers the long-term effects of prenatal exposure to pollution on the health of newborns and infants. Recent studies indicate that maternal exposure to environmental pollutants during pregnancy can lead to various complications, such as preterm birth,

low birth weight, and developmental delays [41; 166]. Furthermore, studies such as those by Picciotto et al. [75] and Sun et al. [170] have shown that prenatal exposure to both persistent and non-persistent organic pollutants can negatively affect the development of the immune system in infants. These findings suggest that prenatal pollution exposure not only impacts newborns but also has the potential to affect infants' overall health and susceptibility to diseases. Thus, in the context of our model, the individuals in the pollution-affected compartment are those who, while not yet infected, have a heightened risk of acquiring the infection and potentially experiencing more severe disease progression due to the detrimental effects of pollution on their health status. This allows us to explicitly quantify the impact of environmental pollution on the dynamics of infectious respiratory diseases.

Now, in an epidemic model, the progression of a disease is largely influenced by its incidence rate [146]. Incidence rate is a measure used to describe how frequently new cases of a disease or condition occur in a specific population over a certain period of time. Given the complexities involved in how diseases are transmitted, numerous nonlinear incidence models have been introduced to more effectively reflect the dynamics between susceptible and infected populations. This chapter considers a non-monotonic incidence rate of the form $\frac{\beta SI}{1+\gamma I^2}$, which captures realistic aspects of disease transmission and reflects a wider range of dynamic behaviours [26; 36; 157]. The term $\frac{1}{1+\gamma I^2}$ captures how susceptible individuals adjust their behavior due to fear or caution when many people are infected. The βI component represents how strongly the disease spreads, factoring in how behavioral changes can reduce contact. This non-linear pattern of transmission is called the Monod-Haldane (M-H) incidence rate [99]. The M-H incidence rate is considered more realistic than bilinear, saturated, or fractional incidence rates as the infection rate initially increases with the increasing number of infected individuals but eventually decreases when infections become very high, thus depicting its ability to capture saturation, behaviour-driven epidemics and realistic peak modeling.

The structure of the chapter is as follows: In Section 5.2, the mathematical model is formulated along with underlying assumptions. Section 5.3 addresses the fundamental properties of the model, such as existence, uniqueness, positivity, and boundedness of solutions. Section 5.4 focuses on the derivation of the basic reproduction number and analysis of the equilibrium points. Stability of the equilibria, both local and global, is discussed in Section 5.5. The potential occurrence of bifurcation at the

critical threshold $\mathscr{R}_0 = 1$ is investigated in Section 5.6. In Section 5.7, an analytical formulation and solution of the corresponding fractional optimal control problem (FOCP) are presented. Numerical simulations supporting the theoretical results are presented in Section 5.8, followed by conclusions in Section 5.9.

5.2 Model development

In this section, inspired by relevant literature, a novel fractional-order nonlinear compartmental model is introduced using the Caputo derivative. The total human population at any time t is denoted by $N(t)$ and is subdivided into four mutually exclusive compartments:

- $S(t)$: Susceptible individuals not affected by environmental pollution,
- $P(t)$: Individuals experiencing stress or physiological impact due to pollution,
- $I(t)$: Infectious individuals capable of transmitting the disease,
- $R(t)$: Individuals recovered either by treatment or autoimmune.

The development of the model relies on the following assumptions:

(A1) A fraction p of the recruitment rate Λ enters the susceptible class S, while the remaining portion $(1-p)$ enters the pollution-affected class P, accounting for prenatal exposure to pollution.

(A2) The movement of individuals from the S and P compartments into the infected class I is governed by non-monotone Monod-Haldane-type transmission term. This formulation captures non-linear effects in transmission, particularly those arising from psychological responses to increasing infection levels. The infection rate is given by β, and γ quantifies the psychological impact of the disease on the population.

(A3) Due to increased vulnerability, pollution-affected individuals in the class P exhibit a greater susceptibility to infection. This increased risk is modeled through an enhanced transmission rate given by $\beta(1+\delta\beta')$, where β' quantifies the impact of pollution on the baseline transmission rate β and δ scales the influence of environmental pollution on the transmission rate.

(A4) Individuals in the susceptible class may become pollution-affected over time, transitioning to the P compartment at a rate λ.

(A5) All compartments are subject to natural mortality at a constant rate μ, while infected individuals also experience disease-induced mortality at a rate d.

(A6) Infected individuals recover at a rate ϕ, either due to immune system response or effective treatment.

(A7) Recovered individuals are assumed to gain lasting immunity and do not revert to the susceptible class. The model also assumes homogeneous mixing, where every individual has an equal chance of coming into contact with others.

Based on these assumptions, the proposed fractional-order epidemic model is formulated as follows:

$$\begin{aligned}
\frac{d^{\alpha}S(t)}{dt} &= p\Lambda - \frac{\beta SI}{1+\gamma I^2} - \lambda S - \mu S,\\
\frac{d^{\alpha}P(t)}{dt} &= (1-p)\Lambda + \lambda S - \frac{\beta(1+\delta\beta')PI}{1+\gamma I^2} - \mu P,\\
\frac{d^{\alpha}I(t)}{dt} &= \frac{\beta SI}{1+\gamma I^2} + \frac{\beta(1+\delta\beta')PI}{1+\gamma I^2} - dI - \phi I - \mu I,\\
\frac{d^{\alpha}R(t)}{dt} &= \phi I - \mu R,
\end{aligned} \tag{5.1}$$

with initial conditions $S(0) = S_0 \geq 0,\ P(0) = P_0 \geq 0,\ I(0) = I_0 \geq 0,\ R(0) = R_0 \geq 0$ and $t \in [0, t_0],\ t_0 \in \mathbb{R}^+$. The schematic diagram of the disease progression dynamics of model (5.1) is shown in Figure 5.1.

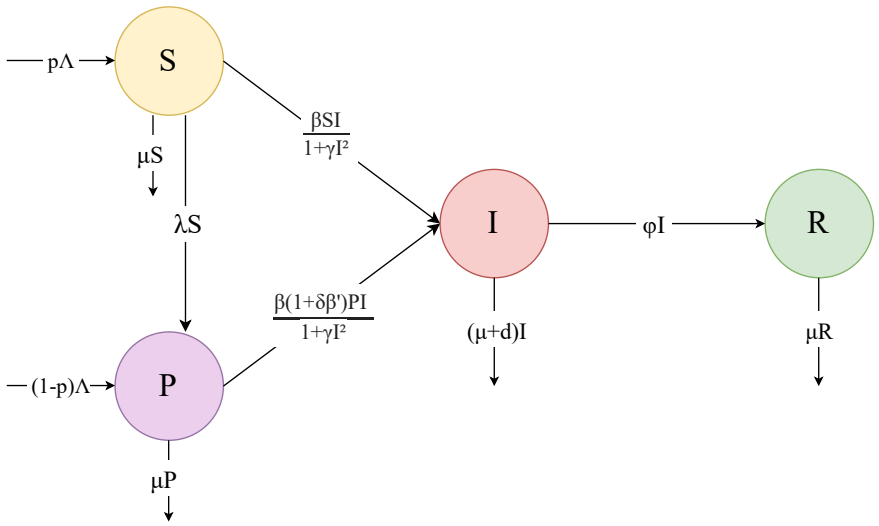

Figure 5.1: Schematic diagram of disease progression dynamics.

5.3 Basic Properties

In this section, the existence and uniqueness of the solution are first shown, followed by the determination of the region of attraction in which the solution remains positive and bounded.

5.3.1 Existence and uniqueness

To verify the existence and uniqueness of solutions for system (5.1), Lemma 1.1.11 has been utilized. For this purpose, consider the domain $[t_0, Q] \times \Omega$, where $\Omega = \{(S,P,I,R) \in \mathbb{R}^4 : \max\{|S|,|P|,|I|,|R|\} \leq M\}$, and both $Q > 0$ and $M > 0$ are real constants.

Theorem 5.3.1 *A unique solution* $\Gamma(t) = (S(t),P(t),I(t),R(t)) \in \Omega$ *to the system* (5.1) *exists for every initial value* $\Gamma_{t_0} = (S_{t_0},P_{t_0},I_{t_0},R_{t_0}) \in \Omega$, *for all* $t > t_0$.

Proof 5.3.2 *Consider any two points* $\Gamma = (S,P,I,R)$ *and* $\Gamma_1 = (S_1,P_1,I_1,R_1)$ *and mapping* $H : \Omega \to \mathbb{R}^4$ *in* Ω *by* $H(\Gamma) = (H_1(\Gamma),H_2(\Gamma),H_3(\Gamma),H_4(\Gamma))$, *where*

$$
\begin{aligned}
H_1(\Gamma) &= p\Lambda - \frac{\beta SI}{1+\gamma I^2} - (\mu+\lambda)S,\\
H_2(\Gamma) &= (1-p)\Lambda + \lambda S - \frac{\beta(1+\delta\beta')PI}{1+\gamma I^2} - \mu P,\\
H_3(\Gamma) &= \frac{\beta SI}{1+\gamma I^2} + \frac{\beta(1+\delta\beta')PI}{1+\gamma I^2} - (\mu+d+\phi)I,\\
H_4(\Gamma) &= \phi I - \mu R
\end{aligned}
$$

For any $\Gamma,\Gamma_1 \in \Omega$, *we have*

$$
\begin{aligned}
\|H(\Gamma)-H(\Gamma_1)\| &= |H_1(\Gamma)-H_1(\Gamma_1)| + |H_2(\Gamma)-H_2(\Gamma_1)| + |H_3(\Gamma)-H_3(\Gamma_1)| + |H_4(\Gamma)-H_4(\Gamma_1)|\\
&= \left| p\Lambda - \frac{\beta SI}{1+\gamma I^2} - (\mu+\lambda)S - p\Lambda + \frac{\beta S_1I_1}{1+\gamma {I_1}^2} + (\mu+\lambda)S_1 \right|\\
&\quad + \left| (1-p)\Lambda + \lambda S - \frac{\beta(1+\delta\beta')PI}{1+\gamma I^2} - \mu P - (1-p)\Lambda - \lambda S_1 + \frac{\beta(1+\delta\beta')P_1I_1}{1+\gamma {I_1}^2} - \mu P_1 \right|\\
&\quad + \left| \frac{\beta SI}{1+\gamma I^2} + \frac{\beta(1+\delta\beta')PI}{1+\gamma I^2} - (\mu+d+\phi)I - \frac{\beta S_1I_1}{1+\gamma {I_1}^2} - \frac{\beta(1+\delta\beta')P_1I_1}{1+\gamma {I_1}^2} + (\mu+d+\phi)I_1 \right|\\
&\quad + |\phi I - \mu R - \phi I_1 + \mu R_1|\\
&\le 2\beta \left| \frac{SI}{1+\gamma I^2} - \frac{S_1I_1}{1+\gamma {I_1}^2} \right| + 2\beta(1+\delta\beta') \left| \frac{PI}{1+\gamma I^2} - \frac{P_1I_1}{1+\gamma {I_1}^2} \right| + (\mu+2\lambda)\,|S-S_1|\\
&\quad + \mu\,|P-P_1| + (\mu+d+2\phi)\,|I-I_1| + \mu\,|R-R_1|\\
&\le 2\beta \left| \frac{SI+\gamma SI{I_1}^2 - S_1I_1 - \gamma S_1I_1I^2}{(1+\gamma I^2)(1+\gamma {I_1}^2)} \right| + 2\beta(1+\delta\beta') \left| \frac{PI+\gamma PI{I_1}^2 - P_1I_1 - \gamma P_1I_1I^2}{(1+\gamma I^2)(1+\gamma {I_1}^2)} \right|\\
&\quad + (\mu+2\lambda)\,|S-S_1| + \mu\,|P-P_1| + (\mu+d+2\phi)\,|I-I_1| + \mu\,|R-R_1|\\
&\le 2\beta M(1+\gamma M^2)|S-S_1| + 2\beta M(1+\gamma M^2)|I-I_1| + 2\beta(1+\delta\beta')M(1+\gamma M^2)|P-P_1|\\
&\quad + 2\beta(1+\delta\beta')M(1+\gamma M^2)|I-I_1| + (\mu+2\gamma)|S-S_1| + \mu|P-P_1| + (\mu+d+2\phi)|I-I_1|\\
&\quad + \mu|R-R_1|\\
&\le K_1|S-S_1| + K_2|P-P_1| + K_3|I-I_1| + K_4|R-R_1|\\
&\le K\,|\Gamma-\Gamma_1|,
\end{aligned}
$$

where $K = max\{K_1,K_2,K_3,K_4\}$ *and*

$$
\begin{aligned}
K_1 &= 2\beta M(1+\gamma M^2) + (\mu+2\lambda), \qquad K_2 = 2\beta M(1+\gamma M^2)(1+\delta\beta') + \mu,\\
K_3 &= 2\beta M(1+\gamma M^2)(2+\delta\beta') + (\mu+d+2\phi), \quad K_4 = \mu.
\end{aligned}
$$

So, $H(\Gamma)$ *satisfies the Lipschitz condition with respect to* $\Gamma \in \Omega$. *According to Lemma 1.1.11, our system* (5.1) *has a unique solution* $\Gamma \in \Omega$. *This proves the theorem.*

5.3.2 Non-negativity and boundedness

To ensure biological validity, the system (5.1) must possess solutions that remain non-negative and bounded. Let us define

$$\Omega^+ = \{(S,P,I,R) \in \Omega : S,P,I,R \in [0,\infty)\}.$$

Theorem 5.3.3 *For any initial condition within Ω^+, the corresponding solution to system* (5.1) *stays non-negative and uniformly bounded over time.*

Proof 5.3.4 *The system's initial solution $\Gamma_{t_0} = (S_{t_0}, P_{t_0}, I_{t_0}, R_{t_0}) \in \Omega^+$ is considered, and from system* (5.1)*, it follows that:*

$$\begin{aligned} D^\alpha S|_{S_{t_0}=0} &= p\Lambda > 0, \\ D^\alpha P|_{P_{t_0}=0} &= (1-p)\Lambda + \lambda S > 0, \\ D^\alpha I|_{I_{t_0}=0} &= 0, \\ D^\alpha R|_{R_{t_0}=0} &= \phi I \geq 0. \end{aligned}$$

By Lemma 1.1.13, $S(t), P(t), I(t), R(t) \geq 0$ for all $t \geq t_0$. This implies that the solution to system (5.1) *will always lie within the set Ω^+.*

Since $N(t) = S(t) + P(t) + I(t) + R(t)$ is the function representing the total population, then

$$\begin{aligned} D^\alpha N &= D^\alpha S + D^\alpha P + D^\alpha I + D^\alpha R \\ &\leq \Lambda - \mu N - dI \\ i.e.\ \ D^\alpha N + \mu N &\leq \Lambda \quad as\ \ I > 0. \end{aligned}$$

We get $N(t) \leq \left(N(t_0) - \frac{\Lambda}{\mu}\right) E_\alpha[-\mu(t-t_0)^\alpha] + \frac{\Lambda}{\mu} \to \frac{\Lambda}{\mu}$ as $t \to \infty$.

Consequently, for any solution of the system (5.1) *that begins in Ω^+, the trajectory remains within the region defined by*

$$\left\{(S,P,I,R) \in \Omega : 0 \leq S+P+I+R \leq \frac{\Lambda}{\mu}\right\}.$$

5.4 Equilibria and the basic reproduction number

It is observed that the variable $R(t)$ is not present in the first four equations. Therefore, it can be excluded from the system (5.1) for further mathematical analysis. Conse-

quently, the resulting system is:

$$\begin{aligned}
\frac{d^{\alpha}S(t)}{dt} &= p\Lambda - \frac{\beta SI}{1+\gamma I^2} - \lambda S - \mu S,\\
\frac{d^{\alpha}P(t)}{dt} &= (1-p)\Lambda + \lambda S - \frac{\beta(1+\delta\beta')PI}{1+\gamma I^2} - \mu P,\\
\frac{d^{\alpha}I(t)}{dt} &= \frac{\beta SI}{1+\gamma I^2} + \frac{\beta(1+\delta\beta')PI}{1+\gamma I^2} - dI - \phi I - \mu I
\end{aligned} \tag{5.2}$$

The above system (5.2) always possesses a disease free equilibrium point $E_0 = E_0(S_0,P_0,I_0) = E_0\left(\frac{p\Lambda}{(\mu+\lambda)}, \frac{(1-p)\Lambda}{(\mu+\lambda)} + \frac{\lambda\Lambda}{\mu(\mu+\lambda)}, 0\right)$. Now, the basic reproduction number using next generation approach [47] is calculated as:

$$\mathscr{R}_0 = \frac{\beta\Lambda\left[p\mu + (\lambda+\mu(1-p))\,(1+\delta\beta')\right]}{\mu(\mu+\lambda)(\mu+d+\phi)}.$$

Further, we will show there exists an endemic equilibrium point $E_1 = E_1(S_*,P_*,I_*)$, where

$$S_* = \frac{\Lambda p\left(\gamma I_*^2+1\right)}{(\mu+\lambda)\left(\gamma I_*^2+1\right)+\beta I_*},\ P_* = \frac{\Lambda\left(\gamma I_*^2+1\right)\left(\mu(1-p)\left(\gamma I_*^2+1\right)+(1-p)\beta I_* + \lambda\left(\gamma I_*^2+1\right)\right)}{\left((\mu+\lambda)\left(\gamma I_*^2+1\right)+\beta I_*\right)\left(\mu\left(\gamma I_*^2+1\right)+\beta(1+\delta\beta')I_*\right)}$$

and I_* is the root of following polynomial

$$A_4{I_*}^4 + A_3{I_*}^3 + A_2{I_*}^2 + A_1 I_* + A_0 = 0, \tag{5.3}$$

where,

$$\begin{aligned}
A_4 &= -\gamma^2\mu(\lambda+\mu)(d+\mu+\phi),\\
A_3 &= -\beta\gamma(d+\mu+\phi)\left(\left(1+\delta\beta'\right)(\lambda+\mu)+\mu\right),\\
A_2 &= \beta\left(1+\delta\beta'\right)(\gamma\lambda\Lambda - \beta(d+\mu+\phi) + \gamma\Lambda\mu(1-p)) + \gamma\mu(\beta\Lambda p - 2(\lambda+\mu)(d+\mu+\phi)),\\
A_1 &= \beta\left(1+\delta\beta'\right)(\beta\Lambda - (\lambda+\mu)(d+\mu+\phi)) - \beta\mu(d+\mu+\phi),\\
A_0 &= \mu(\mu+\lambda)(\mu+d+\phi)(\mathscr{R}_0-1).
\end{aligned}$$

From above, it can be observed that, $A_4,\ A_3 < 0$ and also $A_0 > 0$ for $\mathscr{R}_0 > 1$. So, according to Descarte's rule of sign, the polynomial (5.3) will have at least one positive root I_* exist for $\mathscr{R}_0 > 1$. The current study focuses on the existence of a unique positive equilibrium point. Consider $\mathscr{R}_0 > 1$, then the combinations of signs of coefficients A_1 and A_2 in which unique positive root for polynomial (5.3) exists are as follows:

(i) $A_2 > 0$ and $A_1 > 0$,

(ii) $A_2 < 0$ and $A_1 > 0$,

(iii) $A_2 < 0$ and $A_1 < 0$.

Once the value of I_* is determined, the unique positive endemic equilibrium point $E_1 = E_1(S_*, P_*, I_*)$ is obtained. As a consequence, the following theorem establishes that this equilibrium exists.

Theorem 5.4.1 *If $\mathscr{R}_0 > 1$, then the system* (5.2) *has a unique endemic equilibrium* $E_1 = E_1(S_*, P_*, I_*)$.

5.5 Stability Analysis

Here, the local and global stability of the equilibria is examined. Local stability assesses whether small disturbances near an equilibrium return to it (stable) or move away (unstable). In contrast, global stability examines the system's behavior across the entire state space. Let us assume the subsequent coordinate transform $S(t) = S_*(t) + s(t)$; $P(t) = P_*(t) + p(t)$; $I(t) = I_*(t) + i(t)$, where $(S_*(t), P_*(t), I_*(t))$ denotes the equilibrium point of the model. The linearised system at any steady state is given by

$$\begin{cases} {}_0D_t^{\alpha} S(t) = -\left(\dfrac{\beta I_*}{1+\gamma {I_*}^2} + (\mu+\lambda)\right) S - \dfrac{\beta S_*(1-\gamma {I_*}^2)}{(1+\gamma {I_*}^2)^2} I, \\ {}_0D_t^{\alpha} P(t) = (\lambda) S - \left(\dfrac{\beta(1+\delta\beta')I_*}{1+\gamma {I_*}^2} + \mu\right) P - \dfrac{\beta(1+\delta\beta')P_*(1-\gamma {I_*}^2)}{(1+\gamma {I_*}^2)^2} I, \\ {}_0D_t^{\alpha} I(t) = \left(\dfrac{\beta I_*}{1+\gamma {I_*}^2}\right) S + \left(\dfrac{\beta(1+\delta\beta')I_*}{1+\gamma {I_*}^2}\right) P + \left(\dfrac{\beta S_*(1-\gamma {I_*}^2)}{(1+\gamma {I_*}^2)^2} + \dfrac{\beta(1+\delta\beta')P_*(1-\gamma {I_*}^2)}{(1+\gamma {I_*}^2)^2} - (\mu+d+\phi)\right) I. \end{cases} \tag{5.4}$$

5.5.1 Local stability

Applying the Laplace transform on both side of equation (5.4), we get

$$\begin{aligned} s^{\alpha}\mathscr{L}\{S(t)\} - s^{\alpha-1}S(0) &= -\left(\frac{\beta I_*}{1+\gamma {I_*}^2} + (\mu+\lambda)\right)\mathscr{L}\{S(t)\} - \frac{\beta S_*(1-\gamma {I_*}^2)}{(1+\gamma {I_*}^2)^2}\mathscr{L}\{I(t)\}, \\ s^{\alpha}\mathscr{L}\{P(t)\} - s^{\alpha-1}P(0) &= (\lambda)\mathscr{L}\{S(t)\} - \left(\frac{\beta(1+\delta\beta')I_*}{1+\gamma {I_*}^2} + \mu\right)\mathscr{L}\{P(t)\} \\ &\quad - \frac{\beta(1+\delta\beta')P_*(1-\gamma {I_*}^2)}{(1+\gamma {I_*}^2)^2}\mathscr{L}\{I(t)\}, \\ s^{\alpha}\mathscr{L}\{I(t)\} - s^{\alpha-1}I(0) &= \left(\frac{\beta I_*}{1+\gamma {I_*}^2}\right)\mathscr{L}\{S(t)\} + \left(\frac{\beta(1+\delta\beta')I_*}{1+\gamma {I_*}^2}\right)\mathscr{L}\{P(t)\} \\ &\quad + \left(\frac{\beta S_*(1-\gamma {I_*}^2)}{(1+\gamma {I_*}^2)^2} + \frac{\beta(1+\delta\beta')P_*(1-\gamma {I_*}^2)}{(1+\gamma {I_*}^2)^2} - (\mu+d+\phi)\right)\mathscr{L}\{I(t)\}. \end{aligned} \tag{5.5}$$

Above system(5.5), can be written in the following matrix form:

$$\bigtriangledown(s)\begin{pmatrix}\mathscr{L}\{S(t)\}\\ \mathscr{L}\{P(t)\}\\ \mathscr{L}\{I(t)\}\end{pmatrix}=\begin{pmatrix}\nu_1(s)\\ \nu_2(s)\\ \nu_3(s)\end{pmatrix},$$

where,

$$\nu_1(s)=s^{\alpha-1}S(0),\ \nu_2(s)=s^{\alpha-1}P(0),\ \nu_3(s)=s^{\alpha-1}I(0),$$

and

$$\bigtriangledown(s)=\begin{pmatrix} s^{\alpha}+\frac{\beta I_*}{1+\gamma {I_*}^2}+(\mu+\lambda) & 0 & \frac{\beta S_*(1-\gamma {I_*}^2)}{(1+\gamma {I_*}^2)^2}\\ -\lambda & s^{\alpha}+\frac{\beta(1+\delta\beta')I_*}{1+\gamma {I_*}^2}+\mu & \frac{\beta(1+\delta\beta')P_*(1-\gamma {I_*}^2)}{(1+\gamma {I_*}^2)^2}\\ -\frac{\beta I_*}{1+\gamma {I_*}^2} & -\frac{\beta(1+\delta\beta')I_*}{1+\gamma {I_*}^2} & s^{\alpha}-\frac{\beta S_*(1-\gamma {I_*}^2)}{(1+\gamma {I_*}^2)^2}\\ & & -\frac{\beta(1+\delta\beta')P_*(1-\gamma {I_*}^2)}{(1+\gamma {I_*}^2)^2}+(\mu+d+\phi)\end{pmatrix}. \tag{5.6}$$

For the given system, the characteristic polynomial is $\det(\bigtriangledown(s))$, and $\bigtriangledown(s)$ represents the associated characteristic matrix. The local stability of system (5.2) can be analyzed by examining the eigenvalue distribution of the characteristic polynomial $\det(\bigtriangledown(s))$.

5.5.1.a Local stability of disease-free equilibrium

This subsection is devoted to analyze the local stability of the disease-free equilibrium point $E_0=E_0\left(\frac{p\Lambda}{(\mu+\lambda)},\frac{(1-p)\Lambda}{(\mu+\lambda)}+\frac{\lambda\Lambda}{\mu(\mu+\lambda)},0\right)$, for which the characteristic matrix at DFE is as follows:

$$\bigtriangledown(s)=\begin{pmatrix} s^{\alpha}+\mu+\lambda & 0 & \frac{\beta p\Lambda}{\mu+\lambda}\\ -\lambda & s^{\alpha}+\mu & \beta(1+\delta\beta')\left(\frac{(1-p)\Lambda}{(\mu+\lambda)}+\frac{\lambda\Lambda}{\mu(\mu+\lambda)}\right)\\ 0 & 0 & s^{\alpha}-\frac{\beta p\Lambda}{\mu+\lambda}-\beta(1+\delta\beta')\left(\frac{(1-p)\Lambda}{(\mu+\lambda)}+\frac{\lambda\Lambda}{\mu(\mu+\lambda)}\right)\\ & & +(\mu+d+\phi)\end{pmatrix}. \tag{5.7}$$

So, the characteristic equation is,

$$det(\bigtriangledown(s))=(s^{\alpha}+\mu)(s^{\alpha}+\mu+\lambda)\left(s^{\alpha}+\mu+d+\phi-\frac{\beta\Lambda p}{\lambda+\mu}-\beta\left(1+\delta\beta'\right)\left(\frac{\lambda\Lambda}{\mu(\lambda+\mu)}+\frac{\Lambda(1-p)}{\lambda+\mu}\right)\right)=0.$$

Let $s^{\alpha} = \omega$, then the characteristic equation can be expressed as:

$$(\omega+\mu)(\omega+\mu+\lambda)\left(\omega+\frac{\mu(\mu+\lambda)(\mu+d+\phi)-\beta\mu p\Lambda-\beta(1+\delta\beta')\mu(1-p)\Lambda-\beta(1+\delta\beta')\lambda\Lambda}{\mu(\mu+\lambda)}\right)=0. \tag{5.8}$$

Since stability is determined by the negative eigenvalues of the characteristic equation, two negative eigenvalues are obtained from equation (5.8): $\omega_1 = -\mu$ and $\omega_2 = -(\mu+\lambda)$. The remaining eigenvalues can be analyzed using the following factor of equation (5.8):

$$\left(\omega+\frac{\mu(\mu+\lambda)(\mu+d+\phi)-\beta\mu p\Lambda-\beta(1+\delta\beta')\mu(1-p)\Lambda-\beta(1+\delta\beta')\lambda\Lambda}{\mu(\mu+\lambda)}\right)=0,$$

which is simplified as,

$$\omega+\frac{\mu(\mu+\lambda)(\mu+d+\phi)-\beta\Lambda[p\mu+(\lambda+\mu(1-p))(1+\delta\beta')]}{\mu(\mu+\lambda)}=0,$$
$$\omega+(\mu+d+\phi)(1-\mathscr{R}_0)=0.$$

Therefore, the third eigen value is $\omega_3 = -(\mu+d+\phi)(1-\mathscr{R}_0)$. The sign of ω_3 depends on $\mathscr{R}_0$. When $\mathscr{R}_0$ is less than one, ω_3 has negative sign and consequently, all the eigenvalues have negative sign.

Therefore, the disease-free equilibrium E_0 of system (5.2) exhibits local asymptotic stability when $\mathscr{R}_0 < 1$, and instability when $\mathscr{R}_0 > 1$. This leads to the following theorem.

Theorem 5.5.1 *The equilibrium point E_0 corresponding to the disease-free state is locally asymptotically stable if and only if the threshold value $\mathscr{R}_0$ is less than one, otherwise unstable.*

The local stability behavior of E_0 at $\mathscr{R}_0 = 1$ and the possibility of bifurcation are explored in Section 5.6.

5.5.1.b Local stability of endemic equilibrium

This subsection discusses the local stability of the endemic equilibrium $E_1 = E_1(S_*, P_*, I_*)$, for which the characteristic matrix $\bigtriangledown(s)$ from equation (5.6) at E_1, is given by:

$$\bigtriangledown(s)=\begin{pmatrix} s^{\alpha}+\frac{\beta I_*}{1+\gamma {I_*}^2}+(\mu+\lambda) & 0 & \frac{\beta S_*(1-\gamma {I_*}^2)}{(1+\gamma {I_*}^2)^2} \\ -\lambda & s^{\alpha}+\frac{\beta(1+\delta\beta')I_*}{1+\gamma {I_*}^2}+\mu & \frac{\beta(1+\delta\beta')P_*(1-\gamma {I_*}^2)}{(1+\gamma {I_*}^2)^2} \\ -\frac{\beta I_*}{1+\gamma {I_*}^2} & -\frac{\beta(1+\delta\beta')I_*}{1+\gamma {I_*}^2} & s^{\alpha}-\frac{\beta S_*(1-\gamma {I_*}^2)}{(1+\gamma {I_*}^2)^2} \\ & & -\frac{\beta(1+\delta\beta')P_*(1-\gamma {I_*}^2)}{(1+\gamma {I_*}^2)^2}+(\mu+d+\phi) \end{pmatrix}. \tag{5.9}$$

Let $s^{\alpha}=\psi$, then the characteristic equation corresponding to characteristic matrix (5.9) is:

$$\begin{aligned} det(\bigtriangledown(s))=\frac{}{}&\big({I_*}^2\gamma(\lambda+\mu+\psi)+I_*\beta+\lambda+\mu+\psi\big)\big({I_*}^4\gamma^2(\mu+\psi)(d+\mu+\psi+\phi)\\ &+{I_*}^3\beta\gamma(d+\mu+\psi+\phi)+{I_*}^2\gamma(\mu+\psi)(2d+2\mu+\beta P_*+\beta S_*+2\psi+2\phi)\\ &+I_*\beta(d+\mu+\psi+\phi)+(\mu+\psi)(d+\mu-\beta P_*-\beta S_*+\psi+\phi)\big)\\ &+\beta\beta'\delta\big({I_*}^5\gamma^2(\lambda+\mu+\psi)(d+\mu+\psi+\phi)+{I_*}^4\gamma(\beta(\mu+\psi+\phi)\\ &+\beta d+\gamma P_*(\mu+\psi)(\lambda+\mu+\psi))+{I_*}^3\gamma\big(2d(\lambda+\mu+\psi)+2\lambda\mu\\ &+2\lambda\psi+2\lambda\phi+2\mu^2+4\mu\psi+2\mu\phi+\beta P_*(\mu+\psi)+\beta\mu S_*+\beta S_*\psi\\ &+2\psi^2+2\psi\phi\big)+{I_*}^2\beta(d+\mu+\psi+\phi)+I_*\big(d(\lambda+\mu+\psi)+\lambda\mu\\ &+\lambda\psi+\lambda\phi+\mu^2+2\mu\psi+\mu\phi-\beta P_*(\mu+\psi)-\beta\mu S_*-\beta S_*\psi+\psi^2+\psi\phi\big)\\ &-P_*(\mu+\psi)(\lambda+\mu+\psi)\big)\\ &\Big/\big({I_*}^2\gamma+1\big)^3=0 \end{aligned}$$

This can be rewritten as,

$$\left.\begin{aligned} det(\bigtriangledown(s))=\ &\big({I_*}^2\gamma(\lambda+\mu+\psi)+I_*\beta+\lambda+\mu+\psi\big)\big({I_*}^4\gamma^2(\mu+\psi)(d+\mu+\psi+\phi)\\ &+{I_*}^3\beta\gamma(d+\mu+\psi+\phi)+{I_*}^2\gamma(\mu+\psi)(2d+2\mu+\beta P_*+\beta S_*+2\psi+2\phi)\\ &+I_*\beta(d+\mu+\psi+\phi)+(\mu+\psi)(d+\mu-\beta P_*-\beta S_*+\psi+\phi)\big)\\ &+\beta\beta'\delta\big({I_*}^5\gamma^2(\lambda+\mu+\psi)(d+\mu+\psi+\phi)+{I_*}^4\gamma(\beta(\mu+\psi+\phi)\\ &+\beta d+\gamma P_*(\mu+\psi)(\lambda+\mu+\psi))+{I_*}^3\gamma\big(2d(\lambda+\mu+\psi)+2\lambda\mu\\ &+2\lambda\psi+2\lambda\phi+2\mu^2+4\mu\psi+2\mu\phi+\beta P_*(\mu+\psi)+\beta\mu S_*+\beta S_*\psi\\ &+2\psi^2+2\psi\phi\big)+{I_*}^2\beta(d+\mu+\psi+\phi)+I_*\big(d(\lambda+\mu+\psi)+\lambda\mu\\ &+\lambda\psi+\lambda\phi+\mu^2+2\mu\psi+\mu\phi-\beta P_*(\mu+\psi)-\beta\mu S_*-\beta S_*\psi+\psi^2+\psi\phi\big)\\ &-P_*(\mu+\psi)(\lambda+\mu+\psi)\big) \end{aligned}\right\}=0$$

which can be simplified into the following polynomial form:

$$A_3\psi^3 + A_2\psi^2 + A_1\psi + A_0 = 0, \tag{5.10}$$

where,

$$\begin{aligned}
A_3 &= \left(1+\gamma {I_*}^2\right)^3,\\
A_2 &= \left({I_*}^2\gamma+1\right)\left({I_*}^4\gamma^2\mu + {I_*}^4\gamma^2(d+\mu+\phi) + {I_*}^3\beta\gamma + \left({I_*}^2\gamma+1\right)^2(\lambda+\mu)\right.\\
&\quad + 2{I_*}^2\gamma\mu + 2{I_*}^2\gamma(d+\mu+\phi) + {I_*}^2\beta\gamma S_* + \beta\left(1+\delta\beta'\right)\left({I_*}^3\gamma + {I_*}^2\gamma P_* + I_* - P_*\right)\\
&\quad \left. + I_*\beta + d + 2\mu - \beta S_* + \phi\right),\\
A_1 &= \left({I_*}^2\gamma+1\right)\left(\left({I_*}^2\gamma+1\right)(d+\mu+\phi)\left({I_*}^2\gamma\mu + I_*\beta + \mu\right) + (\lambda+\mu)\left(\mu\left({I_*}^2\gamma+1\right)^2\right.\right.\\
&\quad \left.\left. + \left({I_*}^2\gamma+1\right)^2(d+\mu+\phi) + \beta S_*\left({I_*}^2\gamma - 1\right)\right) + \beta\mu\left({I_*}^3\gamma + {I_*}^2\gamma S_* + I_* - S_*\right)\right)\\
&\quad + \beta\left(1+\delta\beta'\right)\left({I_*}^4\beta\gamma + {I_*}^4\gamma^2\mu P_* + {I_*}^3\beta\gamma P_* + {I_*}^3\beta\gamma S_* + {I_*}^2\beta\right.\\
&\quad + I_*\left({I_*}^2\gamma+1\right)^2(d+\mu+\phi) + \left({I_*}^2\gamma+1\right)(\lambda+\mu)\left({I_*}^3\gamma + {I_*}^2\gamma P_* + I_* - P_*\right)\\
&\quad \left. - I_*\beta P_* - I_*\beta S_* - \mu P_*\right),\\
A_0 &= \mu\left({I_*}^2\gamma+1\right)\left(I_*\beta\left({I_*}^2\gamma+1\right)(d+\mu+\phi) + (\lambda+\mu)\left(\left({I_*}^2\gamma+1\right)^2(d+\mu+\phi)\right.\right.\\
&\quad \left.\left. + \beta S_*\left({I_*}^2\gamma - 1\right)\right)\right) + \beta\left(1+\delta\beta'\right)\left((\lambda+\mu)\left(I_*\left({I_*}^2\gamma+1\right)^2(d+\mu+\phi)\right.\right.\\
&\quad + \left({I_*}^2\gamma - 1\right)\left({I_*}^2\gamma\mu P_* + I_*\beta S_* + \mu P_*\right)\right) + I_*\beta\left(\left({I_*}^3\gamma + I_*\right)(d+\mu+\phi)\right.\\
&\quad \left.\left. - \left({I_*}^2\gamma - 1\right)(\lambda S_* - \mu P_*)\right)\right)
\end{aligned}$$

Considering $B_0 = \dfrac{A_0}{A_3}$, $B_1 = \dfrac{A_1}{A_3}$, and $B_2 = \dfrac{A_2}{A_3}$, equation (5.10) transforms into

$$P(\psi) = \psi^3 + B_2\psi^2 + B_1\psi + B_0. \tag{5.11}$$

According to the Routh-Hurwitz criteria for fractional-order systems [4], the roots of this polynomial satisfying $|\arg\psi_i| > \frac{\alpha\pi}{2}$, $i = 1,2,3$ indicate local stability. For the polynomial $P(\psi)$, the discriminant $D(\psi)$ is given by

$$D(\psi) = 18B_2B_1B_0 + (B_2B_1)^2 - 4B_0{B_2}^3 - 4{B_1}^3 - 27{B_0}^2.$$

If all three roots of $P(\psi) = 0$ have negative real parts, then the equilibrium point $E_1(S_*, P_*, I_*)$ is locally stable, as stated in the following theorem [4]:

Theorem 5.5.2 *The endemic equilibrium $E_1 = E_1(S_*, P_*, I_*)$ is locally asymptotically stable if any of the following conditions hold:*

(i) $B_2 > 0,\ B_0 > 0,\ B_2B_1 > B_0$ *when* $D(\psi) > 0,$

(ii) If $D(\psi) < 0,\ B_2 \geq 0,\ B_1 \geq 0,\ B_0 > 0,\ \alpha < \frac{2}{3},$

(iii) If $D(\psi) < 0,\ B_2 > 0,\ B_1 > 0,\ B_2B_1 = B_0,\ \alpha \in (0,1].$

Otherwise, the endemic equilibrium $E_1 = E_1(S_*, P_*, I_*)$ *is unstable if the condition* $D(\psi) < 0,\ B_2 < 0,\ B_1 < 0,\ \alpha > \frac{2}{3}$ *holds, as in this case, all roots satisfy* $|\arg(\psi_i)| < \frac{\alpha\pi}{2}$.

5.5.2 Global stability

This subsection investigates the global stability of the disease-free equilibrium E_0 and the endemic equilibrium E_1 using the Lyapunov stability method for fractional-order systems.

5.5.2.a Global stability of disease-free equilibrium

The suitable positive definite Lyapunov function, to discuss the global stability of disease free equilibrium E_0, is constructed as:

$$\mathscr{L}(t) = I(t),$$

then for order α, differentiating both side along-with E_0 we have,

$$\begin{aligned}
D_t^{\alpha}\mathscr{L} &= D_t^{\alpha} I(t) \\
&= \left[\frac{\beta SI}{1+\gamma I^2} + \frac{\beta(1+\delta\beta')PI}{1+\gamma I^2} - (\mu+d+\phi)I\right] \\
&\leq \left[\beta S + \beta(1+\delta\beta')P - (\mu+d+\phi)\right] I(t) \\
&\leq \left[\frac{\beta p\Lambda}{\mu+\lambda} + \beta(1+\delta\beta')\left(\frac{(1-p)\Lambda}{\mu+\lambda} + \frac{\lambda\Lambda}{\mu(\mu+\lambda)}\right) - (\mu+d+\phi)\right] I(t) \\
&\leq \left[\frac{\beta\Lambda\left[p\mu + (\mu(1-p)+\lambda)(1+\delta\beta')\right]}{\mu(\mu+\lambda)} - (\mu+d+\phi)\right] I(t) \\
&\leq (\mu+d+\phi)(\mathscr{R}_0 - 1)I(t) \\
&\leq 0 \quad \text{if } \mathscr{R}_0 < 1.
\end{aligned}$$

It is evident that $D_t^{\alpha}\mathscr{L}(t)$ is negative when $\mathscr{R}_0 < 1$ and equals zero at E_0. Thus, by the Lyapunov stability theorem [44], E_0 is globally asymptotically stable when $\mathscr{R}_0 < 1$, leading to the following theorem:

Theorem 5.5.3 *The DFE point* E_0 *of the system* (5.2) *is GAS (Globally asymptotically Stable) if the basic reproduction number* $\mathscr{R}_0$ *is strictly less than unity i.e.* $\mathscr{R}_0 < 1$.

5.5.2.b Global stability of endemic equilibrium

To discuss the global stability of endemic equilibrium point E_1, we have constructed the following positive definite Lyapunov function:

$$\mathscr{L}(t) = \left(S - S_* - S_* \log \frac{S}{S_*}\right) + \left(P - P_* - P_* \log \frac{P}{P^*}\right) + \left(I - I_* - I_* \log \frac{I}{I_*}\right),$$

the fractional derivative of both side of order α along-with the endemic equilibrium point E_1 and with help of Lemma 1.1.9 is:

$$\begin{aligned} D_t^\alpha \mathscr{L}(t) &\leq \left(1 - \frac{S_*}{S}\right) D_t^\alpha S(t) + \left(1 - \frac{P_*}{P}\right) D_t^\alpha P(t) + \left(1 - \frac{I_*}{I}\right) D_t^\alpha I(t) \\ &\leq \left(1 - \frac{S_*}{S}\right)\left(p\Lambda - \frac{\beta SI}{1+\gamma I^2} - (\mu+\lambda)S\right) \\ &+ \left(1 - \frac{P_*}{P}\right)\left((1-p)\Lambda + \lambda S - \frac{\beta(1+\delta\beta')PI}{1+\gamma I^2} - \mu P\right) \\ &+ \left(1 - \frac{I_*}{I}\right)\left(\frac{\beta SI}{1+\gamma I^2} + \frac{\beta(1+\delta\beta')PI}{1+\gamma I^2} - (\mu+d+\phi)I\right). \end{aligned}$$

Let $f(I) = \frac{I}{1+\gamma I^2}$, then from the steady state equation, we also have,

$$p\Lambda = \beta S_* f(I_*) + (\mu+\lambda)S_*, \quad (1-p)\Lambda = -\lambda S_* + \beta(1+\delta\beta')P_* f(I_*) + \mu P_*,$$

$$(\mu+d+\phi) = \frac{\beta S_* f(I_*)}{I_*} + \frac{\beta(1+\delta\beta')P_* f(I_*)}{I_*}.$$

Thus,

$$\begin{aligned} D_t^\alpha \mathscr{L}(t) &\leq \left(1 - \frac{S_*}{S}\right)\left(\beta S_* f(I_*) + (\mu+\lambda)S_* - \beta S f(I) - (\mu+\lambda)S\right) \\ &+ \left(1 - \frac{P_*}{P}\right)\left(-\lambda S_* + \beta(1+\delta\beta')P_* f(I_*) + \mu P_* + \lambda S - \beta(1+\delta\beta')P f(I) - \mu P\right) \\ &+ \left(1 - \frac{I_*}{I}\right)\left(\beta S f(I) + \beta(1+\delta\beta')P f(I) - \frac{\beta S_* f(I_*) I}{I_*} - \frac{\beta(1+\delta\beta')P_* f(I_*) I}{I_*}\right) \\ &\leq (\mu+\lambda)S_*\left(2 - \frac{S_*}{S} - \frac{S}{S_*}\right) + \mu P_*\left(2 - \frac{P_*}{P} - \frac{P}{P_*}\right) \\ &\quad + \beta S_* f(I_*)\left(1 - \frac{S_*}{S} - \frac{S}{S_*}\frac{f(I)}{f(I_*)} + \frac{f(I)}{f(I_*)}\right) \\ &\quad + \beta S f(I)\left(1 - \frac{I_*}{I} - \frac{S_*}{S}\frac{I}{I_*}\frac{f(I_*)}{f(I)} + \frac{S_*}{S}\frac{f(I_*)}{f(I)}\right) \\ &\quad + \beta(1+\delta\beta')P_* f(I_*)\left(1 - \frac{P_*}{P} - \frac{P}{P_*}\frac{f(I)}{f(I_*)} + \frac{f(I)}{f(I_*)}\right) \\ &\quad + \beta(1+\delta\beta')P f(I)\left(1 - \frac{I_*}{I} - \frac{P_*}{P}\frac{I}{I_*}\frac{f(I_*)}{f(I)} + \frac{P_*}{P}\frac{f(I_*)}{f(I)}\right) \\ &\quad + \lambda S\left(1 - \frac{P_*}{P} - \frac{S_*}{S} + \frac{S_*}{S}\frac{P_*}{P}\right). \end{aligned}$$

Since, $\frac{a+b}{2} \geq \sqrt{ab}$ for any a and b. This relation suggests that,

$$\left(2-\frac{S_*}{S}-\frac{S}{S_*}\right)\leq 0, \quad \text{and} \quad \left(2-\frac{P_*}{P}-\frac{P}{P_*}\right)\leq 0$$

and if

$$\left.\begin{aligned}
&\left(1-\frac{S_*}{S}-\frac{S}{S_*}\frac{f(I)}{f(I_*)}+\frac{f(I)}{f(I_*)}\right)\leq 0,\\
&\left(1-\frac{I_*}{I}-\frac{S_*}{S}\frac{I}{I_*}\frac{f(I_*)}{f(I)}+\frac{S_*}{S}\frac{f(I_*)}{f(I)}\right)\leq 0,\\
&\left(1-\frac{P_*}{P}-\frac{P}{P_*}\frac{f(I)}{f(I_*)}+\frac{f(I)}{f(I_*)}\right)\leq 0,\\
&\left(1-\frac{I_*}{I}-\frac{P_*}{P}\frac{I}{I_*}\frac{f(I_*)}{f(I)}+\frac{P_*}{P}\frac{f(I_*)}{f(I)}\right)\leq 0,\\
&\left(1-\frac{P_*}{P}-\frac{S_*}{S}+\frac{S_*}{S}\frac{P_*}{P}\right)\leq 0,
\end{aligned}\right\} \tag{5.12}$$

then, $D_t^{\alpha}\mathscr{L}(t)\leq 0$. Therefore, by the Lyapunov stability theorem [44], the endemic equilibrium $E_1(S_*,P_*,I_*)$ is globally asymptotically stable when $\mathscr{R}_0>1$. Thus, we have the following theorem.

Theorem 5.5.4 *The endemic equilibrium $E_1(S_*,P_*,I_*)$ is globally asymptotically stable, for all $\alpha\in(0,1]$, when $\mathscr{R}_0>1$.*

5.6 Bifurcation analysis at $\mathscr{R}_0=1$ around E_0

This section analyzes system (5.2) in the context of a non-hyperbolic equilibrium, where the linearized matrix has at least one eigenvalue with a real part equal to zero. This analysis is crucial as it provides valuable insights into the stability of the coexistence equilibrium near the critical point E_0 and the threshold $\mathscr{R}_0=1$. This investigation determines the bifurcation direction and describes the local behavior of E_0 at $\mathscr{R}_0=1$. To evaluate the local stability of E_0 near this threshold, bifurcation theory is applied as described in [35], which is based on the center manifold theory [34]. This approach is used to study system (5.2) with the assumption that $(S,P,I)=(x_1,x_2,x_3)$, as follows:

$$\begin{aligned}
\frac{d^{\alpha}S(t)}{dt}&=p\Lambda-\frac{\beta x_1x_3}{1+\gamma {x_3}^2}-(\lambda+\mu)x_1=f_1,\\
\frac{d^{\alpha}P(t)}{dt}&=(1-p)\Lambda+\lambda x_1-\frac{\beta(1+\delta\beta')x_2x_3}{1+\gamma {x_3}^2}-\mu x_2=f_2,\\
\frac{d^{\alpha}I(t)}{dt}&=\frac{\beta x_1x_3}{1+\gamma {x_3}^2}+\frac{\beta(1+\delta\beta')x_2x_3}{1+\gamma {x_3}^2}-(\mu+d+\phi)x_3=f_3
\end{aligned} \tag{5.13}$$

Recall that $\mathscr{R}_0 = \dfrac{\beta\Lambda[p\mu + (\lambda + \mu(1-p))(1+\delta\beta')]}{\mu(\mu+\lambda)(\mu+d+\phi)}$ and select β as a bifurcation parameter for $\mathscr{R}_0 = 1$ which takes the following form:

$$\beta = \beta^* = \frac{\mu(\mu+\lambda)(\mu+d+\phi)}{\Lambda[p\mu + (\lambda+\mu(1-p))(1+\delta\beta')]}.$$

Further, the jacobian matrix of the system (5.2) at E_0

$$J_{[E_0]} = \begin{pmatrix} \mu+\lambda & 0 & \dfrac{\beta p\Lambda}{\mu+\lambda} \\ -\lambda & \mu & \beta(1+\delta\beta')\left(\dfrac{(1-p)\Lambda}{(\mu+\lambda)} + \dfrac{\lambda\Lambda}{\mu(\mu+\lambda)}\right) \\ 0 & 0 & (\mu+d+\phi)(1-\mathscr{R}_0) \end{pmatrix},$$

and at the chosen bifurcation parameter $\beta = \beta^*$ it is given by $J_{[E_0,\beta^*]}$ as:

$$J_{[E_0,\beta^*]} = \begin{pmatrix} \mu+\lambda & 0 & \dfrac{\beta^* p\Lambda}{\mu+\lambda} \\ -\lambda & \mu & \beta^*(1+\delta\beta')\left(\dfrac{(1-p)\Lambda}{(\mu+\lambda)} + \dfrac{\lambda\Lambda}{\mu(\mu+\lambda)}\right) \\ 0 & 0 & 0 \end{pmatrix}. \tag{5.14}$$

The eigenvalues of matrix (5.14) are obtained as $\omega_1 = -(\mu+\lambda),\ \omega_2 = -\mu,\ \omega_3 = 0$. It is clear that two eigen values are with negative real part an the remaining one is 0, and hence for $\mathscr{R}_0 = 1$ the disease free equilibrium E_0 becomes a non-hyperbolic equilibrium.

Now, consider $w = (w_1, w_2, w_3)$ as the right eigen vector corresponding to third eigen value 0. Then, it can be computed as follow:

$$\begin{pmatrix} \mu+\lambda & 0 & \dfrac{\beta^* p\Lambda}{\mu+\lambda} \\ -\lambda & \mu & \beta^*(1+\delta\beta')\left(\dfrac{(1-p)\Lambda}{(\mu+\lambda)} + \dfrac{\lambda\Lambda}{\mu(\mu+\lambda)}\right) \\ 0 & 0 & 0 \end{pmatrix} \begin{pmatrix} w_1 \\ w_2 \\ w_3 \end{pmatrix} = \begin{pmatrix} 0 \\ 0 \\ 0 \end{pmatrix},$$

which is,

$$(\mu+\lambda)w_1 + \left(\frac{\beta^* p\Lambda}{\mu+\lambda}\right)w_3 = 0,$$
$$-\lambda w_1 + \mu w_2 + \left[\beta^*(1+\delta\beta')\left(\frac{(1-p)\Lambda}{(\mu+\lambda)} + \frac{\lambda\Lambda}{\mu(\mu+\lambda)}\right)\right]w_3 = 0.$$

Since, w_3 is free variable, so considering $w_3 = 1$ and solving above equations, we get

$$\{w_1, w_2, w_3\} = \left\{-\frac{\beta^*\Lambda p}{(\mu+\lambda)^2}, -\frac{\beta^*\Lambda(1+\delta\beta')(\mu+\lambda)[\lambda+\mu(1-p)] + \mu p\lambda\beta^*\Lambda}{\mu^2(\mu+\lambda)^2}, 1\right\}$$

In a similar way, consider $u=(u_1,u_2,u_3)$ as the left eigen vector corresponding to 0 eigen value and computed as:

$$\begin{pmatrix} u_1 & u_2 & u_3 \end{pmatrix}\begin{pmatrix} \mu+\lambda & 0 & \dfrac{\beta^* p\Lambda}{\mu+\lambda} \\ -\lambda & \mu & \beta^*(1+\delta\beta')\left(\dfrac{(1-p)\Lambda}{(\mu+\lambda)}+\dfrac{\lambda\Lambda}{\mu(\mu+\lambda)}\right) \\ 0 & 0 & 0 \end{pmatrix}=\begin{pmatrix} 0 \\ 0 \\ 0 \end{pmatrix},$$

which is

$$\begin{aligned} (\mu+\lambda)u_1-\lambda u_2&=0,\\ \mu u_2&=0,\\ \left(\frac{\beta^* p\Lambda}{\mu+\lambda}\right)u_1+\left[\beta^*(1+\delta\beta')\left(\frac{(1-p)\Lambda}{(\mu+\lambda)}+\frac{\lambda\Lambda}{\mu(\mu+\lambda)}\right)\right]u_2&=0. \end{aligned}$$

In this case also u_3 is treated as a free variable and is assumed to equal 1. By solving the above equations, we get

$$\{u_1,u_2,u_3\}=\{0,0,1\}.$$

Now, by using Theorem 4.1 given in [35] the coefficients A and B can be computed as

$$A=\sum_{k,i,j=1}^{3}u_k w_i w_j\left(\frac{\partial^2 f_k}{\partial x_i\partial x_j}\right)_{[E_0,\beta^*]} \quad \text{and} \quad B=\sum_{k,i=1}^{3}u_k w_i\left(\frac{\partial^2 f_k}{\partial x_i\partial\beta^*}\right)_{[E_0,\beta^*]}$$

The non-zero partial derivatives of $f_k's$ at E_0 and $\beta=\beta^*$ are evaluated as follows:

$$\begin{aligned} \frac{\partial^2 f_1}{\partial x_1\partial x_3}&=-\beta^*=\frac{\partial^2 f_1}{\partial x_3\partial x_1},\\ \frac{\partial^2 f_2}{\partial x_2\partial x_3}&=-\beta^*(1+\delta\beta')=\frac{\partial^2 f_2}{\partial x_3\partial x_2},\\ \frac{\partial^2 f_3}{\partial x_1\partial x_3}&=\beta^*=\frac{\partial^2 f_3}{\partial x_3\partial x_1},\\ \frac{\partial^2 f_3}{\partial x_2\partial x_3}&=\beta^*(1+\delta\beta')=\frac{\partial^2 f_3}{\partial x_3\partial x_2},\\ \frac{\partial^2 f_1}{\partial x_3\partial\beta^*}&=-\frac{p\Lambda}{\mu+\lambda},\\ \frac{\partial^2 f_2}{\partial x_3\partial\beta^*}&=-\frac{\Lambda(1+\delta\beta')(\lambda+\mu(1-p))}{\mu(\mu+\lambda)},\\ \frac{\partial^2 f_3}{\partial x_3\partial\beta^*}&=\frac{\Lambda[\mu p+(1+\delta\beta')(\lambda+\mu(1-p))]}{\mu(\mu+\lambda)}. \end{aligned}$$

The expression A and B are simplified as

$$A = 2w_1w_3\left[u_1\frac{\partial^2 f_1}{\partial x_1\partial x_3}+u_3\frac{\partial^2 f_3}{\partial x_1\partial x_3}\right]+2w_3w_2\left[u_2\frac{\partial^2 f_2}{\partial x_3\partial x_2}+u_3\frac{\partial^2 f_3}{\partial x_3\partial x_2}\right]$$
$$= -\frac{2\Lambda\beta^{*2}}{\mu^2(\mu+\lambda)}\left[\mu\delta\beta'(1-p)+\lambda\delta\beta'+(\mu+\lambda)\right]<0,$$

and

$$B = u_3w_3\frac{\partial^2 f_3}{\partial x_3\partial\beta^*}$$
$$= \frac{\Lambda[\mu p+(1+\delta\beta')(\lambda+\mu(1-p))]}{\mu(\mu+\lambda)}>0.$$

As, all the parameters in the coefficient of bifurcation A and B are positive and the sign of A is '-'ve and B is '+'ve, which results in the forward transcritical bifurcation at disease free equilibrium E_0, based on Theorem 4.1 of [35]. To support this numerically, a graphical illustration is presented in Figure 5.2, based on the parameter values provided in Table 5.1. The figure further demonstrates that the disease-free equilibrium remains stable when $\mathscr{R}_0 < 1$. However, as $\mathscr{R}_0$ exceeds unity, the system admits a stable and unique endemic equilibrium.

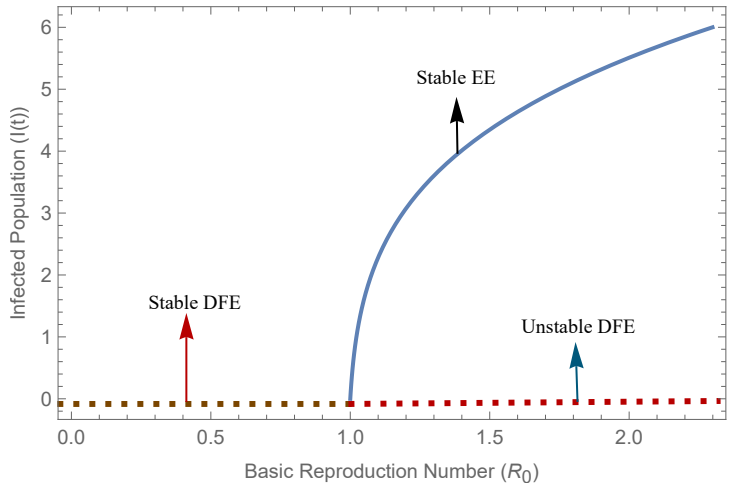

Figure 5.2: Transcritical forward bifurcation.

5.7 Optimal Control Formulations

In this section, the mathematical model (5.1) is extended to a fractional optimal control framework by introducing two time-dependent control variables, $v_1(t)$ and $v_2(t)$,

which represent the influence of information-based (non-pharmaceutical) interventions. These interventions include strategies such as public health campaigns, awareness initiatives, social distancing mandates, and behavioral modifications guided by real-time information on disease prevalence. These control strategies play a crucial role in mitigating the spread of infectious diseases, especially when pharmaceutical measures (such as vaccines or antivirals) are either limited or unavailable.

In this formulation of the optimal control problem, fractional differential equations are employed, providing a more accurate description of system dynamics than traditional integer-order models [164]. The primary objective is to analyze the effect of these control strategies on the progression of disease and optimize the related implementation costs.

It is assumed that the transmission rate among both the susceptible and pollution affected populations is reduced by the factors $(1-v_1(t))$ and $(1-v_2(t))$, respectively, due to the control measures taken. Here, $v_i(t);\ i=1,2;$ represents the intensity of response to information, where $0 \leq v_i(t) \leq 1$. A value of 0 indicates no response, while a value of 1 signifies a full behavioral response from informed individuals.

The application of such controls incurs a cost, modeled as a nonlinear function of $v_i(t);\ i=1,2;$ to encourage individuals to alter their behavior in response to information. The set of admissible control functions $v_i(t)$ is given by:

$$V = \{v_i(t);\ i=1,2;|\ v_i \text{ is Lebesgue measurable for } t \in [0,T],\ 0 \leq v_i(t) \leq 1\},$$

where T refers to the final time of control application and each $v_i(t)$ is a bounded and measurable.

The introduction of control variables $v_i(t)$ is aimed at minimizing both the proportion of the infected population and the corresponding implementation costs of implementing the control measures, which is given by:

$$\mathscr{J}[v] = \int_0^T \left(g_1 I + \frac{1}{2} z_1 {v_1}^2 + \frac{1}{2} z_2 {v_2}^2 \right) dt, \tag{5.15}$$

subject to model system

$$\begin{aligned}
\frac{d^{\alpha}S(t)}{dt} &= p\Lambda - (1-v_1(t))\frac{\beta SI}{1+\gamma I^2} - \lambda S - \mu S,\\
\frac{d^{\alpha}P(t)}{dt} &= (1-p)\Lambda + \lambda S - (1-v_2(t))\frac{\beta(1+\delta\beta')PI}{1+\gamma I^2} - \mu P,\\
\frac{d^{\alpha}I(t)}{dt} &= (1-v_1(t))\frac{\beta SI}{1+\gamma I^2} + (1-v_2(t))\frac{\beta(1+\delta\beta')PI}{1+\gamma I^2} - dI - \phi I - \mu I,\\
\frac{d^{\alpha}R(t)}{dt} &= \phi I - \mu R,
\end{aligned} \tag{5.16}$$

with $S(0) \geq 0,\ P(0) \geq 0,\ I(0) \geq 0$ and $R(0) \geq 0$. Here, the function $\mathscr{J}$ represents the overall cost, while the expression $L(I, v_1(t), v_2(t)) = g_1 I + \frac{1}{2} z_1 {v_1}^2 + \frac{1}{2} z_2 {v_2}^2$ denotes the instantaneous cost at any given time t. The parameter g_1 is positive weight constants used to balance the units within the cost expression. The control effort is represented by the quadratic term ${v_i}^2$. For convenience, we use $v_i(t) = v_i$.

Pontryagin's Maximum Principle [105] is applied to demonstrate the existence and characterization of optimal control functions that minimize the cost functional over a finite time. Following the methodologies presented in the literature [17; 74], the necessary and sufficient conditions for optimality are stated and proved.

Theorem 5.7.1 *There exists a control pair $(\bar{v_1}, \bar{v_2}) \in V$ that satisfies the system* (5.16) *if the following conditions hold:*

1. *For $(\bar{v_1}, \bar{v_2}) \in V$, the solution set of the system* (5.16) *is non-empty.*

2. *The state system* (5.16) *can be expressed as a linear function of the control variables, with coefficients that depend on time and state variables. Moreover, the admissible control set V is closed and convex.*

3. *The integrand $L = g_1 I + \frac{1}{2} z_1 {v_1}^2 + + \frac{1}{2} z_2 {v_2}^2$ is convex in v and $L \geq \phi(v_1, v_2)$, where ϕ is continuous function such that $\frac{\phi(v_1, v_2)}{|(v_1, v_2)|} \to \infty$ as $|(v_1, v_2)| \to \infty$.*

Proof 5.7.2 *The solutions of system* (5.16) *are positively invariant and remain bounded within the region Ω. Furthermore, the right-hand side of each equation in the model satisfies the Lipschitz condition with respect to the state variables, as demonstrated in the theorems presented in Section 5.3. Consequently, the first condition is satisfied by invoking the Picard-Lindelof theorem [103].*

The admissible control set V is, by definition, closed and convex. Moreover, the system (5.16) *is linear in control variables, thus satisfying the second condition. Additionally, the integrand* $L = g_1 I + \frac{1}{2} z_1 {v_1}^2 + + \frac{1}{2} z_2 {v_2}^2$ *is convex due to its quadratic form, which follows directly from the definition of convexity [122]. Let* $Z = min(z_1, z_2) > 0$ *and define* $\phi(v_1, v_2) = Z({v_1}^2 + {v_2}^2)$. *Then* $L \geq \phi(v_1, v_2)$, *and clearly,* ϕ *is continuous and satisfies* $\frac{\phi(v_1, v_2)}{|(v_1, v_2)|} \to \infty$ *as* $|(v_1, v_2)| \to \infty$. *Therefore, the last condition is also satisfied. This completes the proof.*

To obtain the optimal control solution, we need to define Lagrangian function

$$L = g_1 I + \frac{1}{2} z_1 {v_1}^2 + + \frac{1}{2} z_2 {v_2}^2,$$

and Hamiltonian function

$$\begin{aligned} H(S,P,I,R,v_1,v_2,\lambda_i) &= L + \lambda_1 \frac{d^\alpha S(t)}{dt} + \lambda_2 \frac{d^\alpha P(t)}{dt} + \lambda_3 \frac{d^\alpha I(t)}{dt} + \lambda_4 \frac{d^\alpha R(t)}{dt} \\ &= g_1 I + \frac{1}{2} z_1 {v_1}^2 + \frac{1}{2} z_2 {v_2}^2 \\ &\quad + \lambda_1 \left(p\Lambda - (1 - v_1(t)) \frac{\beta SI}{1 + \gamma I^2} - (\lambda + \mu) S \right) \\ &\quad + \lambda_2 \left((1-p)\Lambda + \lambda S - (1 - v_2(t)) \frac{\beta(1 + \delta\beta')PI}{1 + \gamma I^2} - \mu P \right) \\ &\quad + \lambda_3 \left((1 - v_1(t)) \frac{\beta SI}{1 + \gamma I^2} + (1 - v_2(t)) \frac{\beta(1 + \delta\beta')PI}{1 + \gamma I^2} - (\mu + d + \phi) I \right) \\ &\quad + \lambda_4 (\phi I - \mu R). \end{aligned}$$

Here, $\lambda_i = (\lambda_1, \lambda_2, \lambda_3, \lambda_4)$ is referred to as the adjoint variable that satisfies the following canonical equations:

$$D^{\alpha}\lambda_1(t) = -\frac{\partial H}{\partial S} = \left((1-\bar{v_1})\frac{\beta\bar{I}}{1+\gamma\bar{I}^2} + (\mu+\lambda)\right)\lambda_1 - (\lambda)\lambda_2 - \left((1-\bar{v_1})\frac{\beta\bar{I}}{1+\gamma\bar{I}^2}\right)\lambda_3,$$

$$D^{\alpha}\lambda_2(t) = -\frac{\partial H}{\partial P} = \left((1-\bar{v_2})\frac{\beta(1+\delta\beta')\bar{I}}{1+\gamma\bar{I}^2} + \mu\right)\lambda_2 - \left((1-\bar{v_2})\frac{\beta(1+\delta\beta')\bar{I}}{1+\gamma\bar{I}^2}\right)\lambda_3,$$

$$\begin{aligned} D^{\alpha}\lambda_3(t) = -\frac{\partial H}{\partial I} = -g_1 &+ \left((1-\bar{v_1})\frac{\beta\bar{S}(1-\gamma\bar{I}^2)}{(1+\gamma\bar{I}^2)^2}\right)\lambda_1 \\ &+ \left((1-\bar{v_2})\frac{\beta(1+\delta\beta')\bar{P}(1-\gamma\bar{I}^2)}{(1+\gamma\bar{I}^2)^2}\right)\lambda_2 \\ &- \left((1-\bar{v_1})\frac{\beta\bar{S}(1-\gamma\bar{I}^2)}{(1+\gamma\bar{I}^2)^2} + (1-\bar{v_2})\frac{\beta(1+\delta\beta')\bar{P}(1-\gamma\bar{I}^2)}{(1+\gamma\bar{I}^2)^2}\right. \\ &\left. - (\mu+d+\phi)\right)\lambda_3 - (\phi)\lambda_4, \end{aligned}$$

$$D^{\alpha}\lambda_4(t) = -\frac{\partial H}{\partial R} = (\mu)\lambda_4, \tag{5.17}$$

with transversality conditions

$$\lambda_1(T) = 0, \lambda_2(T) = 0, \lambda_3(T) = 0, \lambda_4(T) = 0. \tag{5.18}$$

Theorem 5.7.3 *In the control system* (5.15)-(5.16)*, let* $\bar{v_i}$ *be the optimal control variables and* $\bar{S}$, $\bar{P}$, $\bar{I}$, *and* $\bar{R}$ *the corresponding optimal state variables. Then, there exists* $\lambda_1, \lambda_2, \lambda_3$ *and* λ_4 *satisfying the adjoint system* (5.17) *and transversality conditions* (5.18)*, then the doublet of optimal controls can be characterized as follows:*

$$\bar{v_1} = \min\left\{max\left\{0, \frac{(\lambda_3-\lambda_1)\beta\bar{S}\bar{I}}{z_1(1+\gamma\bar{I}^2)}\right\}, 1\right\},$$

$$\bar{v_2} = \min\left\{max\left\{0, \frac{(\lambda_3-\lambda_2)\beta(1+\delta\beta')\bar{P}\bar{I}}{z_2(1+\gamma\bar{I}^2)}\right\}, 1\right\}. \tag{5.19}$$

Proof 5.7.4 *As per the approach followed in [105], the optimal doublet* $(\bar{v_1}, \bar{v_2})$*, given in* (5.19) *is obtained by using the Potryagin's maximum principle and optimality conditions,* $\frac{\partial H}{\partial v_1} = 0$ *and* $\frac{\partial H}{\partial v_2} = 0$.

5.8 Simulation and Discussion

In this section, computations are performed to support the analytical findings using MATLAB 2012b and the Adams-Bashforth-Moulton predictor-corrector approach

[52]. Using real-world data can be tricky because things like prices and technology changes can affect the results [125; 164]. But using example data makes it easier to see how different groups in the model interact over time. Therefore, a qualitative analysis is conducted to better understand how the disease spreads and to identify aspects of the model that may require improvement.

Table 5.1: Parameters of the model *SPIR* and their numerical values for simulation.

Parameters	**Description**	**Values**
Λ	Growth rate	7
p	Fraction of growth rate into S class	0.6
β	Transmission rate from S to I	0.003
γ	Psychological saturation constant	0.02
λ	Rate at which susceptible becomes stressed	0.004
μ	Natural death rate	0.055
β'	Pollution related influence on transmission rate β	0.2
d	Disease induced death rate	0.07
ϕ	Recovery rate of infected population	0.09
δ	Scaling parameter	0.3

The initial sub-populations for the simulation purpose have been taken as $S(0) = 75$, $P(0) = 40$, $I(0) = 5$, $R(0) = 5$ and utilized the numerical experimental data given in the Table 5.1. First, simulations of the model are performed without control and then with optimal control in the following subsections.

5.8.1 Simulation without control strategy

In this subsection, we will first validate the theoretical results regarding existence and stability of the equilibria and thereafter perform some computations to observe the effect of memory α.

For, the parameter values given in the Table 5.1, the coefficients of the equation (5.3) comes out to be as $A_4 = -2.7907 \times 10^{-7}, A_3 = -1.5163 \times 10^{-6}, A_2 = -4.5229 \times 10^{-6}, A_1 = -9.0333 \times 10^{-6}, A_0 = 5.7408 \times 10^{-4}$. These coefficient values satisfy Theorem 5.4.1 and the possibility of the existence of unique positive equilibrium. Thus, the endemic equilibrium is $E_1(S_*, P_*, I_*) = (60.7791, 46.3121, 5.1627)$ for which the basic reproduction number $\mathscr{R}_0$ is 1.8229.

The values of coefficients of equation (5.10) are calculated as $A_3 = 3.60318$, $A_2 = 1.02449$, $A_1 = 0.0914362$, $A_0 = 0.00261647$. The eigen values corresponding the equation (5.10) are the root of the equation (5.11) i.e. of the equation $\psi^3 + 0.284328\ \psi^2 + 0.0253766\ \psi + 0.000726155$ which are $\psi_1 = -0.140491$, $\psi_2 = -0.0738135$, $\psi_3 = -0.0700235$. The discriminant of polynomial term of the equation (5.11) is calculated as $D(\psi) = 3.17136 \times 10^{-10}$. The values of the coefficients of equation (5.11) are $B_0 = 0.000726155, B_1 = 0.0253766, B_2 = 0.284328$ and these also satisfy the condition $B_2B_1 > B_0$, so together with the discriminant $D(\lambda)$, these are satisfying the first condition of the Theorem 5.5.2, and hence endemic equilibrium is locally asymptotically stable.

To demonstrate how memory affects the dynamics of *SPIR* model (5.1), Figures 5.3, 5.4, 5.5 and 5.6 are plotted with the help of initial conditions of populations which depict the impact of various fractional order $(\alpha = 0.8, 0.85, 0.9, 1.0)$ on the sub-populations. By varying the fractional-order values, different scenarios can be observed.

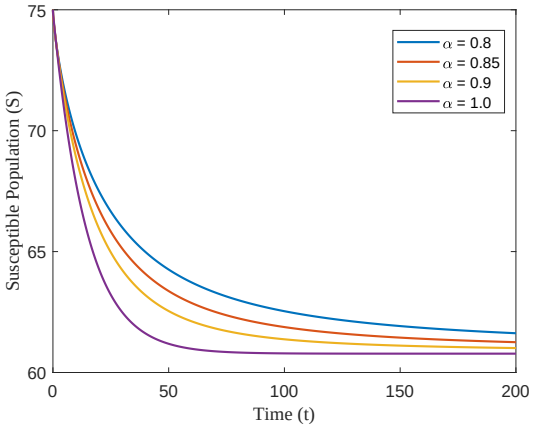

Figure 5.3: Time series plot of susceptible population with different fractional order.

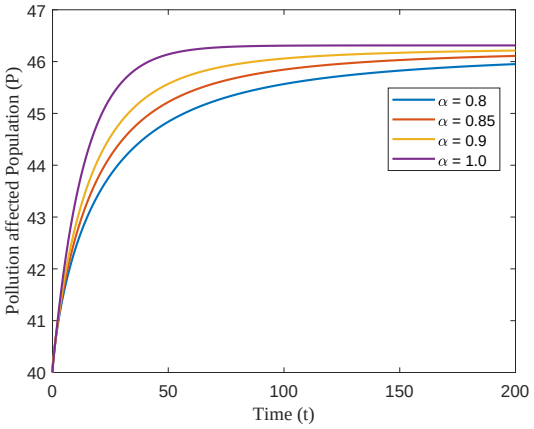

Figure 5.4: Time series plot of pollution affected population with different fractional order.

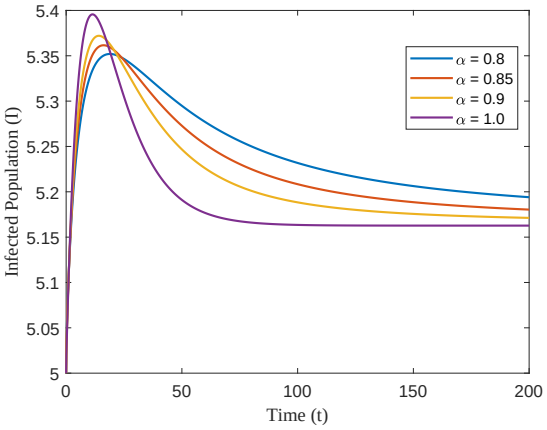

Figure 5.5: Time series plot of infected population with different fractional order.

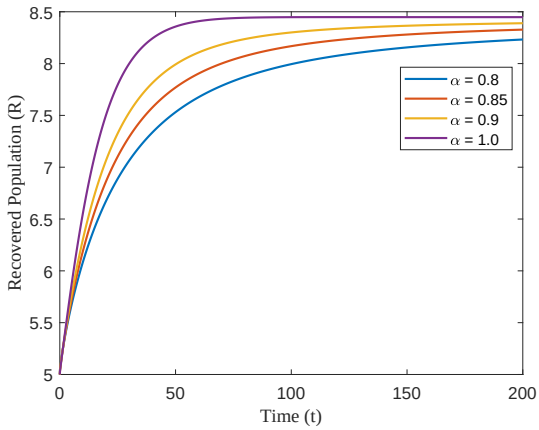

Figure 5.6: Time series plot of recovered population with different fractional order.

The fractional-order parameter α significantly influences the system's convergence behavior, as shown in Figures 5.3, 5.4, 5.5, and 5.6. When $\alpha = 1$, the system behaves like a classical integer-order model, where the susceptible, pollution affected, infected, and recovered populations all reach their steady states relatively quickly. However, as α decreases, the system exhibits stronger memory effects, leading to slower convergence across all compartments.

This memory effect becomes especially evident in the susceptible population (Figure 5.3), where lower α values result in a longer time to reach equilibrium. Biologically, this can be interpreted as the population retaining more influence from past disease exposure, which slows the overall system response. In contrast, higher values of α reflect weaker memory, where individuals are less influenced by historical disease data, allowing the system to stabilize faster.

Interestingly, this faster stabilization at higher α may come at a cost. A weaker memory effect can delay recognition and response to infection, often leading to a higher peak in the infected population. On the other hand, stronger memory associated with lower α could indicate increased public awareness or behavioral changes based on prior outbreaks, thus spreading the disease over a longer period but possibly reducing the peak.

Despite these variations in convergence speed, Theorem 5.5.4 confirms that the endemic equilibrium point $(60.7791, 46.3121, 5.1627)$ remains stable for all considered values of α $(0.8, 0.85, 0.9, 1)$, as demonstrated in the figures. This highlights that

while the path to equilibrium changes with α, the final outcome of the system remains robust.

When the fractional order is relatively high (for instance, $\alpha = 1$) and the transmission rate is low (e.g., $\beta = 0.001$), the basic reproduction number is $\mathscr{R}_0 = 0.60762$, which is less than one. Under these conditions, the number of infected individuals decreases rapidly and eventually reaches zero, meaning the disease dies out and the system quickly stabilizes at the disease-free equilibrium. However, when the fractional order is lower (such as $\alpha \leq 0.90$), the system still trends toward a disease-free state, but the decline in infections happens more gradually. In this slower phase, the infection persists for a longer time, displaying dynamics that resemble an endemic phase before fading out. The findings indicate that fractional-order models play a key role in capturing how previous disease interactions affect current transmission dynamics. The same can be seen from Figure 5.7.

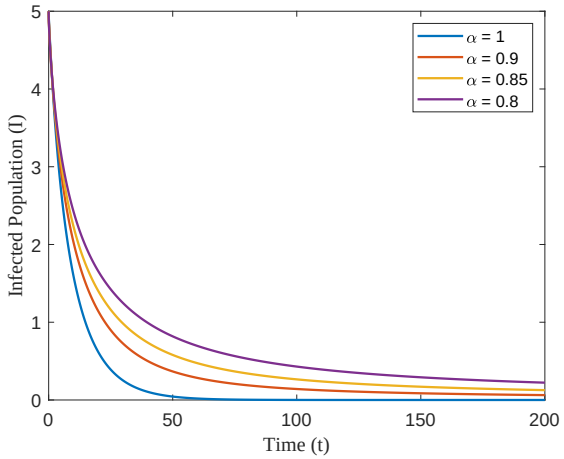

Figure 5.7: Time series plot of infected population with for $\mathscr{R}_0 = 0.60762 < 1$ with different fractional order.

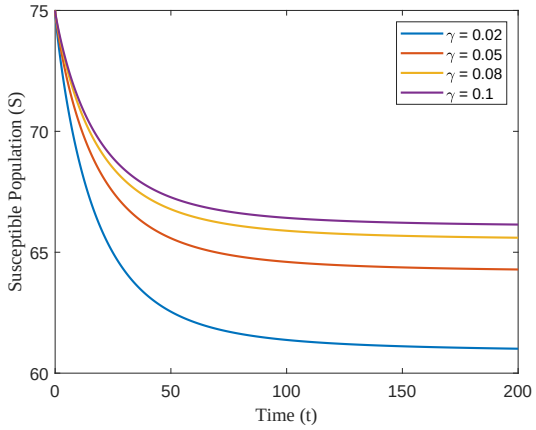

Figure 5.8: Variation of psychological effect γ and their effect on susceptible population for fixed $\alpha = 0.9$.

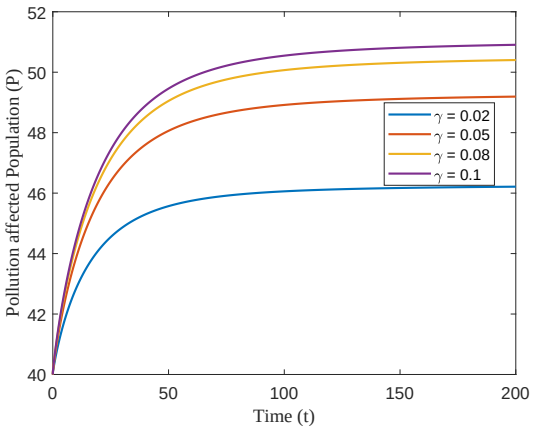

Figure 5.9: Variation of psychological effect γ and their effect on pollution affected population for fixed $\alpha = 0.9$.

Figures 5.8, 5.9, and 5.10 illustrate the influence of psychological factors on different population compartments. As the psychological impact rate, denoted by γ, increases, there is a noticeable rise in the number of susceptible individuals and those affected by pollution. Concurrently, a significant reduction is observed in the peak number of infected individuals. This trend suggests that enhancing psychological awareness can effectively suppress the infection peak during an epidemic, thereby contributing to better disease control.

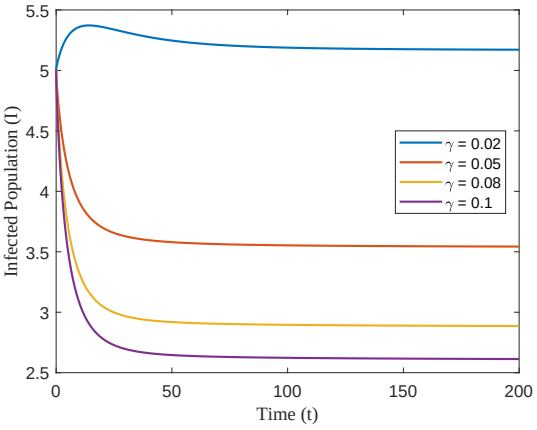

Figure 5.10: Variation of psychological effect γ and their effect on infected population for fixed $\alpha = 0.9$.

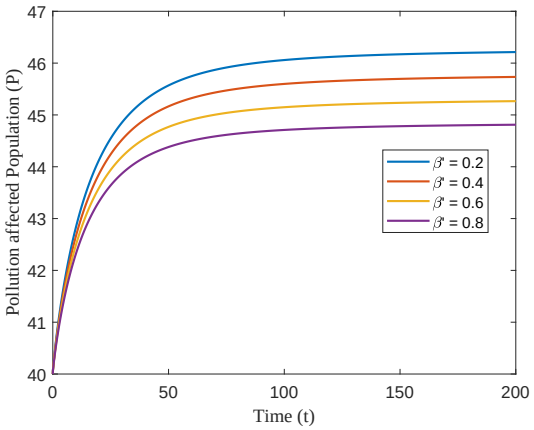

Figure 5.11: Effect of pollution related transmission β' on pollution affected population for fixed $\alpha = 0.9$.

Figure 5.11 explores the effect of the pollution-related transmission rate, represented by β', on the pollution-affected population. An increase in β' leads to a decline in the number of individuals in the pollution-affected class, as more of them transition into the infected category. This dynamic highlights the critical role of managing environmental transmission pathways in reducing infection spread. Therefore, regulating transmission rates can be a practical strategy to mitigate the intensity of outbreaks.

5.8.2 Numerical Analysis with Control Strategy

In this subsection, the outcomes of the Fractional Optimal Control Problem (FOCP) are presented, and various strategies aimed at minimizing the disease burden are discussed. Two time-dependent control variables, $v_1(t)$ and $v_2(t)$, are incorporated into the model. To solve the FOCP and ensure effective optimization, the weight constants in the cost function (5.15) are selected as $g_1 = 50, z_1 = 80$ and $z_2 = 10$. Different permutations of these controls are applied to study the following strategies:

- **Strategy A** ($v_1(t) \neq 0, v_2(t) = 0$)

  We begin by analyzing the implementation of a single control policy, $v_1(t)$, which is applied to reduce the transmission between the susceptible and infected populations. Figure 5.12 shows the graph of the control variable $v_1(t)$ in the absence of another control. For the first 22 days, no control effort is required. After this period, the requirement of control effort gradually increases, reaching its full implementation between days 90 and 173. Following this peak phase, the control intensity gradually decreases and eventually returns to zero. Figures 5.13, 5.14, 5.15, and 5.16 illustrate the dynamics of the population under this control strategy in comparison to the case when no control is applied. From the figures, we observe that there is no impact of the implemented control during the initial days, however after this initial phase, the effect of the control $v_1(t)$ becomes evident. The number of susceptible and pollution-affected individuals increases, while the number of infected individuals decreases. This indicates that the control strategy is effective in reducing the transmission of the disease by preventing susceptible and pollution-affected individuals from becoming infected. Additionally, we observe a decline in the number of recovered individuals. This is because we have applied a non-pharmaceutical control, thus fewer people become infected due to the control, which means fewer eventually recover.

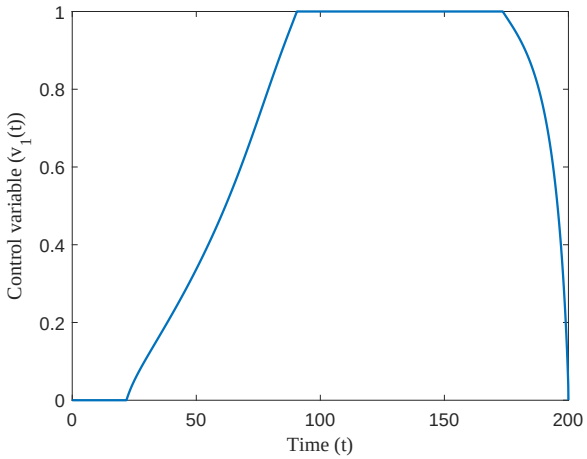

Figure 5.12: Optimal control path of single control $v_1(t)$ when $v_2(t) = 0$.

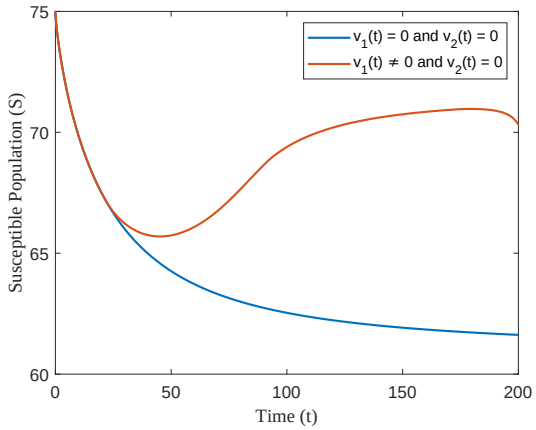

Figure 5.13: Effect of applying only $v_1(t)$ on susceptible individuals compared to the case when no control is applied $(v_1(t) = 0 = v_2(t))$.

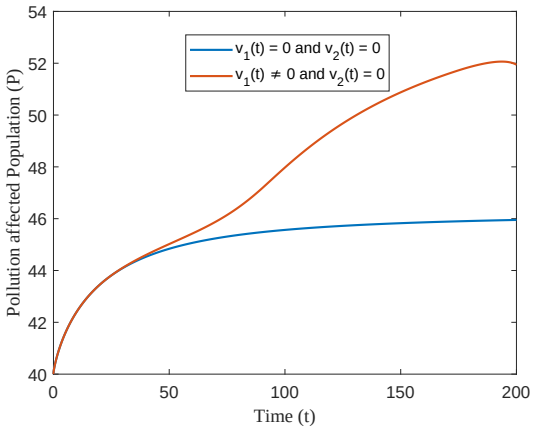

Figure 5.14: Effect of applying only $v_1(t)$ on pollution-affected individuals compared to the case when no control is applied $(v_1(t) = 0 = v_2(t))$.

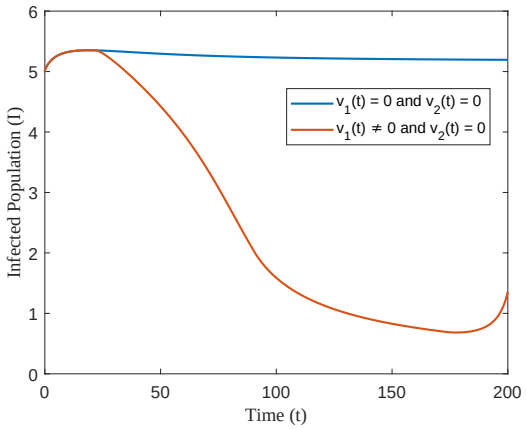

Figure 5.15: Effect of applying only $v_1(t)$ on infected individuals compared to the case when no control is applied $(v_1(t) = 0 = v_2(t))$.

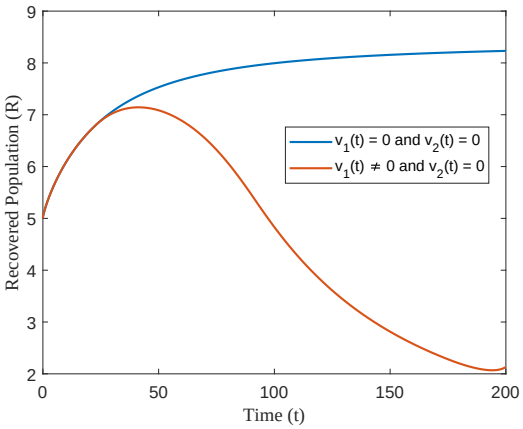

Figure 5.16: Effect of applying only $v_1(t)$ on recovered individuals compared to the case when no control is applied $(v_1(t) = 0 = v_2(t))$.

- **Strategy B** $(v_1(t) = 0, v_2(t) \neq 0)$

  Next, the effect of a single control policy, $v_2(t)$, which regulates the interaction between pollution-affected and infected individuals, is examined. Figure 5.17 shows the graph of control variable $v_2(t)$ when applied independently, in the absence of $v_1(t)$. As seen in the figure, this control requires full implementation for nearly the entire duration of the simulation, approximately 198 days, before it can be gradually withdrawn near the end. Figures 5.18, 5.19, 5.20, and 5.21 depict the population dynamics under this strategy, compared to the case when no control is applied. The results indicate an increase in both susceptible and pollution-affected individuals, while the number of infected and recovered individuals decreases. Unlike Strategy A, Strategy B begins influencing the system immediately, as it is applied at its maximum level from the start. This immediate intervention leads to an earlier and more consistent impact, suggesting that $v_2(t)$ may be more effective than $v_1(t)$ when implemented alone. A detailed comparison can be seen in the subsequent section.

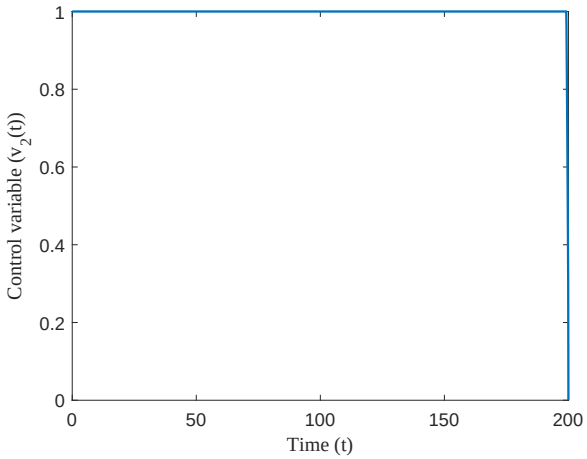

Figure 5.17: Optimal control path of single control $v_2(t)$ when $v_1(t) = 0$.

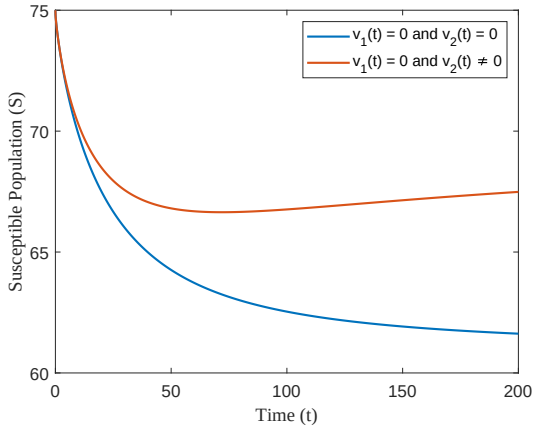

Figure 5.18: Effect of applying only $v_2(t)$ on susceptible individuals compared to the case when no control is applied $(v_1(t) = 0 = v_2(t))$.

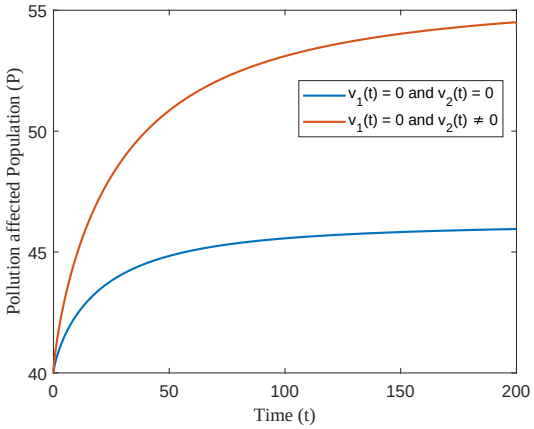

Figure 5.19: Effect of applying only $v_2(t)$ on pollution-affected individuals compared to the case when no control is applied $(v_1(t) = 0 = v_2(t))$.

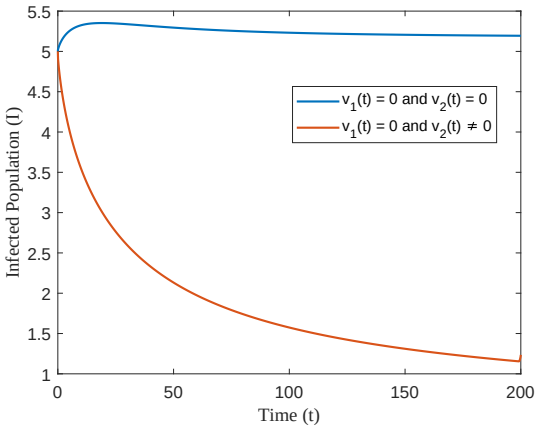

Figure 5.20: Effect of applying only $v_2(t)$ on infected individuals compared to the case when no control is applied $(v_1(t) = 0 = v_2(t))$.

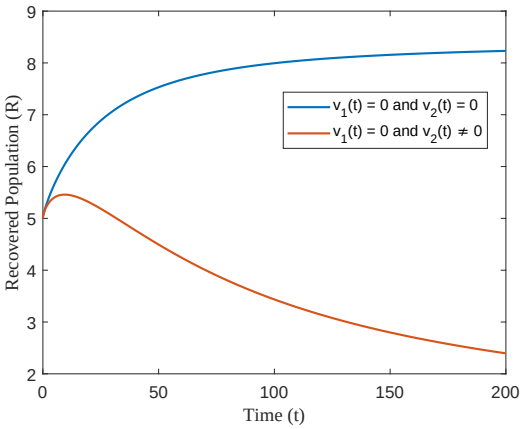

Figure 5.21: Effect of applying only $v_2(t)$ on recovered individuals compared to the case when no control is applied $(v_1(t) = 0 = v_2(t))$.

- **Strategy C** $(v_1(t) \neq 0, v_2(t) \neq 0)$

  This strategy explores the combined effect of simultaneously applying both control measures, $v_1(t)$ and $v_2(t)$, within the model. Figures 5.22 and 5.23 illustrate the profiles of each control when implemented together. Initially, $v_1(t)$ is applied at full strength but gradually decreases to zero as the simulation progresses. In contrast, $v_2(t)$ remains at its maximum level for nearly the entire duration, approximately 195 days, before being phased out toward the end. The resulting population dynamics are shown in Figures 5.24, 5.25, 5.26, and 5.27. Compared to the scenario without any control, the number of susceptible and pollution-affected individuals increases, while the number of infected and recovered populations decreases significantly. This dual-control strategy leads to more substantial changes than those observed in Strategies A and B, where only one control was applied at a time. Thus, the simultaneous application of both $v_1(t)$ and $v_2(t)$ proves more effective in mitigating disease spread, highlighting the advantage of a combined intervention approach.

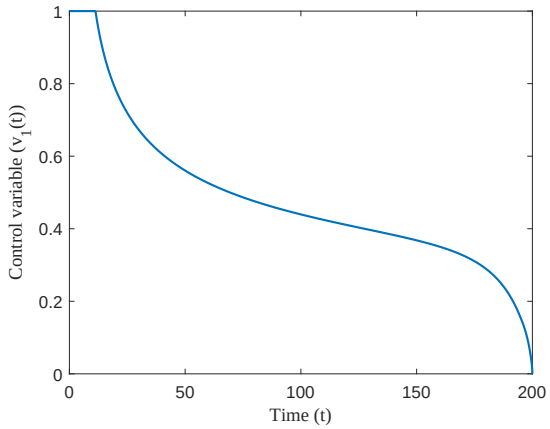

Figure 5.22: Optimal control path of $v_1(t)$ when both controls are applied.

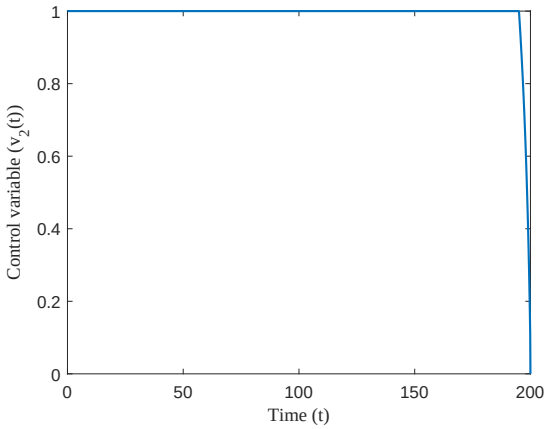

Figure 5.23: Optimal control path of $v_2(t)$ when both controls are applied.

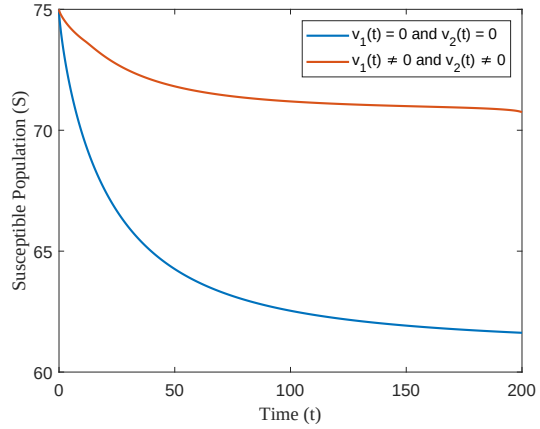

Figure 5.24: Effect of applying both $v_1(t)$ and $v_2(t)$ simultaneously on susceptible individuals compared to the case when no control is applied $(v_1(t) = 0 = v_2(t))$.

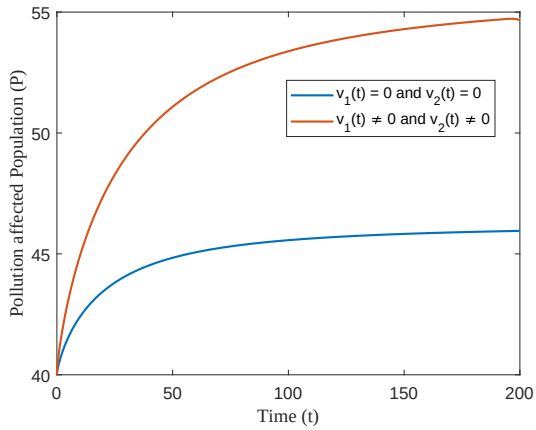

Figure 5.25: Effect of applying both $v_1(t)$ and $v_2(t)$ simultaneously on pollution affected individuals compared to the case when no control is applied $(v_1(t) = 0 = v_2(t))$.

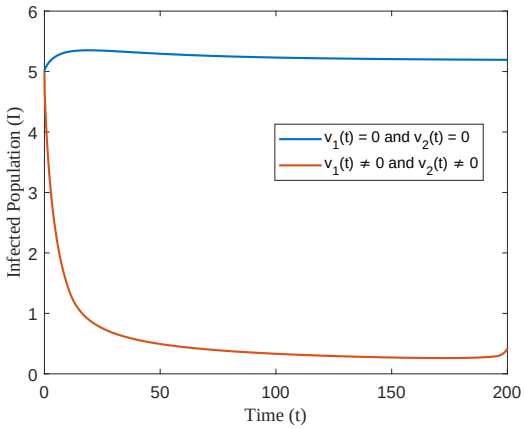

Figure 5.26: Effect of applying both $v_1(t)$ and $v_2(t)$ simultaneously on infected individuals compared to the case when no control is applied $(v_1(t) = 0 = v_2(t))$.

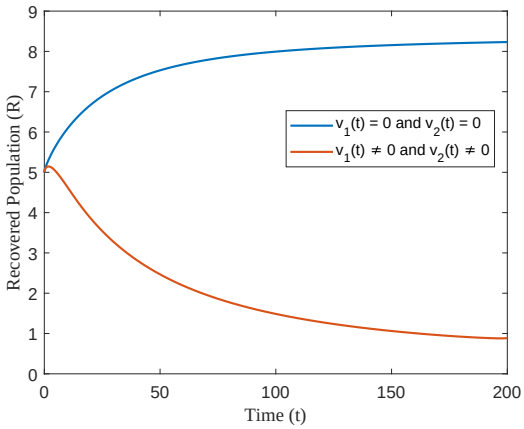

Figure 5.27: Effect of applying both $v_1(t)$ and $v_2(t)$ simultaneously on recovered individuals compared to the case when no control is applied $(v_1(t) = 0 = v_2(t))$.

5.8.3 Comparative study

In this subsection, we present a comparative analysis of all three control strategies discussed earlier, along with the scenario where no control is applied. Strategy A involves the use of only $v_1(t)$, Strategy B uses only $v_2(t)$, and Strategy C applies both $v_1(t)$ and $v_2(t)$ simultaneously.

Figure 5.28 illustrates the progression of the susceptible population under each scenario. The results indicate that Strategy C, which implements both controls together, is the most effective in maintaining a higher number of susceptible individuals throughout the progression. Strategy A performs nearly as well in terms of preserving susceptibility but shows minimal impact during the initial phase of the epidemic. In contrast, Strategy B initially works better than Strategy A for the first 69 days but is eventually overtaken by Strategy A as time progresses.

However, when it comes to the pollution-affected population (Figure 5.29), Strategy B proves more effective than Strategy A. It significantly limits the progression of pollution-affected individuals into the infected class, performing almost as well as Strategy C. Although Strategy C remains the best overall, Strategy B shows a clear advantage over Strategy A in this aspect.

Figure 5.30 compares the number of infected individuals across all strategies. All three control strategies lead to a reduction in infections compared to the uncontrolled

case, with Strategy C once again being the most effective. Strategy B initially outperforms Strategy A in reducing infections, for approximately 100 days, but in the latter half of the simulation, Strategy A becomes more effective.

Figure 5.31 shows the recovery trends in all the four cases. Strategy C results in the lowest number of recovered individuals, not due to inefficacy, but because fewer people become infected in the first place, leading to a smaller group requiring recovery. Strategy A maintains higher recovery counts than Strategy B for the first 150 days, while Strategy B slightly surpasses it in the final 50 days.

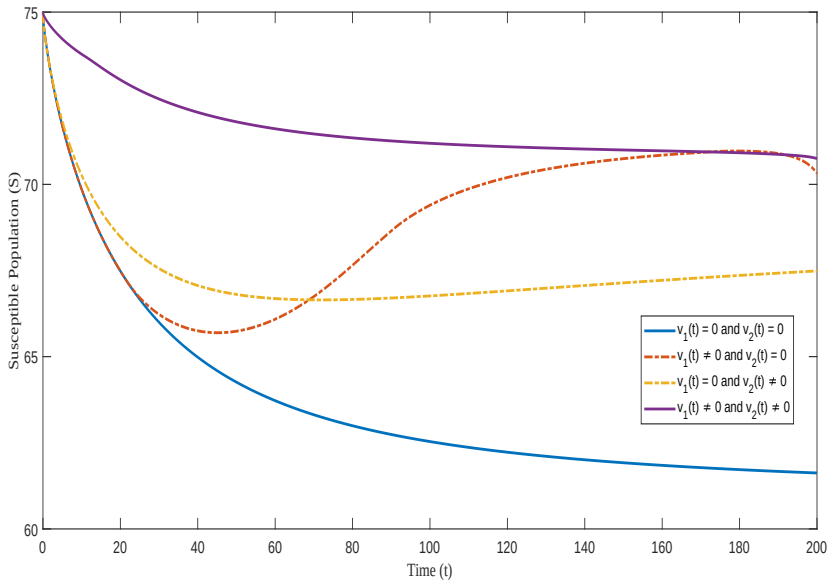

Figure 5.28: Profiles of susceptible population (S) with different control strategies.

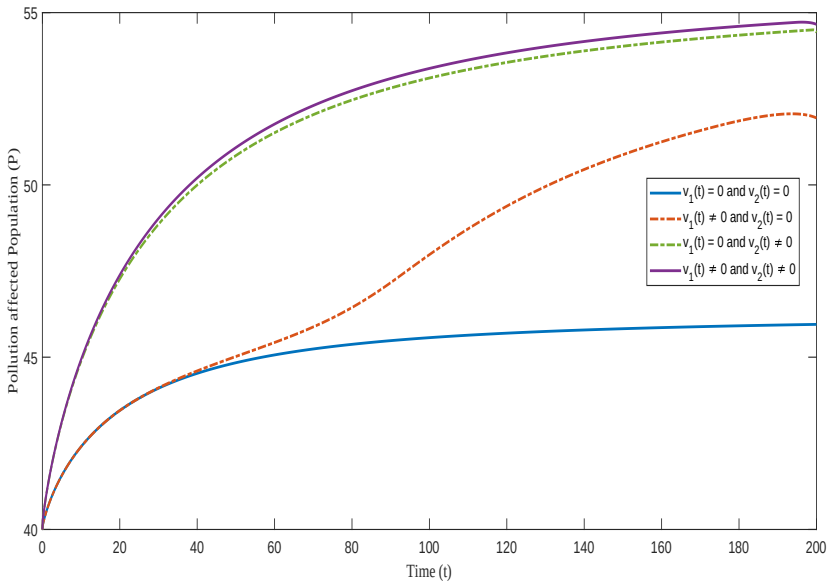

Figure 5.29: Profiles of pollution-affected (P) with different control strategies.

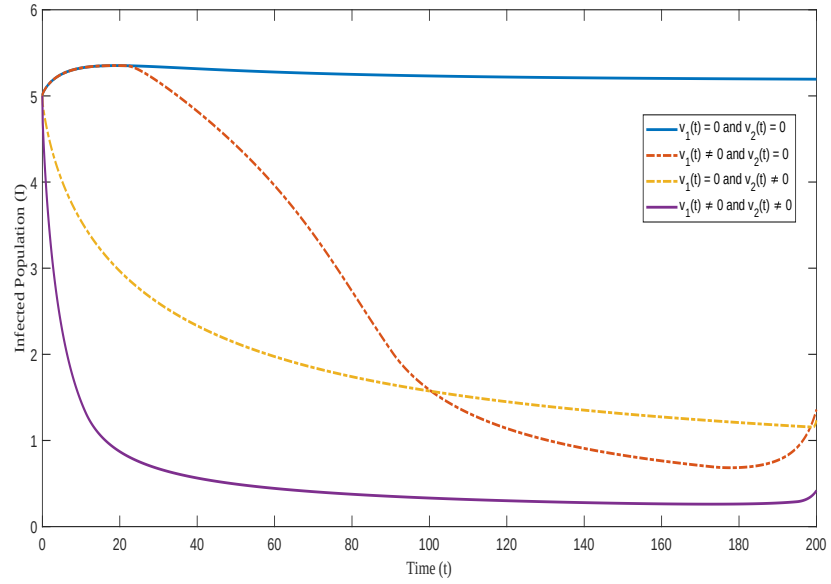

Figure 5.30: Profiles of infected population (I) with different control strategies.

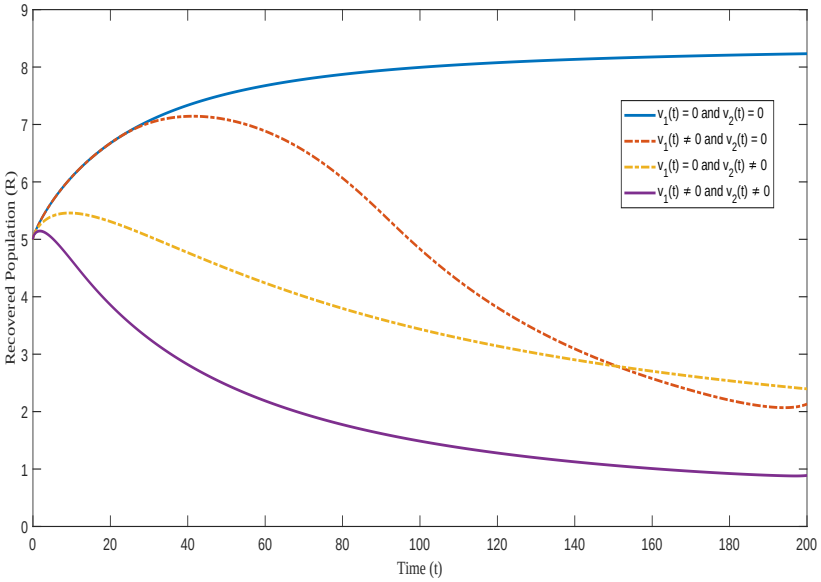

Figure 5.31: Profiles of recovered population (R) with different control strategies.

5.9 Conclusion

The goal of this study is to develop and analyze the stability properties of a new fractional-order *SPIR* epidemiological model that explores the influence of environmental pollution on the transmission of infectious diseases. The model employs the Caputo fractional derivative to describe the rate of change in each sub-population, with the fractional order reflecting memory effects inherent in disease spread. By accounting for individuals' past exposure, this framework improves the predictive capability of the model.

Our formulation highlights how prenatal exposure to environmental pollution shapes initial population compartments, with a fraction p of newborns entering the susceptible class S and the remaining $(1-p)$ entering the pollution-affected class P. The disease transmission between classes is governed by Monod-Haldane-type incidence rates: $\frac{\beta SI}{1+\gamma I^2}$ for S and I, and $\frac{\beta(1+\delta\beta')PI}{1+\gamma I^2}$ for P and I. These expressions capture non-monotonic transmission effects driven by psychological and environmental influences. The parameter δ scales the influence of environmental pollution on transmission and β' quantifies its effect on the base transmission rate β, reinforcing the role of environmental exposure in shaping epidemic dynamics.

The analysis confirms that the model is mathematically well-posed, with solutions that are unique, positive, and bounded within the feasible region Ω. Two equilibrium states emerge: a disease-free equilibrium and an endemic equilibrium. Using Laplace transform techniques for linearization, the stability of these equilibria is examined in detail. The basic reproduction number $\mathscr{R}_0$, derived through the next generation matrix method, serves as a critical threshold parameter. When $\mathscr{R}_0 < 1$, the disease-free equilibrium is shown to be locally asymptotically stable, indicating that under such conditions, the infection cannot persist in the population.

The bifurcation analysis around the non-hyperbolic equilibrium point E_0 at the threshold $\mathscr{R}_0 = 1$ reveals that the model does not support backward bifurcation. Instead, a transcritical forward bifurcation is observed, as shown in Figure 5.2, indicating a smooth transition from disease-free to endemic states as $\mathscr{R}_0$ crosses unity. When $\mathscr{R}_0 > 1$, the existence of an endemic equilibrium is confirmed. Its local stability is ensured for all $\alpha \in (0,1]$ under the conditions specified in Theorem 5.5.2, while global stability is established using a Lyapunov function, as detailed in Theorem 5.5.4. These results collectively highlight the model's well-structured and predictable dynamical behavior near the epidemic threshold.

Additionally, we reformulate the model into an optimal control problem, described in Section 5.7, by introducing two time-dependent control efforts $v_1(t)$ and $v_2(t)$, aimed at reducing transmission from the S and P compartments to the I class. The existence and analytical characterization of the optimal control strategy are derived using Pontryagin's Maximum Principle.

Numerical simulations were also performed to support the analytical results, using the experimental parameter values listed in Table 5.1.

Further, the effect of psychological factors on sub-populations is analyzed, demonstrating their potential in reducing both the disease burden and the infection peak. Additionally, the impact of pollution-related transmission rate β' on the pollution-affected class P is examined, showing that even partial control of transmission can effectively mitigate the spread of infection.

In addition to the simulations, the model is evaluated with the implementation of control strategies. Three strategies are discussed, each demonstrating varying levels of effectiveness in mitigating disease transmission. Strategy C, combining both $v_1(t)$ and $v_2(t)$, proves to be the most effective in controlling the disease spread. While Strategy A and Strategy B individually show partial success, their combined implementation

yields a more substantial and sustained reduction in the number of infected individuals. This demonstrates that a dual-control approach not only enhances effectiveness but also compensates for the limitations of applying each control independently.

This study emphasizes on the critical role of public awareness in controlling the spread of infectious diseases, especially in environments where pollution influences disease transmission dynamics. One of the most effective ways to reduce the emergence of new cases is by educating the public, particularly those who are susceptible or pollution-affected, about the risks of coming into close contact with infected individuals. Raising public awareness involves more than just sharing information. It requires strategic communication campaigns, community engagement, and behavioral change initiatives that inform people about how the disease spreads, who is most at risk, and what practical actions can help prevent transmission. For instance, individuals need to understand why minimizing unnecessary contact, maintaining hygiene, wearing protective gear (such as masks), and avoiding polluted or crowded areas can significantly lower their risk of infection. Policy makers and health workers should implement targeted interventions that encourage behavioural changes among susceptible and pollution-affected populations, provide resources and support that enable people to avoid risky interactions (e.g., facilitating remote work, subsidizing protective equipment, improving access to clean environments), enforce guidelines that limit contact between vulnerable individuals and confirmed or suspected cases.

Chapter 6

Analysis of a fractional order SIR model for infectious diseases spread by household waste with optimal control strategies

---

With the increasing urban population, the accumulation of household waste (HHW) and its disposal has become an arduous issue. Household wastes spread several kinds of deadly diseases and have aroused attention from all sectors of society. In this chapter, a Caputo-type fractional-order SIR model is developed by incorporating two types of bacteria populations, namely bacteria in the environment (B_e) and bacteria in organism (B_o). The analysis establishes the well-posedness of the model and demonstrates the existence and uniqueness of the solution. The basic reproduction number $\mathscr{R}_0$ is derived, and its sensitivity analysis is performed. Furthermore, the stability of the system is investigated in the sense of the Ulam-Hyers stability criteria. Given the high burden of vector-borne diseases, an optimal control problem (OCP) is also formulated to reduce the disease burden at an optimal cost, incorporating three controls, $u_1(t)$, $u_2(t)$ and $u_3(t)$, which are primarily aimed at reducing transmission rates. Seven different types of optimal control strategies have been performed and compared, along with the study of their respective cost functions. This study offers a realistic, cost-effective approach to guide decision-makers in controlling diseases spread by household waste.

6.1 Introduction

Households are an indispensable part of human life. Not only do they provide a space for individual growth, but they also contribute to the economy by providing labour and by consuming goods and services. However, in recent years, the onset of urbanization has increased the living standards of people in both developed and developing countries. Urbanization, along with rapid growth in population, has led to a significant increase in the generation of the daily household wastes, such as plastic materials, cans, bottles, clothes, food packaging, paper, food scraps, disposables, glass, compost etc. Management of these household wastes (HHW) is a major concern [6]. To manage such issues, several steps have been taken by the government of various countries, but due to improper work, lack of knowledge, careless behaviour of the people and lack of landfills, all the HHWs cannot be collected and therefore it is impossible to dispose all these wastes into dump sites [6; 152]. Furthermore, the problem does not stop here. The waste that is disposed in these dumpsites accumulates and forms a 'trash mountain', which serves as a breeding ground for various types of germs and hazardous bacteria.

Moreover, due to the destruction of dumpsites for infrastructure development and a sudden rise in HHW, the growth of bacteria has increased day by day [61]. These bacteria spread into the environment and via carriers such as flies, mosquitoes, fleas, rodents etc. [189], enters human households through sources like food and water. The intake of such contaminated food and water infects the human population, which results in both fatal and non-fatal vector-borne diseases such as cholera, chikungunya, dengue, plague (transmitted from rats to humans), dysentery, Legionnaires' disease, and many more [189; 127]. This creates an alarming situation globally.

Numerous studies and literature have been provided by researchers addressing the household waste problem which includes various surveys and applicable suggestions that highlight how different sources of hazardous wastes contribute to the contamination of air, water, soil and overall environment (see [21; 133], and references therein). Despite these efforts, the management of HHW along with the diseases spread by the generated hazardous bacteria is still a very big concern. This can be interpreted from the fact sheet of World Health Organization, which states that vector-borne illnesses account for the death of more than 700,000 people each year which accounts for more

than 17% of all infectious diseases [193]. These illnesses can be caused by viruses, bacteria, or parasites. Thus, it is very crucial to study the dynamics of disease transmission caused by hazardous bacteria generated from household waste. To address such situations in a realistic manner, the bacterial population is divided into two categories: the bacteria generated from household waste that spread into the environment, referred to as bacteria in environment and the bacteria that further spreads from the environment to organisms through carriers, referred to as bacteria in organisms.

Over the past few decades, researchers have utilized mathematical modeling as an essential tool to explore real-life situations by dividing the population of interest into different compartments [159; 160; 161].

Since the prevalence of vector-borne diseases is very high, especially in low and middle-income countries where vector populations are in large amounts and healthcare systems are not sufficient, it is crucial to formulate an epidemic model which not just focuses on lowering the disease burden but also on minimizing the cost incurred. Thus, we have considered an optimal control strategy based on Pontryagin's Maximum Principle [74]. Incorporating an optimal control problem into epidemic models is essential for effectively managing infectious disease burden [17; 164]. By an optimal control strategy, our model becomes a tool not only for understanding the dynamics of the epidemic but also serves as an aid to achieve economic benefits by designing effective strategies to ease the disease burden.

Conclusively, the proposed *SIR* model with two groups of bacteria population i.e., environmental and organism bacteria along with an optimal control problem can be considered as a novel work, which can prove to be beneficial for the health sector and for policy makers as well.

The framework of this chapter is as follows: In Section 6.2, the required assumptions and mathematical formulation of our proposed model is discussed. Further, in the next section positivity and boundedness of the model is performed. Section 6.4 deals with the existence and uniqueness results using Banach contraction principle and Schaefer's fixed point theorem. In Section 6.5, the basic reproduction number $\mathscr{R}_0$ is calculated, and the highly sensitive parameters are identified through sensitivity analysis. Ulam-Hyers stability is performed for the model in the very next section. An optimal control problem (OCP) is also formulated in Section 6.7 which is helpful in lowering disease burden with optimal cost, with inclusion of three controls $u_1(t)$, $u_2(t)$ and $u_3(t)$ that are basically focused in reducing the transmission rates. The existence

and characterization of controls are performed by using Pontryagin's maximum principle. Moreover, in Section 6.8, the numerical scheme of the Adams-Bashforth-Moulton Predictor-Corrector method is presented, and numerical simulations are performed to illustrate the findings in Section 6.9. Finally, the conclusion of the chapter is summarized in the last section.

6.2 Model development

In this section, a mathematical model is developed to study the effect of bacteria generated by HHWs on the population. When hazardous bacteria generated by HHWs spread in the environment, then the susceptible individuals come in contact with the environmental bacteria and the carrier bacteria in organisms. To express the propagation dynamics, the human population $N(t)$ is divided into three compartments: Susceptible $S(t)$, Infected $I(t)$, and Recovered $R(t)$ at any time t and the class of bacteria in the environment and the carrier bacteria in organisms are denoted by B_e and B_o respectively. The basic assumptions for the model development are as follows:

(A1) The constant growth rate of susceptible population is considered as Λ and the natural death rate for all human compartments $S(t), I(t)$ and $R(t)$ is taken as μ.

(A2) Growth rate of environmental bacteria through the HHWs is taken as A_1 and washout rate is taken as h. Also, the washout rate is assumed to be greater than the growth rate of bacteria, i.e., $h > A_1$ for the present study, because $h < A_1$ is biologically meaningless.

(A3) Growth of bacteria in organisms is considered as directly proportional to the environmental bacteria with rate b because these organism bacteria are like carriers from environment to residential areas and also rate of depletion, which includes washout rate as well, of these bacteria is taken as g.

(A4) When susceptible individuals will come in contact with the bacteria in organisms and bacteria in environment then they will acquire bacterial infection at rates β_o and β_e, respectively. Later on, susceptible may come in close contact with infected individuals and acquire the infection by rate β with some level of protection ρ, where $0 \leq \rho \leq 1$. When $\rho = 0$, there is no protection against infection whereas when $\rho = 1$, there is full protection against infection.

(A5) The rate of recovery for infected individuals is considered to be δ, and the infected can contribute to bacterial production in the environment at a rate of σ.

Thus, under these assumptions, the formulated fractional order compartmental model is given by:

$$\begin{aligned}
\frac{d^{\alpha}S(t)}{dt} &= \Lambda - \beta(1-\rho)S(t)I(t) - \beta_o S(t)B_o(t) - \beta_e S(t)B_e(t) - \mu S(t),\\
\frac{d^{\alpha}I(t)}{dt} &= \beta(1-\rho)S(t)I(t) + \beta_o S(t)B_o(t) + \beta_e S(t)B_e(t) - \delta I(t) - (\mu+d)I(t),\\
\frac{d^{\alpha}R(t)}{dt} &= \delta I(t) - \mu R(t),\\
\frac{d^{\alpha}B_e(t)}{dt} &= (A_1 - h)B_e(t) + \sigma I(t),\\
\frac{d^{\alpha}B_o(t)}{dt} &= bB_e(t) - gB_o(t),
\end{aligned} \tag{6.1}$$

with initial conditions $S(0) = S_0 \geq 0,\ I(0) = I_0 \geq 0,\ R(0) = R_0 \geq 0,\ B_e = (B_e)_0 \geq 0,\ B_o = (B_o)_0 \geq 0$ and $t \in [0, t_0],\ t_0 \in \mathbb{R}^+$. The pictorial representation of this disease propagation dynamics and the interaction between human and bacteria population is given in the flow diagram 6.1.

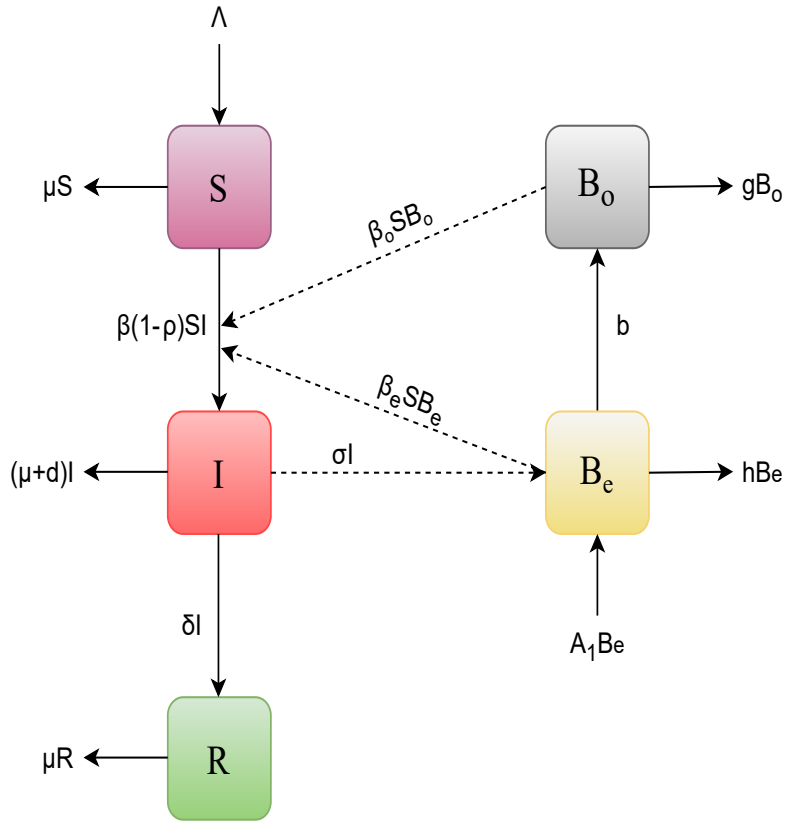

Figure 6.1: Flow diagram of the model (6.1).

Let us rewrite the system (6.1) for the sake of convenience. Let

$$M(t) = [S(t), I(t), R(t), B_e(t), B_o(t)]^T$$

$$\text{and } f(t, M(t)) = [\psi_1(t), \psi_2(t), \psi_3(t), \psi_4(t), \psi_5(t)]^T,$$

where

$$\begin{aligned}
\psi_1(t) &= \Lambda - \beta(1-\rho)S(t)I(t) - \beta_o S(t)B_o(t) - \beta_e S(t)B_e(t) - \mu S(t),\\
\psi_2(t) &= \beta(1-\rho)S(t)I(t) + \beta_o S(t)B_o(t) + \beta_e S(t)B_e(t) - \delta I(t) - (\mu + d)I(t),\\
\psi_3(t) &= \delta I(t) - \mu R(t),\\
\psi_4(t) &= (A_1 - h)B_e(t) + \sigma I(t),\\
\psi_5(t) &= bB_e(t) - gB_o(t).
\end{aligned}$$

So, system (6.1) can be written as follows:

$$D^{\alpha} M(t) = f(t, M(t)); \;\; M(0) = M_0 \geq 0, \;\; t \in [0, t_0]; \;\; 0 < \alpha \leq 1. \tag{6.2}$$

Equation (6.2) is equivalent to the fractional integral equation of the form

$$M(t) = M_0 + \frac{1}{\Gamma\alpha}\int_0^t (t-\xi)^{\alpha-1} f(\xi, M(\xi))d\xi.$$

Let $\Omega = C([0,t_0] : \mathbb{R})$, which denotes the complete normed linear space of all continuous functions from $[0,t_0]$ to $\mathbb{R}$ endowed with the norm $\|M\|_\Omega = \sup_{t\in[0,t_0]}\{|M(t)|\}$, where $|M(t)| = |S(t)| + |I(t)| + |R(t)| + |B_e(t)| + |B_0(t)|$.

6.3 Positivity and Boundedness

Theorem 6.3.1 *For $M(0) > 0$, the solution $M(t)$ of system* (6.1) *is positive and bounded for $t \in [0,t_0]$, $t_0 \in \mathbb{R}^+$.*

Proof 6.3.2 *First of all, we establish non-negativity of solutions. It follows from the first equation of system* (6.1)*, that*

$$D^\alpha S(t) \geq (-\beta(1-\rho)I - \beta_0 B_o - \beta_e B_e - \mu)S.$$

The solution of the above equation is

$$S(t) \geq S_o E_\alpha[-(\beta(1-\rho) + \beta_0 B_o + \beta_e B_e + \mu)t^\alpha].$$

Since $S_0 > 0$, it implies that $S(t) > 0$, $\forall t > 0$.

So, following similar procedure, we have

$$\begin{aligned} I(t) &\geq I_0 E_\alpha[-(\mu + d + \delta)t^\alpha], \\ R(t) &\geq R_0 E_\alpha[-\mu t^\alpha], \\ B_e(t) &\geq (B_e)_0 E_\alpha[(A_1 - h)t^\alpha];\ \ h > A_1, \\ B_o(t) &\geq (B_o)_0 E_\alpha[-gt^\alpha]. \end{aligned}$$

Since $I_0 > 0$, $R_0 > 0$, $(B_e)_0 > 0$ and $(B_o)_0 > 0$, we get $I(t) > 0$, $R(t) > 0$, $B_e(t) > 0$ and $B_o(t) > 0$. Hence, the desired result.

Now, for the boundedness, the sum of the total human population size is given by

$$N(t) = S(t) + I(t) + R(t).$$

$$\begin{aligned} \text{Clearly, } D^\alpha N(t) &= \Lambda - \mu(S+I+R) - dI \\ &= \Lambda - \mu N - dI \\ &\leq \Lambda - \mu N, \end{aligned}$$

$$\text{which implies, } N(t) \leq \frac{\Lambda}{\mu} + \left(N(0) - \frac{\Lambda}{\mu}\right) E_\alpha(-\mu t^\alpha).$$

So, $\lim_{t\to\infty} \sup N(t) \leq \frac{\Lambda}{\mu}$.

$$\begin{aligned}\text{Now, } D^\alpha B_e(t) &= (A_1 - h) B_e(t) + \sigma I(t) \\ &\leq \sigma \frac{\Lambda}{\mu} - (h - A_1) B_e(t),\end{aligned}$$

$$\text{which implies that, } B_e(t) \leq \frac{\sigma\Lambda}{\mu(h-A_1)} + \left(B_e(0) - \frac{\sigma\Lambda}{\mu(h-A_1)} E_\alpha\left(-(h-A_1)t^\alpha\right)\right).$$

So, $\lim_{t\to\infty} \sup B_e(t) \leq \frac{\sigma\Lambda}{\mu(h-A_1)}$.

$$\text{Now, } D^\alpha B_o(t) = bB_e(t) - gB_o(t) \leq \frac{b\sigma\Lambda}{\mu(h-A_1)} - gB_o,$$

$$\text{which implies that, } B_o \leq \frac{b\sigma\Lambda}{\mu(h-A_1)g} + \left(B_o(0) - \frac{b\sigma\Lambda}{\mu(h-A_1)g}\right) E_\alpha(-gt^\alpha).$$

So, $\lim_{t\to\infty} \sup B_o(t) \leq \frac{b\sigma\Lambda}{\mu g(h-A_1)}$.

This indicates that both the total human population and each individual population class remain constrained within finite bounds. Thus, let $x(t) = (S(t), I(t), R(t), B_e(t), B_o(t))$ represent the solution of the system. Then, for biological relevance, the region of attraction of the system (6.1) is defined by the closed set:

$$\mathscr{U} = \left\{ x(t) \in \mathbb{R}^6_+ : 0 \leq N(t) = S(t) + I(t) + R(t) \leq \frac{\Lambda}{\mu},\ B_e(t) \leq \frac{\sigma\Lambda}{\mu(h-A_1)},\right.$$
$$\left. B_o(t) \leq \frac{b\sigma\Lambda}{\mu g(h-A_1)};\ \text{with } h > A_1 \right\}.$$

6.4 Existence and Uniqueness

Lemma 6.4.1 *The function $f(t, M(t))$, defined above, satisfies*
$\left\| f(t,M(t)) - f(t,\hat{M}) \right\| \leq \in^+_M \left\| M - \hat{M} \right\|_\Omega$ *for some* $\in^+_M > 0$ *and* $\hat{M} = \left(\hat{S}, \hat{I}, \hat{R}, \hat{B}_e, \hat{B}_o\right)$.

Proof 6.4.2 *By the definition of function $f(t, M(t))$,*

$$\left\| f(t,M(t)) - f(t,\hat{M}) \right\| \leq \sup_{t\in[0,t_0]} \sum_{i=1}^{5} \left| \Psi_i(t,M(t)) - \Psi_i(t,\hat{M}(t)) \right|. \tag{6.3}$$

We observe that the first component,

$$\left|\Psi_1(t,M(t))-\Psi_1(t,\hat{M}(t))\right| \leq \mu\left|S-\hat{S}\right|+\beta(1-\rho)\left|SI-\hat{S}\hat{I}\right|+\beta_o\left|SB_o-\hat{S}\hat{B}_o\right| + \beta_e\left|SB_e-\hat{S}\hat{B}_e\right|. \tag{6.4}$$

Consider the term,

$$\left|SI-\hat{S}\hat{I}\right| = \left|SI-S\hat{I}+S\hat{I}-\hat{S}\hat{I}\right| \leq w_1(t)\left|I-\hat{I}\right|+w_2(t)\left|S-\hat{S}\right|, \tag{6.5}$$

where $w_1(t)=|S(t)|$ *and* $w_2(t)=|I(t)|$.

$$\textit{Similarly,}\quad \left|SB_o-\hat{S}\hat{B}_o\right| = w_1(t)\left|B_o-\hat{B}_o\right|+w_3(t)\left|S-\hat{S}\right|, \tag{6.6}$$

where $w_3(t)=|B_o(t)|$, *and*

$$\left|SB_e-\hat{S}\hat{B}_e\right| = w_1(t)\left|B_e-\hat{B}_e\right|+w_4(t)\left|S-\hat{S}\right|, \tag{6.7}$$

where $w_4(t)=|B_e(t)|$.

So, equation (6.4) *implies*

$$\begin{aligned}\left|\Psi_1(t,M(t))-\Psi_1(t,\hat{M}(t))\right| &\leq \mu\left|S-\hat{S}\right|+\beta(1-\rho)w_1(t)\left|I-\hat{I}\right| \\ &\quad+\beta(1-\rho)w_2(t)\left|S-\hat{S}\right|+\beta_o w_3(t)\left|S-\hat{S}\right| \\ &\quad+\beta_o w_1(t)\left|B_o-\hat{B}_o\right|+\beta_e w_1(t)\left|B_e-\hat{B}_e\right| \\ &\quad+\beta_e w_4(t)\left|S-\hat{S}\right| \\ &\leq \{\mu+\beta(1-\rho)w_2(t)+\beta_o w_3(t)+\beta_e w_4(t)\}\left|S-\hat{S}\right| \\ &\quad+\beta(1-\rho)w_1(t)\left|I-\hat{I}\right|+\beta_o w_1(t)\left|B_o-\hat{B}_o\right| \\ &\quad+\beta_e w_1(t)\left|B_e-\hat{B}_e\right|.\end{aligned}$$

Which implies that,

$$\left|\Psi_1(t,M(t))-\Psi_1(t,\hat{M}(t))\right| \leq \in_1^+(t)\left\{\left|S-\hat{S}\right|+\left|I-\hat{I}\right|+\left|B_e-\hat{B}_e\right|+\left|B_o-\hat{B}_o\right|\right\},$$

where

$$\begin{aligned}\in_1^+(t) &= \mu+\max_{t\in[0,t_0]}\Big\{\beta(1-\rho)w_2(t)+\beta_o w_3(t)+\beta_e w_4(t)+\beta(1-\rho)w_1(t) \\ &\qquad+\beta_o w_1(t)+\beta_e w_1(t)\Big\} \\ &= \mu+\max_{t\in[0,t_0]}\Big\{\beta(1-\rho)(w_1(t)+w_2(t))+\beta_o(w_1(t)+w_3(t)) \\ &\qquad+\beta_e(w_1(t)+w_4(t))\Big\}.\end{aligned}$$

In a similar manner,

$$\begin{aligned}
\left|\Psi_2(t,M(t))-\Psi_2(t,\hat{M}(t))\right| &\leq \in_2^+(t)\left\{\left|S-\hat{S}\right|+\left|I-\hat{I}\right|+\left|B_e-\hat{B}_e\right|+\left|B_o-\hat{B}_o\right|\right\},\\
\left|\Psi_3(t,M(t))-\Psi_3(t,\hat{M}(t))\right| &\leq \in_3^+(t)\left\{\left|I-\hat{I}\right|+\left|R-\hat{R}\right|\right\},\\
\left|\Psi_4(t,M(t))-\Psi_4(t,\hat{M}(t))\right| &\leq \in_4^+(t)\left\{\left|I-\hat{I}\right|+\left|B_e-\hat{B}_e\right|\right\},\\
\left|\Psi_5(t,M(t))-\Psi_5(t,\hat{M}(t))\right| &\leq \in_5^+(t)\left\{\left|B_e-\hat{B}_e\right|+\left|B_o-\hat{B}_o\right|\right\},
\end{aligned}$$

where

$$\begin{aligned}
\in_2^+(t) &= (\mu+d+\delta)+\max_{t\in[0,t_0]}\Big\{\beta(1-\rho)(w_1(t)+w_2(t))+\beta_e(w_1(t)+w_4(t))\\
&\qquad +\beta_o(w_1(t)+w_3(t))\Big\},\\
\in_3^+(t) &= \delta+\mu,\\
\in_4^+(t) &= (A_1-h)+\sigma,\\
\in_5^+(t) &= b+g.
\end{aligned}$$

So, from equation (6.3)*, we have*

$$\begin{aligned}
\left\|f(t,M(t))-f(t,\hat{M}(t))\right\|_\Omega &\leq \max_{t\in[0,t_0]}\left\{\in_1^+(t)+\in_2^+(t)+\in_3^+(t)+\in_4^+(t)+\in_5^+(t)\right\}\\
&\quad\times\left\{\left|S-\hat{S}\right|+\left|I-\hat{I}\right|+\left|R-\hat{R}\right|+\left|B_e-\hat{B}_e\right|+\left|B_o-\hat{B}_o\right|\right\}\\
&\leq \in_M^+\left\|M-\hat{M}\right\|;\ \textit{for}\ \leq \in_M^+ = \in_1^+ + \in_2^+ + \in_3^+ + \in_4^+ + \in_5^+ .
\end{aligned}$$

Hence, the result.

Theorem 6.4.3 *There exist a unique solution for the proposed model* (6.1) *on* $[0,t_0]$*, if* $\frac{{t_0}^\alpha \in_M^+}{\Gamma(1+\alpha)} < 1$ *holds.*

Proof 6.4.4 *Let us define the set* $X_m = \{M \in \Omega : \|M\| \leq m\}$ *and the operator* $\mathscr{J} : \Omega \to \Omega$ *as follows:*

$$\mathscr{J}(M(t)) = M_0 + \frac{1}{\Gamma\alpha}\int_0^t (t-\xi)^{\alpha-1} f(\xi,M(\xi))d\xi.$$

We need to show that $\mathscr{J}X_m \subset X_m$, *i.e.* $\|\mathscr{J}X_m\| \leq m$. *Using Lemma 6.4.1, we get the following inequality:*

$$\begin{aligned}
\|\mathscr{J}(M)\|_{X_m} &= \sup_{t\in[0,t_0]}\left\{\left|M_0+\frac{1}{\Gamma\alpha}\int_0^t (t-\xi)^{\alpha-1} f(\xi,M(\xi))d\xi\right|\right\}\\
&\leq |M_0|+\frac{1}{\Gamma\alpha}\int_0^t (t-\xi)^{\alpha-1}\|f(\xi,M(\xi))-f(\xi,0)\|d\xi\\
&\quad+\frac{1}{\Gamma\alpha}\int_0^t (t-\xi)^{\alpha-1}\|f(\xi,0)\|d\xi\\
&\leq |M_0|+\frac{\in_M^+ m{t_0}^\alpha}{\Gamma(1+\alpha)}+\frac{M_0{t_0}^\alpha}{\Gamma(1+\alpha)}.
\end{aligned}$$

Let us suppose the contrary, i.e. $\|\mathscr{J}X_m\| > m$,

$$\begin{aligned}
\text{which implies that, } |M_0|+\frac{{t_0}^\alpha}{\Gamma(1+\alpha)}(\in_M^+ m+M_0) &> m\\
\frac{|M_0|}{m}+\frac{{t_0}^\alpha \in_M^+}{\Gamma(1+\alpha)}+\frac{{t_0}^\alpha M_0}{m\Gamma(1+\alpha)} &> 1.
\end{aligned}$$

On taking limit $m\to\infty$ *on both sides, we get* $\frac{{t_0}^\alpha\in_M^+}{\Gamma(1+\alpha)} > 1$, *which is a contradiction to our supposition. So,* $\|\mathscr{J}X_m\| \leq m$. *This proves that* $\mathscr{J}$ *is indeed a self-map.*

For $M,\hat{M}\in\Omega$, *consider*

$$\begin{aligned}
\left\|\mathscr{J}M-\mathscr{J}\hat{M}\right\| &= \sup_{t\in[0,t_0]}\left\{\left|\mathscr{J}M(t)-\mathscr{J}\hat{M}(t)\right|\right\}\\
&\leq \frac{1}{\Gamma\alpha}\int_0^{t_0}(t-\xi)^{\alpha-1}\left\|f(\xi,M(\xi))-f(\xi,\hat{M}(\xi))\right\|d\xi\\
&\leq \frac{\in_M^+ {t_0}^\alpha}{\Gamma(1+\alpha)}\left\|M-\hat{M}\right\|_\Omega\\
&< 1.\left\|M-\hat{M}\right\|_\Omega.
\end{aligned}$$

This confirms that $\mathscr{J}$ *is a contraction mapping. So, by Banach contraction principle,* $\mathscr{J}$ *has a unique fixed point on* $[0,t_0]$, *which is a solution of the model.*

Theorem 6.4.5 *If* $|f(t,M(t))| \leqslant g(t)$ *for all* $g(t)\in C([0,t_0])$, *then the proposed model* (6.2) *has at least one solution provided*

$$\in_M^+ \left\|M(t_0)-\hat{M}(t_0)\right\| < 1.$$

Proof 6.4.6 *Consider* $\xi \geqslant \|M_0\| + \frac{t_0^\alpha}{\Gamma(1+\alpha)}\|g\|$ *and the set* $B_\xi = \{M \in C([0,t_0]) : \|M\| \leqslant \xi\}$. *From [79], consider the operators* $\mathscr{J}_1$, $\mathscr{J}_2$ *on* B_ξ *defined by*

$$(\mathscr{J}_1 M)(t) = \frac{1}{\Gamma(\alpha)} \int_0^t (t-\rho)^{\alpha-1} f(t, M(t))\, d\rho,$$

and

$$(\mathscr{J}_2 M)(t) = M(t_0).$$

Thus, for any $M, \hat{M} \in B_\xi$, *we get*

$$\begin{aligned} \left\|(\mathscr{J}_1 M)(t) + \left(\mathscr{J}_2 \hat{M}\right)(t)\right\| &\leqslant \|M_0\| + \frac{1}{\Gamma(\alpha)} \int_0^t (t-\rho)^{\alpha-1} \|f(\rho, M(\rho))\|\, d\rho \\ &\leqslant \|M_0\| + \frac{t_0^\alpha}{\Gamma(1+\alpha)}\|g\| \\ &\leqslant \xi < \infty. \end{aligned}$$

Hence, $\mathscr{J}_1 M + \mathscr{J}_2 \hat{M} \in B_\xi$. *Now, we will prove the contraction of the operator* $\mathscr{J}_2$. *Given any* $t \in [0,t_0]$ *and* $M, \hat{M} \in B_\xi$, *we have*

$$\left\|(\mathscr{J}_1 M)(t) + \left(\mathscr{J}_2 \hat{M}\right)(t)\right\| \leqslant \left\|M(t_0) - \hat{M}(t_0)\right\|.$$

Moreover, the continuity of the operator $\mathscr{J}_1$ *is implied by the continuity of* f. *For any* $t \in [0,t_0]$ *and* $M \in B_\xi$, $\|\mathscr{J}_1 M\| \leqslant \frac{t_0^\alpha}{\Gamma(1+\alpha)}\|g\| \leqslant \infty$. *Thus, we can say that* $\mathscr{J}_1$ *is uniformly bounded.*

Now, to show $\mathscr{J}_1$ *is compact, define* $f^* = \sup(t, M) \in [0,t_0] \times B_\xi |f(t, M(t))|$. *Thus,*

$$\begin{aligned} \|(\mathscr{J}_1 M)(t_1) - (\mathscr{J}_1 M)(t_2)\| &= \frac{1}{\Gamma(\alpha)} \Bigg| \int_0^{t_1} \left[(t_2-\rho)^{\alpha-1} - (t_1-\rho)^{\alpha-1}\right] f(\rho, M(\rho))\, d\rho \\ &\quad + \int_{t_1}^{t_2} (t_2-\rho)^{\alpha-1} f(\rho, M(\rho))\, d\rho \Bigg| \\ &\leqslant \frac{f^*}{\Gamma(\alpha)} \left[2(t_2-t_1)^\alpha + (t_2-t_1)^\alpha\right] \\ &\to 0, \quad as\ t_2 \to t_1. \end{aligned}$$

This proves that $\mathscr{J}_1$ is equicontinuous and consequently, relatively compact on B_ξ. Hence, by Arzelá Ascoli theorem, $\mathscr{J}_1$ is compact on B_ξ. Using Schaefer's fixed point theorem, the model has a fixed point which is a solution of (6.2).

6.5 Basic Reproduction number and its Sensitivity Analysis

To determine the basic reproduction number, the disease-free equilibrium (DFE) point is first found. For model (6.1), the DFE is:

$$\left(\bar{S},\bar{I},\bar{R},\bar{B}_e,\bar{B}_o\right) = \left(\frac{\Lambda}{\mu},0,0,0,0,\right).$$

The basic reproduction number $\mathscr{R}_0$ is determined using the next-generation approach. For that, let

$$D_t^\alpha(z) = \mathscr{F}(z) - \mathscr{V}(z),$$

where $z = (I,R,B_e)$. The non-negative matrix $\mathscr{F}$, which represents the new infection terms, and the matrix $\mathscr{V}$, comprising the remaining terms, are provided as follows:

$$\mathscr{F} = \begin{pmatrix} \beta(1-\rho)SI + \beta_0 SB_o + \beta_e SB_e \\ \delta I \\ \sigma I \end{pmatrix} \text{ and } \mathscr{V} = \begin{pmatrix} (\delta+\mu+d)I \\ \mu R \\ -(A_1-h)B_e \end{pmatrix}$$

The corresponding linearized matrices evaluated at DFE $\left(\bar{S},\bar{I},\bar{R},\bar{B}_e,\bar{B}_o\right)$ are respectively,

$$F = \begin{pmatrix} \frac{\beta(1-\rho)\Lambda}{\mu} & 0 & \frac{\beta_e\Lambda}{\mu} \\ \delta & 0 & 0 \\ \sigma & 0 & 0 \end{pmatrix} \text{ and } V = \begin{pmatrix} (\delta+\mu+d) & 0 & 0 \\ 0 & \mu & 0 \\ 0 & 0 & -(A_1-h) \end{pmatrix}.$$

Since, the largest eigen value, i.e., the spectral radius of the matrix FV^{-1}, represents the basic reproduction number $\mathscr{R}_0$, therefore,

$$FV^{-1} = \begin{pmatrix} \frac{\beta\Lambda(1-\rho)}{\mu(\delta+\mu+d)} & 0 & \frac{\Lambda\beta_e}{\mu(h-A_1)} \\ \frac{\delta}{(\delta+\mu+d)} & 0 & 0 \\ \frac{\sigma}{(\delta+\mu+d)} & 0 & 0 \end{pmatrix},$$

and hence,

$$\mathscr{R}_0 = \frac{\beta\Lambda(1-\rho)(h-A_1) + \sqrt{\beta^2\Lambda^2(1-\rho)^2(h-A_1)^2 + 4\mu\sigma\beta_e(d+\delta+\mu)}}{2\mu(h-A_1)(d+\delta+\mu)}.$$

6.5.1 Sensitivity Analysis

Sensitivity analysis is used to understand how different model parameters affect the spread of a disease. Specifically, it helps calculate the sensitivity indices of the basic reproductive number, $\mathscr{R}_0$. These indices show how important each parameter is in influencing disease spread and guide where intervention efforts should focus. Since errors often occur in data collection and in the assumed values of model parameters, sensitivity analysis is also used to assess how reliable a model's predictions are when these parameter values change. There are different ways to perform sensitivity analysis, and the results provide sensitivity rankings that can differ slightly depending on the method used. Here, we employed the normalized forward sensitivity index, which is the ratio of the relative change in $\mathscr{R}_0$ to the relative change in the parameter being studied [73].

Definition 6.5.1 *[158] For a variable y dependent on parameter x,the normalized forward sensitivity index is defined as*

$$W_x^y = \frac{\partial y}{\partial x} \times \frac{x}{y}.$$

So, for $\mathscr{R}_0$, the sensitivity index is $W_x^{\mathscr{R}_0} = \dfrac{\partial \mathscr{R}_0}{\partial x} \times \dfrac{x}{\mathscr{R}_0}$, which expresses the sensitivity of $\mathscr{R}_0$ to the parameter x. The sensitivity indices for the relevant parameters are:

$$W_\beta^{\mathscr{R}_0} = \frac{\beta\Lambda(1-\rho)(h-A_1)}{\sqrt{[\beta\Lambda(1-\rho)(h-A_1)]^2+4\mu\sigma\beta_e(d+\delta+\mu)}}$$

$$W_\Lambda^{\mathscr{R}_0} = \frac{\beta\Lambda(1-\rho)(h-A_1)}{\sqrt{[\beta\Lambda(1-\rho)(h-A_1)]^2+4\mu\sigma\beta_e(d+\delta+\mu)}}$$

$$W_\rho^{\mathscr{R}_0} = \frac{-\beta\Lambda\rho(h-A_1)}{\sqrt{[\beta\Lambda(1-\rho)(h-A_1)]^2+4\mu\sigma\beta_e(d+\delta+\mu)}}$$

$$W_h^{\mathscr{R}_0} = \frac{\beta h\Lambda(1-\rho)}{\sqrt{[\beta\Lambda(1-\rho)(h-A_1)]^2+4\mu\sigma\beta_e(d+\delta+\mu)}} - \frac{h}{(h-A_1)}$$

$$W_{A_1}^{\mathscr{R}_0} = \frac{A_1}{h-A_1} - \frac{\beta\Lambda A_1(1-\rho)}{\sqrt{[\beta\Lambda(1-\rho)(h-A_1)]^2+4\mu\sigma\beta_e(d+\delta+\mu)}}$$

$$W_\mu^{\mathscr{R}_0} = \frac{-(d+\delta+2\mu)\left(1+\frac{\beta\Lambda(1-\rho)(h-A_1)}{\sqrt{[\beta\Lambda(1-\rho)(h-A_1)]^2+4\mu\sigma\beta_e(d+\delta+\mu)}}\right)}{2(d+\delta+\mu)}$$

$$W_\sigma^{\mathscr{R}_0} = \frac{2\mu\sigma\beta_e(d+\delta+\mu)}{\sqrt{[\beta\Lambda(1-\rho)(h-A_1)]^2+4\mu\sigma\beta_e(d+\delta+\mu)}\left(\begin{array}{l}\sqrt{[\beta\Lambda(1-\rho)(h-A_1)]^2+4\mu\sigma\beta_e(d+\delta+\mu)}\\ +b\Lambda(1-\rho)(h-A_1)\end{array}\right)}$$

$$W_{\beta_e}^{\mathscr{R}_0} = \frac{2\mu\sigma\beta_e(d+\delta+\mu)}{\sqrt{[\beta\Lambda(1-\rho)(h-A_1)]^2+4\mu\sigma\beta_e(d+\delta+\mu)}\left(\begin{array}{l}\sqrt{[\beta\Lambda(1-\rho)(h-A_1)]^2+4\mu\sigma\beta_e(d+\delta+\mu)}\\ +b\Lambda(1-\rho)(h-A_1)\end{array}\right)}$$

$$W_d^{\mathscr{R}_0} = \frac{2d\mu\sigma\beta_e}{\sqrt{[\beta\Lambda(1-\rho)(h-A_1)]^2+4\mu\sigma\beta_e(d+\delta+\mu)}\left(\begin{array}{l}\sqrt{[\beta\Lambda(1-\rho)(h-A_1)]^2+4\mu\sigma\beta_e(d+\delta+\mu)}\\ +b\Lambda(1-\rho)(h-A_1)\end{array}\right)} - \frac{d}{d+\delta+\mu}$$

$$W_\delta^{\mathscr{R}_0} = \frac{2\delta\mu\sigma\beta_e}{\sqrt{[\beta\Lambda(1-\rho)(h-A_1)]^2+4\mu\sigma\beta_e(d+\delta+\mu)}\left(\begin{array}{l}\sqrt{[\beta\Lambda(1-\rho)(h-A_1)]^2+4\mu\sigma\beta_e(d+\delta+\mu)}\\ +b\Lambda(1-\rho)(h-A_1)\end{array}\right)} - \frac{\delta}{d+\delta+\mu}$$

To evaluate these sensitivity indices, the parameter values provided in Section 6.9 are used, and the corresponding bar diagram is plotted in Figure 6.2 as follows:

$$W_\beta^{\mathscr{R}_0} = 0.944829,\ W_\Lambda^{\mathscr{R}_0} = 0.944829,\ W_\rho^{\mathscr{R}_0} = -0.684187,\ W_h^{\mathscr{R}_0} = -0.128732,$$
$$W_{A_1}^{\mathscr{R}_0} = 0.0735611,\ W_\mu^{\mathscr{R}_0} = -1.31163,\ W_\sigma^{\mathscr{R}_0} = 0.0275854,\ W_{\beta_e}^{\mathscr{R}_0} = 0.0275854,$$
$$W_d^{\mathscr{R}_0} = -0.407057,\ W_\delta^{\mathscr{R}_0} = -0.226143.$$

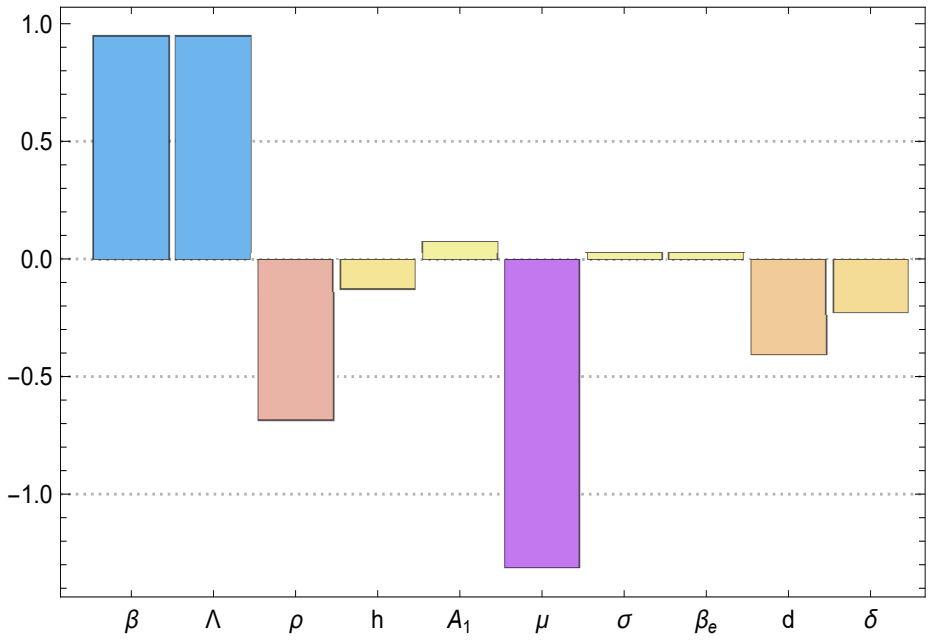

Figure 6.2: Sensitivity indices of $\mathscr{R}_0$.

From the above explanation, we see that these parameters can either increase or decrease $\mathscr{R}_0$. Specifically, the parameters β, Λ have the strongest positive impact and A_1, σ and β_e have a less positive impact on $\mathscr{R}_0$. This means that if these parameters increase while keeping the others unchanged, the basic reproduction number $\mathscr{R}_0$ will also increase, leading to a faster spread of the disease. Similarly, if they decrease, the spread of the disease will slow down.

For example, $W_\beta^{\mathscr{R}_0} = 0.944829$ indicates that if the parameter β increases (or decreases) by 10%, then $\mathscr{R}_0$ will increase (or decrease) by 9.45%. Similarly, $W_\rho^{\mathscr{R}_0} = -0.684187$ means that if ρ increases (or decreases) by 10%, then $\mathscr{R}_0$ will decrease (or increase) by 6.84%, respectively. This helps us understand the sensitivity of the parameters and their impact on $\mathscr{R}_0$ in both positive and negative ways.

6.6 Ulam-Hyers Stability

In this section, the global stability of the fractional-order model is analyzed within the framework of the Ulam-Hyers stability criteria, following the approach in [179; 83]. To begin, the following inequality is introduced:

$$|D_t^\alpha M(t) - f(t, M(t))| \leq \varepsilon, \quad t \in [0, t_0]. \tag{6.8}$$

A function M^o satisfies (6.8), if there exists $\chi \in \Omega$ such that:

- $|\chi(t)| \leq \varepsilon$
- $D_t^{\alpha} M^o(t) = f(t, M^o(t)) + \chi(t);\ \ t \in [0, t_0]$.

Definition 6.6.1 *[25] The model* (6.1) *is Ulam-Hyers stable if* $\exists$ *a real number* $\phi > 0$ *such that for given* $\varepsilon > 0$ *and for any solution* $M^o(t)$ *of equation* (6.8)*, there exists a unique solution* $M(t)$ *of model equation*(6.1) *with*

$$\|M(t) - M^o(t)\| \leq \varepsilon\phi;\ \ t \in [0, t_0].$$

Consider the inequality,

$$|D_t^{\alpha} M(t) - f(t, M(t))| \leq \varepsilon\theta(t),\ \text{ for some }\ \theta(t) \in C([0, t_0]; \mathbb{R}^+). \tag{6.9}$$

A function M^o satisfies equation (6.9) iff there exists a function $\nu(t) \in \Omega$ such that

- $|\nu(t)| \leq \varepsilon\theta(t)$
- $D_t^{\alpha} M^o(t) = f(t, M^o(t)) + \nu(t);\ \ t \in [0, t_0]$.

Definition 6.6.2 *[25] The fractional order model* (6.1) *is generalized Ulam-Hyers stable with respect to function* $\theta(t)$ *if there exists real number* $\phi > 0$ *such that for given* $\varepsilon > 0$ *and for any solution* $M^o(t)$ *of equation* (6.9)*, there exists a unique solution* $M(t)$ *of model equation* (6.1) *with*

$$\|M(t) - M^o(t)\| \leq \varepsilon\phi\theta(t);\ \ t \in [0, t_0].$$

Theorem 6.6.3 *Suppose Lemma 6.4.1 holds and* $X_\theta > 0$ *be such that* $\int_0^t \theta(s)ds \leq X_\theta\theta(t),\ \ t \in [0, t_0]$. *Then the proposed model* (6.1) *is Ulam-Hyers generalized stable with respect to function* $\theta(t)$ *if*

$$\in_M^+ {t_0}^{\alpha} < \Gamma(\alpha + 1),\ \ \textit{or equivalently}\ \ \frac{\in_M^+ {t_0}^{\alpha}}{\Gamma(\alpha + 1)} < 1.$$

Proof 6.6.4 *Let M be a unique solution of the model system* (6.1) *by Theorem 6.4.3. Since,* M^o *satisfies inequality* (6.9)*, thus we have*

$$M^o(t) = M_0 + \frac{1}{\Gamma\alpha}\int_0^t (t - \xi)^{\alpha - 1}\{f(\xi, M^o(\xi)) + \nu(\xi)\}d\xi,$$

which implies that,

$$\left| M^o(t) - M_0 - \frac{1}{\Gamma\alpha}\int_0^t (t-\xi)^{\alpha-1} f(\xi, N^o(\xi))d\xi \right| = \left| \frac{1}{\Gamma\alpha}\int_0^t (t-\xi)^{\alpha-1}\nu(\xi)d\xi \right|$$
$$\leq \left| \frac{1}{\Gamma\alpha}\int_0^t (t-\xi)^{\alpha-1}\varepsilon\theta(\xi)d\xi \right|$$
$$\leq \varepsilon X_\theta \theta(t)\frac{{t_0}^\alpha}{\Gamma(\alpha+1)}. \tag{6.10}$$

For $\varepsilon > 0$ *and* $t \in [0, t_0]$,

$$\begin{aligned}
\|M(t) - M^o(t)\|_\Omega &= \sup_{t\in[0,t_0]} |M(t) - M^o(t)| \\
&= \sup_{t\in[0,t_0]} \left| M^o(t) - M_0 - \frac{1}{\Gamma\alpha}\int_0^t (t-\xi)^{\alpha-1} f(\xi, N(\xi))d\xi \right| \\
&= \left| M^o(t) - M_0 - \frac{1}{\Gamma\alpha}\int_0^t (t-\xi)^{\alpha-1} f(\xi, N^o(\xi))d\xi \right| \\
&\quad + \frac{1}{\Gamma\alpha}\int_0^t (t-\xi)^{\alpha-1} \|f(\xi, N^o(\xi)) - f(\xi, N(\xi))\| d\xi \\
&\leq \varepsilon X_\theta \theta(t)\frac{{t_0}^\alpha}{\Gamma(\alpha+1)} + \frac{\in_M^+ {t_0}^\alpha}{\Gamma(\alpha+1)}\|M - M^o\|_\Omega.
\end{aligned}$$

This implies that

$$\|M(t) - M^o(t)\|_\Omega \leq \frac{\varepsilon X_\theta \theta(t) {t_0}^\alpha}{(\Gamma(\alpha+1) - \in_M^+ {t_0}^\alpha)},$$

and hence,

$$\|M(t) - M^o(t)\|_\Omega \leq \varepsilon\phi\theta(t),$$

where $\phi = \frac{X_\theta {t_0}^\alpha}{(\Gamma(\alpha+1) - \in_M^+ {t_0}^\alpha)}$ *and* $\in_M^+ {t_0}^\alpha < \Gamma(\alpha+1)$.

This proves that the model system (6.1) is Ulam-Hyers generalized stable. In a similar way, it is easy to check that model system (6.1) is Ulam-Hyers stable also.

6.7 Optimal Control Formulations

Optimal control theory primarily deals with constraints and systematic approaches to enhance the performance metrics of control systems. In this section, we introduce

a well-structured control strategy designed to minimize the effects of diseases while keeping intervention costs as low as possible. During the spread of an epidemic, reducing the infection rate among susceptible individuals is crucial. This can be achieved by influencing their behaviors to decrease direct contact with both infected individuals and disease-carrying vectors, thereby lowering transmission risks. The control variable $u_1(t)$ represents personal protection measures through the use of face masks, social distancing, isolation and awareness of disease transmission from an infected person. Control $u_2(t)$ represents the level of awareness about cleanliness practices in our surroundings, such as households, workplaces and public spaces. This includes understanding the importance of regularly cleaning surfaces, disposing of waste properly, washing hands frequently, and taking other preventative measures to reduce contamination. The control variable $u_3(t)$ reflects the understanding of hygiene practices, such as actions like using sanitizers, washing vegetables properly before consumption and ensuring proper sanitation, especially in food preparation areas or healthcare settings. By adding these three control measures, the system (6.1) is modified as follows:

$$\begin{aligned}
D^{\alpha}S(t) &= \Lambda - \beta(1-u_1(t))S(t)I(t) - \beta_o(1-u_2(t))S(t)B_o(t) - \beta_e(1-u_3(t))S(t)B_e(t) \\
&\qquad - \mu S(t), \\
D^{\alpha}I(t) &= \beta(1-u_1(t))S(t)I(t) + \beta_o(1-u_2(t))S(t)B_o(t) + \beta_e(1-u_3(t))S(t)B_e(t) \\
&\qquad - \delta I(t) - (\mu+d)I(t), \\
D^{\alpha}R(t) &= \delta I(t) - \mu R(t), \\
D^{\alpha}B_e(t) &= (A_1 - h)B_e(t) + \sigma I(t), \\
D^{\alpha}B_o(t) &= bB_e(t) - gB_o(t),
\end{aligned} \tag{6.11}$$

with $S(0) \geq 0$, $I(0) \geq 0$, $R(0) \geq 0$, $B_e(0) \geq 0$, $B_o(0) \geq 0$.

We begin by exploring the formulation of objective functional, which helps quantify the trade-offs between disease burden and intervention efforts. The overall objective functional consists of two main components: the cumulative cost related to the disease, denoted as J_b, and the cost associated with implementing control measures, represented by J_c.

The total intervention cost can be expressed as a nonlinear function of the control variables, given by:

$$J_c = \int_0^T \left(\frac{1}{2} z_1 u_1^2(t) + \frac{1}{2} z_2 u_2^2(t) + \frac{1}{2} z_3 u_3^2(t) \right) dt,$$

where z_1, z_2 and z_3 are positive constants representing the cost of implementing different intervention strategies.

The cost incurred due to the disease ,J_b, is determined by the specific disease model under consideration and the accessible information. It is given by:

$$J_b = \int_0^T A_b I(t) dt,$$

where A_b is a positive scaling factor that accounts for the overall economic impact of the disease. This includes direct costs, such as medical treatment and indirect costs, such as productivity loss and mortality.

The optimal control strategy is influenced by the relative magnitudes of the coefficients A_b, z_1, z_2 and z_3, which determine the balance between disease-related losses and intervention expenses.

6.7.1 Combined objective functional

The objective functional aims to minimize both the disease burden and the associated intervention costs. This is mathematically expressed as:

$$\min_{u_i \in U} \int_0^T \left[A_b I(t) + \frac{1}{2} z_1 u_1^2(t) + \frac{1}{2} z_2 u_2^2(t) + \frac{1}{2} z_3 u_3^2(t) \right] dt,$$

where $A_b I(t)$ represents the cost attributed to disease prevalence, while the remaining terms account for the costs associated with implementing control strategies. The control variables $u_1(t)$, $u_2(t)$ and $u_3(t)$ belong to the set U, which is defined as:

$$U = \{(u_1, u_2, u_3) | u_i(t) \text{ is Lebesgue measurable on } [0,1], 0 \leq u_i(t) \leq 1, i = 1,2,3\}.$$

Here, $u_i(t) = 0$ indicates no implementation of the i^{th} control, while $u_i(t) = 1$ corresponds to the full application of the available intervention. Since these control functions represent proportions or effort levels, it is not meaningful to consider values below 0 or above 1.

6.7.2 Existence of optimal control

The following conditions ensure the existence of the optimal control functions:

1. **Non-emptiness of the solution set:** The system (6.11) has at least one solution when the control variables are chosen from the set U.

2. **Properties of the Control Set:** The set U is closed and convex. Additionally, the right-hand side of the system (6.11) is bounded by a linear function in terms of the control and state variables.

3. **Convexity of the Integrand:** The function $L = A_b I(t) + \frac{1}{2}z_1 u_1^2(t) + \frac{1}{2}z_2 u_2^2(t) + \frac{1}{2}z_3 u_3^2(t)$ is convex over the set U. Additionally, the function satisfies the condition $L(I,u_1,u_2,u_3) \geq \kappa(u_1,u_2,u_3)$, where κ is continuous. Furthermore, as $|(u_1,u_2,u_3)| \to \infty$, the ratio $|(u_1,u_2,u_3)|^{-1}\kappa(u_1,u_2,u_3) \to \infty$, where $|.|$ represents the norm.

6.7.3 Characterization of optimal control function

To determine the necessary conditions for optimal control, Pontryagin's Maximum Principle [105] is utilised. This principle is crucial in linking the cost functional with the system's state equations by introducing adjoint variables. These adjoint variables help in deriving conditions that must be satisfied for the control function to be optimal.

To facilitate this process, define the Hamiltonian function as follows:

$$\begin{aligned} H = {} & A_b I + \frac{1}{2}z_1 u_1^2 + \frac{1}{2}z_2 u_2^2 + \frac{1}{2}z_3 u_3^2 \\ & + \lambda_1 \left[\Lambda - \beta(1-u_1)SI - \beta_o(1-u_2)SB_o - \beta_e(1-u_3)SB_e - \mu S\right] \\ & + \lambda_2 \left[\beta(1-u_1)SI + \beta_o(1-u_2)SB_o + \beta_e(1-u_3)SB_e - \delta I - (\mu+d)I\right] \\ & + \lambda_3 \left[\delta I - \mu R\right] + \lambda_4 \left[(A_1-h)B_e + \sigma I\right] + \lambda_5 \left[\mathrm{bB}_e - \mathrm{gB}_o\right]. \end{aligned}$$

Here, $\lambda_i = (\lambda_1,\lambda_2,\lambda_3,\lambda_4,\lambda_5)$ are referred to as the adjoint variable, which satisfy the following canonical equations:

$$\frac{d^\alpha \lambda_1}{dt} = -\frac{\partial H}{\partial S}, \frac{d^\alpha \lambda_2}{dt} = -\frac{\partial H}{\partial I}, \frac{d^\alpha \lambda_3}{dt} = -\frac{\partial H}{\partial R}, \frac{d^\alpha \lambda_4}{dt} = -\frac{\partial H}{\partial B_e}, \frac{d^\alpha \lambda_5}{dt} = -\frac{\partial H}{\partial B_o}.$$

Therefore, the adjoint system is:

$$\begin{aligned} D^\alpha \lambda_1 &= -[-\lambda_1\beta(1-u_1)I - \lambda_1\beta_o(1-u_2)B_o - \lambda_1\beta_e(1-u_3)B_e - \lambda_1\mu \\ &\qquad +\lambda_2\beta(1-u_1)I + \lambda_2\beta_o(1-u_2)B_o + \lambda_2\beta_e(1-u_3)B_e] \\ D^\alpha \lambda_2 &= -[A_b - \lambda_1\beta(1-u_1)S + \lambda_2\beta(1-u_1)S - \lambda_2(\mu+d+\delta) + \lambda_3\delta + \lambda_4\sigma] \\ D^\alpha \lambda_3 &= \lambda_3\mu \\ D^\alpha \lambda_4 &= -[-\lambda_1\beta_e(1-u_3)S + \lambda_2\beta_e(1-u_3)S + \lambda_4(A_1-h) + \lambda_5 b] \\ D^\alpha \lambda_5 &= -[-\lambda_1\beta_o(1-u_2)S + \lambda_2\beta_o(1-u_2)S - \lambda_5 g], \end{aligned}$$

with the transversality condition

$$\lambda_1(T) = 0,\ \lambda_2(T) = 0,\ \lambda_3(T) = 0,\ \lambda_4(T) = 0,\ \lambda_5(T) = 0.$$

We can then characterize the optimal control on the interior of the control set using the optimality condition $\frac{\partial H}{\partial u_i} = 0$ at $u_i = u_i^*$, which gives,

$$\begin{aligned}
{u_1}^* &= \min\left\{max\left\{0, \frac{(\lambda_2 - \lambda_1)\beta SI}{z_1}\right\}, 1\right\},\\
{u_2}^* &= \min\left\{max\left\{0, \frac{(\lambda_2 - \lambda_1)\beta_o SB_o}{z_2}\right\}, 1\right\},\\
{u_3}^* &= \min\left\{max\left\{0, \frac{(\lambda_2 - \lambda_1)\beta_e SB_e}{z_3}\right\}, 1\right\}.
\end{aligned} \tag{6.12}$$

6.8 Numerical Scheme Adams-Bashforth-Moulton Predictor-Corrector Method

In this section, numerical scheme is presented for the model (6.1) in the Caputo sense, utilizing the Adams-Bashforth-Moulton predictor-corrector method. This approach is widely used for solving fractional-order differential equations with initial conditions [50]. The implementation of this method is outlined below, considering the following non-autonomous household waste system:

$$\begin{aligned}
D^\alpha S(t) &= f_1\big(t, S, I, R, B_e, B_o\big),\\
D^\alpha I(t) &= f_2\big(t, S, I, R, B_e, B_o\big),\\
D^\alpha R(t) &= f_3\big(t, S, I, R, B_e, B_o\big),\\
D^\alpha B_e(t) &= f_4\big(t, S, I, R, B_e, B_o\big),\\
D^\alpha B_o(t) &= f_5\big(t, S, I, R, B_e, B_o\big),
\end{aligned} \tag{6.13}$$

with $S(0) = S_0,\ I(0) = I_0,\ R(0) = R_0,\ B_e(0) = (B_e)_0$ and $B_o(0) = (B_o)_0$, where $0 < \alpha \leq 1$. Let $t_j = jh,\ j = 0, 1, 2, \ldots, N$ with some integer N and $h = T/N$, in the interval $[0, T]$. By utilizing the method given in [50], system (6.13) can be written as follows:

Predictor values for (6.13) are

$$S^P_{n+1} = S_0 + \frac{1}{\Gamma(\alpha)}\sum_{j=0}^{n} b_{j,n+1} f_1\big(t_j, S_j, I_j, R_j, (B_e)_j, (B_o)_j\big),$$

$$I^P_{n+1} = I_0 + \frac{1}{\Gamma(\alpha)}\sum_{j=0}^{n} b_{j,n+1} f_2\big(t_j, S_j, I_j, R_j, (B_e)_j, (B_o)_j\big),$$

$$R^P_{n+1} = R_0 + \frac{1}{\Gamma(\alpha)}\sum_{j=0}^{n} b_{j,n+1} f_3\big(t_j, S_j, I_j, R_j, (B_e)_j, (B_o)_j\big),$$

$$B_{e}{}^P_{n+1} = B_{e0} + \frac{1}{\Gamma(\alpha)}\sum_{j=0}^{n} b_{j,n+1} f_4\big(t_j, S_j, I_j, R_j, (B_e)_j, (B_o)_j\big),$$

$$B_{o}{}^P_{n+1} = B_{o0} + \frac{1}{\Gamma(\alpha)}\sum_{j=0}^{n} b_{j,n+1} f_5\big(t_j, S_j, I_j, R_j, (B_e)_j, (B_o)_j\big),$$

where, $b_{j,n+1} = \frac{h^\alpha}{\alpha}\big((n-j+1)^\alpha - (n-j)^\alpha\big)$.

Corrector values are obtained by using predictor values as follows:

$$S_{n+1} = S_0 + \frac{h^\alpha}{\Gamma(\alpha+2)} f_1\big(t_{n+1}, S^P_{n+1}, I^P_{n+1}, R^P_{n+1}, B_{e}{}^P_{n+1}, B_{o}{}^P_{n+1}\big) + \frac{h^\alpha}{\Gamma(\alpha+2)}\sum_{j=0}^{n} a_{j,n+1} f_1\big(t_j, S_j, I_j, R_j, B_{ej}, B_{oj}\big),$$

$$I_{n+1} = I_0 + \frac{h^\alpha}{\Gamma(\alpha+2)} f_2\big(t_{n+1}, S^P_{n+1}, I^P_{n+1}, R^P_{n+1}, B_{e}{}^P_{n+1}, B_{o}{}^P_{n+1}\big) + \frac{h^\alpha}{\Gamma(\alpha+2)}\sum_{j=0}^{n} a_{j,n+1} f_2\big(t_j, S_j, I_j, R_j, B_{ej}, B_{oj}\big),$$

$$R_{n+1} = R_0 + \frac{h^\alpha}{\Gamma(\alpha+2)} f_3\big(t_{n+1}, S^P_{n+1}, I^P_{n+1}, R^P_{n+1}, B_{e}{}^P_{n+1}, B_{o}{}^P_{n+1}\big) + \frac{h^\alpha}{\Gamma(\alpha+2)}\sum_{j=0}^{n} a_{j,n+1} f_3\big(t_j, S_j, I_j, R_j, B_{ej}, B_{oj}\big),$$

$$B_{en+1} = B_{e0} + \frac{h^\alpha}{\Gamma(\alpha+2)} f_4\big(t_{n+1}, S^P_{n+1}, I^P_{n+1}, R^P_{n+1}, B_{e}{}^P_{n+1}, B_{o}{}^P_{n+1}\big) + \frac{h^\alpha}{\Gamma(\alpha+2)}\sum_{j=0}^{n} a_{j,n+1} f_4\big(t_j, S_j, I_j, R_j, B_{ej}, B_{oj}\big),$$

$$B_{on+1} = B_{o0} + \frac{h^\alpha}{\Gamma(\alpha+2)} f_5\big(t_{n+1}, S^P_{n+1}, I^P_{n+1}, R^P_{n+1}, B_{e}{}^P_{n+1}, B_{o}{}^P_{n+1}\big) + \frac{h^\alpha}{\Gamma(\alpha+2)}\sum_{j=0}^{n} a_{j,n+1} f_5\big(t_j, S_j, I_j, R_j, B_{ej}, B_{oj}\big),$$

where

$$a_{j,n+1} = \begin{cases} n^{\alpha+1} - (n-\alpha)(n+1)^{\alpha}, & j = 0 \\ (n-j+2)^{\alpha+1} + (n-j)^{\alpha+1} - 2(n-j+1)^{\alpha+1}, & 1 \leq j \leq n. \end{cases}$$

6.9 Simulation and Discussion

In this section, the dynamics of the household waste fractional model are explained using MATLAB 2012b and the Adams-Bashforth-Moulton predictor corrector approach. Since the numerical experimental data is easier and essential for observing the long-term behaviour, because when we use real data, it might be challenging to identify the cause and effects due to fluctuations in pricing, expenditures etc. [125; 164]. Therefore, a qualitative analysis is performed to provide a deeper understanding of the model. For the computational analysis, the initial population is chosen as $S(0) = 50$, $I(0) = 30$, $R(0) = 5$, $B_e(0) = 20$, $B_o(0) = 25$, and the following set of experimental data is considered as an example:
$\Lambda = 5$, $\beta = 0.0033$, $\rho = 0.42$, $\beta_e = 0.0024$, $\beta_o = 0.0021$, $\mu = 0.03$, $\delta = 0.02$,
$d = 0.036$, $A_1 = 0.4$, $h = 0.7$, $\sigma = 0.04$, $b = 0.26$, $g = 0.18$.

To demonstrate how memory affects the dynamics of the HHW model (6.1), Figures 6.3, 6.4, 6.5, 6.6, and 6.7 are plotted, illustrating the impact of various fractional-order values $(\alpha = 0.7, 0.8, 0.9, 1.0)$ on the sub-populations. Increasing the fractional-order values reveals different scenarios for the considered model.

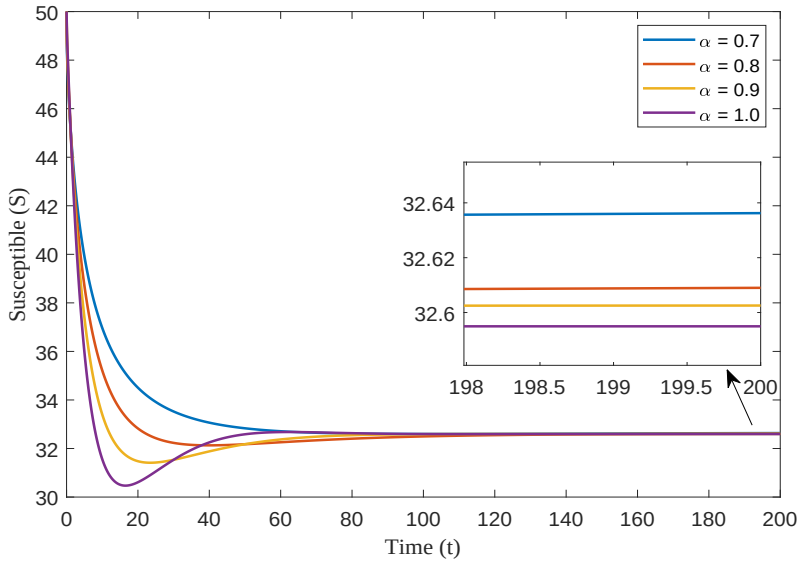

Figure 6.3: Time series plot of susceptible population with different fractional order.

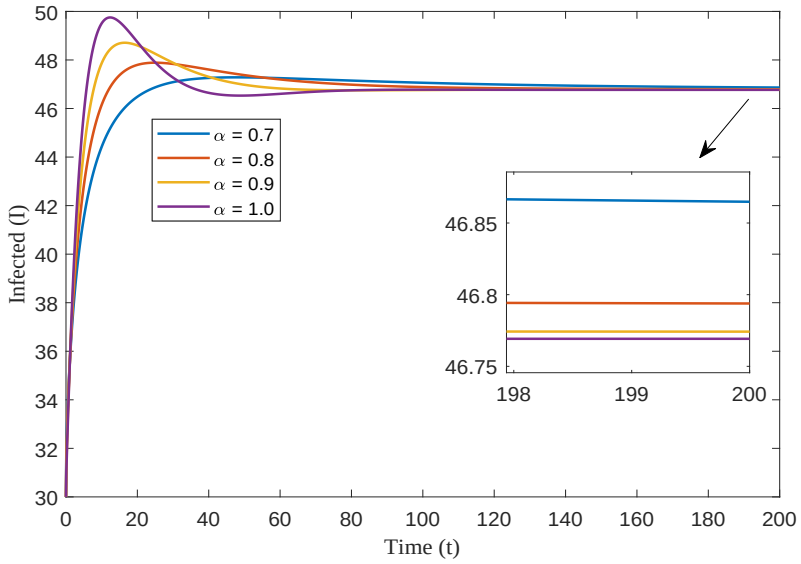

Figure 6.4: Time series plot of infected population with different fractional order.

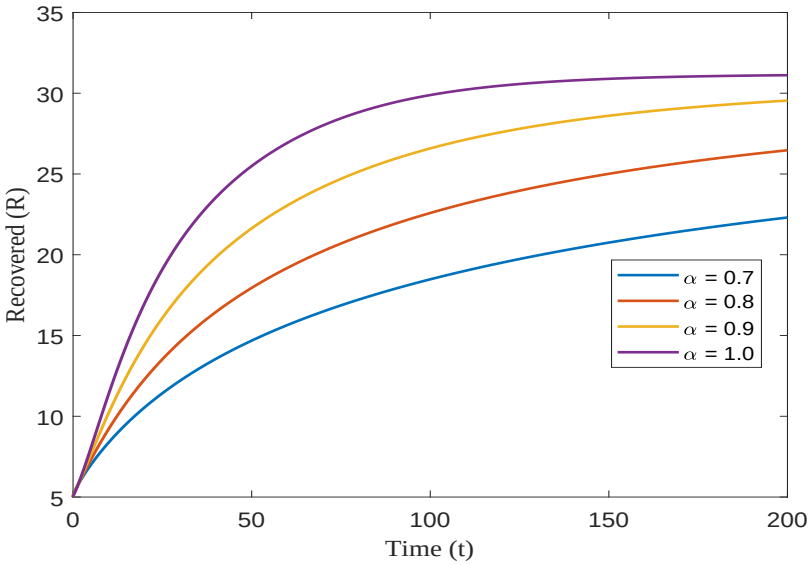

Figure 6.5: Time series plot of recovered population with different fractional order.

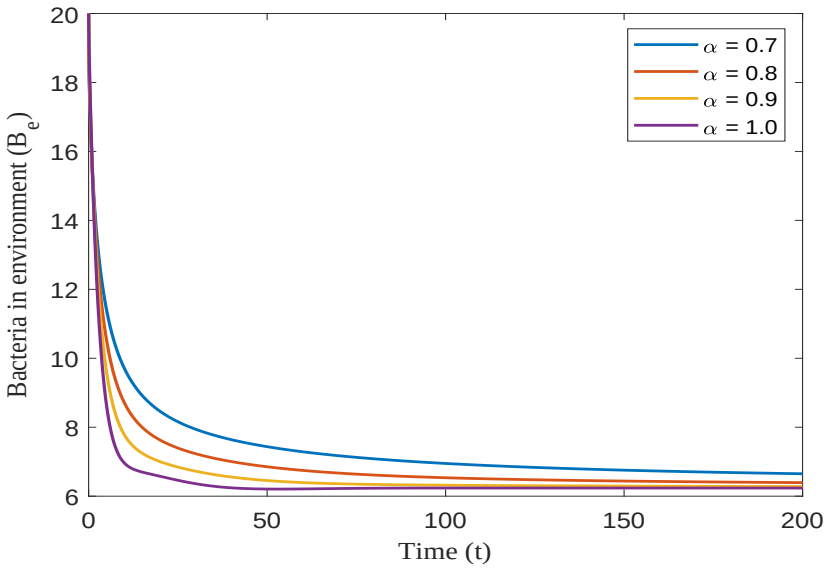

Figure 6.6: Time series plot of environmental bacteria population with different fractional order.

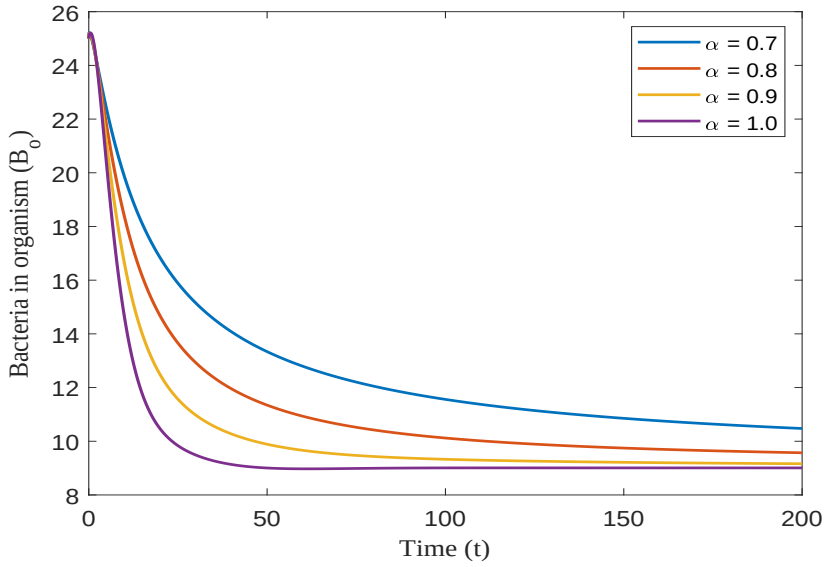

Figure 6.7: Time series plot of organism bacteria population with different fractional order.

As, it can be observed from Figure 6.3, convergence rate of the system (6.1) is influenced by variation of the memory effect α. In particular, by decreasing the memory i.e. increasing the fractional order α, the susceptible population reaches its steady state quickly. At the same time, the decreasing fractional order α leads to a

slower convergence, which means if the system has larger memory i.e. lesser value of α, then it will take more time for convergence. Simply said, decreasing α will require more time to eradicate the disease.

Similarly, it can be observed in Figures 6.4, 6.5, 6.6 and 6.7 that when $\alpha = 1$, the populations I, R, B_e, and B_o, respectively, acquire steady state quickly. However, as the value of α decreases, it takes more time to reach the steady state. This shows the evolution of epidemic over time.

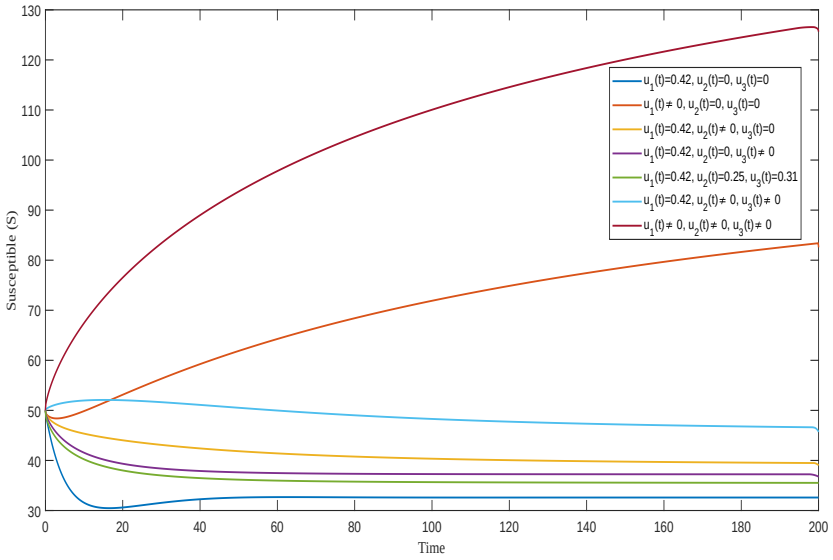

Figure 6.8: Profiles of susceptible population (S) with different control strategies.

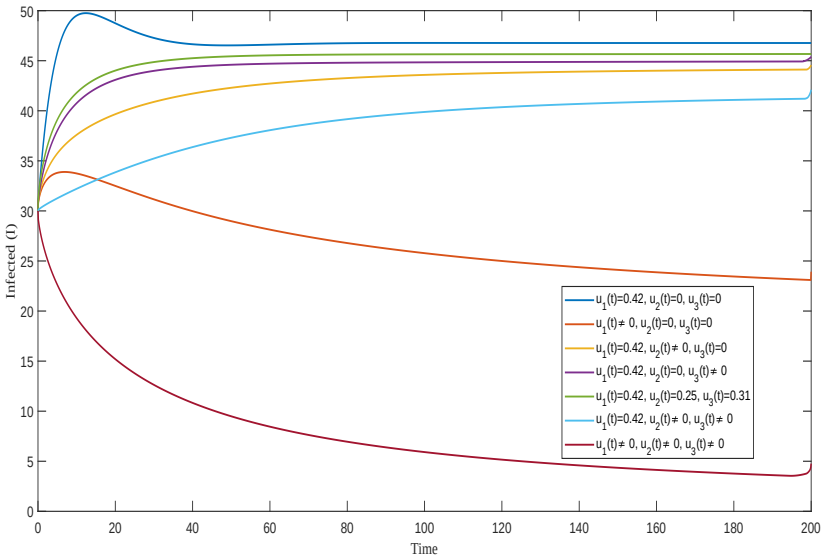

Figure 6.9: Profiles of infected population (I) with different control strategies.

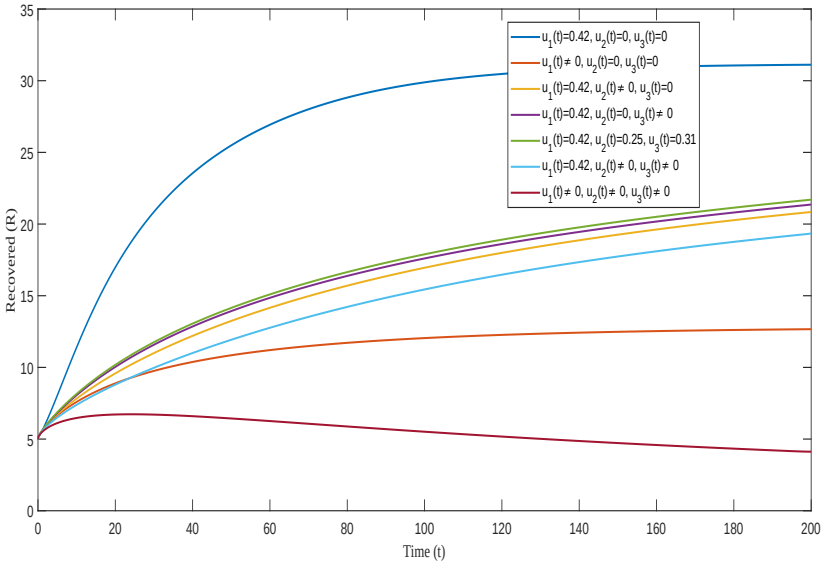

Figure 6.10: Profiles of recovered population (R) with different control strategies.

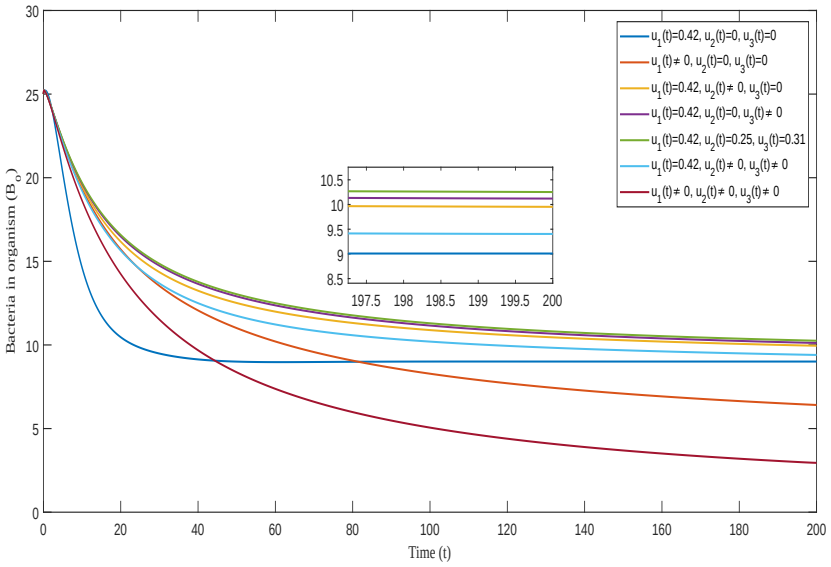

Figure 6.11: Profiles of organism bacteria (B_o) with different control strategies.

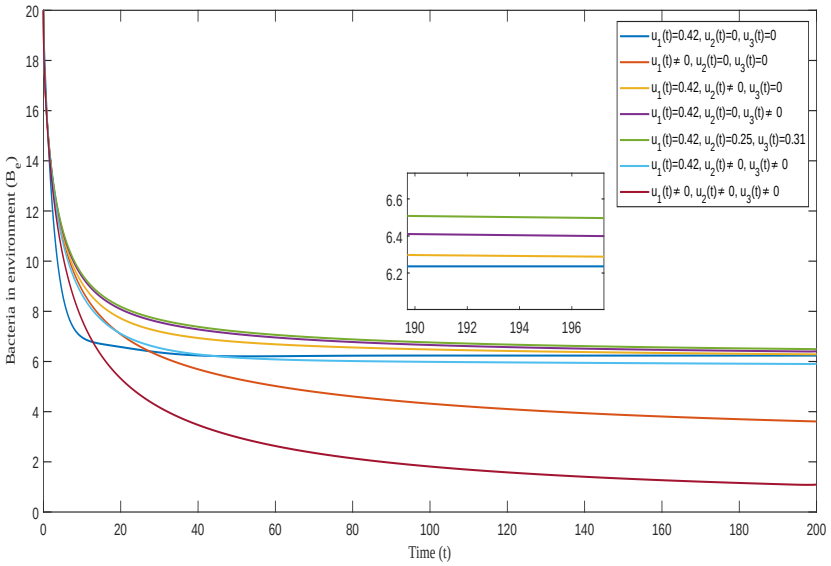

Figure 6.12: Profiles of environmental bacteria (B_e) with different control strategies.

Further, incorporating an optimal control strategy in our model will greatly affect the progress of the epidemic. To best match real-life, we have incorporated three controls, namely $u_1(t)$, $u_2(t)$ and $u_3(t)$, representing the level of protection as mentioned in Section 6.7. Figures 6.8, 6.9, 6.10, 6.11 and 6.12 show the time series plot, for 200 days, of the various sub-population for different values of these controls. Differ-

ent permutations of these controls can be applied in our model out of which several strategies have been considered depending upon whether $u_i(t); i = 1,2,3$, is constant or time-dependent, where $u_i(t)$ is taken as time-dependent and expressions (6.12) have been used for simulation purposes. The detailed study of the strategies is given below:

- **Strategy 1** ($u_1(t) = 0.42, u_2(t) = 0, u_3(t) = 0$)
  Constant personal protection u_1 only: First we study the dynamics of the epidemic when a constant rate of personal protection, $u_1(t) = 0.42$, is applied in the absence of awareness regarding cleanliness and hygiene. Figure 6.8 shows that by using this strategy, there is a sudden decrease in the susceptible population for approximately 15 days and then a slight increase till a certain level. The infected population reaches its peak in the first 15 days and then slightly decreases (Figure 6.9). As constant personal protection, such as wearing masks and isolation from the infected individuals, is followed throughout the course of the epidemic, the recovered population increases till it reaches a steady state (Figure 6.10). The population of both bacteria in environment and organism initially decreases, but eventually reaches a stable count (Figures 6.11 and 6.12).

- **Strategy 2** ($u_1(t) \neq 0, u_2(t) = 0, u_3(t) = 0$)
  Time-dependent personal protection $u_1(t)$ only: As we apply a time-dependent control $u_1(t)$ in the absence of $u_2(t)$ and $u_3(t)$, the susceptible population decreases slightly for the first 2-3 days then increases eventually as the epidemic progresses. The recovered population also increases throughout the course of disease. The bacteria population reduces till it reaches a stable count. After employing this strategy, the infected population peaks within the first 2-3 days, which is still a much lower peak as compared to the one observed in Strategy 1. Moreover, the number of infected individuals eventually drops below initial number of infected individuals. In contrast, while the infection count in Strategy 1 decreases after 15 days, it still remains higher than the initial number of infected individuals. Conclusively, we can say that a time-dependent control yields better results than a constant control.

- **Strategy 3** ($u_1(t) = 0.42, u_2(t) \neq 0, u_3(t) = 0$)
  Constant personal protection u_1 combined with time-dependent spread of awareness on cleanliness $u_2(t)$: In this strategy, a constant personal protection control, $u_1(t) = 0.42$, along with a time-dependent control $u_2(t)$, which focuses

on the spread of awareness regarding cleanliness, have been used to reduce the objective functional $J(u)$, while the control $u_3(t)$ based on hygiene conditions has been set to zero. The susceptible population reduces slightly and the infected population increases. While this combination of controls is applied, the recovered population increases and the amount of bacteria in environment and organism reduces.

- **Strategy 4** ($u_1(t) = 0.42, u_2(t) = 0, u_3(t) \neq 0$)
  Constant personal protection u_1 combined with time-dependent hygiene practices $u_3(t)$: Similar to Strategy 3, in this strategy, we study the effects of a constant personal protection control, $u_1(t) = 0.42$, in the absence of $u_2(t)$ but in the presence of a time-dependent control $u_3(t)$, aiming at reducing the rate of contact between susceptible and bacteria in our surroundings by following some basic hygiene practices, such as proper sanitation in kitchens. The number of susceptible individuals decreases, while the number of infected individuals increases over time, eventually reaching a steady state. Meanwhile, the number of recovered individuals also increases. The application of this strategy leads to a reduction in the count of both bacteria in environment and bacteria in organisms. While this reduction is noticeable, the bacterial count observed under this strategy is still higher than the count observed when Strategy 3 is implemented. This suggests that although Strategy 4 is effective in decreasing bacteria around us, Strategy 3 still results in more reduction overall.

- **Strategy 5** ($u_1(t) = 0.42, u_2(t) = 0.25, u_3(t) = 0.31$)
  Constant personal protection, cleanliness and hygiene practices: This strategy employs all the three controls, that is, u_1, u_2 and u_3, simultaneously at a constant rate of 0.42, 0.25 and 0.31, respectively. This results in an increase in the recovered population and a decrease in the bacteria count. Moreover, it is interesting to note that, even though all the three controls are applied in this strategy, still it gives far worse results than Strategy 2, where only a time-dependent control $u_1(t)$ is applied. The susceptible individuals are significantly lower and infected individuals are higher in this case as compared to those observed under Strategy 2.

- **Strategy 6** ($u_1(t) = 0.42, u_2(t) \neq 0, u_3(t) \neq 0$)
  Constant personal protection u_1 with time-dependent controls $u_2(t)$ and

$u_3(t)$**, regarding cleanliness and hygiene practices:** Taking a constant control $u_1 = 0.42$ and time-dependent controls $u_2(t)$ and $u_3(t)$, increases the number of recovered individuals and decreases the bacteria count over a span of 200 days. Compared to Strategy 2, the number of infected individuals is lesser for approximately 20 days in this case. After this period, the number of infected individuals gradually increases till it reaches a steady state. Additionally, this number is way lesser than the case when constant u_1, u_2 and u_3 are applied (Strategy 5).

- **Strategy 7** ($u_1(t) \neq 0, u_2(t) \neq 0, u_3(t) \neq 0$)
  Time-dependent personal protection, cleanliness and hygiene practices: Applying all three time-dependent controls $u_1(t)$, $u_2(t)$ and $u_3(t)$, simultaneously, increases the susceptible population and reduces the infected population significantly. In fact, the number of susceptible individuals are the most and the number of infected individuals are the least in this case as compared to all the above strategies. The recovered population decreases in this case, but this is because the population of both bacteria in environment and bacteria in organisms reduces drastically, thereby effectively lessening the spread of the disease. Thus we can say that employing three time-dependent controls reduces the disease burden notably.

Table 6.1 provides a comparative analysis of various control strategies in terms of their implementation cost (unit), the maximum number of individuals infected at any time during the disease propagation period ($I_{\max}$), and the number of infected individuals at the end of 200 days (I_{end}), for the fractional order $\alpha = 0.7$. The results clearly show that strategies employing time-dependent controls lead to lower values of both the cost functional and the number of infected individuals, compared to those using constant controls. Among all the strategies analyzed, Strategy 7 proves to be the most effective approach by achieving the lowest implementation cost, the smallest peak infection level, and the minimum number of infections at the end of the 200-day period. This highlights the effectiveness of optimal, time-dependent control measures in mitigating disease spread while minimizing the expenditure cost.

Table 6.1: Values of cost function (unit), maximum number of infected individuals per day ($I_{\max}$), and the number of infected individuals in the end (I_{end}), for $\alpha = 0.7$.

	Cost (unit)	I_{max}	I_{end}
Strategy 1	9340.8	47.2841	46.8648
Strategy 2	5462.1	33.8916	23.9285
Strategy 3	8637.5	44.5642	44.5642
Strategy 4	4537.9	45.3937	45.3937
Strategy 5	9038.1	45.6716	45.6716
Strategy 6	7942.4	42.1036	42.1036
Strategy 7	1872.5	30.0000	4.7623

6.10 Conclusion

This chapter studies the impact of household waste on human health, highlighting how uncollected waste fosters harmful bacteria that spread diseases and pose serious environmental and public health risks. This scenario is modeled in this chapter for which a Caputo type fractional order *SIR* model is developed with the inclusion of two types of bacteria class: Bacteria in environment (B_e) and Bacteria in organism (B_o).

Further, in the analysis of this model we have first found the region of attractor, in which the solution remains bounded. The existence and uniqueness of the solution of the model (6.1) has been discussed using fixed point theorems and Banach contraction principle. The basic reproduction number $\mathscr{R}_0$ is calculated with the help of next generation approach and its sensitivity analysis is performed using the normalized forward sensitivity index. The sensitivity analysis displays that the the growth rate (Λ), the virus transmission rate from susceptible to infected (β), level of protection (ρ) and death rate (μ) are highly sensitive parameters. These factors can be controlled significantly by some appropriate steps. Additionally, the stability analysis in light of Ulam-Hyers and generalized Ulam-Hyers criteria is discussed.

Moreover, we have formulated an optimal control problem (OCP) (6.11) corresponding to our vector borne disease model (6.1). In this OCP, we have considered three time-dependent controls $u_1(t), u_2(t)$ and $u_3(t)$. All the controls are focused on reducing the transmission rate as discussed in Section 6.7. Existence results and characterization of optimal controls are performed with the help of Pontryagin's maximum principle.

Furthermore, in numerical analysis, we have plotted the time series plot, for 200 days, of each sub-population with different fractional order α in Figures 6.3, 6.4, 6.5, 6.6 and 6.7. These graphical representations reveal a significant pattern: as the fractional order α approaches one, the time required for each sub-population to settle into its steady state decreases, indicating a faster convergence. However, despite this variation in convergence speed, the fundamental stability characteristics of the equilibrium points remain unchanged. This means that varying α does not affect the stability nature; rather, it only influences how quickly the system reaches its equilibrium. This highlights the role of fractional-order derivatives in capturing memory effect while maintaining the overall stability properties of the system.

The numerical simulation of the optimal control problem is also performed. To study the varying impacts of different control measures on the dynamics of the epidemic, we have taken into account different strategies, as illustrated in Figures 6.8, 6.9, 6.10, 6.11 and 6.12, evaluated the costs corresponding to each strategy along with the maximum number of infected individuals per day and the number of infected individuals in the end in Table 6.1. Among all the strategies, Strategy 7, which employs time-dependent controls for personal protection, cleanliness, and hygiene practices, proves to be the most effective in reducing the infected population and bacterial counts, leading to a significant reduction in the disease burden as well as its implementation cost. In contrast, Strategy 5, despite incorporating all three controls, yields relatively poor results when compared to Strategy 2, which relies on time-dependent personal protection alone. This suggests that a time-dependent approach, particularly when focused on personal protection and hygiene, is more efficient than constant controls. Strategies that combine time-dependent controls, especially with attention to cleanliness and hygiene (as seen in Strategies 6 and 7), provide good outcomes in controlling the spread of the disease and minimizing the cost of implementation of these strategies.

Thus, this study presents a flexible vector-borne *SIR* model that can be adapted to real-world situations by incorporating additional parameters or compartments. Given the persistent challenge of managing household waste and production of hazardous bacteria, the results of this chapter provide valuable insights into cost-effective and impactful disease control strategies. Policy makers should focus on spreading awareness about self protection, cleanliness and hygiene from time-to-time so as to minimize the disease burden. This study serves as a crucial step towards minimizing both eco-

nomic burden and public health risk, ultimately helping to create a stronger and more adaptable healthcare system.

Chapter 7

Conclusion, Future scope and Social Impact

7.1 Conclusion

The aim of this chapter is to present a concluding remarks to our thesis and illustrate some of the prospects that define our current and future endeavours in scientific research.

This thesis has focused on the development and analysis of several fractional-order epidemic models that integrate real-world complexities such as vaccination strategies, behavioural responses, psychological effects, environmental factors, and optimal control measures. By combining mathematical theory with numerical simulations and policy-oriented insights, this work has aimed to contribute both to the advancement of fractional calculus in epidemiology and to the design of effective public health strategies.

The thesis began with a discussion of vaccination strategies adopted by five highly affected countries during the COVID-19 pandemic: the USA, India, Brazil, France, and the UK. This comparative study revealed how population structure, median age, immunity, and healthcare capacity shaped vaccination priorities. For example, countries with older populations such as France and the UK focused heavily on elderly groups, while India, with a much younger population, initially targeted frontline workers and adults over 45. The analysis showed that median age played an important role in determining infection spread and mortality, and that vaccination strategies had to be

adapted according to demographic realities. This introductory study provided useful context and motivation for the mathematical models developed in later chapters.

The next contribution was the development of a fractional-order SIS model with fear effect and preventive measures. By incorporating behavioral responses such as fear and protection, the model showed how psychological and social factors can significantly influence epidemic outcomes. Numerical simulations confirmed that increasing the level of fear or the adoption of preventive measures reduces infection levels and slows disease spread. This result highlights the importance of considering human behavior in disease modeling, as public fear and awareness campaigns can play a central role in controlling epidemics.

Building on this, the thesis proposed a fractional-order $SVIR$ model that distinguished between partially vaccinated and fully vaccinated individuals. This extension was motivated by real-world vaccination programs where not everyone receives full protection. The analysis demonstrated that while partial vaccination reduces infection, it is not sufficient to control the epidemic. In contrast, full vaccination significantly lowers disease prevalence and increases recovery, proving more cost-effective and impactful. This chapter underlined the need for health authorities to promote full vaccination coverage rather than relying on incomplete vaccination, which may not adequately reduce the epidemic burden.

The third mathematical model was a fractional-order $SEIQR$ system, which incorporated both quarantined individuals and psychological effects on susceptibles. This framework allowed the study of how quarantine policies and information-driven behavior shape epidemic dynamics. The findings showed that timely quarantine of infected individuals, combined with behavioral changes through information campaigns, effectively reduces the number of infections. Moreover, the incorporation of memory effects through fractional calculus demonstrated how past experiences and responses influence present outcomes. An optimal control problem was also formulated, showing that information-based interventions are both effective and economical in the early phase of an outbreak.

The thesis then turned to environmental factors by proposing a fractional-order $SPIR$ model with pollution effects. This model captured how environmental pollution can contribute to disease transmission, with some newborns entering a pollution-affected compartment. The analysis confirmed that pollution intensifies epidemic spread and that controlling transmission in pollution-affected groups is crucial. Op-

timal control simulations suggested that dual interventions - targeting both susceptible and pollution-affected groups - yield the most effective results. The study emphasized the importance of considering environmental health in epidemic preparedness, as pollution can exacerbate disease risks.

Finally, a fractional-order *SIR* model with bacterial classes was developed to study the impact of uncollected household waste. Two bacterial compartments, environmental and organism-based, were introduced to capture the role of harmful bacteria in disease spread. The results showed that poor waste management can fuel epidemics, but appropriate controls such as cleanliness, hygiene, and personal protection can significantly reduce infection and bacterial counts. Importantly, time-dependent strategies focusing on awareness and hygiene were shown to be more effective than constant interventions. This chapter demonstrated the close link between public health, waste management, and epidemic control.

Overall, the thesis makes several contributions. First, it shows that fractional calculus is a versatile and effective framework for modeling infectious diseases, as it captures memory effects that integer-order models overlook. Second, it highlights the role of non-biological factors - such as fear, behavior, vaccination strategy, pollution, and waste management - in shaping epidemic outcomes. Third, it demonstrates the importance of full vaccination, timely quarantine, and environmental controls as effective strategies to reduce disease burden.

The findings have practical implications for policymakers, healthcare professionals, and environmental authorities. Epidemic control cannot rely solely on medical interventions but must also consider behavioral responses, demographic structures, and environmental conditions. Mathematical models, especially those enriched with fractional dynamics, can serve as valuable tools to guide such decisions.

In conclusion, this thesis provides both theoretical and applied insights into the modeling of infectious diseases. By combining fractional calculus with realistic social, psychological, and environmental factors, it advances our understanding of epidemic dynamics and offers strategies for better management of future outbreaks. The work also opens pathways for further research, such as extending models to include age-structure, time delays, or network effects, and applying them to specific diseases beyond COVID-19. Such efforts can help build more resilient public health systems and prepare society for future epidemic challenges.

7.2 Future Directions and Research Plans

The work presented in this thesis provides a comprehensive study of fractional-order epidemic models incorporating vaccination strategies, fear effects, quarantine measures, environmental pollution, and waste-borne bacterial infections. While the current work has generated meaningful theoretical and numerical results, it also serves as a foundation for future research. Possible extensions of this work include the following directions:

(i) The construction of more generalized epidemic models that include additional compartments such as age groups, asymptomatic carriers, hospitalized individuals, and spatial heterogeneity. Such extensions aim to capture more realistic disease dynamics and to enable applications to region-specific case studies, particularly in densely populated countries like India.

(ii) The incorporation of stochastic effects into fractional-order epidemic models. This approach allows the study of randomness in disease spread, especially during the initial phase of outbreaks or in small populations. In addition, the inclusion of time delays (e.g., incubation periods, vaccination lags, and behavioral response delays) is planned, as these are biologically and socially relevant.

(iii) The application of statistical and computational approaches for the estimation of real data, which can subsequently be integrated into fractional-order models. This step is crucial for validating theoretical results and demonstrating their applicability in public health decision-making.

(iv) The coupling of epidemic models with environmental indicators such as air pollution levels, waste management efficiency, and climate variables (temperature, humidity, rainfall), thereby extending the study of pollution and waste-borne infections.

(v) Collaboration with epidemiologists, environmental scientists, and public health experts to apply these models in real-world policy contexts. The long-term objective is to develop decision-support systems based on fractional epidemic models, which may guide governments and health organizations in designing effective interventions during future epidemics.

7.3 Social Impact

The findings of this thesis hold significant social relevance as they provide practical insights for controlling and managing infectious diseases. By incorporating fractional calculus into epidemic modeling, the research enhances the accuracy of predictions and supports informed decision-making for public health authorities. The analysis of vaccination strategies, quarantine measures, environmental influences, and waste management demonstrates that disease control is not only a medical challenge but also a social responsibility requiring community participation. The emphasis on full vaccination, awareness campaigns, and hygienic practices highlights strategies that can reduce infection risks and promote healthier societies. Ultimately, this work bridges mathematical theory with public health practice, offering tools that can guide policymakers, influence health education, and strengthen social resilience against future epidemics and pandemics.

This thesis aligns with SDG 3 (Good Health and Well-Being) by providing mathematical models to predict and control infectious diseases. It contributes to SDG 9 (Industry, Innovation and Infrastructure) through innovative applications of fractional calculus in epidemiology. By analyzing disease spread in urban contexts, it supports SDG 11 (Sustainable Cities and Communities), offering insights for safer and more resilient cities. Finally, by incorporating environmental and pollution-related factors, it connects with SDG 13 (Climate Action), emphasizing the link between environmental health and epidemic risks.

References

[1] Agarwal, R., Purohit, S. D., and Kritika, 2024, "Introduction to fractional calculus and modelling," in *Modeling Calcium Signaling: A Fractional Perspective* (Springer). ISBN 9789819716517, pp. 1–28.

[2] Agrawal, O. P., 2002, "Formulation of Euler–Lagrange equations for fractional variational problems," *Journal of Mathematical Analysis and Applications* **272**, 368–379.

[3] Agrawal, O. P., 2004, "A general formulation and solution scheme for fractional optimal control problems," *Nonlinear Dynamics* **38**, 323–337.

[4] Ahmed, E., El-Sayed, A., and El-Saka, H. A., 2006, "On some Routh–Hurwitz conditions for fractional order differential equations and their applications in Lorenz, Rössler, Chua and Chen systems," *Physics Letters A* **358**, 1–4.

[5] Ahmed, E., and Elgazzar, A., 2007, "On fractional order differential equations model for nonlocal epidemics," *Physica A: Statistical Mechanics and its Applications* **379**, 607–614.

[6] Albattat, A., Singh, A., Tyagi, P., and Haghi, A., 2024, *Solid waste management and disposal practices in rural tourism*, Advances in Hospitality, Tourism, and the Services Industry (IGI Global). ISBN 9798369396230.

[7] Alexanderian, A., Gobbert, M. K., Fister, K. R., Gaff, H., Lenhart, S., and Schaefer, E., 2011, "An age-structured model for the spread of epidemic cholera: analysis and simulation," *Nonlinear Analysis: Real World Applications* **12**, 3483–3498.

[8] Algehyne, E. A., and ud Din, R., 2021, "On global dynamics of COVID-19 by using SQIR type model under non-linear saturated incidence rate," *Alexandria Engineering Journal* **60**, 393–399.

[9] Alm, E., Broberg, E. K., Connor, T., Hodcroft, E. B., Komissarov, A. B., Maurer-Stroh, S., Melidou, A., Neher, R. A., O'Toole, Á., Pereyaslov, D., *et al.*, 2020, "Geographical and temporal distribution of SARS-CoV-2 clades in the WHO European Region, January to June 2020," *Eurosurveillance* **25**, 2001410.

[10] Amin, M., Farman, M., Akgül, A., and Alqahtani, R. T., 2022, "Effect of vaccination to control COVID-19 with fractal fractional operator," *Alexandria Engineering Journal* **61**, 3551–3557.

[11] Anderson, R. M., and May, R. M., 1991, *Infectious Diseases of Humans: Dynamics and Control* (Oxford University Press). ISBN 9780198545996.

[12] Andre, F. E., Booy, R., Bock, H. L., Clemens, J., Datta, S. K., John, T. J., Lee, B. W., Lolekha, S., Peltola, H., Ruff, T., *et al.*, 2008, "Vaccination greatly reduces disease, disability, death and inequity worldwide," *Bulletin of the World health organization* **86**, 140–146.

[13] Anthony, S. M., and Bhatia, S. K., 2024, "Mathematical modeling and dynamical analysis of an SPIR epidemic model with fuzzy parameters under environmental pollution," *Modeling Earth Systems and Environment* **10**, 6977–6996.

[14] Artalejo, J. R., Economou, A., and Lopez-Herrero, M. J., 2015, "The stochastic SEIR model before extinction: Computational approaches," *Applied Mathematics and Computation* **265**, 1026–1043.

[15] Atangana, A., 2017, *Fractional Operators with Constant and Variable Order with Application to Geo-hydrology* (Academic Press). ISBN 9780128097960.

[16] Awadalla, M., Alahmadi, J., Cheneke, K. R., and Qureshi, S., 2024, "Fractional optimal control model and bifurcation analysis of human syncytial respiratory virus transmission dynamics," *Fractal and Fractional* **8**, 44.

[17] Azoua, M., Azouani, A., and Hafidi, I., 2023, "Optimal control and global stability of the SEIQRS epidemic model," *Communications in Mathematical Biology and Neuroscience* **2023**, 1–24.

[18] Baba, B. A., and Bilgehan, B., 2021, "Optimal control of a fractional order model for the COVID–19 pandemic," *Chaos, Solitons & Fractals* **144**, 110678.

[19] Baba, I. A., and Nasidi, B. A., 2021, "Fractional order epidemic model for the dynamics of novel COVID-19," *Alexandria Engineering Journal* **60**, 537–548.

[20] Bacaër, N., 2011, "Daniel Bernoulli, d'Alembert and the inoculation of smallpox (1760)," in *A Short History of Mathematical Population Dynamics* (Springer). ISBN 9780857291158, pp. 21–30.

[21] Banerjee, S., and Sarkhel, P., 2019, "Municipal solid waste management, household and local government participation: a cross country analysis," *Journal of Environmental Planning and Management* **63**, 210–235.

[22] Bank, W., 2018, "The World Bank, Fertility rate, total (births per woman) - Hong Kong SAR, China," `https://data.worldbank.org`

[23] Bank, W., 2021 June, "Global Economic Prospects: A Weak and Uneven Recovery," `https://www.worldbank.org/en/publication/global-economic-prospects`.

[24] Beddington, J. R., 1975, "Mutual interference between parasites or predators and its effect on searching efficiency," *The Journal of Animal Ecology* **44**, 331–340.

[25] Bedi, P., Kumar, A., Abdeljawad, T., and Khan, A., 2021, "S-asymptotically ω-periodic mild solutions and stability analysis of Hilfer fractional evolution equations," *Evolution Equations and Control Theory* **10**, 733–748.

[26] Bentaleb, D., and Amine, S., 2019, "Lyapunov function and global stability for a two-strain SEIR model with bilinear and non-monotone incidence," *International Journal of Biomathematics* **12**, 1950021.

[27] Bjørkdahl, K., and Carlsen, B., 2017, "Fear of the fear of the flu: Assumptions about media effects in the 2009 pandemic," *Science communication* **39**, 358–381.

[28] Brauer, F., Castillo-Chavez, C., and Castillo-Chavez, C., 2012, *Mathematical models in population biology and epidemiology*, Texts in Applied Mathematics, Vol. 2 (Springer). ISBN 9781475735161.

[29] Cai, L.-M., Li, Z., and Song, X., 2018, "Global analysis of an epidemic model with vaccination," *Journal of Applied Mathematics and Computing* **57**, 605–628.

[30] Cai, Y., Kang, Y., and Wang, W., 2017, "A stochastic SIRS epidemic model with nonlinear incidence rate," *Applied Mathematics and Computation* **305**, 221–240.

[31] Callender, D., 2016, "Vaccine hesitancy: more than a movement," *Human Vaccines & Immunotherapeutics* **12**, 2464–2468.

[32] Capasso, V., and Serio, G., 1978, "A generalization of the Kermack-McKendrick deterministic epidemic model," *Mathematical Biosciences* **42**, 43–61.

[33] Caputo, M., and Fabrizio, M., 2017, "On the notion of fractional derivative and applications to the hysteresis phenomena," *Meccanica* **52**, 3043–3052.

[34] Carr, J., 2012, *Applications of centre manifold theory*, Applied Mathematical Sciences, Vol. 35 (Springer). ISBN 9781461259299.

[35] Castillo-Chavez, C., and Song, B., 2004, "Dynamical models of tuberculosis and their applications," *Mathematical Biosciences & Engineering* **1**, 361–404.

[36] Chang, X., Wang, J., Liu, M., and Yan, X., 2025, "An SIS infectious disease model with nonlinear incidence and disease awareness on complex networks," *Chaos, Solitons & Fractals* **196**, 116349.

[37] Chen, Q., Liu, Y., and Wang, F.-L., 2003, "A chronicle on the SARS epidemic," *Chinese Law & Government* **36**, 12–15.

[38] Coddington, A., and Levinson, N., 1955, *Theory of Ordinary Differential Equations*, International series in pure and applied mathematics (Tata McGraw-Hill Education). ISBN 9780070992566.

[39] Cui, J., Mu, X., and Wan, H., 2008, "Saturation recovery leads to multiple endemic equilibria and backward bifurcation," *Journal of Theoretical Biology* **254**, 275–283.

[40] Cui, X., Xue, D., and Pan, F., 2022, "Dynamic analysis and optimal control for a fractional-order delayed SIR epidemic model with saturated treatment," *The European Physical Journal Plus* **137**, 1–18.

[41] Dadvand, P., Parker, J., Bell, M. L., Bonzini, M., Brauer, M., Darrow, L. A., Gehring, U., Glinianaia, S. V., Gouveia, N., Ha, E.-h., *et al.*, 2013, "Maternal exposure to particulate air pollution and term birth weight: a multi-country evaluation of effect and heterogeneity," *Environmental health perspectives* **121**, 267–373.

[42] Das, S., and Gupta, P., 2011, "A mathematical model on fractional Lotka–Volterra equations," *Journal of Theoretical Biology* **277**, 1–6.

[43] DeAngelis, D. L., Goldstein, R., and O'Neill, R. V., 1975, "A model for tropic interaction," *Ecology* **56**, 881–892.

[44] Delavari, H., Baleanu, D., and Sadati, J., 2012, "Stability analysis of Caputo fractional-order nonlinear systems revisited," *Nonlinear Dynamics* **67**, 2433–2439.

[45] Diagne, M., Rwezaura, H., Tchoumi, S., and Tchuenche, J., 2021, "A mathematical model of COVID-19 with vaccination and treatment," *Computational and Mathematical Methods in Medicine* **2021**, 1250129.

[46] Diaz, P., Constantine, P., Kalmbach, K., Jones, E., and Pankavich, S., 2018, "A modified SEIR model for the spread of Ebola in Western Africa and metrics for resource allocation," *Applied mathematics and computation* **324**, 141–155.

[47] Diekmann, O., Heesterbeek, J., and Roberts, M. G., 2010, "The construction of next-generation matrices for compartmental epidemic models," *Journal of the Royal society interface* **7**, 873–885.

[48] Diekmann, O., Heesterbeek, J. A. P., and Metz, J. A. J., 1990, "On the definition and the computation of the basic reproduction ratio R_0 in models for infectious diseases in heterogeneous populations," *Journal of mathematical biology* **28**, 365–382.

[49] Diethelm, K., 2016, "Monotonicity of functions and sign changes of their Caputo derivatives," *Fractional Calculus and Applied Analysis* **19**, 561–566.

[50] Diethelm, K., Ford, N. J., and Freed, A. D., 2002, "A predictor-corrector approach for the numerical solution of fractional differential equations," *Nonlinear Dynamics* **29**, 3–22.

[51] Diethelm, K., Ford, N. J., and Freed, A. D., 2004, "Detailed error analysis for a fractional Adams method," *Numerical algorithms* **36**, 31–52.

[52] Diethelm, K., Ford, N. J., Freed, A. D., and Luchko, Y., 2005, "Algorithms for the fractional calculus: a selection of numerical methods," *Computer methods in applied mechanics and engineering* **194**, 743–773.

[53] Diethelm, K., and Luchko, Y., 2004, "Numerical solution of linear multi-term initial value problems of fractional order," *J. Comput. Anal. Appl* **6**, 243–263.

[54] Dietz, K., 1988, "The first epidemic model: a historical note on PD En'ko," *Australian Journal of Statistics* **30**, 56–65.

[55] Ding, Y., Wang, Z., and Ye, H., 2011, "Optimal control of a fractional-order HIV-immune system with memory," *IEEE Transactions on Control Systems Technology* **20**, 763–769.

[56] Van den Driessche, P., and Watmough, J., 2002, "Reproduction numbers and sub-threshold endemic equilibria for compartmental models of disease transmission," *Mathematical biosciences* **180**, 29–48.

[57] Dubey, B., Dubey, P., and Dubey, U. S., 2015, "Dynamics of an SIR model with nonlinear incidence and treatment rate," *Applications and Applied Mathematics: An International Journal (AAM)* **10**, 718–737.

[58] Dubey, B., Patra, A., Srivastava, P., and Dubey, U. S., 2013, "Modeling and analysis of an SEIR model with different types of nonlinear treatment rates," *Journal of Biological Systems* **21**, 1350023.

[59] Dubey, P., Dubey, B., and Dubey, U. S., 2016, "An SIR model with nonlinear incidence rate and Holling type III treatment rate," in *Applied Analysis in Biological and Physical Sciences: ICMBAA, Aligarh, India, June 2015* (Springer). pp. 63–81.

[60] Ellwanger, J. H., Veiga, A. B. G. d., Kaminski, V. d. L., Valverde-Villegas, J. M., Freitas, A. W. Q. d., and Chies, J. A. B., 2021, "Control and prevention of infectious diseases from a one health perspective," *Genetics and Molecular Biology* **44**, e20200256.

[61] Ferdinan, Utomo, S. W., Soesilo, T. E. B., and Herdiansyah, H., 2022, "Household waste control index towards sustainable waste management: A study in bekasi city, indonesia," *Sustainability* **14**, 14403.

[62] Gaff, H., and Schaefer, E., 2009, "Optimal control applied to vaccination and treatment strategies for various epidemiological models," *Mathematical Biosciences and Engineering* **6**, 469–492.

[63] Ghosh, I., Tiwari, P. K., Samanta, S., Elmojtaba, I. M., Al-Salti, N., and Chattopadhyay, J., 2018, "A simple SI-type model for HIV/AIDS with media and self-imposed psychological fear," *Mathematical biosciences* **306**, 160–169.

[64] Ghosh, M., Lashari, A. A., and Li, X.-Z., 2013, "Biological control of malaria: A mathematical model," *Applied Mathematics and Computation* **219**, 7923–7939.

[65] Glencross, D. A., Ho, T.-R., Camina, N., Hawrylowicz, C. M., and Pfeffer, P. E., 2020, "Air pollution and its effects on the immune system," *Free Radical Biology and Medicine* **151**, 56–68.

[66] Göllmann, L., Kern, D., and Maurer, H., 2009, "Optimal control problems with delays in state and control variables subject to mixed control–state constraints," *Optimal Control Applications and Methods* **30**, 341–365.

[67] Gomes, M., Margheri, A., Medley, G., and Rebelo, C., 2005, "Dynamical behaviour of epidemiological models with sub-optimal immunity and nonlinear incidence," *Journal of Mathematical Biology* **51**, 414–430.

[68] Gomez-Mejiba, S. E., Zhai, Z., Akram, H., Pye, Q. N., Hensley, K., Kurien, B. T., Scofield, R. H., and Ramirez, D. C., 2009, "Inhalation of environmental stressors & chronic inflammation: autoimmunity and neurodegeneration," *Mutation research/genetic toxicology and environmental mutagenesis* **674**, 62–72.

[69] González-Parra, G., Arenas, A. J., and Chen-Charpentier, B. M., 2014, "A fractional order epidemic model for the simulation of outbreaks of influenza A (H1N1)," *Mathematical methods in the Applied Sciences* **37**, 2218–2226.

[70] Granger, C. W., and Joyeux, R., 1980, "An introduction to long-memory time series models and fractional differencing," *Journal of time series analysis* **1**, 15–29.

[71] Greenberg, R. S., and Kleinbawm, D., 1985, "Mathematical modeling strategies for the analysis of epidemiologic research," *Annual review of public health* **6**, 223–245.

[72] Gumel, A. B., McCluskey, C. C., and Watmough, J., 2006, "An SVEIR model for assessing potential impact of an imperfect anti-SARS vaccine," *Mathematical Biosciences and Engineering* **3**, 485–512.

[73] Hamby, D. M., 1994, "A review of techniques for parameter sensitivity analysis of environmental models," *Environmental monitoring and assessment* **32**, 135–154.

[74] Harmand, J., Lobry, C., Rapaport, A., and Sari, T., 2019, *Optimal Control in Bioprocesses: Pontryagin's Maximum Principle in Practice* (Wiley). ISBN 9781119597230.

[75] Hertz-Picciotto, I., Park, H.-Y., Dostal, M., Kocan, A., Trnovec, T., and Sram, R., 2008, "Prenatal exposures to persistent and non-persistent organic compounds and effects on immune system development," *Basic & clinical pharmacology & toxicology* **102**, 146–154.

[76] Hethcote, H. W., 2000, "The mathematics of infectious diseases," *SIAM review* **42**, 599–653.

[77] Hethcote, H. W., and van den Driessche, P., 1991, "Some epidemiological models with nonlinear incidence," *Journal of Mathematical Biology* **29**, 271–287.

[78] Hilfer, R., 2000, *Applications of fractional calculus in physics* (World scientific). ISBN 9789814496209.

[79] Hincal, E., and Alsaadi, S. H., 2021, "Stability analysis of fractional order model on corona transmission dynamics," *Chaos, Solitons & Fractals* **143**, 110628.

[80] Hu, Z., Liu, S., and Wang, H., 2008, "Backward bifurcation of an epidemic model with standard incidence rate and treatment rate," *Nonlinear Analysis: Real World Applications* **9**, 2302–2312.

[81] Hu, Z., Ma, W., and Ruan, S., 2012, "Analysis of SIR epidemic models with nonlinear incidence rate and treatment," *Mathematical biosciences* **238**, 12–20.

[82] Huo, J., Zhao, H., and Zhu, L., 2015, "The effect of vaccines on backward bifurcation in a fractional order HIV model," *Nonlinear Analysis: Real World Applications* **26**, 289–305.

[83] Hyers, D. H., 1941, "On the stability of the linear functional equation," *Proceedings of the National Academy of Sciences* **27**, 222–224.

[84] Iqbal, Z., Rehman, M. A. U., Baleanu, D., Ahmed, N., Raza, A., and Rafiq, M., 2020, "Mathematical and numerical investigations of the fractional order epidemic model with constant vaccination strategy," *Rom. Rep. Phys* **73**, 1–19.

[85] Jana, S., Haldar, P., and Kar, T., 2016, "Optimal control and stability analysis of an epidemic model with population dispersal," *Chaos, Solitons & Fractals* **83**, 67–81.

[86] Jones, K. E., Patel, N. G., Levy, M. A., Storeygard, A., Balk, D., Gittleman, J. L., and Daszak, P., 2008, "Global trends in emerging infectious diseases," *Nature* **451**, 990–993.

[87] Just, W., Saldaña, J., and Xin, Y., 2018, "Oscillations in epidemic models with spread of awareness," *Journal of Mathematical Biology* **76**, 1027–1057.

[88] Kabir, K. A., Kuga, K., and Tanimoto, J., 2019, "Analysis of SIR epidemic model with information spreading of awareness," *Chaos, Solitons & Fractals* **119**, 118–125.

[89] Kar, T., Nandi, S. K., Jana, S., and Mandal, M., 2019, "Stability and bifurcation analysis of an epidemic model with the effect of media," *Chaos, Solitons & Fractals* **120**, 188–199.

[90] Kassa, S. M., and Ouhinou, A., 2015, "The impact of self-protective measures in the optimal interventions for controlling infectious diseases of human population," *Journal of Mathematical Biology* **70**, 213–236.

[91] Keeling, M. J., and Rohani, P., 2008, *Modeling infectious diseases in humans and animals* (Princeton university press). ISBN 9781400841035.

[92] Kermack, W. O., and McKendrick, A. G., 1927, "A contribution to the mathematical theory of epidemics," *Proceedings of the royal society of london. Series A, Containing papers of a mathematical and physical character* **115**, 700–721.

[93] Khajji, B., Kouidere, A., Elhia, M., Balatif, O., and Rachik, M., 2021, "Fractional optimal control problem for an age-structured model of COVID-19 transmission," *Chaos, Solitons & Fractals* **143**, 110625.

[94] Kilbas, A., Anatoli, Srivastava, H. M., and Trujillo, J. J., 2006, *Theory and applications of fractional differential equations*, North-Holland Mathematics Studies (Elsevier). ISBN 9780444518323.

[95] Kiss, I. Z., Cassell, J., Recker, M., and Simon, P. L., 2010, "The impact of information transmission on epidemic outbreaks," *Mathematical biosciences* **225**, 1–10.

[96] Kumar, A., 2020, "Stability of a fractional-order epidemic model with nonlinear incidences and treatment rates," *Iranian Journal of Science and Technology, Transactions A: Science* **44**, 1505–1517.

[97] Kumar, A., Kumar, M., and Nilam, 2020, "A study on the stability behavior of an epidemic model with ratio-dependent incidence and saturated treatment," *Theory in Biosciences* **139**, 225–234.

[98] Kumar, A., and Nilam, 2019, "Mathematical analysis of a delayed epidemic model with nonlinear incidence and treatment rates," *Journal of Engineering Mathematics* **115**, 1–20.

[99] Kumar, A., and Nilam, 2022, "Effects of nonmonotonic functional responses on a disease transmission model: modeling and simulation," *Communications in Mathematics and Statistics* **10**, 195–214.

[100] Kumar, U., Mandal, P. S., Tripathi, J. P., Bajiya, V. P., and Bugalia, S., 2021, "SIRS epidemiological model with ratio-dependent incidence: Influence of preventive vaccination and treatment control strategies on disease dynamics," *Mathematical Methods in the Applied Sciences* **44**, 14703–14732.

[101] Kumari, N., and Sharma, S., 2018, "Modeling the dynamics of infectious disease under the influence of environmental pollution," *International Journal of Applied and Computational Mathematics* **4**, 1–24.

[102] Lafferty, K. D., and Holt, R. D., 2003, "How should environmental stress affect the population dynamics of disease?." *Ecology Letters* **6**, 654–664.

[103] LaSalle, J. P., 1968, "Stability theory for ordinary differential equations," *Journal of Differential equations* **4**, 57–65.

[104] Lazarević, M. P., Rapaić, M. R., Šekara, T. B., Mladenov, V., and Mastorakis, N., 2014, "Introduction to fractional calculus with brief historical background," *Advanced topics on applications of fractional calculus on control problems, system stability and modeling*, 3–16.

[105] Lenhart, S., and Workman, J. T., 2007, *Optimal control applied to biological models*, Chapman & Hall/CRC Mathematical Biology Series (CRC Press). ISBN 9781420011418.

[106] de León, U. A.-P., Pérez, Á. G., and Avila-Vales, E., 2020, "An SEIARD epidemic model for COVID-19 in Mexico: mathematical analysis and state-level forecast," *Chaos, Solitons & Fractals* **140**, 110165.

[107] Leontitsis, A., Senok, A., Alsheikh-Ali, A., Al Nasser, Y., Loney, T., and Alshamsi, A., 2021, "SEAHIR: A Specialized Compartmental Model for COVID-19," *International journal of environmental research and public health* **18**, 2667.

[108] Li, G.-H., and Zhang, Y.-X., 2017, "Dynamic behaviors of a modified SIR model in epidemic diseases using nonlinear incidence and recovery rates," *PLoS One* **12**, e0175789.

[109] Li, H.-L., Zhang, L., Hu, C., Jiang, Y.-L., and Teng, Z., 2017, "Dynamical analysis of a fractional-order predator-prey model incorporating a prey refuge," *Journal of Applied Mathematics and Computing* **54**, 435–449.

[110] Li, M. Y., Graef, J. R., Wang, L., and Karsai, J., 1999, "Global dynamics of a SEIR model with varying total population size," *Mathematical biosciences* **160**, 191–213.

[111] Li, M. Y., and Wang, L., 2002, "Global stability in some SEIR epidemic models," in *Mathematical approaches for emerging and reemerging infectious diseases: models, methods, and theory*, Vol. 126 (Springer). pp. 295–311.

[112] Li, X.-P., Gul, N., Khan, M. A., Bilal, R., Ali, A., Alshahrani, M. Y., Muhammad, T., and Islam, S., 2021, "A new Hepatitis B model in light of asymptomatic carriers and vaccination study through Atangana–Baleanu derivative," *Results in Physics* **29**, 104603.

[113] Li, X.-Z., Li, W.-S., and Ghosh, M., 2009, "Stability and bifurcation of an SIR epidemic model with nonlinear incidence and treatment," *Applied Mathematics and Computation* **210**, 141–150.

[114] Li, Y., Chen, Y., and Podlubny, I., 2010, "Stability of fractional-order nonlinear dynamic systems: Lyapunov direct method and generalized Mittag–Leffler stability," *Computers & Mathematics with Applications* **59**, 1810–1821.

[115] Lipsitch, M., and Santillana, M., 2019, "Enhancing situational awareness to prevent infectious disease outbreaks from becoming catastrophic," *Global Catastrophic Biological Risks* **424**, 59–74.

[116] Liu, S., Jiang, W., Li, X., and Zhou, X.-F., 2016, "Lyapunov stability analysis of fractional nonlinear systems," *Applied Mathematics Letters* **51**, 13–19.

[117] Liu, W.-m., Hethcote, H. W., and Levin, S. A., 1987, "Dynamical behavior of epidemiological models with nonlinear incidence rates," *Journal of mathematical biology* **25**, 359–380.

[118] Liu, W.-M., Levin, S. A., and Iwasa, Y., 1986, "Influence of nonlinear incidence rates upon the behavior of SIRS epidemiological models," *Journal of mathematical biology* **23**, 187–204.

[119] Liu, Y., and Cui, J.-a., 2008, "The impact of media coverage on the dynamics of infectious disease," *International Journal of Biomathematics* **1**, 65–74.

[120] Lu, Z., and Zhu, Y., 2018, "Comparison principles for fractional differential equations with the Caputo derivatives," *Advances in Difference Equations* **237**, 1–11.

[121] Lueck, J. A., and Callaghan, T., 2022, "Inside the 'black box'of COVID-19 vaccination beliefs: Revealing the relative importance of public confidence and news consumption habits," *Social Science & Medicine* **298**, 114874.

[122] Lukes, D. L., 1982, *Differential equations: Classical to Controlled*, Mathematics in Science and Engineering (Academic Press). ISBN 9780080956688.

[123] Ma, L., and Li, C., 2016, "Center manifold of fractional dynamical system," *Journal of Computational and Nonlinear Dynamics* **11**, 021010.

[124] Majee, S., Jana, S., Das, D. K., and Kar, T., 2022, "Global dynamics of a fractional-order HFMD model incorporating optimal treatment and stochastic stability," *Chaos, Solitons & Fractals* **161**, 112291.

[125] Majee, S., Jana, S., Kar, T., Barman, S., and Das, D., 2024, "Modeling and analysis of Caputo-type fractional-order SEIQR epidemic model," *International Journal of Dynamics and Control* **12**, 148–166.

[126] Majee, S., Kar, T. K., Jana, S., Das, D. K., and Nieto, J., 2023, "Complex dynamics and fractional-order optimal control of an epidemic model with saturated treatment and incidence," *International Journal of Bifurcation and Chaos* **33**, 2350192.

[127] Mamidi, S., 2024 May, "Waste management and vector-borne diseases," `https://d-scholarship.pitt.edu/47230/`.

[128] Mandal, M., Jana, S., Nandi, S. K., and Kar, T., 2020, "Modelling and control of a fractional-order epidemic model with fear effect," *Energy, Ecology and Environment* **5**, 421–432.

[129] Mandale, R., Kumar, A., Vamsi, D., and Srivastava, P. K., 2021, "Dynamics of an infectious disease in the presence of saturated medical treatment of Holling Type-III and self-protection," *Journal of Biological Systems* **29**, 245–289.

[130] Martcheva, M., 2015, *An introduction to mathematical epidemiology*, Texts in Applied Mathematics, Vol. 61 (Springer). ISBN 9781489976123.

[131] Matignon, D., 1996, "Stability results for fractional differential equations with applications to control processing," in *Computational engineering in systems applications*, Vol. 2, pp. 963–968.

[132] Miller, K. S., and Ross, B., 1993, *An introduction to the fractional calculus and fractional differential equations* (Wiley). ISBN 9780471588849.

[133] Minelgaitė, A., and Liobikienė, G., 2019, "Waste problem in European Union and its influence on waste management behaviours," *Science of The Total Environment* **667**, 86–93.

[134] Miranda, M. N., Pingarilho, M., Pimentel, V., Torneri, A., Seabra, S. G., Libin, P. J., and Abecasis, A. B., 2022, "A tale of three recent pandemics: Influenza, HIV and SARS-CoV-2," *Frontiers in Microbiology* **13**, 889643.

[135] Mishra, A., and Gakkhar, S., 2017, "A micro-epidemic model for primary dengue infection," *Communications in Nonlinear Science and Numerical Simulation* **47**, 426–437.

[136] Momenyan, S., and Torabi, M., 2022, "Modeling the spatio-temporal spread of COVID-19 cases, recoveries and deaths and effects of partial and full vaccination coverage in Canada," *Scientific Reports* **12**, 17817.

[137] Morens, D. M., and Fauci, A. S., 2013, "Emerging infectious diseases: threats to human health and global stability," *PLoS pathogens* **9**, e1003467.

[138] Murray, J. D., 2007, *Mathematical biology: I. An introduction*, Vol. 17 (Springer). ISBN 9780387952239.

[139] Nabil, T., 2019, "Krasnoselskii n-tupled fixed point theorem with applications to fractional nonlinear dynamical system," *Advances in Mathematical Physics* **2019**, 6763842.

[140] Naik, P. A., Yavuz, M., Qureshi, S., Zu, J., and Townley, S., 2020, "Modeling and analysis of COVID-19 epidemics with treatment in fractional derivatives using real data from Pakistan," *The European Physical Journal Plus* **135**, 1–42.

[141] Naz, R., and Torrisi, M., 2022, "The transmission dynamics of a compartmental epidemic model for COVID-19 with the asymptomatic population via closed-form solutions," *Vaccines* **10**, 2162.

[142] Odibat, Z. M., and Shawagfeh, N. T., 2007, "Generalized Taylor's formula," *Applied Mathematics and Computation* **186**, 286–293.

[143] Oke, M., Ogunmiloro, O., Akinwumi, C., and Raji, R., 2019, "Mathematical modeling and stability analysis of a SIRV epidemic model with non-linear force of infection and treatment," *Communications in Mathematics and Applications* **10**, 717.

[144] Oldham, K., and Spanier, J., 1974, *The fractional calculus theory and applications of differentiation and integration to arbitrary order*, Mathematics in Science and Engineering, Vol. 111 (Elsevier). ISBN 9780080956206.

[145] Omae, Y., Kakimoto, Y., Sasaki, M., Toyotani, J., Hara, K., Gon, Y., and Takahashi, H., 2022, "SIRVVD model-based verification of the effect of first and second doses of COVID-19/SARS-CoV-2 vaccination in Japan," *Math Biosci Eng* **19**, 1026–40.

[146] Pan, Q., Huang, J., and Wang, H., 2022, "An SIRS model with nonmonotone incidence and saturated treatment in a changing environment," *Journal of mathematical biology* **85**, 23.

[147] Paul, S., Mahata, A., Mukherjee, S., Roy, B., Salimi, M., and Ahmadian, A., 2022, "Study of fractional order SEIR epidemic model and effect of vaccination on the spread of COVID-19," *International Journal of Applied and Computational Mathematics* **8**, 237.

[148] Podlubny, I., 1998, *Fractional differential equations: an introduction to fractional derivatives, fractional differential equations, to methods of their solution and some of their applications*, Mathematics in Science and Engineering, Vol. 198 (Academic Press). ISBN 9780080531984.

[149] Pooseh, S., Rodrigues, H. S., and Torres, D. F., 2011, "Fractional derivatives in dengue epidemics," in *AIP Conference Proceedings*, Vol. 1389 (American Institute of Physics). pp. 739–742.

[150] Rajak, A. K., and Nilam, 2022, "A fractional-order epidemic model with quarantine class and nonmonotonic incidence: Modeling and simulations," *Iranian Journal of Science and Technology, Transactions A: Science* **46**, 1249–1263.

[151] Rezapour, S., Mohammadi, H., and Samei, M. E., 2020, "SEIR epidemic model for COVID-19 transmission by caputo derivative of fractional order," *Advances in difference equations* **2020**, 1–19.

[152] Ridho, H., Thamrin, M. H., Nasution, F. A., and Indainanto, Y. I., 2023, "Disposition of waste management policy implementers through the regional cooperation scheme," *International Journal of Sustainable Development & Planning* **18**, 275–282.

[153] Rosa, S., and Torres, D. F., 2023, "Numerical fractional optimal control of respiratory syncytial virus infection in Octave/ MATLAB," *Mathematics* **11**, 1511.

[154] Ross, R., 1916, "An application of the theory of probabilities to the study of a priori pathometry-Part I," *Proceedings of the Royal Society of London. Series A, Containing papers of a mathematical and physical character* **92**, 204–230.

[155] Ruan, S., and Wang, W., 2003, "Dynamical behavior of an epidemic model with a nonlinear incidence rate," *Journal of differential equations* **188**, 135–163.

[156] Sabatier, J., Agrawal, O. P., and Machado, J. T., 2007, *Advances in Fractional Calculus: Theoretical Developments and Applications in Physics and Engineering*, Vol. 4 (Springer). ISBN 9781402060427.

[157] Sadki, M., and Allali, K., 2023, "Stochastic two-strain epidemic model with bilinear and non-monotonic incidence rates," *The European Physical Journal Plus* **138**, 1–15.

[158] Sahu, G. P., and Dhar, J., 2015, "Dynamics of an SEQIHRS epidemic model with media coverage, quarantine and isolation in a community with pre–existing immunity," *Journal of Mathematical Analysis and Applications* **421**, 1651–1672.

[159] Shah, K., Ahmad, S., Ullah, A., and Abdeljawad, T., 2024, "Study of chronic myeloid leukemia with T-cell under fractal-fractional order model," *Open Physics* **22**, 20240032.

[160] Shah, K., Sarwar, M., Abdeljawad, T., *et al.*, 2024, "A comprehensive mathematical analysis of fractal–fractional order nonlinear re-infection model," *Alexandria Engineering Journal* **103**, 353–365.

[161] Shah, K., Sarwar, M., Abdeljawad, T., *et al.*, 2024, "On mathematical model of infectious disease by using fractals fractional analysis," *Discrete and Continuous Dynamical Systems-S* **17**, 3064–3085.

[162] Shulgin, B., Stone, L., and Agur, Z., 1998, "Pulse vaccination strategy in the SIR epidemic model," *Bulletin of mathematical biology* **60**, 1123–1148.

[163] Smith, K. F., Goldberg, M., Rosenthal, S., Carlson, L., Chen, J., Chen, C., and Ramachandran, S., 2014, "Global rise in human infectious disease outbreaks," *Journal of the Royal Society Interface* **11**, 20140950.

[164] Srivastava, A., and Nilam, 2024, "Optimal control of a fractional order SEIQR epidemic model with non-monotonic incidence and quarantine class," *Computers in Biology and Medicine* **178**, 108682.

[165] Stefan G. Samko, O. I. M., Anatoly A. Kilbas, 1993, *Fractional Integrals and Derivatives: Theory and Applications* (Taylor & Francis). ISBN 9782881248641.

[166] Stieb, D. M., Chen, L., Eshoul, M., and Judek, S., 2012, "Ambient air pollution, birth weight and preterm birth: a systematic review and meta-analysis," *Environmental research* **117**, 100–111.

[167] Straif-Bourgeois, S., Ratard, R., and Kretzschmar, M., 2014, "Infectious disease epidemiology," in *Handbook of epidemiology* (Springer). ISBN 9780387098340, pp. 2041–2119.

[168] Strogatz, S. H., 2024, *Nonlinear dynamics and chaos: with applications to physics, biology, chemistry, and engineering* (CRC Press). ISBN 9780429676284.

[169] Sun, D., Li, Q., and Zhao, W., 2023, "Stability and optimal control of a fractional SEQIR epidemic model with saturated incidence rate," *Fractal and Fractional* **7**, 533.

[170] Sun, X., Luo, X., Zhao, C., Chung Ng, R. W., Lim, C. E. D., Zhang, B., and Liu, T., 2015, "The association between fine particulate matter exposure during pregnancy and preterm birth: a meta-analysis," *BMC pregnancy and childbirth* **15**, 1–12.

[171] Swati, and Nilam, 2022, "Fractional order SIR epidemic model with Beddington–De Angelis incidence and Holling type II treatment rate for COVID-19," *Journal of Applied Mathematics and Computing* **68**, 3835–3859.

[172] Tang, B., Zhang, X., Li, Q., Bragazzi, N. L., Golemi-Kotra, D., and Wu, J., 2022, "The minimal COVID-19 vaccination coverage and efficacy to compensate for a potential increase of transmission contacts, and increased transmission probability of the emerging strains," *BMC Public Health* **22**, 1258.

[173] Tang, Y., Huang, D., Ruan, S., and Zhang, W., 2008, "Coexistence of limit cycles and homoclinic loops in a SIRS model with a nonlinear incidence rate," *SIAM Journal on Applied Mathematics* **69**, 621–639.

[174] Tanwar, K., Kumawat, N., Tripathi, J. P., Chauhan, S., and Mubayi, A., 2024, "Evaluating vaccination timing, hesitancy and effectiveness to prevent future outbreaks: insights from COVID-19 modelling and transmission dynamics," *Royal Society Open Science* **11**, 240833.

[175] Taubenberger, J. K., and Morens, D. M., 2008, "The Pathology of Influenza virus infections," *Annu. Rev. Pathol. Mech. Dis.* **3**, 499–522.

[176] Tchuenche, J. M., Dube, N., Bhunu, C. P., Smith, R. J., and Bauch, C. T., 2011, "The impact of media coverage on the transmission dynamics of human influenza," *BMC Public Health* **11**, S5.

[177] Torvik, P. J., and Bagley, R. L., 1984, "On the appearance of the fractional derivative in the behavior of real materials," *Journal of Applied Mechanics* **51**, 294–298.

[178] Uddin, M., Mustafa, F., Rizvi, T. A., Loney, T., Al Suwaidi, H., Al-Marzouqi, A. H. H., Kamal Eldin, A., Alsabeeha, N., Adrian, T. E., Stefanini, C., *et al.*, 2020, "SARS-CoV-2/COVID-19: viral genomics, epidemiology, vaccines, and therapeutic interventions," *Viruses* **12**, 526.

[179] Ulam, S., 2004, *Problems in Modern Mathematics*, Dover phoenix editions (Dover Publications). ISBN 9780486495835.

[180] Ullah, A., Abdeljawad, T., Ahmad, S., and Shah, K., 2020, "Study of a fractional-order epidemic model of childhood diseases," *Journal of Function Spaces* **2020**, 5895310.

[181] University, J. H., 2021, "COVID-19 Dashboard by the Center for Systems Science and Engineering (CSSE)," `https://coronavirus.jhu.edu/map.html`

[182] Upadhyay, R. K., and Acharya, S., 2022, "Modeling the recent outbreak of COVID-19 in india and its control strategies," *Nonlinear Analysis: Modelling and Control* **27**, 254–274.

[183] Upadhyay, R. K., Pal, A. K., Kumari, S., and Roy, P., 2019, "Dynamics of an SEIR epidemic model with nonlinear incidence and treatment rates," *Nonlinear Dynamics* **96**, 2351–2368.

[184] Wang, T., Wu, Y., Lau, J. Y.-N., Yu, Y., Liu, L., Li, J., Zhang, K., Tong, W., and Jiang, B., 2020, "A four-compartment model for the COVID-19 infection- implications on infection kinetics, control measures, and lockdown exit strategies," *Precision Clinical Medicine* **3**, 104–112.

[185] Wang, W., 2006, "Backward bifurcation of an epidemic model with treatment," *Mathematical biosciences* **201**, 58–71.

[186] Wang, W., and Ruan, S., 2004, "Bifurcations in an epidemic model with constant removal rate of the infectives," *Journal of Mathematical Analysis and Applications* **291**, 775–793.

[187] Wang, X., Tao, Y., and Song, X., 2011, "Global stability of a virus dynamics model with Beddington–DeAngelis incidence rate and CTL immune response," *Nonlinear Dynamics* **66**, 825–830.

[188] Wang, X., 2004, "A simple proof of Descartes's rule of signs," *The American Mathematical Monthly* **111**, 525–526.

[189] WHO, 2014, *A global brief on vector-borne diseases*, Tech. Rep.

[190] WHO, 2019 Dec, "World Health Organization: Top ten threats to global health in 2019," `https://www.who.int/news-room/spotlight/ten-threats-to-global-health-in-2019`.

[191] WHO, 2020, "WHO Director-General's opening remarks at the media briefing on COVID-19 – 11 March 2020," `https://www.who.int/director-general/speeches/detail/who-director-general-s-opening-remarks-at-the-media-briefing\-on-covid-19---11-march-2020`.

[192] WHO, 2023, "Managing epidemics: key facts about major deadly diseases," https://www.who.int/publications/i/item/managing-epidemics-key-facts-about-major-deadly-diseases.

[193] WHO, 2024 Sep., *World Health Organization, Factsheet (Vector-borne-diseases).*

[194] Xiao, D., and Ruan, S., 2007, "Global analysis of an epidemic model with non-monotone incidence rate," *Mathematical biosciences* **208**, 419–429.

[195] Xu, C., Yu, Y., Ren, G., Sun, Y., and Si, X., 2023, "Stability analysis and optimal control of a fractional-order generalized SEIR model for the COVID-19 pandemic," *Applied Mathematics and Computation* **457**, 128210.

[196] Yang, Y., and Xu, L., 2020, "Stability of a fractional order SEIR model with general incidence," *Applied Mathematics Letters* **105**, 106303.

[197] Yavuz, M., Coşar, F. Ö., Günay, F., and Özdemir, F. N., 2021, "A new mathematical modeling of the COVID-19 pandemic including the vaccination campaign," *Open Journal of Modelling and Simulation* **9**, 299–321.

[198] Ye, X., and Xu, C., 2019, "A fractional order epidemic model and simulation for avian influenza dynamics," *Mathematical Methods in the Applied Sciences* **42**, 4765–4779.

[199] Yuan, S., and Li, B., 2009, "Global dynamics of an epidemic model with a ratio-dependent nonlinear incidence rate," *Discrete Dynamics in Nature and Society* **2009**, 609306.

[200] Zhang, X., and Liu, X., 2008, "Backward bifurcation of an epidemic model with saturated treatment function," *Journal of mathematical analysis and applications* **348**, 433–443.

[201] Zhonghua, Z., and Yaohong, S., 2010, "Qualitative analysis of a SIR epidemic model with saturated treatment rate," *Journal of Applied Mathematics and Computing* **34**, 177–194.

List of Publications

1. Abhay Srivastava and Nilam (2024). *Optimal control of a fractional order SEIQR epidemic model with non-monotonic incidence and quarantine class*. Computers in Biology and Medicine, 178, 108682. DOI-10.1016/j.compbiomed.2024.108682 [**SCIE, Impact Factor: 7.7**]

2. Abhay Srivastava and Nilam (2025). *Stability analysis and quantification of effects of partial and full vaccination using fractional order SVIR model*. Mathematical Medicine and Biology: A Journal of the IMA, 42(3), 331–358. DOI-10.1093/imammb/dqaf007 [**SCIE, Impact Factor: 1.5**]

3. Abhay Srivastava and Nilam (2025). *Analysis of a Fractional Order SIR Model for Infectious Diseases Spread by Household Waste with Optimal Control Strategies*. Optimal Control Applications and Methods, 47(1), 116-133. DOI-10.1002/oca.70046 [**SCIE, Impact Factor: 1.5**]

4. Abhay Srivastava and Nilam (2026). *A Study of Fractional Order SIS Model with Fear Effect and Beddington-De Angelis Incidence Rate*. Boletim da Sociedade Paranaense de Matematica (BSPM). [**ESCI and Scopus, Impact Factor: 0.4 (Accepted)**]

5. Abhay Srivastava and Nilam. *Study on Vaccination Strategy Employed by the Five Countries Most Affected by Covid-19*. [**Communicated**]

6. Abhay Srivastava and Nilam. *Mathematical Modeling and Qualitative Analysis of a Fractional-Order SPIR Epidemic Model with Non-monotonic Incidences and Optimal Control*. [**Communicated**]

Papers Presented in International Conferences

1. Presented a research paper entitled "**The Role of Strong and weak antivirus in the computer virus propagation model**" in *International Conference on "Dynamical Systems, Control and their Applications"*, organized by the Department of Mathematics, IIT Roorkee, India, during July 01-03, 2022.

2. Presented a research paper entitled "**Dynamic Study of Weak and Strong Vaccination of Covid-19 Using Fractional order *SIR* model**" in the *International Conference on "Mathematics and Applications (ICMA-2024)"*, organized by the Department of Mathematics, Mata Sundri College for Women, University of Delhi, Delhi, India, during January 10-12, 2024.

3. Presented a research paper entitled "**Optimal Control of a Fractional Order *SEIQR* Epidemic Model with Non-monotonic Incidence and Quarantine class**" in the "*International Conference on Multidisciplinary Approaches to Sustainability and Current Challenges (MACCS 2024)*", organized by G H Raisoni University, Amravati, India, during May 17-18, 2024.

4. Presented a research paper entitled "**Review and analysis of vaccination strategy employed by the five most affected countries during Covid-19**" in the "*International Conference on Nonlinear Dynamics: Modeling and Computation (ICNDMC 2025)*", organized by Department of Mathematics, Bharathiar University, Coimbatore, India, during February 17-19, 2025.